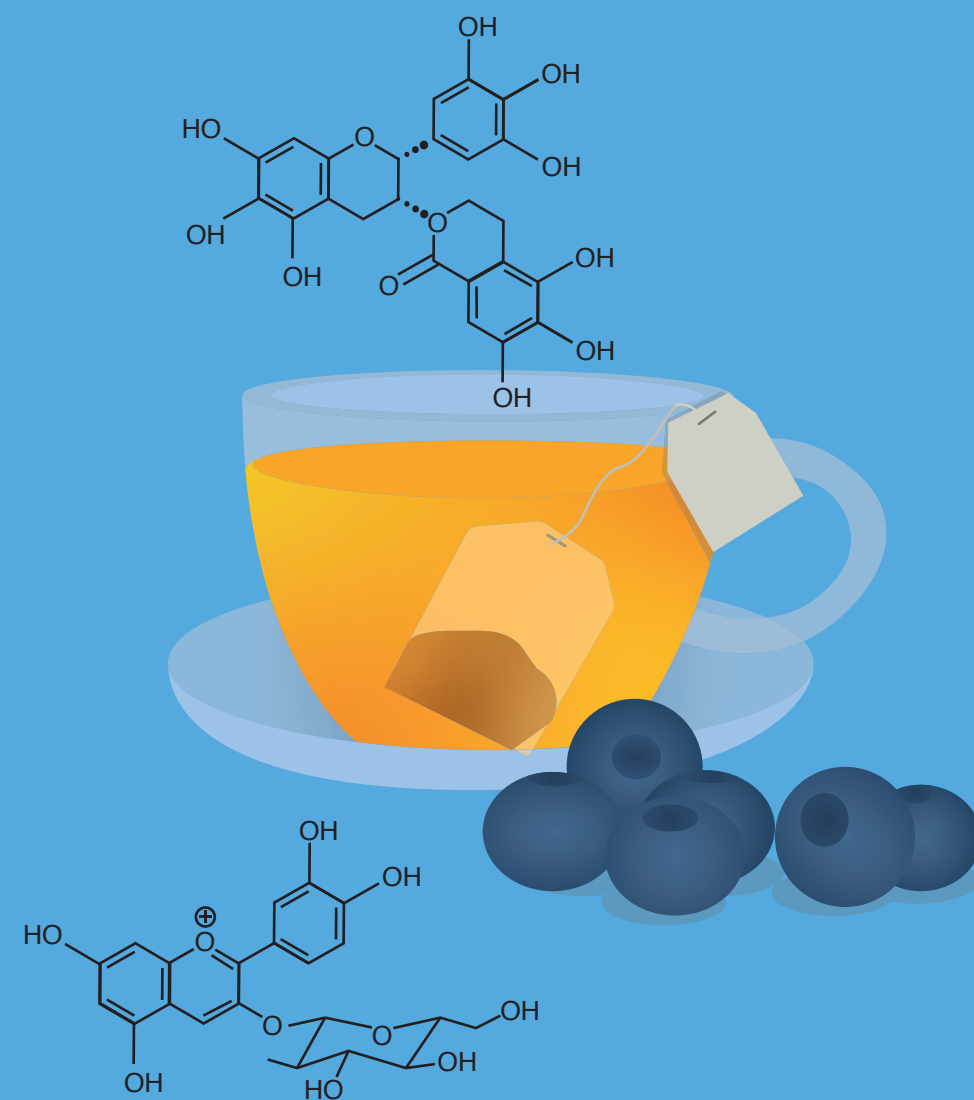


A study on polyphenols modulation of starch digestion

Lijiao Kan

## A study on polyphenols modulation of starch digestion



Lijiao Kan

## **Propositions**

1. The role of polyphenols in limiting starch digestibility is influenced by food matrix structure.  
(this thesis)
2. Caco-2 cells can be used to study inhibition of polyphenols on brush border enzymatic activity which has similar functionality with the brush border enzymatic activity in the human intestine.  
(this thesis)
3. Consumers should be guided by scientists rather than advertisements.
4. Quality is more important than quantity in terms of research publications.
5. Collaboration is necessary if you want to do something impactful.
6. Hard-working can take you far, but smart-working will move you further.
7. Self-discipline is far more important to protect yourself from Covid-19 than any rules.

Propositions belonging to the thesis, entitled

A study on polyphenols modulation of starch digestion

Lijiao Kan

Wageningen, 4 October 2021

# A study on polyphenols modulation of starch digestion

Lijiao Kan

## **Thesis Committee**

### **Promotor**

Prof. Dr V. Fogliano

Professor of Food Quality and Design

Wageningen University & Research

### **Co-promotor**

Dr E. Capuano

Associate professor, Food Quality and Design

Wageningen University & Research

Dr T. Oliviero

Teacher, Food Quality and Design

Wageningen University & Research

### **Other members**

Prof. Dr. Walter Gerrits, Wageningen University & Research

Dr. WJC de Bruijn, Wageningen University & Research

Prof. M. Ferruzzi, North Carolina state University, North Carolina, the United States

Prof. L. Bravo, Institute of Food Science, Technology and Nutrition of the Spanish National Research Council (ICTAN-CSIC), Madrid, Spain

This research was conducted under the auspices of the Graduate School VLAG (Advanced studies in Food Technology, Agrobiotechnology and Health Sciences)



# A study on polyphenols modulation of starch digestion

Lijiao Kan

Thesis

submitted in the fulfilment of the requirements for the degree of doctor

at Wageningen University

by the authority of the Rector Magnificus,

Prof. Dr A.P.J. Mol,

in the presence of the

Thesis Committee appointed by the Academic Board

to be defended in public

on Monday 4 October 2021

at 11 a.m. in the Aula.

Lijiao Kan

A study on polyphenols modulation of starch digestion, 206 pages

PhD thesis, Wageningen University, Wageningen, the Netherlands (2021).

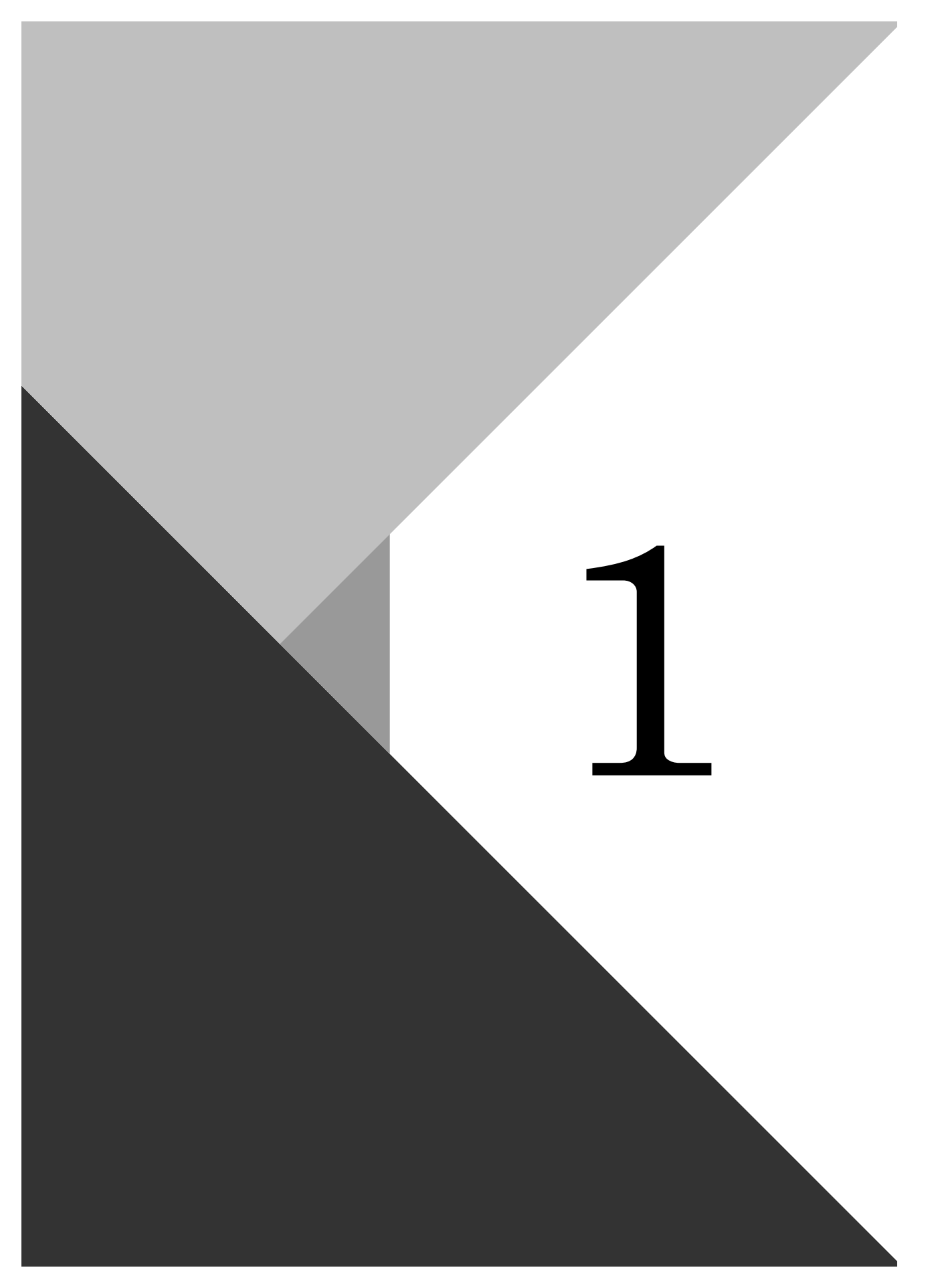
With references, with summary in English.

ISBN: 978-94-6395-883-7

DOI: <https://doi.org/10.18174/549695>

## Table of Contents

<b>Chapter 1</b>	<b>7</b>
General Introduction and Thesis outline	
<b>Chapter 2</b>	<b>25</b>
Interaction of bread and berry polyphenols affects starch digestibility and polyphenols bio-accessibility	
<b>Chapter 3</b>	<b>53</b>
Tea polyphenols as a strategy to control starch digestion in bread: effect of polyphenols type and gluten	
<b>Chapter 4</b>	<b>81</b>
Different effects of inclusion and non-inclusion wheat starch-tannic acid complexes on rheological properties and digestibility of wheat starch	
<b>Chapter 5</b>	<b>117</b>
Non-inclusion starch-tannins interactions formed in starch differing in crystalline type and different amylose content	
<b>Chapter 6</b>	<b>145</b>
Inhibition of $\alpha$ -glucosidases by tea polyphenols in rat intestinal extract and Caco-2 cells grown on Transwell	
<b>Chapter 7</b>	<b>175</b>
General Discussion	
<b>Summary</b>	<b>193</b>
<b>Acknowledgment</b>	<b>197</b>
<b>About the author</b>	<b>201</b>



1

# Chapter 1

General Introduction and Thesis outline

## 1.1 Background

Starch is the most abundant carbohydrate in our diet. Long-term excessive intake of starchy foods has been regarded as the main reason causing overweight or type II diabetes. Besides controlling the intake of starch, slowing down starch digestibility is considered to be an effective way to control glycemic response. Many technological strategies are developed to achieve the aim of controlling glycemic response, such as selection of slowly digestible starch, controlling cell wall integrity, and manipulating the level of starch gelatinization/retrogradation (Hou et al., 2020; Rovalino-Córdova, Fogliano, & Capuano, 2019; Xiao et al., 2011). Another option is using compounds that can inhibit carbohydrate digestive enzymes. This can be done with medicine, such as acarbose, or with natural food components such as polyphenols. Recently it has been shown that polyphenols may reduce starch digestibility by inhibiting carbohydrates digestive enzymes or coating starch granules (Cao et al., 2019; Pyner, Nyambe-Silavwe, & Williamson, 2017; Lijun Sun, Gidley, & Warren, 2017, 2018; Xing, Zhang, Qi, Tsao, & Mine, 2019).

## 1.2 Structures of starch

Starch is an  $\alpha$ -glucans chain and it is composed of amylose and amylopectin. Amylose is a linear glucan. Amylopectin is a highly branched glucan. The structure of native type starch is composed of amorphous and crystalline regions (Waigh, Gidley, Komanshek, & Donald, 2000). The crystalline regions consist of double helices of amylopectin (Waigh et al., 2000). The amylopectin chains can be found in one, two, or more clusters (Donald, 2004). According to the amylose/amylopectin ratio, starch was classified as waxy starch, normal starch, and high amylose starch (Wang, Wang, Yu, & Wang, 2014). Waxy starch consists almost completely of amylopectin. The amylose contents of normal starches range from 14 to 29% (Waterschoot, Gomand, Fierens, & Delcour, 2015). The amylose contents of high amylose starch range from 65 to 85% (Richardson, Jeffcoat, & Shi, 2000). The arrangement and length of the amylopectin chains resulted in the classification of A, B, and C types of X-ray diffraction patterns (Magallanes-Cruz, Flores-Silva, & Bello-Perez, 2017). Cereal starch, for instance, wheat starch, corn starch, and rice starch exhibit an A-type diffraction pattern. Tuber starch, for instance, potato starch, sweet potato starch is known as B-type starch (Matignon & Tecante, 2017). Legume starches, for instance, bean starch is known as C type starch, which is a combination of the A and B C-type granules (Wang, Bogracheva, & Hedley, 1998).

### 1.3 Physiology of starch digestibility

In Figure 1.1. an overview of the physiology of starch digestion is depicted. Starch digestion starts in the mouth where salivary  $\alpha$ -amylase hydrolyze starch into oligosaccharides, maltose, and maltodextrin (Squires, 1953). Upon arriving in the stomach, despite salivary amylase is inactivated at low pH, its activity can continue in the stomach if the pH is sufficiently high due to the buffering effect of foods. Starch digestion mainly occurs in the small intestine. Starch is hydrolyzed into oligosaccharides by pancreatic  $\alpha$ -amylase (Ishikawa & Hirata, 1989). Then the brush border enzymes hydrolyze the oligosaccharides into glucose (Van Beers, Büller, Grand, Einerhand, & Dekker, 1995). Then these monosaccharides enter the bloodstream, which gives a signal to the endocrine organs such as the pancreas to secrete insulin (Cura & Carruthers, 2012). A fraction of starch cannot be digested in the small intestine, and will finally arrive in the colon for fermentation, and this starch is called resistant starch (RS). RS can be further divided into five types (Asp & Björck, 1992). RS1 can be found in whole grains and the cell walls surrounding the starch make the starch inaccessible to digestive enzymes. RS2 is represented by native granules where the presence of crystallites would make starch inaccessible to amylases. RS 3 is retrograded starch, and the produced crystalline structure is difficult to digest. RS 4 is chemically modified starch by various techniques like crosslinking and RS type 5 is a non-digestible complex formed, for instance, amylose-lipid complex in cereal starch.

### 1.4 Potential mechanisms of starch digestion reduction by polyphenols.

Whether the polyphenols can cause certain health effects depends on their chemical structure. As summarized in Figure 1.2, the basic classification of phenolics includes five main phenolic classes: phenolic acids, flavonoids, stilbenes, lignans, and others. Flavonoids are the most widely distributed phenolic compounds in plant foods and have been widely studied (Galanakis, 2018). Flavonoids are among the most promising type of polyphenolic antioxidants because they have structural elements involved in the antiradical activity (Bravo, 1998).

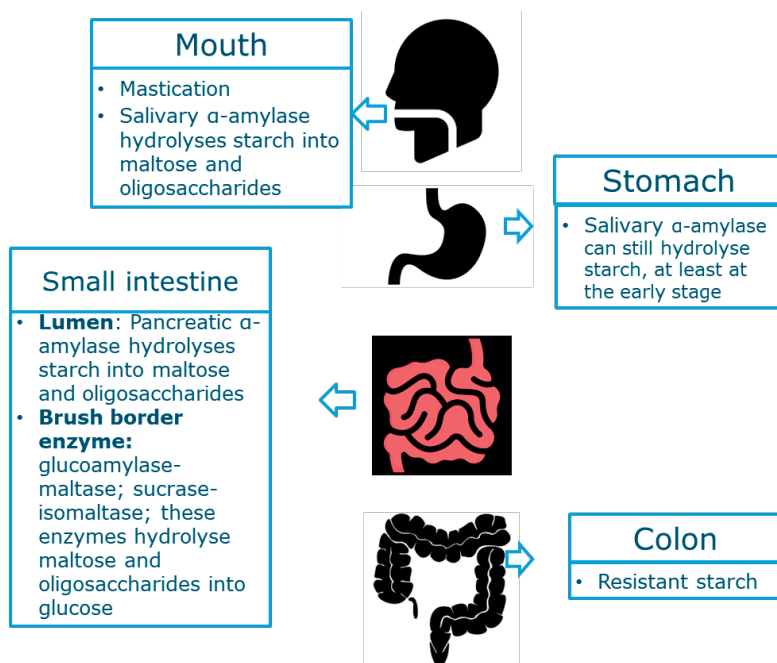


Figure 1.1 Starch digestion in the gastrointestinal tract. Adapted from Molnar, Charles, and Jane Gair. "Concepts of Biology: 1st Canadian Edition." (2015).

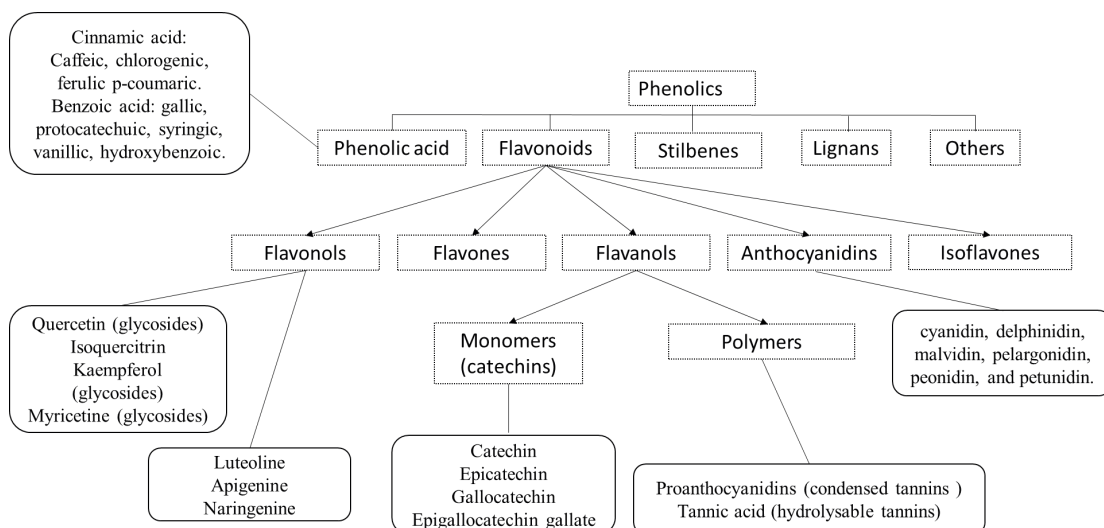


Figure 1.2. Classification of polyphenols. Adapted from (Galanakis, 2018).



### 1.4.1 Inhibitory effects of polyphenols on digestive enzymes

It has been widely accepted that  $\alpha$ -amylase inhibition by polyphenols, in most cases is caused by the binding interactions between the two molecules. The interactions of digestive enzymes and polyphenols are produced by van der Waals forces, hydrogen bonding, and other electrostatic forces (Figure 1.3).

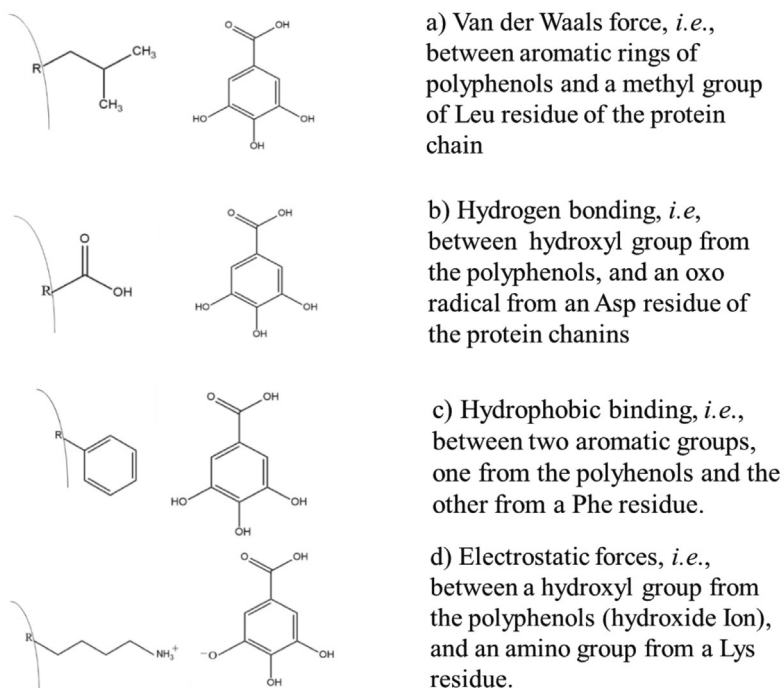
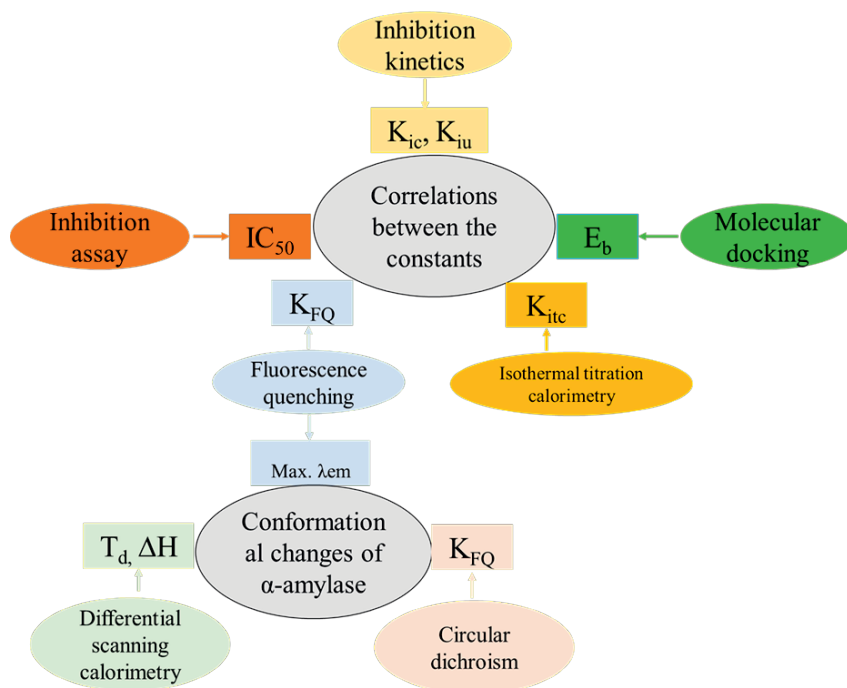


Figure 1.3. Non-covalent binding involves polyphenols–enzyme interactions. Examples of (a) van der Waals forces; (b) hydrogen bonding; (c) hydrophobic binding; and (d) electrostatic forces. The protein chain is represented by R and a curved line.

The binding between digestive enzymes and polyphenols has been studied through inhibitory assays, inhibition kinetics, fluorescence quenching, isothermal titration calorimetry, and molecular docking methods. Techniques commonly used for measuring  $\alpha$ -amylase inhibition are summarized in Figure 1.4. The inhibitory activity of a polyphenol is typically described by its half inhibitory concentration value ( $IC_{50}$ ). Inhibition kinetics results can be

obtained by combining Lineweaver-Burk plot, Dixon plot, Cornish-Bowden plots. Competitive ( $K_{ic}$ ) and uncompetitive inhibition constant ( $K_{iu}$ ) can be used to describe the inhibitory type, including the competitive, uncompetitive, mixed type of inhibition. Fluorescence quenching (FQ) can be used to study the binding of polyphenols and starch at a molecular level. Based on the Stern-Volmer equation, the fluorescence quenching constant ( $K_{FQ}$ ) can be calculated. As  $K_{FQ}$  can reflect the interaction (binding) of polyphenols with  $\alpha$ -amylase, higher  $K_{FQ}$  values correspond to higher binding properties of polyphenols. DSC can be used to measure the thermostability of  $\alpha$ -amylase by determining the denaturation temperature ( $T_d$ ) and denaturation enthalpy ( $\Delta H$ ). The denaturation process of  $\alpha$ -amylase is affected by interacting with dietary polyphenols, which can be suggested by the  $T_d$  and  $\Delta H$  values from DSC thermograms. Circular dichroism spectroscopy (CD) is a technique for investigating the secondary structures of proteins. Based on CD, we can calculate the contents of  $\alpha$ -helix,  $\beta$ -sheet,  $\beta$ -turn, and random coil in a protein. Therefore, the CD can be used to study the effect of dietary polyphenols on the secondary structures of  $\alpha$ -amylase. Isothermal titration calorimetry (ITC) can be used for the determination of the binding enthalpy and binding constant of the reaction between  $\alpha$ -amylase and polyphenols. The binding affinity between  $\alpha$ -amylase and polyphenols can be described by the binding constant ( $K_{itc}$ ). Higher  $K_{itc}$  values reflect a higher binding affinity between polyphenol and  $\alpha$ -amylase. In addition, molecular docking is a computer-assisted technique to simulate the binding of polyphenols and  $\alpha$ -amylase. Docking studies can show not only the hydrogen bonding between the hydroxyl groups of polyphenols and amino acids but also the hydrophobic interactions between the aromatic groups of polyphenols and the enzyme. Figure 1.4 shows the methodologies that have been used to investigate the inhibitory effects on  $\alpha$ -amylase by various polyphenols.



**Figure 1.4.** Overview of the techniques available to study  $\alpha$ -amylase inhibition by polyphenols and the relevant kinetic or thermodynamic parameters.  $K_{FQ}$ , the fluorescence quenching,  $K_{ic}$ , constant competitive,  $K_{iu}$ , uncompetitive inhibition constant,  $IC_{50}$ , half inhibitory concentration value,  $T_d$ , denaturation temperature,  $\Delta H$ , denaturation enthalpy,  $K_{itc}$ , the binding constant,  $E_b$ , total binding energy,  $\lambda_{em}$ , maximum emission wavelength. Adapted from (Sun, Warren, & Gidley, 2019).

Among all types of polyphenols, berry and tea polyphenols were widely studied by many researchers due to their wide use for food consumption. Regarding  $\alpha$ -amylase, the inhibitory effect of berry anthocyanins (investigated in [Chapter 2](#)) and tea polyphenols (investigated in [Chapter 3](#)) including half inhibitory concentration value ( $IC_{50}$ ), competitive ( $K_{ic}$ ) constant, uncompetitive inhibition constant ( $K_{iu}$ ), and inhibitory type were summarized in [Table 1.1](#). Anthocyanins are the main polyphenols in berries. All four anthocyanins inhibited  $\alpha$ -amylase competitively. Catechins and theaflavins are the main polyphenols in tea. Tea polyphenols such as epigallocatechin gallate and theaflavin-3, 3'-digallate inhibited  $\alpha$ -amylase

competitively, whereas epicatechin gallate, theaflavin-3'-gallate, and theaflavin inhibited  $\alpha$ -amylase competitively and un-competitively.

Table 1.1. The inhibitory effect of berry anthocyanins and tea polyphenols on  $\alpha$ -amylase, including half inhibitory concentration value ( $IC_{50}$ ), competitive ( $K_{ic}$ ) constant, uncompetitive inhibition constant ( $K_{iu}$ ), and inhibitory type

Polyphenols	$IC_{50}$ (mg/mL)	$K_{ic}$ (mM)	$K_{iu}$ (mM)	Inhibition type
Cyanidin-3-glucoside	0.024	0.014	NA	Competitive
Cyanidin-3,5-glucoside	0.040	0.020	NA	Competitive
Cyanidin-3-rutinoside	0.031	0.019	NA	Competitive
Peonidin-3-glucoside	0.075	0.045	NA	Competitive
Epigallocatechin gallate	5.489	104.13	NA	Competitive
Epicatechin gallate	3.911	84.831	100.83	Mixed
Theaflavin-3, 3'-digallate	0.149	1.322	NA	Competitive
Theaflavin-3'-gallate	0.341	5.942	27.828	Mixed
Theaflavin	0.730	15.452	55.594	Mixed

Adapted from (Lijun Sun, Warren, Netzel, & Gidley, 2016)(Sui, Zhang, & Zhou, 2016)

Besides  $\alpha$ -amylase,  $\alpha$ -glucosidase can be inhibited by tea polyphenols as well. Mammalian  $\alpha$ -glucosidase is composed of two complexes, i.e., maltase-glucoamylase (MGAM) and sucrase-isomaltase (SI). Each complex consists of two unites, N-terminal subunit (Ct) and Nt (N-terminal subunit). All four subunits have high maltase activities ( $\alpha$ -1,4) (Shin et al., 2019). But each subunit has different  $\alpha$ -glycosidic catalytic properties related to their independent active sites (Matsui et al., 2007). For instance, Ct-SI and Nt-SI subunits display distinctive sucrase and isomaltase activities, respectively (Simsek, Quezada-Calvillo, Ferruzzi, Nichols, & Hamaker, 2015). Ct-MAGAM and Nt-MGAM subunits display distinctive glucoamylase and maltase activities, respectively. The inhibition of polyphenols on  $\alpha$ -glucosidase should be measured based on different active sites, since  $\alpha$ -glucosidase shows different activities on various substrates. One study reported that catechin, chlorogenic acid, and epigallocatechin gallate inhibit  $\alpha$ -glucosidase selectively (Simsek et al., 2015). Among all the  $\alpha$ -glycosidic activities, inhibitory effects on maltase and sucrase are mostly reported. A summary of inhibitory effects on maltase and sucrase by tea polyphenols (investigated in Chapters 3&6) were summarized in Table 1.2.

Table 1.2 The inhibitory effects of tea polyphenols on maltase and sucrase

Inhibitor	maltase IC <sub>50</sub> (μM)	sucrase IC <sub>50</sub> (μM)
epicatechin	770	1080
epicatechin-gallate	53	172
epigallocatechin	1260	921
epigallocatechin-gallate	40	169
theaflavin	500	>10000
theaflavin-3-O-gallate	10	1024
theaflavin-3'O-gallate	136	573
theaflavin-3,3'-digallate	58	159
Green tea extract (mg/mL)	0.035	1.8

The results are expressed as half inhibitory concentration values (IC<sub>50</sub>). Adapted from (Matsui et al., 2007; Pyner et al., 2017).

#### 1.4.2 Starch-polyphenols interactions inhibit starch digestibility

Besides inhibition on digestive enzymes, starch-polyphenols interaction has been reported as another crucial mechanisms to slow down starch digestibility. Phenolics can be either encapsulated within the inner hydrophobic helix of starch to form V-type inclusion complexes, or interacted with starch to form non-inclusion types of complexes (Zhu, 2015). Similar to amylose-lipid inclusion complexes, the V-type phenolics-starch complexes could be characterized by X-ray diffraction (XRD) with characteristic diffraction peaks at about 7°, 13°, and 20°. For instance, rice starch-gallic acid complexes, the corn starch-soy isoflavone complexes, and the amylose-proanthocyanin complexes have been reported as inclusion complexes by a distinct and prominent peak at about 7°, 13°, and 20° (Amoako & Awika, 2016; Liu, Chen, Xu, Liang, & Zheng, 2019). The DSC can be also used to identify inclusion types of complexes. Amylose-proanthocyanin inclusion complex was found by a melting peak at around 120 °C (Amoako & Awika, 2019). The non-inclusion interaction between starch and phenolic compounds is through hydrogen bonds without the formation of the V-type inclusion complex, which cannot be detected by characteristic peaks in XRD. Instead of direct evidence, some indirect evidence has been reported for confirming the non-inclusion complexes, *i.e.*, the pasting, swelling, and gelatinization properties of starch are affected in presence of phenolics (Guo, Zhao, Chen, Chen, & Zheng, 2019). Whatever the complexes formed are of inclusion or non-inclusion nature, complexation with polyphenols reduces the

starch digestibility. In Table 1.3 a summary of all inclusion and non-inclusion types of starch-phenolics complexes which can significantly slow down starch digestion is reported.

Table 1.3 Inclusion and non-inclusion types of complexes formed between various starch and phenolics.

Polyphenols	Starch	Complex type	Reference
Gallic acid	Maize starch	Non-inclusion complex	(Chi et al., 2017)
Dodecyl gallate	Rice starch	Inclusion complex	(Chi et al., 2018)
Caffeic acid, gallic acid and ferulic acid	Maize amylopectin and potato starch	Not sure.	(Li, Ndiaye, Corbin, Foegeding, & Ferruzzi, 2020);(Li, Pernell, & Ferruzzi, 2018)
Proanthocyanidins	Amylose	Inclusion complex	(Amoako & Awika, 2019)
Tea polyphenols	Lotus seed starch	Non-inclusion complex	(Guo et al., 2019)
Gallic acid	Rice starch	Inclusion complex	(Liu et al., 2019)
Green tea polyphenols	Lotus seed starch	Inclusion complex	(Zhao et al., 2019)
Caffeic acid	Normal maize starch, waxy maize starch, and high-amylose maize starch	Inclusion complex	(Han, Bao, Wu, & Ouyang, 2020)
Soy isoflavone	Corn starch	Inclusion complex	(C. Wang, Chen, & Liu, 2020)
Caffeic acid	Maize starch	Non-inclusion complex	(Zheng et al., 2020)

Adapted from (Deng et al., 2021).

### 1.4.3 Inhibition on transporters

After starch digestion, the final product glucose is absorbed by glucose transporters, such as glucose transporter 1 (SGLT1), glucose transporter 2 (GLUT2), etc. Glucose transport occurs in the enterocyte in the small intestine. Some studies reported that polyphenols show direct effects on glucose transporters SGLT1 and GLUT2 (Kobayashi et al., 2000). Therefore, effects on glucose transporters could be also a promising way to modulate glycemic response. The dietary polyphenols affect glucose transport either by inhibiting glucose transport into intestinal cells from the intestine lumen or by stimulating glucose transport into other functional tissue cells from blood. Both ways can help reduce postprandial blood glucose level (Lijun Sun & Miao, 2020).

### 1.5 Research objective and outline of this thesis

The inhibitory effect of polyphenols on  $\alpha$ -amylase and  $\alpha$ -glucoamylase has been reported for decades. Studies using various polyphenols and polyphenol-rich extracts have tried to describe the inhibitory efficiency and the possible mechanisms as affected by phenolic structure, amount of phenolics, source of enzymes, etc. Most studies used simple model systems (*i.e.*, just containing enzymes, polyphenols, and a simple substrate like p-nitrophenyl-

$\alpha$ -D-glucopyranoside (*pNPG*) or starch), but this inhibition has been rarely studied in a real food matrix, where compositional and structural properties can modulate such effect. For this reason, the role of the food matrix on the efficacy of polyphenol's inhibition on starch digestion remains to be elucidated. The overall aim of this thesis is to acquire knowledge about the inhibition of polyphenols on starch digestibility influenced by multiple interactions among  $\alpha$ -amylase,  $\alpha$ -glucosidase, polyphenols, starch, and components in the food matrix. The overall outline of this thesis is shown in Figure 1.5.

In Chapter 2, I selected bread as a source of starch and berry extract as a source of polyphenols. The INFOGEST *in vitro* digestion protocol was used to monitor the starch digestibility of bread. We investigated the inhibition of starch digestibility during *in vitro* digestion of white bread (1) fortified with raspberry or blueberry extracts and (2) co-digested with the same raspberry or blueberry extracts. The kinetics of starch digestion and polyphenols bio-accessibility were measured and compared in the two sets of samples. Finally, the influence of the food matrix on the efficacy of inhibition of berry polyphenols was discussed.

In Chapter 3, I investigated the inhibitory effect of tea polyphenols on starch digestibility influenced by polyphenol type and the presence of gluten. Conventional wheat bread and gluten-free bread were prepared as a starchy model. Green tea and black tea extracts were chosen as sources of polyphenols. Polymeric polyphenols were also prepared from black tea extract. Then co-digestion of wheat bread / gluten-free bread and tea extract were performed. The kinetics of starch digestion and polyphenols bio-accessibility were measured. The different behavior of monomeric polyphenols (catechins) and polymeric polyphenols (tannins) was discussed.

In Chapters 4 & 5, I studied the starch-polyphenols interactions from different aspects. In Chapter 4, I investigated the effect of tannic acid on the physicochemical properties and starch digestibility of wheat starch. In Chapter 5, we further investigated the effect of tannic acid on physicochemical properties and starch digestibility of corn starch (A-type), maize amylopectin (A-type, waxy), and potato starch (B-type). Different starches were chosen to investigate how the starch types and amylopectin content influence the starch-tannins interaction. Although the interaction of a variety of polyphenols and starch has been widely reported, insufficient evidence was provided on the interacting mechanisms, for instance, by forming inclusion and non-inclusion complexes and corresponding forming conditions. In this study, I further investigated the effect of the addition of tannic acid (TA), a relatively less

studied polyphenol, on starch physicochemical properties and digestibility. TA was added to starch in two ways, i.e., by complexing or mixing with starch. Starch-tannins complexes were prepared by mixing and incubating native starch and tannins solutions and then removing the unbound tannic acid. Starch-tannins mixtures were prepared by simply mixing native starch and tannins just before starch characterization. The influence of tannins on gelatinization and pasting properties of starch was measured by differential scanning calorimeter and Rapid Visco Analyser, respectively. Steady and dynamic rheological properties were measured as well. Finally, *in vitro* digestion models were used to measure starch digestibility.

In Chapter 6, I investigated the inhibitory effect of tea polyphenols on  $\alpha$ -glucosidase. Rat intestinal enzymes and Caco-2 cells in Transwells were used to provide  $\alpha$ -glucosidase. Four tea extracts from white tea, green tea, oolong tea, and black tea were prepared as sources of tea polyphenols. Besides, some tea polyphenols like epigallocatechin gallate, epicatechin gallate, theaflavins, theaflavin-3-gallate, and theaflavin-3'-gallate were also selected for the inhibitory experiments. Four substrates have been used to determine individual hydrolytic properties, i.e., maltose, maltodextrin, sucrose, and isomaltose. Inhibitory kinetics and synergistic experiments were performed to further analyze the underlying mechanisms. The different sensitivity of tea polyphenols for  $\alpha$ -glucosidase inhibition was discussed.

In Chapter 7, we summarized the main findings of all the chapters presented in this thesis. We overviewed the possible mechanisms for the inhibition of polyphenols on starch digestibility. Furthermore, the scientific challenges and future recommendations for further research are also presented.

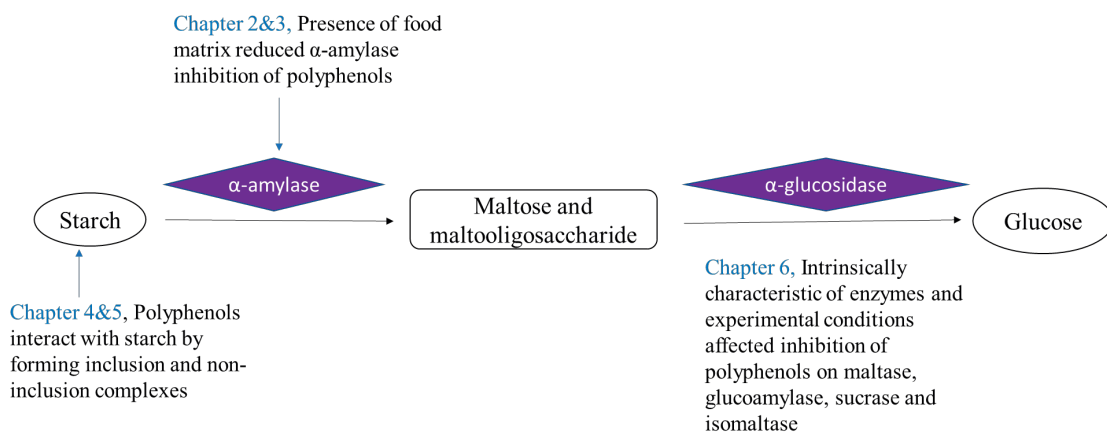


**Figure 1.5.** Graphical outline of the chapters contained in this thesis.



## References

- Amoako, D. B., & Awika, J. M. (2016). Polymeric tannins significantly alter properties and *in vitro* digestibility of partially gelatinized intact starch granule. *Food Chemistry*.  
<https://doi.org/10.1016/j.foodchem.2016.03.096>
- Amoako, D. B., & Awika, J. M. (2019). Resistant starch formation through intrahelical V-complexes between polymeric proanthocyanidins and amylose. *Food Chemistry*.  
<https://doi.org/10.1016/j.foodchem.2019.01.173>
- Asp, N. G., & Björck, I. (1992). Resistant starch. *Trends in Food Science and Technology*.  
[https://doi.org/10.1016/0924-2244\(92\)90153-N](https://doi.org/10.1016/0924-2244(92)90153-N)
- Bravo, L. (1998). Polyphenols: Chemistry, dietary sources, metabolism, and nutritional significance. *Nutrition Reviews*. <https://doi.org/10.1111/j.1753-4887.1998.tb01670.x>
- Cao, H., Ou, J., Chen, L., Zhang, Y., Szkudelski, T., Delmas, D., Daglia, M., & Xiao, J. (2019). Dietary polyphenols and type 2 diabetes: Human Study and Clinical Trial. *Critical Reviews in Food Science and Nutrition*.  
<https://doi.org/10.1080/10408398.2018.1492900>
- Chi, C., Li, X., Feng, T., Zeng, X., Chen, L., & Li, L. (2018). Improvement in Nutritional Attributes of Rice Starch with Dodecyl Gallate Complexation: A Molecular Dynamic Simulation and in Vitro Study. *Journal of Agricultural and Food Chemistry*.  
<https://doi.org/10.1021/acs.jafc.8b02121>
- Chi, C., Li, X., Zhang, Y., Chen, L., Li, L., & Wang, Z. (2017). Digestibility and supramolecular structural changes of maize starch by non-covalent interactions with gallic acid. *Food and Function*. <https://doi.org/10.1039/c6fo01468b>
- Cura, A. J., & Carruthers, A. (2012). Role of monosaccharide transport proteins in carbohydrate assimilation, distribution, metabolism, and homeostasis. *Comprehensive Physiology*. <https://doi.org/10.1002/cphy.c110024>
- Deng, N., Deng, Z., Tang, C., Liu, C., Luo, S., Chen, T., & Hu, X. (2021). Formation, structure and properties of the starch-polyphenol inclusion complex: A review. *Trends in Food Science and Technology*. <https://doi.org/10.1016/j.tifs.2021.04.032>
- Donald, A. M. (2004). Understanding starch structure and functionality. In *Starch in Food: Structure, Function and Applications*. <https://doi.org/10.1016/B978-1-85573-731->

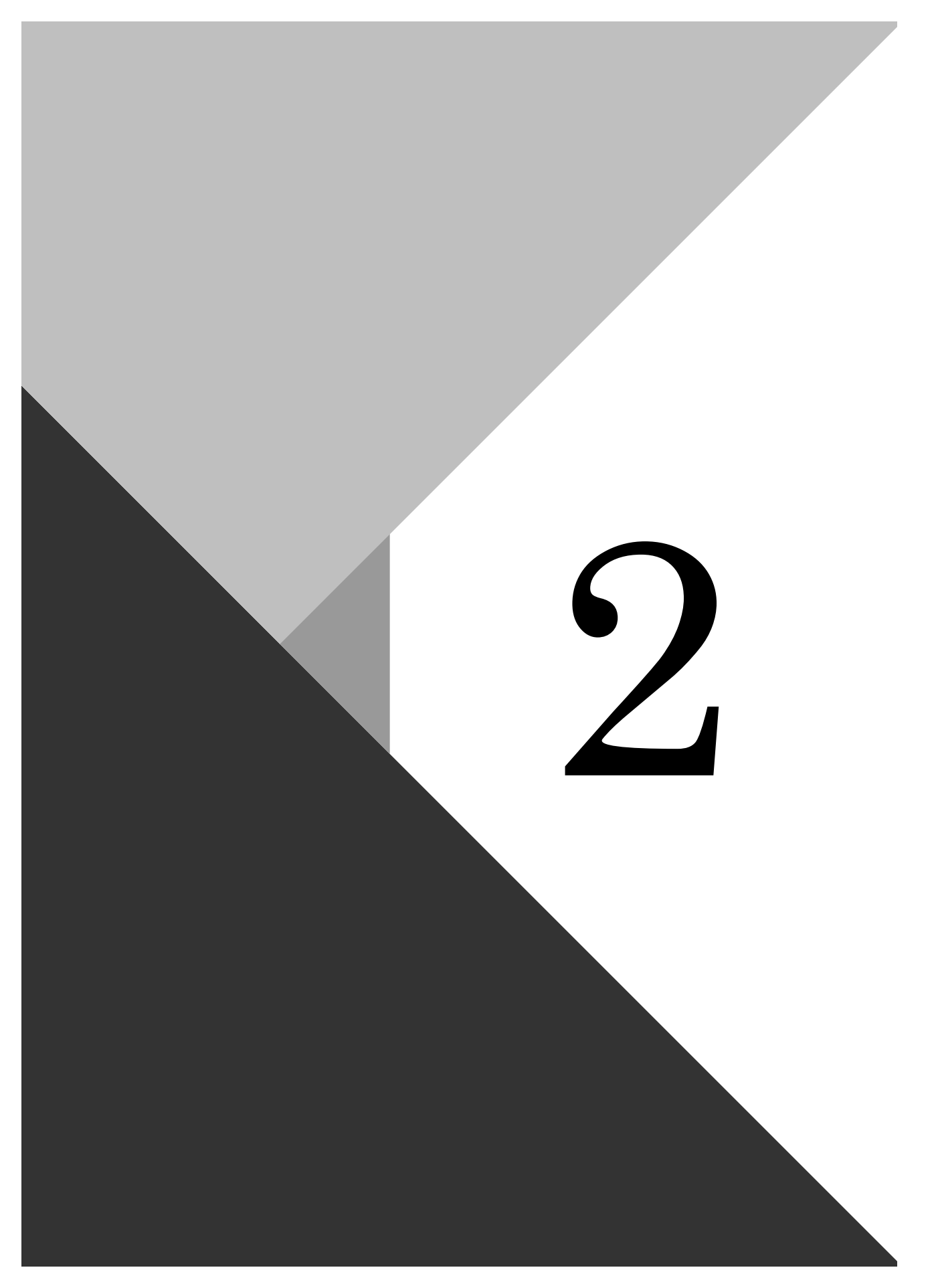
0.50009-8

- Galanakis, C. M. (2018). *Polyphenols: Properties, recovery, and applications. Polyphenols: Properties, Recovery, and Applications*. <https://doi.org/10.1016/C2016-0-05057-X>
- Guo, Z., Zhao, B., Chen, J., Chen, L., & Zheng, B. (2019). Insight into the characterization and digestion of lotus seed starch-tea polyphenol complexes prepared under high hydrostatic pressure. *Food Chemistry*. <https://doi.org/10.1016/j.foodchem.2019.124992>
- Han, M., Bao, W., Wu, Y., & Ouyang, J. (2020). Insights into the effects of caffeic acid and amylose on in vitro digestibility of maize starch-caffeic acid complex. *International Journal of Biological Macromolecules*. <https://doi.org/10.1016/j.ijbiomac.2020.06.200>
- Hou, C., Zhao, X., Tian, M., Zhou, Y., Yang, R., Gu, Z., & Wang, P. (2020). Impact of water extractable arabinoxylan with different molecular weight on the gelatinization and retrogradation behavior of wheat starch. *Food Chemistry*. <https://doi.org/10.1016/j.foodchem.2020.126477>
- Ishikawa, K., & Hirata, H. (1989). New substrate specificity of modified porcine pancreatic  $\alpha$ -amylase. *Archives of Biochemistry and Biophysics*. [https://doi.org/10.1016/0003-9861\(89\)90229-4](https://doi.org/10.1016/0003-9861(89)90229-4)
- Kobayashi, Y., Suzuki, M., Satsu, H., Arai, S., Hara, Y., Suzuki, K., Miyamoto, Y., & Shimizu, M. (2000). Green tea polyphenols inhibit the sodium-dependent glucose transporter of intestinal epithelial cells by a competitive mechanism. *Journal of Agricultural and Food Chemistry*. <https://doi.org/10.1021/jf0006832>
- Li, M., Ndiaye, C., Corbin, S., Foegeding, E. A., & Ferruzzi, M. G. (2020). Starch-phenolic complexes are built on physical CH- $\pi$  interactions and can persist after hydrothermal treatments altering hydrodynamic radius and digestibility of model starch-based foods. *Food Chemistry*. <https://doi.org/10.1016/j.foodchem.2019.125577>
- Li, M., Pernell, C., & Ferruzzi, M. G. (2018). Complexation with phenolic acids affect rheological properties and digestibility of potato starch and maize amylopectin. *Food Hydrocolloids*. <https://doi.org/10.1016/j.foodhyd.2017.11.028>
- Liu, Y., Chen, L., Xu, H., Liang, Y., & Zheng, B. (2019). Understanding the digestibility of rice starch-gallic acid complexes formed by high pressure homogenization. *International Journal of Biological Macromolecules*. <https://doi.org/10.1016/j.ijbiomac.2019.05.083>

- Magallanes-Cruz, P. A., Flores-Silva, P. C., & Bello-Perez, L. A. (2017). Starch Structure Influences Its Digestibility: A Review. *Journal of Food Science*.  
<https://doi.org/10.1111/1750-3841.13809>
- Matignon, A., & Tecante, A. (2017). Starch retrogradation: From starch components to cereal products. *Food Hydrocolloids*. <https://doi.org/10.1016/j.foodhyd.2016.10.032>
- Matsui, T., Tanaka, T., Tamura, S., Toshima, A., Tamaya, K., Miyata, Y., Tanaka, K., & Matsumoto, K. (2007).  $\alpha$ -glucosidase inhibitory profile of catechins and theaflavins. *Journal of Agricultural and Food Chemistry*. <https://doi.org/10.1021/jf0627672>
- Pyner, A., Nyambe-Silavwe, H., & Williamson, G. (2017). Inhibition of human and rat sucrase and maltase activities to assess antiglycemic potential: Optimization of the assay using acarbose and polyphenols. *Journal of Agricultural and Food Chemistry*, 65(39), 8643–8651. <https://doi.org/10.1021/acs.jafc.7b03678>
- Richardson, P. H., Jeffcoat, R., & Shi, Y. C. (2000). High-amylose starches: from biosynthesis to their use as food ingredients. *MRS Bulletin*.  
<https://doi.org/10.1557/mrs2000.249>
- Roalino-Córdova, A. M., Fogliano, V., & Capuano, E. (2019). The effect of cell wall encapsulation on macronutrients digestion: A case study in kidney beans. *Food Chemistry*. <https://doi.org/10.1016/j.foodchem.2019.02.057>
- Shin, H., Seo, D. H., Seo, J., Lamothe, L. M., Yoo, S. H., & Lee, B. H. (2019). Optimization of in vitro carbohydrate digestion by mammalian mucosal  $\alpha$ -glucosidases and its applications to hydrolyze the various sources of starches. *Food Hydrocolloids*.  
<https://doi.org/10.1016/j.foodhyd.2018.08.033>
- Simsek, M., Quezada-Calvillo, R., Ferruzzi, M. G., Nichols, B. L., & Hamaker, B. R. (2015). Dietary Phenolic Compounds Selectively Inhibit the Individual Subunits of Maltase-Glucoamylase and Sucrase-Isomaltase with the Potential of Modulating Glucose Release. *Journal of Agricultural and Food Chemistry*. <https://doi.org/10.1021/jf505425d>
- Squires, B. T. (1953). Human salivary amylase secretion in relation to diet. *The Journal of Physiology*. <https://doi.org/10.1113/jphysiol.1953.sp004835>
- Sui, X., Zhang, Y., & Zhou, W. (2016). In vitro and in silico studies of the inhibition activity of anthocyanins against porcine pancreatic  $\alpha$ -amylase. *Journal of Functional Foods*.

- <https://doi.org/10.1016/j.jff.2015.11.042>
- Sun, L., Warren, F. J., & Gidley, M. J. (2019). Natural products for glycaemic control: Polyphenols as inhibitors of alpha-amylase. *Trends in Food Science and Technology*. <https://doi.org/10.1016/j.tifs.2019.07.009>
- Sun, Lijun, Gidley, M. J., & Warren, F. J. (2017). The mechanism of interactions between tea polyphenols and porcine pancreatic alpha-amylase: Analysis by inhibition kinetics, fluorescence quenching, differential scanning calorimetry and isothermal titration calorimetry. *Molecular Nutrition and Food Research*, 61(10), 1–13. <https://doi.org/10.1002/mnfr.201700324>
- Sun, Lijun, Gidley, M. J., & Warren, F. J. (2018). Tea polyphenols enhance binding of porcine pancreatic  $\alpha$ -amylase with starch granules but reduce catalytic activity. *Food Chemistry*. <https://doi.org/10.1016/j.foodchem.2018.03.017>
- Sun, Lijun, & Miao, M. (2020). Dietary polyphenols modulate starch digestion and glycaemic level: a review. *Critical Reviews in Food Science and Nutrition*. <https://doi.org/10.1080/10408398.2018.1544883>
- Sun, Lijun, Warren, F. J., Netzel, G., & Gidley, M. J. (2016). 3 or 3'-Galloyl substitution plays an important role in association of catechins and theaflavins with porcine pancreatic  $\alpha$ -amylase: The kinetics of inhibition of  $\alpha$ -amylase by tea polyphenols. *Journal of Functional Foods*. <https://doi.org/10.1016/j.jff.2016.07.012>
- Van Beers, E. H., Büller, H. A., Grand, R. J., Einerhand, A. W. C., & Dekker, J. (1995). Intestinal brush border glycohydrolases: Structure, function, and development. *Critical Reviews in Biochemistry and Molecular Biology*. <https://doi.org/10.3109/10409239509085143>
- Waigh, T. A., Gidley, M. J., Komanshek, B. U., & Donald, A. M. (2000). The phase transformations in starch during gelatinisation: A liquid crystalline approach. *Carbohydrate Research*. [https://doi.org/10.1016/S0008-6215\(00\)00098-7](https://doi.org/10.1016/S0008-6215(00)00098-7)
- Wang, C., Chen, X., & Liu, S. (2020). Encapsulation of tangeretin into debranched-starch inclusion complexes: Structure, properties and stability. *Food Hydrocolloids*. <https://doi.org/10.1016/j.foodhyd.2019.105409>
- Wang, S., Wang, J., Yu, J., & Wang, S. (2014). A comparative study of annealing of waxy,

- normal and high-amylose maize starches: The role of amylose molecules. *Food Chemistry*. <https://doi.org/10.1016/j.foodchem.2014.05.055>
- Wang, T. L., Bogracheva, T. Y., & Hedley, C. L. (1998). Starch: As simple as A, B, C? *Journal of Experimental Botany*. <https://doi.org/10.1093/jxb/49.320.481>
- Waterschoot, J., Gomand, S. V., Fierens, E., & Delcour, J. A. (2015). Production, structure, physicochemical and functional properties of maize, cassava, wheat, potato and rice starches. *Starch/Staerke*. <https://doi.org/10.1002/star.201300238>
- Xiao, H., Lin, Q., Liu, G. Q., Wu, Y., Tian, W., Wu, W., & Fu, X. (2011). Effect of green tea polyphenols on the gelatinization and retrogradation of rice starches with different amylose contents. *Journal of Medicinal Plants Research*.
- Xing, L., Zhang, H., Qi, R., Tsao, R., & Mine, Y. (2019). Recent Advances in the Understanding of the Health Benefits and Molecular Mechanisms Associated with Green Tea Polyphenols. *Journal of Agricultural and Food Chemistry*. <https://doi.org/10.1021/acs.jafc.8b06146>
- Zhao, B., Sun, S., Lin, H., Chen, L., Qin, S., Wu, W., Zheng, B., & Guo, Z. (2019). Physicochemical properties and digestion of the lotus seed starch-green tea polyphenol complex under ultrasound-microwave synergistic interaction. *Ultrasonics Sonochemistry*. <https://doi.org/10.1016/j.ultsonch.2018.11.001>
- Zheng, Y., Tian, J., Kong, X., Yang, W., Yin, X., Xu, E., Chen, S., Liu, D., & Ye, X. (2020). Physicochemical and digestibility characterisation of maize starch–caffeic acid complexes. *LWT*. <https://doi.org/10.1016/j.lwt.2019.108857>
- Zhu, F. (2015). Interactions between starch and phenolic compound. *Trends in Food Science & Technology*, 43(2), 129–143. <https://doi.org/10.1016/J.TIFS.2015.02.003>

The background features a diagonal split. The upper-left portion is a light gray triangle, and the lower-right portion is a dark gray triangle. The remaining area is white. A large, black, serif-style number '2' is positioned in the white area, slightly to the right of the center.

2

# Chapter 2

Interaction of bread and berry polyphenols affects starch digestibility  
and polyphenols bio-accessibility

This chapter has been published as:

Kan, L., Oliviero, T., Verkerk, R., Fogliano, V., & Capuano, E. (2020). Interaction of bread and berry polyphenols affects starch digestibility and polyphenols bio-accessibility. *Journal of Functional Foods*, 68, 103924.

### **Abstract**

In this study, the effect of berry polyphenols on starch digestion was tested *in vitro* both by co-digestion of berry extract with bread or by fortifying bread with berry extract. Results show that the co-digestion of bread with berry extracts significantly reduce the rate and extent of starch digestion. Sixty one percent of starch digestion is inhibited by co-digesting 1 g of raspberry extract with 4 g of the bread. The inhibition obtained by co-digesting berry extracts and bread is much higher than the inhibition obtained by digesting berry-fortified bread. Interactions of polyphenols with matrix reduce polyphenols bio-accessibility, thus reducing the amount of polyphenols available for  $\alpha$ -amylase inhibition. The interaction of polyphenols and starch seems also a crucial mechanism for the inhibition of starch digestion. This study shows that the co-ingestion of berry polyphenols with bread is a promising strategy to reduce glycaemic index of starchy food.

**Key words:** bread, berry polyphenols, starch digestibility, *in vitro* digestion, polyphenol bio-accessibility



## 2.1 Introduction

Energy-dense, nutrient-poor diets containing high amounts of carbohydrates combined with sedentary lifestyles are the major drivers of the global obesity epidemic with high prevalence of type-2 diabetes (Medina-Remón, Kirwan, Lamuela-Raventós, & Estruch, 2018). Dietary carbohydrates, mainly occurring as starch in the human diet, can be hydrolysed by enzymes present in the upper gastrointestinal tract and absorbed as monosaccharides. Therefore, reducing the rate of starch digestion through a dietary intervention is a promising strategy for a better glycaemia control and this can be achieved by inhibiting the enzymes responsible for starch digestion ( $\alpha$ -amylase and/or  $\alpha$ -glucosidase) (Lim, Kim, Shin, Hamaker, & Lee, 2019; Takahama & Hirota, 2018).

Polyphenols have been shown to inhibit  $\alpha$ -amylase and/or  $\alpha$ -glucosidase, thus modulating the glycaemic response to carbohydrates (Barrett, Farhadi, & Smith, 2018; Di Stefano, Oliviero, & Udenigwe, 2018; Figueiredo-González et al., 2018; Silva, Sampaio, Freitas, & Torres, 2018). The mechanism of the inhibition depends on the type and concentration of polyphenols. Monomeric polyphenols can inactivate the two primary digestive enzymes by blocking the catalytic sites (Yilmazer-Musa, Griffith, Michels, Schneider, & Frei, 2012). Polymeric polyphenols can precipitate with the digestive enzymes to form a non-digestible complex (Barrett et al., 2018). If the concentration of the polyphenols is high enough, they can also interact with food nutrients (like protein and starch) to form a polyphenol-coated particle or even large complexes (Amoako & Awika, 2016). All these mechanisms can slow digestion of carbohydrates and reduce the rate of glucose uptake in the blood stream. Therefore, the use of polyphenols as a more natural substitute for anti-diabetic drugs such as acarbose was proposed for effective glycaemic control (Boath, Stewart, & McDougall, 2012; Lin, Teo, Leong, & Zhou, 2019).

Among the various polyphenols-rich food blueberry and raspberry are becoming popular in human diet, not only because of their appealing taste, but also for their health benefits (Garcia et al., 2017; Louis et al., 2014). Polyphenol-rich extracts from a range of berries containing anthocyanins and proanthocyanidins can inhibit  $\alpha$ -amylase and  $\alpha$ -glucosidase *in vitro* (Grussu, Stewart, & McDougall, 2011). *In vitro* studies and *silico* molecular docking studies confirmed the inhibitory effect of anthocyanins (like cyanidin-3- glucoside, cyanidin-3,5-glucoside, cyanidin-3-rutinoside, and peonidin-3-glucoside) on pancreatic  $\alpha$ -amylase (Sui, Zhang, & Zhou, 2016). Proanthocyanidins also showed inhibitory effect on  $\alpha$ -amylase (Mullen et al., 2002).

The inhibition of polyphenols on  $\alpha$ -amylase and  $\alpha$ -glucosidase has been often investigated in simple model systems but rarely in a real food matrix (Grussu et al., 2011; McDougall et al., 2005; Yuan et al., 2018). The influence on starch digestive enzymes of the actual availability of the polyphenols under digestive-physiological conditions, as well as the influence of the interactions between polyphenols and food components during digestion are still unknown.

To investigate how the food matrix influences the role of polyphenols on starch digestibility, the berry extracts was either co-digested with bread or used to fortify a bread by mixing it to the dough. The co-digestion of the control bread plus different concentrations of berry polyphenols extracts was performed to simulate a meal in which bread is consumed along with berries; while by preparing a berry-fortified bread the effect of baking and bread matrix was investigated. In this paper, we aim at investigating the inhibition of starch degradation during *in vitro* digestion of white bread 1) fortified with raspberry or blueberry extracts and 2) co-digested with the same raspberry or blueberry extracts. The kinetics of starch digestion and polyphenols bio-accessibility were measured and compared in the two sets of samples.

## 2.2. Methodology

### 2.2.1 Materials

Blueberry, raspberry, wheat flour (carbohydrate 73%, fat 1.6%, gluten 11%) and dry yeast were purchased from a local supermarket.

Cyanidin-3-glucoside, procyanidin B-2, pepsin (800–2500 units/mg), pancreatin (P1750; 4X USP specifications), amyloglucosidase (129 U/mg), ferric ammonium sulphate, butanol, bovine serum albumin (BSA), sodium dodecyl sulphate (SDS), triethanolamine (TEA) were purchased from Sigma–Aldrich (St Louis, MO, USA). Acetonitrile, methanol and absolute ethanol were HPLC grade. All other chemicals were of analytical grade.

### 2.2.2. Polyphenol extract preparation

The preparation of crude polyphenol extracts was carried out according to a previously published method with a slight modification (Kan, Nie, Hu, Liu, & Xie, 2016). The fresh blueberry and raspberry were dried firstly in a freeze dryer (Alpha 2-4 LDplus, Christ). Then, 200 g of dry powder of the fruits were extracted three times with 2 L of methanol. The extraction was carried out through an ultrasound equipment (Sonication, China) for 30 min.

Ice was added to the ultrasound equipment to keep the temperature at 0 °C. After each extraction, extracts were centrifuged at 4000 g for 15 min. The supernatants were combined and concentrated on a rotary evaporator to remove the methanol. Finally, the extracts were freeze-dried. The berries polyphenol extract powder was stored at -20 °C. For the preparation of the heated extracts, 5 g of berry extract was placed in a boiling water bath for 45 min to simulate the baking process. Finally, the heated berry extract was tested for the  $\alpha$ -amylase inhibition assay and *in vitro* digestion assay (see sections 2.4 and 2.6).

### 2.2.3 Polyphenol composition

#### 2.2.3.1 Anthocyanins

Anthocyanin analysis was performed on a HPLC system equipped with a diode array detector based on a previous method with some modification (Kan et al., 2017). The separation was carried out on a Varian Polaris 5 C18-A (4.6 x 150 mm) column. The mobile phase consisted of water (10% of formic acid, eluent A) and methanol (eluent B). The flow rate was 1 mL/min. A multi-step programme was as follows: 5–60% B (20 min), 60–100% B (5 min), 100% B (5 min), 100–5%B (1 min). The run time was 31 min. The injection volume was 10  $\mu$ L. The monitoring was performed at 520 nm. The total anthocyanin content was expressed as mg/g berry extract (cyanidin-3-glucoside equivalents).

#### 2.2.3.2 Proanthocyanidins / Condensed tannins

The acid butanol method was used for condensed tannins quantification (Han et al., 2015). Briefly, 0.5 mL of suitable diluted extract was mixed with 3 mL of butanol-acid reagent (95:5, v/v) and 0.1 mL of ferric reagent (2% ferric ammonium sulphate in 2M HCl). Then, the mixture was boiled for 30 min. After cooling, the absorbance at 550 nm was measured on a spectrophotometer (Agilent Cary 60 UV.VIS). Procyanidin B-2 was used to make a calibration curve. The results were expressed as mg of procyanidin B-2 equivalents per gram of berry extract.

#### 2.2.3.3 Protein precipitation capacity

BSA precipitation assay was used for measuring the protein precipitation capacity of berry tannins (Kyrleou et al., 2015). Briefly, 0.5 mL of dissolved extract was added to 1 mL of buffer 1 (200 mM acetic acid; 170 mM NaCl; pH=4.9, containing BSA (1 mg/mL). Then the mixture was shaken slightly for 15 min. After the shaking, the samples were centrifuged to

pellet the protein-tannin precipitate. The supernatant was discarded. The protein-tannin pellet was dissolved in a buffer containing 5% TEA (v/v) and 5% SDS (w/v). The dissolved tannins solution was mixed with 125  $\mu$ L of ferric chloride reagent (10 mM  $\text{FeCl}_3$  in 10 mM HCl). The mixture was incubated at room temperature for 10 min, and the reading at 510 nm was observed. Catechin was used as a standard, and the results expressed as mg catechin equivalents per gram of berry extract.

#### 2.2.4 $\alpha$ -amylase inhibition assay

The inhibition of  $\alpha$ -amylase was performed according to a previous method (Zhang et al., 2010). Briefly, 1% starch solution was prepared by dissolving 1 g starch in 100 mL of 0.1 M phosphate buffer (pH 6.9 containing 6.7 mM sodium chloride). Porcine pancreatin ( $\alpha$ -amylase activity is 40 U/mg) was dissolved in the same buffer to give a final concentration of 20 mg/mL. Different concentrations of berry extract was dissolved in methanol. Then, 400  $\mu$ L of methanol or berry extract solution or gastric supernatant (see section 2.7) was mixed with 200  $\mu$ L of starch and incubated at 25  $^{\circ}\text{C}$  for 10 min, and finally 200  $\mu$ L of pancreatin was added to start the reaction. The final concentration of the berry extracts in the mixture was 5, 10, 20, 30, 40 and 50 mg/mL. The final concentration of the gastric supernatant in the mixture was the actual concentration for  $\alpha$ -amylase inhibition during *in vitro* digestion. The  $\alpha$ -amylase activity of the final mixture is 200 U/ mL. After 3 min at 25  $^{\circ}\text{C}$ , 400  $\mu$ L of 96 mM dinitrosalicylic acid reagent was added and the mixture was put in boiling water bath for 5 min. After cooling down, 4 mL of water was added before measured at 540 nm on a microplate reader. The  $\alpha$ -amylase inhibition was calculated according to the following equation:

$$\text{Inhibition (\%)} = (1 - (A_{\text{sample}} - A_{\text{blank}}) / (A_{\text{test}} - A_{\text{control}})) \times 100 \quad (1)$$

where  $A_{\text{sample}}$  is the absorbance of the mixture of phenolic samples, starch, enzyme and DNS reagent;  $A_{\text{blank}}$  is the absorbance of the mixture of phenolic samples, starch and DNS reagent without enzyme;  $A_{\text{test}}$  is the absorbance of the mixture of buffer (instead of phenolic sample), starch, enzyme and DNS reagent;  $A_{\text{control}}$  is the absorbance of the mixture of buffer, starch and DNS reagent without enzyme.

Finally, the  $\alpha$ -amylase inhibitory effect of the berry extract was expressed as  $\text{IC}_{50}$ , which was defined as the concentration of extract required to inhibit 50% of the enzyme activity, and

expressed as milligram berry extract per millilitre solvent (mg/mL). The  $\alpha$ -amylase inhibitory effect of the gastric supernatant was calculated according to equation (1).

### 2.2.5 Preparation of berry polyphenol-fortified bread

Baked bread fortified with 0% (control), 2.5% and 5% berry polyphenol extract were prepared using a bread-baking machine. The content of berry extract is based on fresh bread. The bread recipe was shown in Table 2.1. The ingredients of baked bread included wheat flour, water and yeast (Goh et al., 2015). All the ingredients were put in the bread-baking machine (Philips, HD 9020) and the bread was made using a standard program (Table 2.1).

**Table 1** The recipe of berry polyphenol-fortified bread

Ingredients	Control	1%	2.5%	5%
Water /mL	220	220	220	220
Wheat flour /g	350	345	337	324
Berry extract /g	0	5	13	26
Yeast /g	7	7	7	7
Fresh weight /g	516	516	516	516

Standard program of white bread: baking time is 45 min and baking temperature is 120 °C.

### 2.2.6 *In vitro* digestion study

#### 2.2.6.1 *In vitro* digestion model

A standard protocol was used for the *in vitro* digestion study (Minekus et al., 2014) which was modified for the amount of  $\alpha$ -amylase and the absent of the salivary amylase. The fresh bread samples were sieved through a 2 mm sieve. Five grams of sieved bread is mixed with 4 mL of simulated salivary fluid, 25  $\mu$ L of 0.3 M  $\text{CaCl}_2$  and 975  $\mu$ L of water. The mixture was mixed thoroughly. Then two digestion phases (gastric and intestinal phase) were performed. For the gastric phase, 10 mL of the mixed sample were combined with 7.5 mL of simulated gastric fluids and 1.6 mL of pepsin (5.86 mg/mL, 4268 U/mg). The pH was adjusted to 3 by 1M HCl. All the samples were put in the shaking water-bath (37 °C) for 2 hours. For the intestinal phase, the samples from gastric digestion were combined with simulated intestinal fluids and pancreatin (40 mg/mL;  $\alpha$ -amylase activity of the pancreatin is 40 U/mg.) to give an  $\alpha$ -amylase activity of 200 U/mL in the final solution and the pH was adjusted to 7. All the samples were put in the shaking water-bath (37 °C) for 2 hours. Individual sample tubes were prepared for each digestion time point of intestinal phase. Totally 8 time points (0, 10, 20, 40,

60, 80, 100 and 120 min) was chosen for the intestinal phase. Then all the samples from each time point was centrifuged immediately at 4 °C (4000 g, 10 min). Finally 1 mL of the supernatant was mixed with 4 mL of ethanol to stop the reaction and this mixture was used for further analysis of glucose.

To understand the matrix effect of bread on the efficacy of berry polyphenol, a co-digestion study was carried out, aiming to simulate a meal in which bread is consumed along with berry. Then 0, 0.125, 0.25, 0.5 and 1 grams of berry extract were mixed with 5, 4.875, 4.75, 4.5 and 4 g of bread and marked as 0% (control), 2.5%, 5%, 10% and 20% of berry extracts co-digestion.

#### 2.2.6.2 Determination of the percentage of the digested starch

For the glucose measurement, amyloglucosidase was added to complete starch digestion (Rovalino-Córdova, Fogliano, & Capuano, 2018): one millilitre of supernatant was combined with 5 mL of amyloglucosidase solution (27.16 U/mL) in acetate buffer (0.1M, pH 4.8) and incubated at 37°C for 1 hour. The tubes were boiled for 5 min to inactivate the enzyme activity. The samples were centrifuged at 4000 g for 15 min. The supernatant was collected for glucose measurement.

Preliminary experiments have indicated that colorimetric enzymatic methods for glucose measurements are poorly accurate when coloured extracts are used or when the presence of polyphenols may inhibit the enzymes used in the assay. HPLC-ELSD was used to quantify the glucose from starch digestion (Ma, Sun, Chen, Zhang, & Zhu, 2014). The separation was carried out on a Grace prevail carbohydrate ES (5 µm, 250 × 4.6 mm) column. The mobile phase consisted of water (eluent A) and acetonitrile (eluent B). The flow rate was 0.6 mL/min. The programme was 75% B for 25 min. The injection volume was 20 µL. For the ELSD settings, evaporating and nebulizer temperature were 90°C and 50°C, and the carrier gas flow was 1.6 slm (standard litre per minute). The released glucose from bread was quantified based on the peak area from HPLC (The digested starch = released glucose / 0.9). The initial amount of total starch in bread was measured by Total Starch Assay kit (amyloglucosidase / $\alpha$ -amylase method), Megazyme Inc. (Bray, Ireland). The results were expressed as the percentage of digested starch (% of digested starch = digested starch / initial amount of starch).

The digested starch data for this study were fitted to a first order model (equation 2) as previously proposed (Goñi, Garcia-Alonso, & Saura-Calixto, 1997):

$$C_t - C_0 = C_\infty(1 - e^{-kt}) \quad (2)$$

Where  $C_t$ ,  $C_0$  and  $C_\infty$  are the percentage of digested starch at time  $t$ , time 0 and at infinite time, respectively, and  $k$  is a pseudo-first order rate constant. Solver from Excel was used for estimating  $k$  and  $C_\infty$  values by minimizing the residual sum of square values. In this study, the change of the two parameters ( $k$  and  $C_\infty$ ) caused by polyphenols will be discussed.

In this study, the initial reaction rate was calculated by equation (3).

$$\text{Initial reaction rate} = (C_{10} - C_0)/10 \quad (3)$$

Where  $C_{10}$  and  $C_0$  are the percentage of digested starch at time 10 and 0 (min), respectively, and 10 is the time that was chosen for the calculation of initial reaction rate.

The inhibition of the berry polyphenols on starch digestion could be calculated by equation (4):

$$\text{Inhibition (\%)} = ((C_{t(\text{control})} - C_{t(\text{sample})})/C_{t(\text{control})}) \times 100 \quad (4)$$

Where  $C_{t(\text{control})}$  is the percentage of digested starch of control bread at time  $t$ , and  $C_{t(\text{sample})}$  is the percentage of digested starch of berry-fortified or co-digested bread at time  $t$ .

### 2.2.7 Bio-accessibility of polyphenols

During the *in vitro* digestion process, the digested samples at the end of gastric (time point, 0 min) and intestinal phase (time point, 120 min) were collected and centrifuged for 10 min at 4000 g. The both supernatants were collected for measuring anthocyanins and proanthocyanidins directly as described in 2.3. The supernatant from gastric phase was also used for measuring the  $\alpha$ -amylase inhibition as described in 2.4. Then the bio-accessibility of polyphenols was expressed as percentage of polyphenols available in the supernatant compared to the initial amount of polyphenols in the crude extract.

### 2.2.8 The interaction between polyphenols, digestive enzymes and bread matrix

To investigate the interactions between polyphenols, digestive enzymes and bread matrix in co-digestion samples, 250 mg of berry extract were mixed with gastric and intestinal digestive fluids as a control. Then the digestive enzymes (pepsin and pancreatin) or 5 g of bread were added separately. All the mixtures were allowed to stand at room temperature for 2 min. Then

the mixture was centrifuged for 15 min at 4000 g. The supernatant was collected and the percentage of polyphenols in supernatant was determined as described in 2.3. The results were expressed as the percentage of polyphenols distributed in supernatant compared to the initial content in berry extracts.

To study the interaction preference between berry polyphenols and bread components (starch and gluten) in co-digestion samples, starch and gluten were mixed with berry extract separately. Briefly, starch or gluten were added to some water. The mixture was boiled for 5 min and then cooled down to room temperature to allow for starch gelatinization. Then 2.5 g of starch or 0.4 g of gluten (the corresponding amount in 5 g of bread) were mixed with 250 mg of berry extract separately. Then gastric and intestinal fluids were added. The mixture was allowed to stand at room temperature for 2 min. Quantification of polyphenols in the supernatant was carried out as described in 2.3.

To explain the interaction of polyphenols and food matrix in fortified bread, 5 g of 5% berry-fortified bread was mixed with gastric and intestinal digestive fluids. The mixtures were allowed to stand at room temperature for 2 min. Then the mixture was centrifuged for 15 min at 4000 g. The supernatant was collected and the percentage of polyphenols in supernatant was determined as described in 2.3. The results were expressed as the percentage of polyphenols distributed in supernatant compared to the amount of polyphenols in berry-fortified bread. Moreover, 5% berry-fortified dough (before baking) was also prepared to ascertain the influence of baking on polyphenol stability. Then the dough was mixed with gastric and intestinal fluids and the following steps was the same as fortified bread.

#### 2.2.9 Statistical analysis

All experiments were performed in triplicate. The results were expressed as mean  $\pm$  standard deviation (SD). One-way analysis of variance (ANOVA) followed by the Duncan's multiple range test was used to compare the means among different groups by the SAS 9.4 (SAS Institute Inc., Cary, NC, USA). Differences were considered significant at  $P < 0.05$ .



## 2.3. Results

### 2.3.1 $\alpha$ -amylase inhibition and protein precipitation capacity of berry extracts

Table 2.2 shows the polyphenol composition of berry extracts. Anthocyanins (10.0 mg/g) and proanthocyanidins (44.5 mg/g) are detected in blueberry extract. Whereas in raspberry extract, less anthocyanins (4.4 mg/g) and proanthocyanidins (13.5 mg/g) were detected. Raspberry showed some protein precipitation capacity of 9.6 mg/g. No precipitation capacity was detected in blueberry extract. Blueberry and raspberry extract also contained 70.2% and 66.9% of sugars respectively (data not shown). After heating at 100 °C, almost half of the anthocyanins and proanthocyanidins were degraded for both berry extracts. There was no significant change of protein precipitation capacity after heating.

The inhibition of berry extracts on  $\alpha$ -amylase is also shown in Table 2.2. The blueberry extract had a smaller IC<sub>50</sub> value (17.3 mg/mL) than raspberry extract (25.5 mg/mL). The heating also had some influence on the inhibitory effect of both berry extracts. Although half of the anthocyanins and proanthocyanidins were degraded, the direct inhibition on  $\alpha$ -amylase was increased (Table 2.2).

**Table 2.2** The amount of polyphenols in the berry extract or heated berry extract and their IC<sub>50</sub> values for  $\alpha$ -amylase inhibition

Extract	Anthocyanin <sup>a</sup>	Condensed tannins <sup>b</sup>	PPC <sup>c</sup>	IC <sub>50</sub> <sup>d</sup>
BPE	10.0 ± 0.0 a	44.5 ± 1.5 a	nd	17.3 ± 0.4 c
RPE	4.4 ± 0.1 b	13.5 ± 1.0 b	9.6 ± 0.5 a	25.5 ± 0.3 a
Heated BPE	5.5 ± 0.1 c	26.7 ± 0.9 c	nd	15.8 ± 0.5d
Heated RPE	2.1 ± 0.0 d	7.4 ± 0.6 d	9.5 ± 0.6 a	22.0 ± 0.3 b

<sup>a</sup>: Results expressed as mg cyanidin-3-glucoside equivalents per gram of extract or heated extract;

<sup>b</sup>: Results expressed as mg procyanidin B-2 equivalents per gram of extract or heated extract.

<sup>c</sup>: PPC, Protein precipitation capacity. The Results expressed as mg catechin equivalents per gram of extract or heated extract.

<sup>d</sup>: Results expressed as IC<sub>50</sub> values which means the concentration of extract (mg/mL) required to inhibit 50% of the  $\alpha$ -amylase activity

BPE: blueberry polyphenol extract; RPE: raspberry polyphenol extract. nd: not detected

Values followed by the different letter in the same column are significantly different ( $p < 0.05$ )

### 2.3.2 Starch digestibility in co-digestion and fortification samples

The starch digestion curves for bread co-digested with different concentrations of berry extracts and for fortified bread are shown in Figure 2.1. A dose-dependent reduction in the rate and extent of starch digestibility was observed for both extracts that were co-digested with bread. The starch digestion curves are fit to a fractional conversion model (Dona, Pages, Gilbert, & Kuchel, 2010) and the estimated parameters are shown in Table 2.3. In our study the  $C_{\infty}$  value of control white bread was 86.9%. A significant decrease in  $C_{\infty}$  values of 4.9%, 14.7%, 38.2% and 56.5% was observed when the white bread was co-digested with different levels of blueberry extracts and an even larger decrease of 12.9%, 23.7%, 51.1% and 61.2% is found with raspberry extracts. Higher inhibition was found in both heated berry extracts that were co-digested with control bread compared with non-heated extract (16.7% vs 14.7% for blueberry and 28.2% vs 23.7% for raspberry). The initial rate also decreased significantly when co-digested with berry extract. The starch was digested at a similar rate ( $k$  value) as control bread when co-digested at low concentration of polyphenols (2.5%). When co-digested with higher polyphenols concentration (above 5%), the  $k$  value slightly increased.

The results about the fortified bread revealed that the inhibitory effect of polyphenols on starch digestion in berry-fortified bread was lower compared with the co-digestion. Regarding the raspberry bread, the 2.5% and 5% of raspberry extracts fortification led to a significantly inhibitory effect that was confirmed by the decrease of the  $C_{\infty}$  values from 86.9% (control bread) to 80.8% (2.5% fortification) and 74.0% (5% fortification) (Table 2.3). Regarding the blueberry bread, it can be noticed that the addition of extract did not produce any significant effect on starch digestion (Figure 2.1). The  $C_{\infty}$  values from the kinetics model confirmed this trend (Table 2.3).

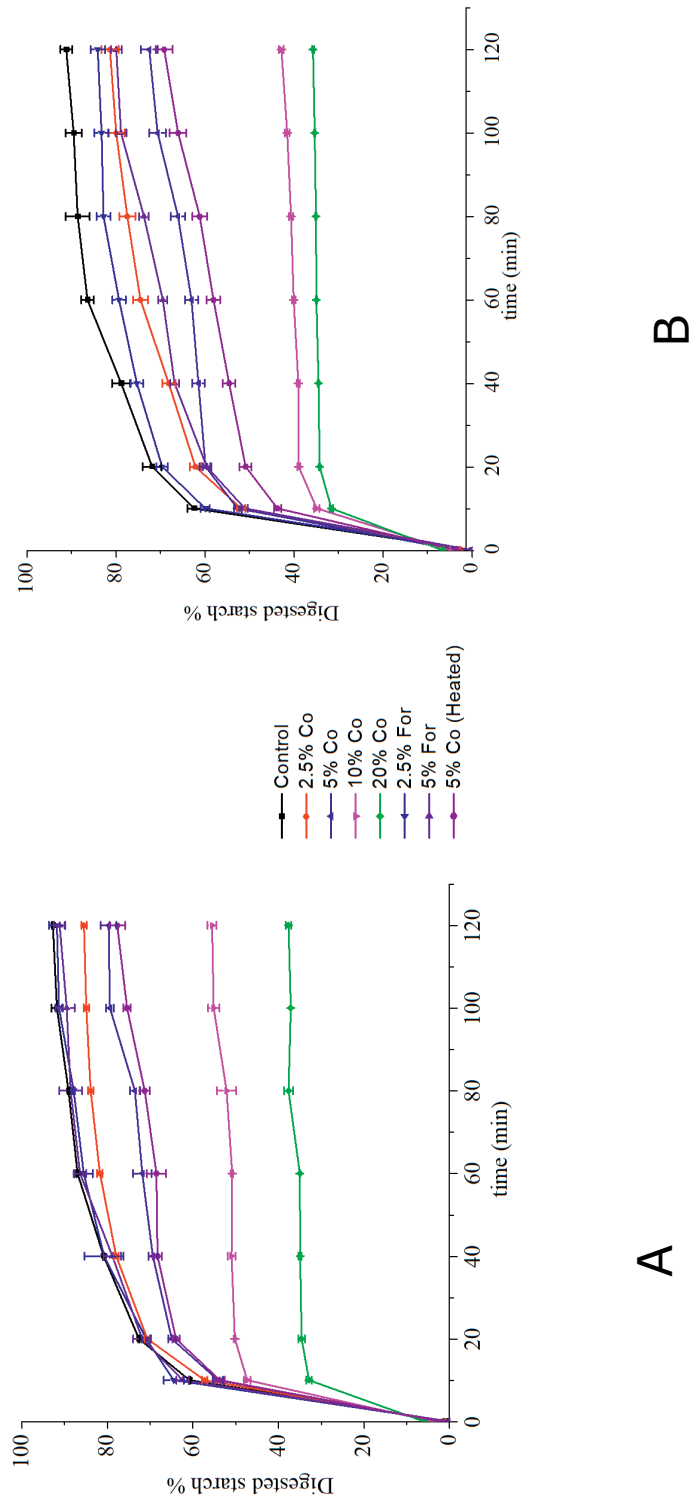


**Figure 2.1:** *In vitro* starch hydrolysis profiles of control bread co-digested or fortified with different concentrations of blueberry polyphenol extract (A) and raspberry polyphenol extract (B). Co: Co-digestion. For: Fortification.

**Table 2.3.** Estimated kinetic parameters for starch digestion obtained from *in vitro* digestion of wheat bread co-digested or fortified with different levels of berry extracts

	Co-digestion						Fortification		
	Control	2.5% Co BPE	5% Co BPE	5% Co heated	10% Co BPE	20% Co BPE	2.5% Fortification	5% Fortification	
blueberry									
$k$ ( $\text{min}^{-1}$ )	0.11 $\pm$ 0.00 cd	0.11 $\pm$ 0.00 cd	0.15 $\pm$ 0.01 b	0.12 $\pm$ 0.01 c	0.21 $\pm$ 0.00 a	0.21 $\pm$ 0.03 a	0.11 $\pm$ 0.00 cd	0.11 $\pm$ 0.00 d	
$C_{\infty}$ (%)	86.9 $\pm$ 1.2 a	82.0 $\pm$ 0.6 b	72.2 $\pm$ 0.2 c	70.2 $\pm$ 0.2 d	48.7 $\pm$ 0.4 e	30.4 $\pm$ 0.1 f	87.2 $\pm$ 0.8 a	87.6 $\pm$ 0.1 a	
Initial rate (%* $\text{min}^{-1}$ )	5.8 $\pm$ 0.2 ab	5.6 $\pm$ 0.2 b	5.4 $\pm$ 0.1 c	5.0 $\pm$ 0.2 d	4.3 $\pm$ 0.1 e	2.7 $\pm$ 0.1 f	5.9 $\pm$ 0.2 a	5.6 $\pm$ 0.0 bc	
Residual sum of squares	136.2 $\pm$ 5.5	40.3 $\pm$ 0.6	27.9 $\pm$ 1.4	86.0 $\pm$ 46.7	32.2 $\pm$ 4.2	11.4 $\pm$ 1.7	180.2 $\pm$ 25.9	105.5 $\pm$ 9.6	
raspberry									
$k$ ( $\text{min}^{-1}$ )	0.11 $\pm$ 0.00 e	0.09 $\pm$ 0.00 g	0.14 $\pm$ 0.00 c	0.10 $\pm$ 0.00 f	0.18 $\pm$ 0.00 f	0.21 $\pm$ 0.01 b	0.12 $\pm$ 0.00 a	0.10 $\pm$ 0.00 d	
$C_{\infty}$ (%)	86.9 $\pm$ 1.2 a	74.0 $\pm$ 1.8 c	63.2 $\pm$ 1.6 d	58.8 $\pm$ 1.7 e	35.8 $\pm$ 0.4 f	25.7 $\pm$ 2.8 g	80.8 $\pm$ 1.5 b	74.0 $\pm$ 1.0 c	
Initial rate (%* $\text{min}^{-1}$ )	5.8 $\pm$ 0.2 a	4.8 $\pm$ 0.1 b	4.5 $\pm$ 0.1 c	3.7 $\pm$ 0.1 d	3.0 $\pm$ 0.1 e	2.5 $\pm$ 0.0 f	5.7 $\pm$ 0.1 a	4.7 $\pm$ 0.1 b	
Residual sum of squares	136.3 $\pm$ 5.7	110.5 $\pm$ 5.9	99.8 $\pm$ 8.1	143.9 $\pm$ 8.1	8.9 $\pm$ 1.0	1.1 $\pm$ 0.3	72.8 $\pm$ 3.1	99.8 $\pm$ 8.1	

Values expressed as mean  $\pm$  sd. Values followed by the different letter in the same row are significantly different ( $p < 0.05$ ).

### 2.3.3 Polyphenols bio-accessibility and $\alpha$ -amylase inhibition of gastric supernatant

Polyphenols bio-accessibility after gastric phase and intestinal phase are shown in Figure 2.2. For both berry samples, the polyphenols bio-accessibility of co-digestion samples is higher than that of fortification samples. Regarding the blueberry co-digestion samples, almost 50 ~ 60% of anthocyanins was bio-accessible after gastric digestion and no clear increase after intestinal digestion. Less proanthocyanidins was bio-accessible after gastric digestion compared to anthocyanins. Regarding the blueberry fortification samples, less than 30% of anthocyanins and 5% of proanthocyanidins was bio-accessible after gastric digestion. The raspberry polyphenols bio-accessibility showed the similar trend with blueberry polyphenols, but no protein precipitation capacity was detected after gastric digestion or intestinal digestion of all the samples. The  $\alpha$ -amylase inhibition of the bio-accessible polyphenols after gastric phase was also investigated (Table 2.4). No enzyme inhibition was detected in all the fortification samples. Regarding bio-accessible blueberry polyphenols after gastric phase, 5.2%, 37.3% and 65.2% of  $\alpha$ -amylase inhibition was found in the bio-accessible polyphenols from 5%, 10% and 20% co-digestion. But less  $\alpha$ -amylase inhibition was found in bio-accessible raspberry polyphenols from co-digestion experiments.

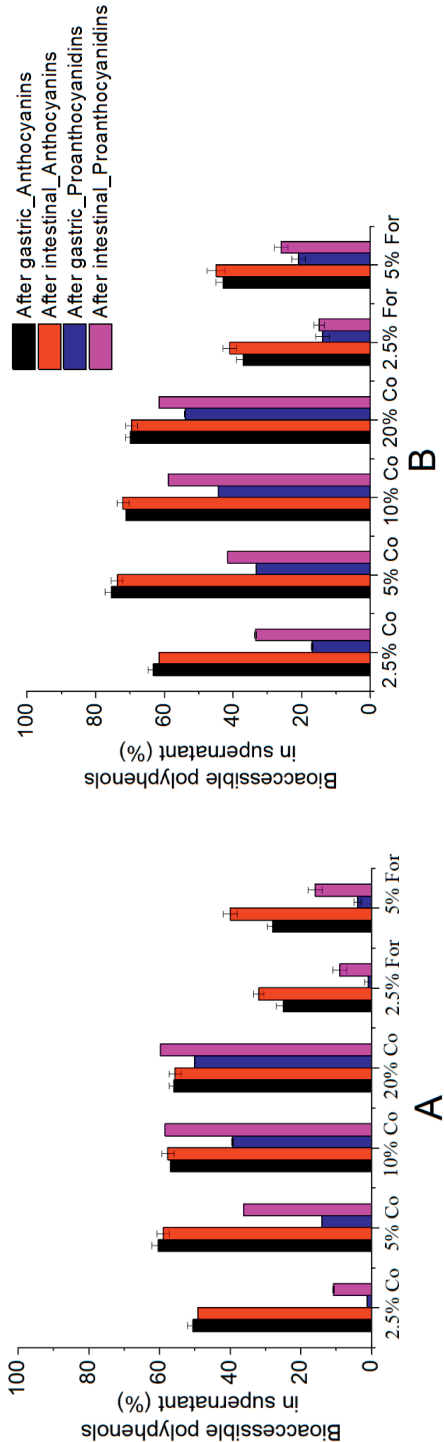


**Figure 2.2.** Bio-accessibility of berry polyphenols after gastric and intestinal digestion. Results expressed as percentage of bio-accessible polyphenols at the end of gastric and intestinal digestion compared to the initial amount of polyphenols in crude extract. A: Blueberry; B: Raspberry; Co: Co-digestion; For: Fortification. No protein precipitation capacity was detected after gastric and intestinal digestion.

**Table 2.4:**  $\alpha$ -amylase inhibition of digested samples after gastric digestion (%)

		Co-digestion				Fortification		
		2.5%	5%	10%	20%	2.5%	5%	
Blueberry	Amylase inhibition	nd	$4.8 \pm 0.2$ c	$33.2 \pm 4.2$ b	$60.6 \pm 4.6$ a	nd	nd	
	Inhibition calculated from $C_{\infty}$	$5.7 \pm 0.7$ d	$16.9 \pm 0.2$ c	$44.0 \pm 0.5$ b	$65.1 \pm 0.1$ a	0	0	
	Inhibition calculated from $C_{10}$	$2.5 \pm 1.7$ d	$6.9 \pm 1.01$ c	$25.9 \pm 1.1$ b	$54.1 \pm 1.5$ a	0	0	
Raspberry	Amylase inhibition	nd	nd	$4.7 \pm 0.4$ b	$33.5 \pm 2.6$ a	nd	nd	
	Inhibition calculated from $C_{\infty}$	$14.8 \pm 2.0$ d	$27.3 \pm 1.9$ c	$58.8 \pm 0.5$ b	$70.4 \pm 3.2$ a	$7.0 \pm 1.8$ c	$14.9 \pm 1.3$ d	
	Inhibition calculated from $C_{10}$	$17.7 \pm 1.1$ d	$22.3 \pm 1.3$ c	$48.7 \pm 1.0$ b	$57.4 \pm 0.0$ a	$1.5 \pm 1.6$ e	$19.5 \pm 0.9$ d	

The results were expressed as the mean  $\pm$  sd; The different letters in the same row mean significant difference

### 2.3.4 Interaction among polyphenols, digestive enzymes and bread matrix

The interaction among polyphenols, digestive enzymes, bread, gluten and starch was measured and shown in Figure 2.3. Regarding the blueberry, 61% of anthocyanins and 52% of the proanthocyanidins were detected in the supernatant after diffusion in the digestive fluids. Less anthocyanins (56%) and proanthocyanidins (50%) were detected when pepsin and pancreatin were added to digestive fluids. The raspberry showed the same trend as blueberry. When both berry extracts were mixed with control bread, much less polyphenols were detected in the supernatant. The interaction of polyphenols with starch and gluten is also shown in Figure 2.3. When both berry extracts were separately mixed with starch and gluten (at the corresponding amount present in the bread), more polyphenols were detected in the supernatant of gluten-polyphenol mixture than starch-polyphenol mixture.

Blueberry-fortified bread and dough were mixed with digestive fluids as well, and few anthocyanins (6.0 and 3.6%) and proanthocyanidins (1.8 and 1.1%) were found in bread and dough, respectively. A similar behaviour was observed in raspberry-fortified bread.

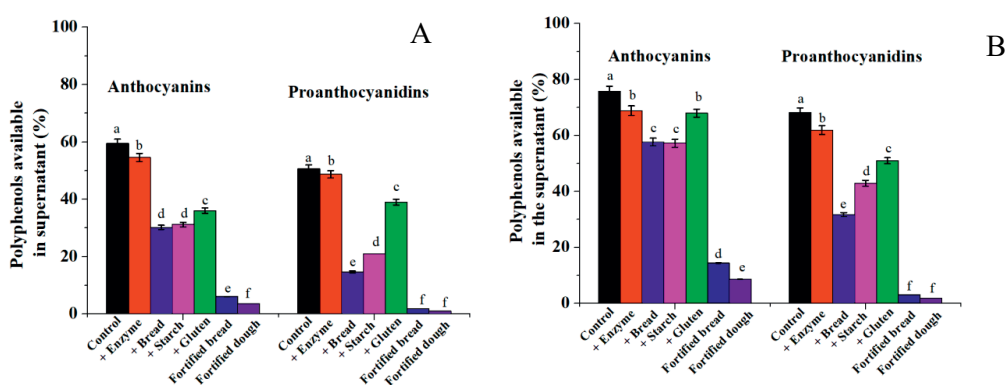


Figure 2.3: Relative percentage of polyphenols in supernatant upon addition of digestive enzymes and bread components (gluten and starch) compared to the initial content in berry extracts. The berry extracts were mixed with digestive fluids as a control. Then the mixture was mixed either with digestive enzyme, or with bread, or with starch, or with gluten (Gluten and starch were added at the corresponding amount as they are present in the bread). In addition, the berry-fortified bread or dough was mixed with digestive fluids and the percentage of polyphenols in supernatant was also measured as well. The different letters mean significant difference. A: blueberry extract, B: raspberry extract. (No protein precipitation capacity was detected in all the samples.)

## 2.4. Discussion

Given the relevance of post-prandial glycaemia on the incidence of chronic diseases, non-communicable strategies to reduce the GI of staple starch-based foods are intensively explored. A promising strategy is the addition of polyphenols which has been reported to reduce the rate of starch digestion. However, the vast majority of the scientific reports have been produced in simple model systems (*i.e.*, just containing enzymes, polyphenols and a simple substrate like p-nitrophenyl- $\alpha$ -D-glucopyranoside (pNPG) or starch), but rarely in a real food matrix (McDougall et al., 2005). We have selected white bread as a model starchy food, berries as sources of polyphenols and used the INFOGEST *in vitro* digestion method to simulate the digestion of bread. The extent of starch digestion we observed was in line with other reports where 87% of starch was hydrolysed in white bread using the same *in vitro* digestion model (Bustos, Vignola, Pérez, & León, 2017). The  $C_{\infty}$  values were markedly reduced when increasing the polyphenol concentration from blueberry and raspberry in the co-digestion and the fortification experiments (Figure 2.1 A & B). However, the rate constant  $k$  became larger when co-digested with higher amount of berry extract, even though the rate of starch digestion during the first minutes was clearly lower as visually judged by the slope of the starch digestion curves during the initial stage of digestion. This counterintuitive finding is rather difficult to explain but might partly be related to the smaller amount of starch available for digestion at very high polyphenols content and thus, to the shorter time needed to reach  $C_{\infty}$ . In such situations, the calculation of the initial rate of digestion would give a more accurate depiction of the digestion kinetics compared to  $k$  (Table 2.3).

Taken together our results suggest that the effect of polyphenols on starch digestion is modulated by the presence of the food matrix and of other digestive enzymes. In particular, when the  $IC_{50}$  values reported in Table 2.2 are compared to the kinetics reported in Table 2.3, it is clear that the behaviour of the berry extracts in the starch digestion of bread cannot be accurately predicted by the  $IC_{50}$  values calculated in the simple model system containing just starch, polyphenols and  $\alpha$ -amylase. For example, in the 20% co-digestion experiment (corresponding to a concentration of raspberry extract in the intestinal digestion of 25 mg/mL) an inhibition of 57.4 % (Table 2.4) was found based on the starch digestion kinetics of the first 10 minutes which is higher than 50% inhibition reported in Table 2.2, and much higher inhibition (70.4%) was found based on the starch kinetics of the infinite time (Table 4). What's more, the order of inhibitory potential of berries that we observed in the experiment with bread (Table 2.3) is the opposite of what observed with the inhibition experiments (Table



2.2). Therefore the IC<sub>50</sub> value cannot accurately predict the inhibition of starch digestibility in food matrix.

When results in Figure 2.1A and B are considered, it is clear that co-digestion of the berry extract with bread is more effective in reducing the rate of starch digestion than incorporating berry extract into the bread matrix. We first hypothesized that this effect may be partially due to the degradation of the phenolic compounds during baking. Indeed, a substantial reduction in the content of extractable polyphenols was observed after baking (Table 2.2). However, heated berry extracts showed better inhibition than non-heated extracts in both the simple inhibition assay (Table 2.2) and in the *in vitro* simulated digestion (Table 2.3 & Figure 2.1). This could mean that the degradation products from anthocyanins or proanthocyanidins can exert an inhibitory effect on  $\alpha$ -amylase at least of the same magnitude as the parent compounds. A recent study has showed that the thermal degradation products from anthocyanins, like chalcone, could inhibit  $\alpha$ -amylase through non-competition inhibition (Zhang et al., 2019).

Interactions with food matrix modulate the amount of polyphenols available to inhibit  $\alpha$ -amylase. To consider how interactions with food matrix influence the role of polyphenols on  $\alpha$ -amylase, we investigated the bio-accessibility of polyphenols in a variety of systems (Figure 2.2 & 2.3). We firstly investigated the bio-accessibility of polyphenols after gastric phase digestion which is an indication of the actual concentration for  $\alpha$ -amylase inhibition. As reported in Figure 2.2, the bio-accessibility of polyphenols in fortification samples was lower than that of co-digestion samples but the loss of phenolics due to the baking step must be considered as well. Since a direct comparison with fortified bread was difficult given this loss, we further compared the bio-accessibility of polyphenols after mixing with bread to the bio-accessibility of polyphenols in a dough matrix. The results in Figure 2.3 shows that the bio-accessibility of polyphenols was higher in the co-digestion experiment compared to the dough. We therefore hypothesize that, regardless the exact type of enzyme inhibition (*i.e.* uncompetitive, non-competitive, *etc.*) (Barrett et al., 2018; Grussu et al., 2011), the intensity of the inhibition on digestive enzymes is proportional to the amount of solubilized polyphenols that can interact with  $\alpha$ -amylase, which represented the bio-accessible fraction, not blocked by other interactions, *e.g.*, with gluten, or starch. This is in line with previous reports discussing the relevance of interactions within the food matrix on the digestive enzyme activities (Capuano, Oliviero, Fogliano, & Pellegrini, 2018; Sun, Gidley, & Warren, 2018).

Although interactions with matrix reduce the amount of polyphenols available for  $\alpha$ -amylase inhibition, the direct interaction with starch could also be a crucial mechanism to inhibit starch digestion. Another possible mechanism of the inhibition of the starch digestion is the absorption of polyphenols on the surface of starch granules, possibly shielding the amylase from its substrates. The accessibility of available binding sites on the starch granules for amylase would be reduced in presence of a large amount of polyphenols. In this case, the inhibitory effect would be proportional to the extent of starch coverage by polyphenols. In fact, the drastic decrease in  $C_{\infty}$  at very high concentration of berry extract (Table 2.3), suggests that the interaction between starch and polyphenols is producing a fraction of starch that is hardly, if ever, digestible *i.e.*, resistant starch. To further confirm to what extent the direct interaction of polyphenols with starch could influence the starch digestion, we investigated the  $\alpha$ -amylase inhibition of the intestinal supernatant after the gastric phase and compared it with the inhibition calculated by the bread digestion experiments ( $C_{10}$  and  $C_{\infty}$ ). Data of Table 2.4 highlights that the inhibition calculated by  $C_{10}$  and  $C_{\infty}$  are higher than the  $\alpha$ -amylase inhibition in most of the cases. Even more importantly, for some of the co-digestion or fortification experiments with 2.5% and 5% extracts, no  $\alpha$ -amylase inhibition was found even if some inhibition was calculated from the  $C_{10}$  and  $C_{\infty}$ . The bio-accessibility of polyphenols at the end of intestinal phase (Figure 2.2) also confirmed that substantial amount of polyphenols stably interacted with food matrix. Therefore,  $\alpha$ -amylase inhibition is not the only way to inhibit starch digestion, interaction with starch is also a crucial mechanism for inhibition of starch digestion.

Whatever mechanism of the inhibition on starch digestion is, the polyphenols bio-accessibility is modulated by the food matrix. To further explore the factors modulating bio-accessibility of polyphenols during digestion of a bread matrix, we showed that this bio-accessible fraction depends on polyphenols solubility and stability and is further reduced by the addition of pancreatic secretions and by the food matrix (Figure 2.3). The addition of digestive enzymes reduces bio-accessibility of polyphenols. This was expected given the protein nature of digestive enzymes but the net effect was rather modest. It must be noted however, this effect depends on the amount of enzymes present in the digestive fluids used *i.e.*, varies depending on the *in vitro* digestion model selected. The effect of adding bread instead was substantial, both for anthocyanins and proanthocyanidins. Further insights were obtained when gluten and starch were separately added to the mixture of digestive fluids and polyphenols. Whereas an interaction of polyphenols with the gluten network was expected,

given the high affinity of polyphenols with proteins, we observed a surprising contribution of starch on polyphenols bio-accessibility. Polyphenols have been already reported to bind directly with starch through hydrophobic forces and hydrogen bonding (Zhu, 2015). Here we show that despite the stronger interactions of polyphenols with proteins, in a starch-rich matrix such as bread, the contribution of starch in binding polyphenols is greater than that of gluten (Figure 2.3). Incidentally, the interaction with digestive enzymes and food matrix will also modify the way polyphenols are delivered to the gut microbiota (bound to starch or proteins versus free) even though the effect these interactions can have on polyphenols utilization by gut microbiota is still unknown.

The bio-accessibility of polyphenols is not the only factors determining the extent of the inhibition on starch digestion, the type of polyphenols being equally important. This is shown by the fact that inhibition is better after addition of raspberry extracts compared to blueberry extracts despite the higher  $IC_{50}$  value of raspberry extract from the results of the simple  $\alpha$ -amylase inhibition assay (Table 2.2). Raspberry is different from other berries for its substantial amount of high molecular weight tannins, *i.e.* ellagitannins. High molecular tannins are reported to show better protein precipitation capacity compared with condensed tannins (McDougall et al., 2005). This was in line with our results that blueberry extract did not show any protein precipitation capacity though it had substantial amount of condensed tannins (Table 2.2). However, we did not detect any protein precipitation capacity after gastric and intestinal phase as shown in Figure 2.2. That means the high molecular weight tannins from raspberry are likely to interact with starch, thus reducing the accessibility of the starch for the  $\alpha$ -amylase as we discussed before. This is also further confirmed by results in Table 2.4, *i.e.*, raspberry bio-accessible polyphenols have lower  $\alpha$ -amylase inhibition compared to blueberry bio-accessible polyphenols, but higher inhibition of starch digestion calculated by  $C_{10}$  and  $C_{\infty}$ . That means some raspberry polyphenols, most likely the high molecular weight tannins, interacted with starch, thus inhibiting the starch digestion. This is in line with the others reports that high molecular weight tannin-starch complexes can block digestibility of starch (Amoako & Awika, 2016).

Our study shows that it is possible to slow down starch digestion in a starchy food like bread providing there is a sufficient amount of polyphenols in the gastrointestinal tract. However, such an amount is hardly achievable through fresh berries. The yield of the extract from fresh berries was around 5%. Based on the extract yield from berries, co-digestion with 2.5% berry extract for 100 grams of bread would require 2.5 g of berry extract, *i.e.* about 50 g

of fresh berries, which is an amount that can be realistically achieved in a meal. However, co-digestion with higher amount of berry extract would require unrealistic amounts of berries. For example, 200 g and 400 g of fresh berries are needed for 100 grams of bread at a level of 10% and 20% of berry extract. On top of that, bio-accessibility of polyphenols from a fruit matrix is limited by the fruit matrix itself which may result in even milder effects compared to berry polyphenols pre-extracted from the fruit matrix (Capuano et al., 2018).

## 2.5. Conclusion

In summary, this study investigated the effects of berry polyphenols on the *in vitro* digestibility of white bread either when they are co-digested or incorporated in bread. A significant reduction was observed in starch digestion kinetics from the co-digestion of bread with berry extract. The fortification of bread with berry extracts was less effective in inhibiting the starch digestion. The effect of polyphenols on starch digestion is modulated by the presence of the food matrix. On one hand, the interactions between polyphenols and the food matrix reduces the bio-accessibility of the polyphenols, thereby reducing the amount of polyphenols available for  $\alpha$ -amylase inhibition. On the other hand, the interaction between starch and polyphenols is also a crucial way to inhibit starch digestion by reducing the accessibility of the starch for  $\alpha$ -amylase. Finally, polyphenols type also influences their way for the inhibition of starch digestion. This study shows that the co-ingestion of berry polyphenols with bread is a promising strategy to reduce glycaemic index, however, the lower bio-accessibility due to the interaction with food matrix must be taken into account.

## Acknowledgement

The authors would like to thank our technicians Geert Meijer and Erik Meulenbroeks for their assistance for the lab work. The author Lijiao Kan received a PhD scholarship from the China Scholarship Council (No. 201706820018).

## Declaration of interests

The authors declare that they have no known competing financial interests.

## References:

- Amoako, D., & Awika, J. M. (2016). Polyphenol interaction with food carbohydrates and consequences on availability of dietary glucose. *Current Opinion in Food Science*, 8, 14–18. <https://doi.org/10.1016/J.COFS.2016.01.010>
- Amoako, D. B., & Awika, J. M. (2016). Polymeric tannins significantly alter properties and in vitro digestibility of partially gelatinized intact starch granule. *Food Chemistry*. <https://doi.org/10.1016/j.foodchem.2016.03.096>
- Barrett, A. H., Farhadi, N. F., & Smith, T. J. (2018). Slowing starch digestion and inhibiting digestive enzyme activity using plant flavanols/tannins— A review of efficacy and mechanisms. *LWT - Food Science and Technology*, 87, 394–399. <https://doi.org/10.1016/J.LWT.2017.09.002>
- Boath, A. S., Stewart, D., & McDougall, G. J. (2012). Berry components inhibit  $\alpha$ -glucosidase in vitro: Synergies between acarbose and polyphenols from black currant and rowanberry. *Food Chemistry*, 135(3), 929–936. <https://doi.org/10.1016/j.foodchem.2012.06.065>
- Capuano, E., Oliviero, T., Fogliano, V., & Pellegrini, N. (2018). Role of the food matrix and digestion on calculation of the actual energy content of food. *Nutrition Reviews*. <https://doi.org/10.1093/NUTRIT/NUX072>
- Di Stefano, E., Oliviero, T., & Udenigwe, C. C. (2018). Functional significance and structure–activity relationship of food-derived  $\alpha$ -glucosidase inhibitors. *Current Opinion in Food Science*. <https://doi.org/10.1016/j.cofs.2018.02.008>
- Dona, A. C., Pages, G., Gilbert, R. G., & Kuchel, P. W. (2010). Digestion of starch: In vivo and in vitro kinetic models used to characterise oligosaccharide or glucose release. *Carbohydrate Polymers*, 80(3), 599–617. <https://doi.org/10.1016/J.CARBPOL.2010.01.002>
- Figueiredo-González, M., Reboredo-Rodríguez, P., González-Barreiro, C., Carrasco-Pancorbo, A., Cancho-Grande, B., & Simal-Gándara, J. (2018). The involvement of phenolic-rich extracts from Galician autochthonous extra-virgin olive oils against the  $\alpha$ -glucosidase and  $\alpha$ -amylase inhibition. *Food Research International*. <https://doi.org/10.1016/j.foodres.2018.08.060>

- Garcia, G., Nanni, S., Figueira, I., Ivanov, I., McDougall, G. J., Stewart, D., Ferreira, R.B., Pinto, P., Silva, R. F., Brites, D., & Santos, C. N. (2017). Bioaccessible (poly)phenol metabolites from raspberry protect neural cells from oxidative stress and attenuate microglia activation. *Food Chemistry*. <https://doi.org/10.1016/j.foodchem.2016.07.128>
- Goh, R., Gao, J., Ananingsih, V. K., Ranawana, V., Henry, C. J., & Zhou, W. (2015). Green tea catechins reduced the glycaemic potential of bread: An in vitro digestibility study. *Food Chemistry*, 180, 203–210. <https://doi.org/10.1016/J.FOODCHEM.2015.02.054>
- Goñi, I., Garcia-Alonso, A., & Saura-Calixto, F. (1997). A starch hydrolysis procedure to estimate glycemic index. *Nutrition Research*. [https://doi.org/10.1016/S0271-5317\(97\)00010-9](https://doi.org/10.1016/S0271-5317(97)00010-9)
- Grussu, D., Stewart, D., & McDougall, G. J. (2011). Berry polyphenols inhibit  $\alpha$ -amylase in vitro: Identifying active components in rowanberry and raspberry. *Journal of Agricultural and Food Chemistry*. <https://doi.org/10.1021/jf1045359>
- Han, K. H., Kitano-Okada, T., Seo, J. M., Kim, S. J., Sasaki, K., Shimada, K. ichiro, & Fukushima, M. (2015). Characterisation of anthocyanins and proanthocyanidins of adzuki bean extracts and their antioxidant activity. *Journal of Functional Foods*, 14, 692–701. <https://doi.org/10.1016/j.jff.2015.02.018>
- Kan, L., Nie, S., Hu, J., Liu, Z., & Xie, M. (2016). Antioxidant activities and anthocyanins composition of seed coats from twenty-six kidney bean cultivars. *Journal of Functional Foods*, 26, 622–631. <https://doi.org/10.1016/j.jff.2016.08.030>
- Kan, L., Nie, S., Hu, J., Wang, S., Cui, S. W., Li, Y., Xu, S., Wu, Y., Wang, J., Bai, Z., & Xie, M. (2017). Nutrients, phytochemicals and antioxidant activities of 26 kidney bean cultivars. *Food and Chemical Toxicology*, 108, 467–477. <https://doi.org/10.1016/j.fct.2016.09.007>
- Kyrleou, M., Kallithraka, S., Koundouras, S., Chira, K., Haroutounian, S., Spinthiropoulou, H., & Kotseridis, Y. (2015). Effect of vine training system on the phenolic composition of red grapes (<em>Vitis vinifera</em> L. cv. Xinomavro). *OENO One*, 49(1), 71. <https://doi.org/10.20870/oeno-one.2015.49.2.92>
- Lim, J., Kim, D. K., Shin, H., Hamaker, B. R., & Lee, B. H. (2019). Different inhibition properties of catechins on the individual subunits of mucosal  $\alpha$ -glucosidases as measured by partially-purified rat intestinal extract. *Food and Function*.

<https://doi.org/10.1039/c9fo00990f>

- Lin, J., Teo, L. M., Leong, L. P., & Zhou, W. (2019). In vitro bioaccessibility and bioavailability of quercetin from the quercetin-fortified bread products with reduced glycemic potential. *Food Chemistry*. <https://doi.org/10.1016/j.foodchem.2019.01.199>
- Louis, X. L., Thandapilly, S. J., Kalt, W., Vinqvist-Tymchuk, M., Aloud, B. M., Raj, P., Yu, L., Le, H., & Netticadan, T. (2014). Blueberry polyphenols prevent cardiomyocyte death by preventing calpain activation and oxidative stress. *Food and Function*. <https://doi.org/10.1039/c3fo60588d>
- Ma, C., Sun, Z., Chen, C., Zhang, L., & Zhu, S. (2014). Simultaneous separation and determination of fructose, sorbitol, glucose and sucrose in fruits by HPLC-ELSD. *Food Chemistry*. <https://doi.org/10.1016/j.foodchem.2013.08.135>
- McDougall, G. J., Shpiro, F., Dobson, P., Smith, P., Blake, A., & Stewart, D. (2005). Different polyphenolic components of soft fruits inhibit  $\alpha$ -amylase and  $\alpha$ -glycosidase. *Journal of Agricultural and Food Chemistry*, 53(7), 2760–2766. <https://doi.org/10.1021/jf0489926>
- Medina-Remón, A., Kirwan, R., Lamuela-Raventós, R. M., & Estruch, R. (2018). Dietary patterns and the risk of obesity, type 2 diabetes mellitus, cardiovascular diseases, asthma, and neurodegenerative diseases. *Critical Reviews in Food Science and Nutrition*, 58(2), 262–296. <https://doi.org/10.1080/10408398.2016.1158690>
- Minekus, M., Alminger, M., Alvito, P., Ballance, S., Bohn, T., Bourlieu, C., Carrière, F., Boutrou, R., Corredig, M., Dupont, D., Dufour, C., Egger, L., Golding, M., Karakaya, S., Kirkhus, B., Feunteun, S. L., Lesmes, U., Macierzanka, A., Mackie, A., Marze, S., McClements, D. J., Mènard, O., Recio, I., Santos, C. N., Singh, R. P., Vegaru, G. E., Wickam, S.J., Weitschies, W., & Brodkorb, A. (2014). A standardised static in vitro digestion method suitable for food-an international consensus. *Food and Function*. <https://doi.org/10.1039/c3fo60702j>
- Mullen, W., McGinn, J., Lean, M. E. J., MacLean, M. R., Gardner, P., Duthie, G. G., Yokota, T., & Crozier, A. (2002). Ellagitannins, Flavonoids, and Other Phenolics in Red Raspberries and Their Contribution to Antioxidant Capacity and Vasorelaxation Properties. *Journal of Agricultural and Food Chemistry*, 50(18), 5191–5196. <https://doi.org/10.1021/jf020140n>


- Roalino-Córdova, A. M., Fogliano, V., & Capuano, E. (2018). A closer look to cell structural barriers affecting starch digestibility in beans. *Carbohydrate Polymers*, 181, 994–1002. <https://doi.org/10.1016/J.CARBPOL.2017.11.050>
- Silva, C. P., Sampaio, G. R., Freitas, R. A. M. S., & Torres, E. A. F. S. (2018). Polyphenols from guaraná after in vitro digestion: Evaluation of bioaccessibility and inhibition of activity of carbohydrate-hydrolyzing enzymes. *Food Chemistry*. <https://doi.org/10.1016/j.foodchem.2017.08.078>
- Sui, X., Zhang, Y., & Zhou, W. (2016). In vitro and in silico studies of the inhibition activity of anthocyanins against porcine pancreatic  $\alpha$ -amylase. *Journal of Functional Foods*, 21, 50–57. <https://doi.org/10.1016/j.jff.2015.11.042>
- Sun, L., Gidley, M. J., & Warren, F. J. (2018). Tea polyphenols enhance binding of porcine pancreatic  $\alpha$ -amylase with starch granules but reduce catalytic activity. *Food Chemistry*. <https://doi.org/10.1016/j.foodchem.2018.03.017>
- Takahama, U., & Hirota, S. (2018). Interactions of flavonoids with  $\alpha$ -amylase and starch slowing down its digestion. *Food & Function*, 9(2), 677–687. <https://doi.org/10.1039/C7FO01539A>
- Yilmazer-Musa, M., Griffith, A. M., Michels, A. J., Schneider, E., & Frei, B. (2012). Grape seed and tea extracts and catechin 3-gallates are potent inhibitors of  $\alpha$ -amylase and  $\alpha$ -glucosidase activity. In *Journal of Agricultural and Food Chemistry*. <https://doi.org/10.1021/jf301147n>
- Yuan, Y., Zhang, J., Fan, J., Clark, J., Shen, P., Li, Y., & Zhang, C. (2018). Microwave assisted extraction of phenolic compounds from four economic brown macroalgae species and evaluation of their antioxidant activities and inhibitory effects on  $\alpha$ -amylase,  $\alpha$ -glucosidase, pancreatic lipase and tyrosinase. *Food Research International*. <https://doi.org/10.1016/j.foodres.2018.07.021>
- Zhang, J., Xiao, J., Giampieri, F., Forbes-Hernandez, T. Y., Gasparrini, M., Afrin, S., Cianciosi, D., Reboledo-Rodriguez, P., Battino, M., & Zheng, X. (2019). Inhibitory effects of anthocyanins on  $\alpha$ -glucosidase activity. *Journal of Berry Research*, 9(1), 109–123. <https://doi.org/10.3233/JBR-180335>
- Zhang, L., Li, J., Hogan, S., Chung, H., Welbaum, G. E., & Zhou, K. (2010). Inhibitory effect of raspberries on starch digestive enzyme and their antioxidant properties and phenolic



composition. *Food Chemistry*, 119(2), 592–599.

<https://doi.org/10.1016/j.foodchem.2009.06.063>

Zhu, F. (2015). Interactions between starch and phenolic compound. *Trends in Food Science and Technology*. <https://doi.org/10.1016/j.tifs.2015.02.003>

The background features a large, light gray triangle in the upper left corner, a dark gray triangle in the lower left corner, and a white triangle in the upper right corner. A smaller, medium gray triangle is positioned between the light and dark gray triangles. The number 3 is centered in the white triangle.

3

# Chapter 3

Tea polyphenols as a strategy to control starch digestion in bread:  
effect of polyphenols type and gluten

This chapter has been published as:

Kan, L., Capuano, E., Fogliano, V., Oliviero, T., & Verkerk, R. (2020). Tea polyphenols as a strategy to control starch digestion in bread: the effects of polyphenol type and gluten. *Food & function*, 11(7), 5933-5943.

**Abstract:**

Inhibition of tea polyphenols on starch digestibility can contribute to control the glycaemic index of starchy food. In this study, wheat bread and gluten-free bread were co-digested *in vitro* with different amount of tea polyphenols. The kinetics of starch digestion and polyphenol bio-accessibility during *in vitro* digestion were monitored. Results showed that co-digestion of bread with tea polyphenols dose-dependently slowed starch digestion kinetics and this effect is influenced by the types of polyphenols and the presence of gluten. The gluten presence lowered the inhibitory efficacy of tannins on starch digestibility of 7.4% and 47.5% when 25 mg of tannins were co-digested with wheat bread and gluten-free bread, respectively. In contrast, the presence of gluten had little impact on the inhibitory efficacy of monomeric polyphenols. This study shows that the release of tea polyphenols in the digestive environment is a promising strategy for controlling glycaemic index of starchy food but that monomeric and polymeric tea polyphenols differently affect starch digestion according to the gluten presence.

**Key works:** tea polyphenols, starch digestibility, gluten, polyphenol bio-accessibility, tannins

### 3.1 Introduction

The number of people affected by type 2 diabetes is growing worldwide (Moradi-Marjaneh, Paseban, & Sahebkar, 2019). Control of postprandial glucose level is critical for diabetic patients. This could be achieved by inhibition of the  $\alpha$ -amylase and  $\alpha$ -glucosidase, the two key digestive enzymes that convert starch to glucose (Forester, Gu, & Lambert, 2012). Some antidiabetic drugs, such as acarbose, miglitol, and voglibose can substantially inhibit  $\alpha$ -amylase and  $\alpha$ -glucosidases, but they often cause side effects (Pyner, Nyambe-Silavwe, & Williamson, 2017). However, studies report that the inhibition of starch digestive enzymes can also be achieved, to certain extent, by compounds present in our diet, such as polyphenols (Sun, Warren, Netzel, & Gidley, 2016).

Among polyphenols, tea polyphenols gained considerable attention because of their health benefits, like anti-inflammation, anti-oxidant as well as management of diabetes (Xing, Zhang, Qi, Tsao, & Mine, 2019). Green tea and black tea are two of the most popular hot beverages in the world. Green tea is a non-fermented tea in which the most abundant polyphenol is epigallocatechin gallate (EGCG) (Forester et al., 2012). Black tea is fermented tea, and its distinctive polyphenols are theaflavins and thearubigins (Pereira-Caro et al., 2017). Theaflavins have benzotropolone structures and therefore give a red colour in a black tea infusion and thearubigins are polymeric polyphenols (Zhang et al., 2018).

Previously, the inhibition of tea polyphenols on digestive enzymes have been characterized by determination of the half inhibition concentration ( $IC_{50}$ ), kinetics of inhibition, fluorescence quenching to further explain the inhibition type and mechanism (Striegel, Kang, Pilkenton, Rychlik, & Apostolidis, 2015). Most studies tested the inhibition in a simple reaction system (simple mixture of digestive enzyme and substrate), ignoring the influence of the interactions among polyphenols, digestive enzymes, starch and other food components on starch digestibility.

In this study, wheat bread and gluten-free bread were chosen as a model starchy food. Green tea and black tea were chosen as sources of polyphenols. Wheat bread and gluten-free bread were co-digested with tea extract to simulate a meal having bread and tea simultaneously. The kinetics of starch digestion and polyphenol bio-accessibility during *in vitro* digestion were monitored. Then, the influence of gluten on the inhibitory efficacy of polyphenols on starch digestibility and bio-accessibility of polyphenols was discussed. To further explain the different behaviour of monomeric polyphenols (catechins) and polymeric

polyphenols (tannins), the polymeric fraction was separated from black tea extract and was investigated for the impact on starch digestibility. Finally, the breakdown of the bread matrix after co-digestion with polymeric fraction was investigated.

## 3.2 Materials and methods

### 3.2.1 Materials

Green tea, black tea, wheat flour (11.4% of moisture, 73% of starch, 11% gluten, 1.6% of fat and 2.2% of fibre), gluten-free flour (AmiFoods, 12.5% of moisture, 86% of wheat starch, 0.21% of protein, 0.02% of fat and 0.05% of fibre), and dry yeast were purchased from the local supermarket.

Polyphenol standards including catechin (C), epicatechin (EC), epigallocatechin (EGC), gallocatechin (GC), catechin gallate (CG), epicatechin gallate (ECG), gallocatechin gallate (GCG), epigallocatechin gallate (EGCG), theaflavins (TF1), theaflavin-3-gallate (TF2A), theaflavins-3'-gallate (TF2B), theaflavins-3,3'-gallate (TF3), pepsin (4268 units/mg), porcine pancreatin (P7545; 4XUSP specifications; amylase activity 40 units/mg), amyloglucosidase (P300 units/mL), porcine  $\alpha$ -amylase (A4268, 1096 units/mg), wheat gluten, bovine serum albumin (BSA), sodium dodecyl sulfate (SDS), triethanolamine (TEA) and ferric chloride were purchased from Sigma-Aldrich (St Louis, MO, USA). Trifluoroacetic acid, acetonitrile, methanol and absolute ethanol were HPLC grade. All other chemicals were of analytical grade.

### 3.2.2 Experimental design

In this study, wheat bread and gluten-free bread were co-digested with different amounts of green tea extract, black tea extract and polymeric fraction from black tea extract. Starch digestibility, bio-accessibility of polyphenols, the interactions of polyphenols and nutrients and the breakdown of bread matrix during digestion were investigated.

### 3.2.3. Tea extract preparation and separation of the polymeric fractions

The extract of tea polyphenols was prepared according to a previous method with some modifications (Lijiao Kan, Oliviero, Verkerk, Fogliano, & Capuano, 2020). Ten grams of green tea and black tea samples was extracted with 100 mL of absolute methanol for 30 min in a ultrasound equipment (Sonication, China) at room temperature. The mixture was centrifuged (4000 g, 15 min) and the residue was re-extracted twice. The supernatants were combined and the tea extract powder was obtained on a freeze dryer (Alpha 2-4 LD plus,

Christ). The green tea extract (GTE) and the black tea extract (BTE) powder were stored at -20 °C until analysed. The yield of GTE and BTE was calculated and it was used for calculation the corresponding amount of tea cups.

The separation of the polymeric fractions from BTE was performed according to a previous method with some modifications (Kyraleou et al., 2015). Briefly, 1 g of BTE was dissolved in 5% of aqueous ethanol (ethanol : water = 5 : 95, v/v). Then 100 mL of ethyl acetate was added to extract the organic fraction. The organic fraction containing monomeric and oligomeric fractions was discarded. The aqueous fraction containing polymeric tannins was collected and concentrated on a rotary evaporator at 40 °C. Finally, the powder of polymeric fractions was obtained by freeze dryer (Alpha 2-4 LD plus, Christ) and stored at -20 °C.

### 3.2.4 Polyphenol characterization

#### 3.2.4.1 HPLC-DAD

HPLC-DAD was used for analysing the catechins composition of tea polyphenol extract according to a previous method with some modifications (Kan et al., 2018). HPLC analysis was conducted on a HPLC system equipped with diode array detector. A Varian Polaris 5 C18-A (4.6 x 150 mm) column was used for separation of tea polyphenols. The UV wavelength was set in the range of 200 – 400 nm. The UV detecting channel was set at 290 nm. The gradient elution was composed of solvent A (water, pH=2.5 adjusted by trifluoroacetic acid) and solvent B (absolute acetonitrile). The flow rate was 1 mL/min. The mobile phase composition started from 100% solvent A to 58% A within 20 min and keep at 58% A for 5 min. Finally bring mobile phase composition back to the initial conditions in 1 min for the next run. All the tea catechins and theaflavins standards are used to make calibrations. The tea polyphenols in the TEs (tea extracts) was expressed as mg/g TE.

#### 3.2.4.2 BSA precipitation

The tannin content of TE (tea extracts) was measured by BSA precipitation method (Zeller et al., 2015). Briefly, 0.5 mL of the sample was mixed with 1.5 mL of acetic acid/NaCl buffer (200 mM acetic acid, 170 mM NaCl, pH=4.9) containing BSA (1 mg/mL). The mixture was incubated at room temperature with slow agitation. After 15 min, the mixture was centrifuged to pellet the protein-tannin precipitation (13000 g, 5 min). The pellet was washed with acetic acid/NaCl buffer and then dissolved in a buffer containing 5% TEA (v/v) and 5% SDS (w/v). For tannin analysis, 875 µL of dissolved sample was mixed with 125 µL of ferric chloride

reagent (10 mm ferric chloride reagent in 10 mm HCl). The mixture was incubated at room temperature for 10 min. The absorbance was measured at 510 nm. Catechin standard was used to make a calibration. The tannin content was expressed as mg catechin equivalents per gram of sample.

### 3.2.5 $\alpha$ -amylase inhibition assay

The inhibition of  $\alpha$ -amylase was performed according to a previous method (Lijiao Kan et al., 2020). Two types of  $\alpha$ -amylase were used in this study: porcine pancreatic  $\alpha$ -amylase and porcine pancreatin. The  $\alpha$ -amylase activity of the two enzymes are 1096 unites/mL and 40 units/mg, respectively. The two enzymes were dissolved in phosphate buffer to give a  $\alpha$ -amylase activity of 400 U/mL. Briefly, 400  $\mu$ L of methanol or TEs solution was mixed with 200  $\mu$ L of starch and incubated at 25 °C for 10 min, and finally 200  $\mu$ L of enzyme was added to start the reaction. The final concentration of the TEs in the reaction solution was 0.025, 0.125, 0.25, 1.25, 2.5, 5, 12.5 and 25 mg/mL. After incubated at 25 °C for 3 min, 400  $\mu$ L of 96 mM dinitrosalicylic acid reagent was added and the mixture was put in boiling water bath for 5 min. After cooling down, 4 mL of water was added before measured at 540 nm on a microplate reader. Finally the  $\alpha$ -amylase inhibitory effect was expressed as IC<sub>50</sub> (mg/mL), which was defined as the concentration of TEs in the reaction solution required to inhibit 50% of the enzyme activity.

### 3.2.6 Bread preparation

Normal wheat bread and gluten-free bread were prepared by mixing 350 g of wheat flour or gluten-free flour, 220 mL of water and 7 g of yeast. No additional ingredients were added. All of the ingredients were added into a baking machine (Philips, HD 9020) and the bread was made using a standard program (baking temperature: 120 °C, baking time: 15 min). All the bread samples were dried using a freeze dryer (Alpha 2-4 LD plus, Christ). Then the dried samples were sieved through 2 sieves (315 and 125  $\mu$ m) to make sure the particle size of the obtained sample is 125~315  $\mu$ m. The sieved bread sample was stored at -20 °C for further analysis.

### 3.2.7 Hydration properties of bread samples

The hydration properties of bread samples was measured according to the previous method (De La Hera, Gomez, & Rosell, 2013). Water holding capacity (WHC) was the amount of



water retained by the bread sample. Briefly, 1 g of dried bread sample was mixed with 10 mL of water and kept at room temperature for 24 h. Then the supernatant was removed gently. WHC was expressed as grams of water retained per grams of bread (g/g). Swelling volume (SV) was calculated by dividing the total swollen volume and the initial weight of the sample. Briefly, 1 g of dried bread sample was placed in a graduated cylinder and mixed with 10 mL of distilled water. After 24 h, the volume of the swollen sample was measured. SV was expressed as volume of the swollen samples per gram of initial sample (mL/g).

### 3.2.8 *In vitro* digestion

#### 3.2.8.1 *In vitro* digestion model

Co-digestion of wheat bread with different amounts of TEs was performed in this study. Firstly 2.5 grams of dried wheat bread was hydrated with 2.5 mL of water. Then 5 g of the mixture was mixed with 0, 50, 125, 250, 500, 1000 mg of TEs and marked as control, 1, 2.5, 5, 10 and 20% co-digestion. Co-digestion of gluten-free bread with 5% of TEs was carried out, *i.e.* 5 g of hydrated gluten-free bread was mixed with 250 mg of TEs. Finally co-digestion of wheat bread and gluten-free bread with 1, 2.5 and 5% of polymeric fraction from BTE was performed, *i.e.*, 5 g of hydrated wheat bread and gluten-free bread was mixed with 50, 125 and 250 mg of polymeric fraction from BTE, respectively.

A standard *in vitro* simulated process was used in this study which was modified for the amount of  $\alpha$ -amylase (Minekus et al., 2014). Briefly, the sample was initially treated with simulated gastric fluids and pepsin. The pH of the mixture was adjusted to 3 and incubated at 37 °C with agitation for 2 h. Then, simulated intestinal fluids and pancreatin were added to the mixture to give a final  $\alpha$ -amylase activity of 200 U/mL and the corresponding trypsin activity is 15 U/mL. Then the pH was adjusted to 7. The mixture was incubated at 37 °C with agitation for 2 h. During the intestinal phase, 0.1 mL of sample was collected at different time points (0, 10, 20, 40, 60, 80, 100, 120 min). Then 0.4 mL of absolute ethanol was added to stop the reaction and the mixture was centrifuged at 13000 g for 10 min. Finally, 2 mL of amyloglucosidase (27.16 U/mL) was added and incubated at 37 °C for an extra hour to complete starch digestion.

### 3.2.8.2 Determination of the percentage of the digested starch

GOPOD kit was used for the glucose measurement. The digested starch = released glucose / 0.9. The initial amount of total starch in bread was measured by Total Starch Assay kit. The results were expressed as the percentage of digested starch (% of digested starch = digested starch / initial amount of starch). A first-order kinetics model was applied to describe the kinetics of glucose release from starch digestion (Dona, Pages, Gilbert, & Kuchel, 2010).

$$C_t - C_0 = C_{\infty}(1 - e^{-kt}) \quad (1)$$

$$\text{Initial rate} = C_{\infty} \times k \quad (2)$$

where  $C_t$ ,  $C_0$  and  $C_{\infty}$  correspond to the percentage of digested starch at time  $t$ , 0 and infinite time, and  $k$  is the kinetic constant. Parameter estimation was performed using the solver of excel software by minimizing the sum of square values.

### 3.2.9 Bio-accessibility of tea polyphenols

The bio-accessibility of tea polyphenols after gastric phase and intestinal digestion was measured according to the previous method with some modifications (Goh et al., 2015). Gastric supernatant and intestinal supernatant was collected at the time points 0 and 120 min, respectively (See 3.2.7). The amount of polyphenols from both supernatants was measured as described in 3.2.3. The bio-accessibility of polyphenols was expressed as the percentage of polyphenols in the supernatant compared to the initial amount in TEs.

### 3.2.10 The interactions between tea polyphenols and bread components.

The interactions among tea polyphenols, digestive enzyme and bread nutrients (gluten and starch) was investigated. Briefly, 250 mg of TEs was mixed with digestive fluids as a control. Then digestive enzymes (pepsin and pancreatin), wheat bread, gelatinized starch and gluten were added separately. All of the chemicals were added the same amount as described in 3.2.7. Gelatinized starch (1.8 g) and gluten (0.3 g) were added considering the amount present in 5 g of hydrated bread. After 2 min, the mixture was centrifuged (4000 g, 15 min), and the amount of polyphenols in supernatant was measured as described in 2.3. The results were expressed as the percentage of polyphenols in the supernatant compared with the initial amount in TEs.

### 3.2.11 Breakdown of wheat bread and gluten-free bread during digestion

Size distribution was analysed according to a previous method (De La Hera et al., 2013). Intestinal digested wheat bread and gluten-free bread when co-digested with different amounts of polymeric fractions from BTE were collected for size distribution analysis. The particle size distribution was analysed using Mastersizer 3000 (Malvern Instruments, Worcestershire UK). D[3, 2] (surface weight mean diameter), D[4, 3] (volume-weight mean diameter) and D (50) (volume median diameter) were obtained.

### 3.2.12 Statistical analysis

All analysis were performed in triplicate. Bread preparation and *in vitro* digestion experiments were repeated twice. The results were expressed as mean  $\pm$  standard deviation (SD). One-way analysis of variance (ANOVA) followed by the Duncan's multiple range test was used to compare the means among different groups by the SAS 9.4 (SAS Institute Inc., Cary, NC, USA). Differences were considered significant at  $P < 0.05$ .

### 3.3. Results

#### 3.3.1 Polyphenol composition and $\alpha$ -amylase inhibition

Table 3.1 shows the polyphenol composition of BTE and GTE. Four flavan-3-ols (EGC, EC, EGCG, ECG) and 3 theaflavins (theaflavin, theaflavin-3-gallate, theaflavin-3'-gallate) were detected in BTE. Totally 410 mg/g of catechins, 43 mg/g of theaflavins and 50 mg/g of tannins were found in BTE. GTE showed a less diverse polyphenol profile. In total, 388 mg/g of flavan-3-ols were quantified, and EGCG was the major catechin in GTE. No theaflavin or tannins were found in GTE.

The inhibitory effect of TEs against  $\alpha$ -amylase was measured as reported in Table 3.1 and Figure S3.1. Both TEs had strong inhibition on  $\alpha$ -amylase, indicated by low  $IC_{50}$  values, *i.e.*, 1.6 and 1.9 mg/mL for GTE and BTE, respectively. Much lower inhibition of both TEs on  $\alpha$ -amylase was observed, indicated by high  $IC_{50}$  values, when pancreatin was used as source of  $\alpha$ -amylase, *i.e.* 16.4 and 26.6 mg/mL for GTE and BTE, respectively.

**Table 3.1.** Polyphenols composition of green tea and black tea extract and polymeric fraction from BTE and their  $IC_{50}$  value of  $\alpha$ -amylase inhibition

Polyphenols		GTE (mg/g)	BTE (mg/g)	Polymeric fraction from BTE (mg/g)
Caffeine		89 $\pm$ 1	72 $\pm$ 2	nd
Epigallocatechin (EGC)		nd	179 $\pm$ 8	nd
Epicatechin (EC)		73 $\pm$ 2	116 $\pm$ 1	nd
Epigallocatechin gallate (EGCG)		276 $\pm$ 3	78 $\pm$ 1	nd
Epicatechin gallate (ECG)		39 $\pm$ 1	37 $\pm$ 0	nd
Theaflavin		nd	16 $\pm$ 0	nd
theaflavin-3-gallate		nd	9 $\pm$ 0	nd
theaflavin-3'-gallate		nd	18 $\pm$ 0	nd
Tannins		nd	50 $\pm$ 1	100 $\pm$ 1
Total amount of monomeric polyphenols		388 $\pm$ 1	453 $\pm$ 9	nd
Total amount of polyphenols		388 $\pm$ 1	503 $\pm$ 10	100 $\pm$ 1
Enzyme		GTE (mg/mL)	BTE (mg/mL)	Polymeric fraction from BTE (mg/mL)
$IC_{50}$	Pancreatin	16.4 $\pm$ 0.0	26.6 $\pm$ 1.6	nd
	$\alpha$ -amylase	1.6 $\pm$ 0.2	1.9 $\pm$ 0.3	2.5 $\pm$ 0.3

Values expressed as mean  $\pm$  standard deviation. BTE, black tea extract; GTE, green tea extract. nd: not detectable.

Total amount of monomeric polyphenols means the sum of all the catechins and theaflavins.

Total amount of polyphenols means the sum of all the catechins, theaflavins and tannins

$IC_{50}$  values mean the concentration of extract (mg/mL) in the final reaction solution required to inhibit 50% of the  $\alpha$ -amylase activity.

### 3.3.2 Starch digestibility of wheat bread and gluten-free bread

#### 3.3.2.1 Starch digestibility of wheat bread

Figure 3.1A&B shows the starch digestibility curve of wheat bread when co-digested with TEs. The starch digestibility of wheat bread was fitted to a first order kinetics model and the kinetic parameters are shown in Table 3.2. A clear dose-dependent inhibition was observed when wheat bread was co-digested with different amount of TEs (Figure 3.1A&B). As shown in Table 3.2, reductions of 23.3%, 31.4% and 66% were found when wheat bread was co-digested with 250, 500 and 1000 mg of BTE, respectively. Similar inhibition was found when wheat bread was co-digested with GTE compared with the same amount of BTE. The initial rate of starch digestion was also clearly reduced by co-digestion with different amount of TEs with wheat bread (Table 3.2). Figure 3.1C shows the starch digestibility curve of wheat bread when co-digested with different amount of polymeric fractions from BTE. As shown in Table 3.2, reductions of 1.9%, 5.2% and 7.4% was observed when wheat bread was co-digested with 50, 125 and 250 mg of polymeric fraction from BTE and a clear reduction can also be observed from the starch digestibility curve as shown in Figure 3.1C.

#### 3.3.2.2 Starch digestibility of gluten-free bread

Figure 3.1D&E shows the starch digestibility curve in gluten-free bread when co-digested with 250 mg of TEs. Only 48.6% of starch was digested in gluten-free bread, which is much lower than the starch digestibility in wheat bread (87%) as shown in Table 3.2. GTE caused similar reduction of starch digestibility in wheat bread (22.5%) and gluten-free bread (21.3%). BTE caused higher reduction of starch digestibility in gluten-free bread (42.5%) than the reduction of starch digestibility in wheat bread (23.3%). Figure 3.1F shows the starch digestibility curve of gluten-free bread when co-digested with different amounts of polymeric fraction from BTE. A clear dose-dependent reduction of the starch digestibility was observed. Only 1.1% of the starch in gluten-free bread were digested when co-digested with 250 mg of polymeric fraction from BTE (Table 3.2).

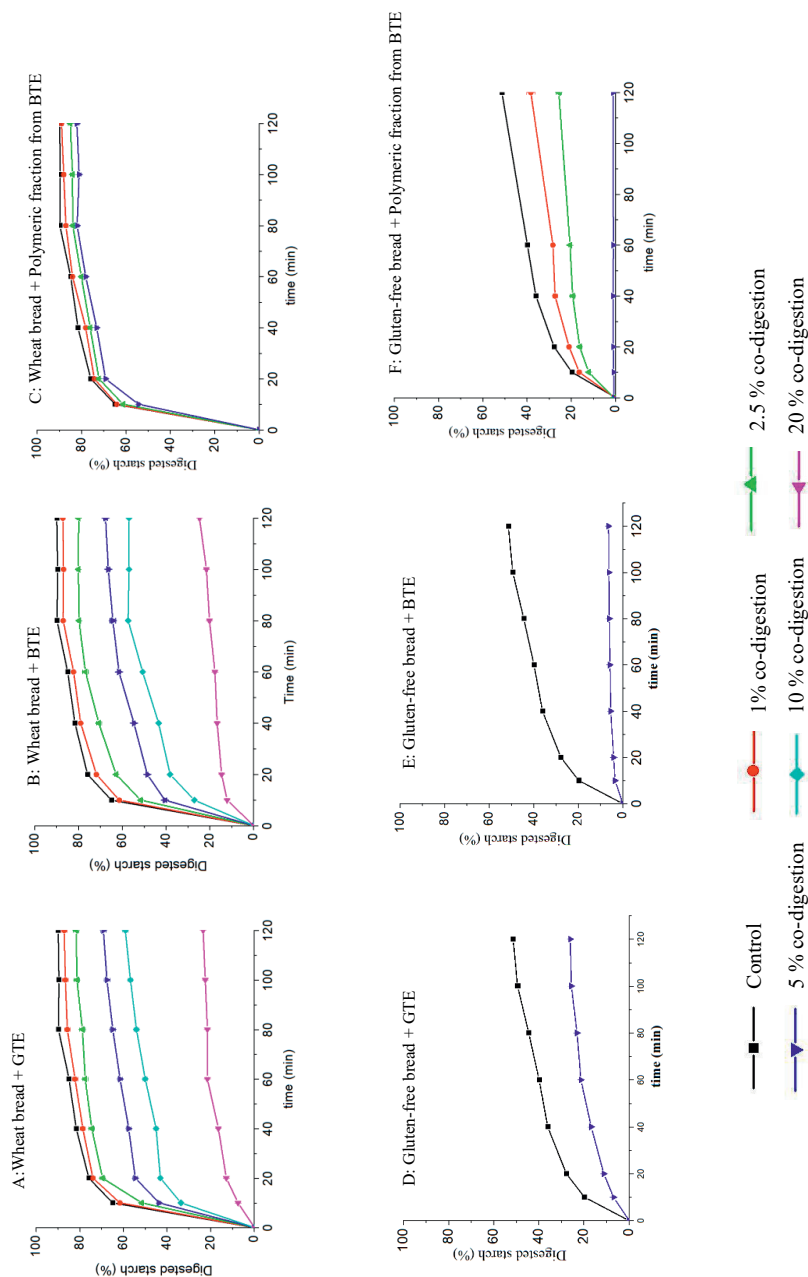


**Figure 3.1:** *In vitro* starch hydrolysis profiles of wheat bread and gluten-free bread co-digested with different amounts of BTE, GTE and polymeric fraction from BTE. The present data was expressed as mean  $\pm$  standard deviation ( $n=3$ ). The statistical analysis of the data was shown in Table 3.2. Note: 5 g of hydrated wheat bread and gluten-free bread was mixed with 0, 50, 125, 250, 500, 1000 mg of TEs or polymeric fraction from BTE and marked as control, 1, 2.5, 5, 10 and 20% co-digestion.

**Table 3.2.** Estimated kinetic parameters for starch digestion obtained from *in vitro* digestion of wheat bread co-digested with different amounts of TEs and polymeric fraction from BTE.

Wheat bread GTE co-digestion	Control (wheat bread)	1% GTE (50 mg)	2.5% GTE (125mg)	5% GTE (250 mg)	10% GTE (500 mg)	20% GTE (1000 mg)
k (min <sup>-1</sup> )	0.13 ± 0.00 a	0.12 ± 0.00 b	0.10 ± 0.00 c	0.10 ± 0.00 c	0.08 ± 0.00 d	0.04 ± 0.00 e
C <sub>∞</sub> (%)	87.0 ± 0.4 a	84.0 ± 1.3 b	79.2 ± 1.3 c	64.5 ± 1.2 d	53.8 ± 1.1 e	23.3 ± 0.5 f
% * min <sup>-1</sup>	10.9 ± 0.3 a	10.4 ± 0.2 a	8.2 ± 0.1 b	6.6 ± 0.1 c	4.5 ± 0.1 d	0.9 ± 0.0 e
Sum of square	75.4 ± 9.9	58.6 ± 1.8	25.1 ± 0.8	81.9 ± 2.7	107.1 ± 4.4	4.0 ± 0.2
Wheat bread BTE co-digestion	Control (wheat bread)	1% BTE (50 mg)	2.5% BTE (125mg)	5% BTE (250 mg)	10% BTE (500 mg)	20% BTE (1000 mg)
k (min <sup>-1</sup> )	0.13 ± 0.00 a	0.11 ± 0.00 b	0.10 ± 0.00 c	0.08 ± 0.00 d	0.05 ± 0.00 f	0.06 ± 0.00 e
C <sub>∞</sub> (%)	87.0 ± 0.4 a	84.3 ± 0.4 b	77.8 ± 0.1 c	63.7 ± 0.8 d	55.6 ± 0.3 e	21.0 ± 0.7 f
% * min <sup>-1</sup>	10.9 ± 0.3 a	9.1 ± 0.6 b	7.4 ± 0.2 c	5.3 ± 0.0 d	3.1 ± 0.0 e	1.3 ± 0.1 f
Sum of square	75.4 ± 9.9	95.4 ± 28.4	74.2 ± 25.4	103.0 ± 11.8	69.3 ± 9.0	35.5 ± 2.2
Wheat bread Polymeric fraction co-digestion	Control (wheat bread)	1% Polymeric fraction (50 mg)	2.5% Polymeric fraction (125 mg)	5% Polymeric fraction (250 mg)		
k (min <sup>-1</sup> )	0.13 ± 0.00 a	0.13 ± 0.00 a	0.13 ± 0.00 a	0.11 ± 0.00 a		
C <sub>∞</sub> (%)	87.0 ± 0.4 a	85.1 ± 0.9 b	81.8 ± 0.8 c	79.6 ± 0.8 d		
% * min <sup>-1</sup>	10.9 ± 0.3 a	10.9 ± 0.1 a	10.5 ± 0.1 a	8.7 ± 0.1 b		
Sum of square	75.4 ± 9.9	96.0 ± 1.9	65.7 ± 1.3	49.5 ± 1.0		
Gluten-free bread Polymeric fraction and TEs co-digestion	Control (gluten-free bread)	1% Polymeric fraction (50 mg)	2.5% Polymeric fraction (125 mg)	5% Polymeric fraction (250 mg)	5% GTE (250 mg)	5% BTE (250 mg)
k (min <sup>-1</sup> )	0.04 ± 0.00 e	0.05 ± 0.00 d	0.06 ± 0.00 c	0.17 ± 0.00 a	0.03 ± 0.00 f	0.07 ± 0.00 b
C <sub>∞</sub> (%)	48.6 ± 0.5 a	34.7 ± 1.6 b	23.1 ± 1.0 d	1.1 ± 0.0 f	27.3 ± 0.3 c	6.1 ± 0.1 e
% * min <sup>-1</sup>	1.9 ± 0.0 a	1.6 ± 0.0 b	1.4 ± 0.0 c	0.2 ± 0.0 f	0.7 ± 0.0 d	0.4 ± 0.0 e
Sum of square	58.5 ± 1.2	51.8 ± 18.7	17.0 ± 3.1	0.0 ± 0.0	1.7 ± 0.0	0.6 ± 0.0

Values expressed as mean ± standard deviation. Values followed by the different letter in the same row are significantly different ( $p < 0.05$ ). BTE, black tea extract; GTE, green tea extract.

Polyphenol content in GTE: 50, 125, 250, 500, 1000 mg of GTE contained 19.4, 48.5, 97, 194 and 388 mg of monomeric polyphenols.

Polyphenol content in BTE: 50, 125, 250, 500, 1000 mg of BTE contained 22.6, 56.6, 113.2, 226.5 and 453 mg of monomeric polyphenols and 2.5, 6.25, 12.5, 25 and 50 mg of tannins.

Polyphenol content in Polymeric fraction: 50, 125 and 250 mg of polymeric fraction contained 5, 12.5 and 25 mg of tannins.

### 3.3.3 Bio-accessibility of tea polyphenols

#### 3.3.3.1 Bio-accessibility of tea polyphenols when co-digested with wheat bread

As shown in Figure 3.2 (upper panels), regarding GTE, EC were the most bio-accessible polyphenol after gastric digestion (33~39%), followed by EGCG (8~12%) and ECG (5~9%). After intestinal digestion, more catechins became bio-accessible from GTE, *i.e.*, 76~87% of EC, 34~45% of EGCG and 31~40% of ECG. The bio-accessibility of catechins from BTE was much lower than the bio-accessibility of catechins from GTE. No tannins from BTE was released after gastric and intestinal digestion.

#### 3.3.3.2 Bio-accessibility of tea polyphenols when co-digested with gluten-free bread

As shown in Figure 3.2 (lower panels), after gastric digestion, the bio-accessibility of tea polyphenols when co-digested with gluten-free bread (Figure 3.2, lower panels) was higher than the bio-accessibility of tea polyphenols co-digested with wheat bread (Figure 3.2, upper panels). E.g., EGCG was more bio-accessible when GTE was co-digested with gluten-free bread (38%) than when the same amount of GTE was co-digested with of wheat bread (10%). Bio-accessibility of polyphenols from BTE showed the similar trend. In gluten-free bread, and for both TEs, no clear increase of the bio-accessibility of the tea polyphenols was observed after intestinal digestion compared with their bio-accessibility after gastric digestion.



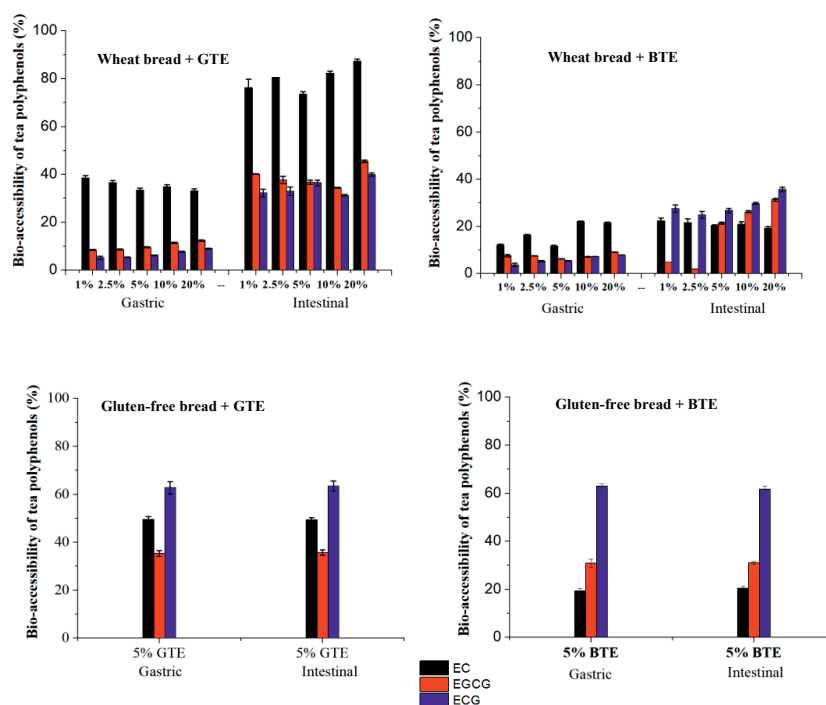
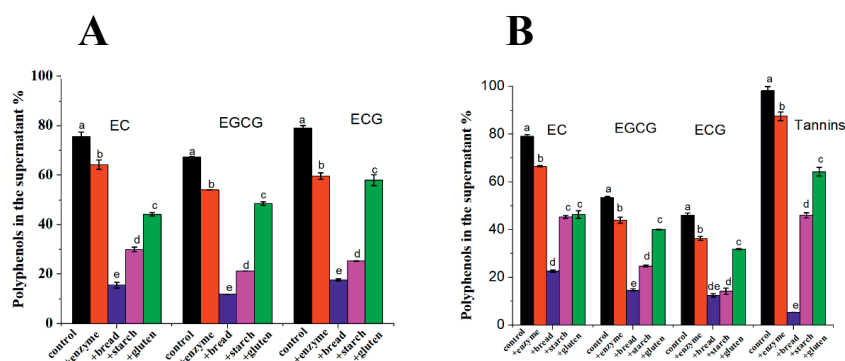


Figure 3.2. Bio-accessibility of tea polyphenols after gastric and intestinal digestion when co-digested with wheat bread or gluten-free bread. Results expressed as percentage of bio-accessible polyphenols at the end of gastric and intestinal digestion compared to the initial amount of polyphenols in TEs. No tannins were detected after gastric and intestinal digestion. The amount of EGC and theaflavins from BTE was not shown because the peak area is too small for accurate calculation. The present data was expressed as mean  $\pm$  standard deviation ( $n=3$ ). EC, epicatechin; EGCG, epigallocatechin gallate; ECG, epicatechin gallate; EGC, epigallocatechin.

### 3.3.4 Interaction of tea polyphenols with the bread matrix

Figure 3.3 shows the percentage of free tea polyphenols in the supernatant after mixing with digestive enzymes (pepsin and pancreatin), wheat bread, wheat starch (corresponding amount in wheat bread) and wheat gluten (corresponding amount in wheat bread). For both TEs, less than 80% of catechin were available in supernatant in control samples. Regarding BTE, 98% of the tannins were found in supernatant in control sample. When digestive enzymes and wheat bread were separately added to the control sample, 87% and 5% of tannins were found in supernatant, respectively. Catechins from both TEs showed the same trend as tannins, *i.e.* substantial amount of polyphenols, interacted with bread matrix. To investigate the preferential interaction of tea polyphenols bread components, starch and gluten were added separately. Surprisingly, a large amount of tea polyphenols interacted with gluten considering its lower content in wheat flour (11%) compared with starch (73%).



**Figure 3.3.** Relative percentage of polyphenols in supernatant upon addition of digestive enzymes and bread components (gluten and starch) compared to the initial content in TEs. The TEs were mixed with digestive fluids as a control. Then the mixture was mixed either with digestive enzyme, or with bread, or with starch, or with gluten (Gluten and starch were added at the corresponding amount as they are present in the bread). The present data was expressed as mean  $\pm$  standard deviation ( $n=3$ ). The different letters mean significant difference. A: GTE, green tea extract, B: BTE, black tea extract. EC, epicatechin; EGCG, epigallocatechin gallate; ECG, epicatechin gallate.

### 3.3.5 Bread hydration and the breakdown of the bread matrix during digestion

Gluten-free bread samples showed the lowest water holding capacity (2.0 g/g) and swelling volume (2.6 mL/g). The water holding capacity and swelling volume of wheat bread were two times higher than gluten-free bread (Table 3.3).

The size distribution of the two intestinal digested bread when co-digested with different amount of polymeric fraction from BTE was measured as well (Table 3.3 and Figure S3.2).  $D_{50}$  (volume median diameter) values of intestinal digested gluten-free samples (16.2  $\mu\text{m}$ ) are much lower than that of intestinal digested wheat bread (41.2  $\mu\text{m}$ ).  $D[3,2]$ , surface area moment mean and  $D[4,3]$ , volume moment mean showed the same trend as  $D_{50}$ . Regarding wheat bread, a significant increase of the size distribution of the intestinal digested bread was observed when co-digestion with different amount of polymeric fraction from BTE. *E.g.*,  $D_{50}$  of the intestinal digested wheat bread increased from 41.2 to 96.3 and 200.5  $\mu\text{m}$  when co-digested with 125 and 250 mg of polymeric fraction from BTE, respectively. Regarding gluten-free bread, only a small increase of  $D_{50}$  of intestinal digested gluten-free bread was observed when co-digested with 250 mg of polymeric fraction from BTE.  $D[3,2]$  and  $D[4,3]$  showed the similar trend.

**Table 3.3.** Hydration properties of bread samples and size distribution of the digested samples from co-digestion of wheat bread and gluten free bread with different amounts of polymers

Wheat bread	Measurement	Control (wheat bread)	1% Polymeric fraction (50 mg)	2.5% Polymeric fraction (125 mg)	5% Polymeric fraction (250 mg)
Undigested bread	WHC (g/g)	4.0 $\pm$ 0.1	na	na	na
	SV (mL/g)	4.7 $\pm$ 0.2	na	na	na
Intestinal digested sample	$D_{50}$ ( $\mu\text{m}$ )	41.2 $\pm$ 1.2 c	41.8 $\pm$ 0.3 c	96.3 $\pm$ 1.3 b	200.5 $\pm$ 2.5 a
	$D[3,2]$ ( $\mu\text{m}$ )	21.0 $\pm$ 1.0 d	23.5 $\pm$ 0.5 c	31.8 $\pm$ 0.3 b	44.4 $\pm$ 0.6 a
	$D[4,3]$ ( $\mu\text{m}$ )	60.2 $\pm$ 1.2 d	64.8 $\pm$ 0.3 c	125.0 $\pm$ 2.0 b	225.5 $\pm$ 1.5 a
Gluten free bread	Measurement	Control (gluten- free)	1% Polymeric fraction (50 mg)	2.5% Polymeric fraction (125 mg)	5% Polymeric fraction (250 mg)
Undigested bread	WHC (g/g)	2.0 $\pm$ 0.1	na	na	na
	SV (mL/g)	2.6 $\pm$ 0.1	na	na	na
Intestinal digested sample	$D_{50}$ ( $\mu\text{m}$ )	16.2 $\pm$ 0.1 c	16.4 $\pm$ 0.0 c	17.0 $\pm$ 0.1 b	18.2 $\pm$ 0.0 a
	$D[3,2]$ ( $\mu\text{m}$ )	13.9 $\pm$ 0.0 b	13.7 $\pm$ 0.1 b	13.9 $\pm$ 0.0 b	14.7 $\pm$ 0.1 a
	$D[4,3]$ ( $\mu\text{m}$ )	17.0 $\pm$ 0.0 c	17.5 $\pm$ 0.1 b	17.7 $\pm$ 0.1 b	21.5 $\pm$ 0.2 a

$D[50]$ , volume median diameter;  $D[3,2]$ , surface area moment mean;  $D[4,3]$ , volume moment mean;

Values expressed as mean  $\pm$  standard deviation. Values followed by the different letter in the same row are significantly different ( $p < 0.05$ ).

### 3.4. Discussion

The inhibition of tea polyphenols on starch digestion has been widely reported, but most of the studies focused on the interaction between polyphenols and  $\alpha$ -amylase, ignoring the effect of the food matrix on such interaction (Fei et al., 2014; He, Lv, & Yao, 2007; Pyner et al., 2017; Yang & Kong, 2016). In our previous study, we reported that the interaction of berry

polyphenols with starch or gluten affected the efficacy of polyphenols on the inhibition of starch digestion (Kan et al., 2020). Moreover, we highlighted that the interaction of polyphenols and starch may be an additional mechanism for polyphenols inhibition of starch digestibility (Kan et al., 2020). In the present study, we investigated more in detail how the multiple interactions among polyphenols,  $\alpha$ -amylase, other digestive enzymes, starch and gluten influence the starch digestibility using tea polyphenols as model phenolics and bread as a model starchy food.

Data showed that co-digestion of bread with both black and green tea polyphenols significantly reduced the kinetics rate and extent of starch digestion (Figure 3.1 & Table 3.2). An *in vitro* study showed that co-digestion with green tea catechins could slow down starch digestion in steamed and baked bread which was in line with our results (Goh et al., 2015). In the present study, we observed a trend for a reduction in both  $k$  and  $C_{\infty}$  when the amount of co-digested polyphenols from black and green tea increased (Figure 3.1). Since a significant reduction of the  $C_{\infty}$  may decrease the time needed to achieve  $C_{\infty}$  and thus increase  $k$  values as we observed in previous study (Kan et al., 2020), initial rates were also calculated and their values confirmed a dose-dependent decrease of the digestion rate (Table 3.2).

Monomeric and polymeric polyphenols showed different inhibition degrees on starch digestibility in wheat bread and gluten-free bread. It is interesting to notice that GTE caused similar reduction of starch digestibility in wheat bread (Figure 3.1A) and gluten-free bread (Figure 3.1D), but BTE caused larger reduction of starch digestibility in gluten-free bread (Figure 3.1E) compared to wheat bread (Figure 3.1B). Considering the different polyphenol profile in BTE and GTE (Table 3.1), we proposed that the polymeric polyphenols from BTE are responsible for the different BTE inhibition efficacy when co-digested with wheat bread and gluten-free bread. It has been already proposed that polymeric polyphenols may be more effective in reducing the rate and the extent of starch digestion compared to monomers. In one study, a sorghum extract rich in tannins increased the resistant starch content in normal corn starch by around two times compared to the extract with monomeric polyphenols (Barros, Awika, & Rooney, 2012). To better understand the role of the polymeric fraction on starch digestibility, the polymeric fraction was separated from BTE for testing the inhibition on starch digestibility. Surprisingly, the polymeric extract was more effective than the whole BTE extract in gluten-free bread but much less effective in wheat bread (Figure 3.1). By comparing the polyphenol composition and inhibitory efficacy of BTE and polymeric fraction, we could quantify the relative contribution of the monomeric and polymeric fraction

to the observed inhibition. In wheat bread, the contribution of the monomeric and the polymeric fraction to the reduction of the starch digestibility caused by 250 mg of BTE (23.3%) was quantified as 18.1% and 5.2% respectively. In gluten-free bread, the contribution of the monomeric and the polymeric fraction to the reduction of the starch digestibility caused by 250 mg of BTE (42.5%) was quantified as 17% and 25.5%, respectively. We concluded that the presence of gluten had a minor influence on inhibitory efficacy of monomeric polyphenols, since the monomeric polyphenols caused similar reduction of starch digestibility in wheat bread (18.1%) and in gluten-free bread (17%) when they were co-digested with BTE. This was in line with the fact that GTE has similar inhibitory efficacy in wheat bread (22.5%) and gluten-free bread (21.3%) as shown in Table 3.2, since GTE only contained monomeric polyphenols (Table 3.1). However, the presence of gluten clearly reduced the inhibitory efficacy of polymeric polyphenols, since tannins caused much larger reduction of starch digestibility in gluten-free bread (25.5%) compared with the reduction of starch digestibility in wheat bread (5.2%) when both bread samples were co-digested with 250 mg of BTE. We can also conclude that the presence of the gluten network is key to understand the efficacy of polymeric polyphenols on starch digestibility in a complex food matrix like bread.

Whatever monomeric or polymeric polyphenols, their inhibitory effect on starch digestibility in bread can be explained by multiple mechanisms involving interactions among tea polyphenols,  $\alpha$ -amylase, other digestive enzymes, starch and gluten. The presence of those interactions is confirmed by the bio-accessibility data reported in Figure 3.2 & 3.3. The first mechanism is a direct inhibition of  $\alpha$ -amylase. We initially hypothesized that this inhibition would be proportional to the amount of polyphenols that are not bound components other than  $\alpha$ -amylase. One of those components is the pancreatic enzymes. Some researchers reported that polyphenol-rich extracts from green tea and black tea competitively inhibit pancreatic  $\alpha$ -amylase and with  $IC_{50}$  values of 0.20 and 0.46 mg/mL for GTE and BTE, respectively, and the inhibition was likely attributed to the galloyl moiety, a common substitute in tea polyphenols (Sun et al., 2016). Although a lot of research has been done on  $\alpha$ -amylase inhibition (Fei et al., 2014; Yilmazer-Musa, Griffith, Michels, Schneider, & Frei, 2012), most studies used isolated pancreatic  $\alpha$ -amylase, rather than the whole pancreatin. Pancreatin is a mixture of  $\alpha$ -amylase, trypsin, chymotrypsin, lipase and colipase and frequently used for the *in vitro* digestion study. Therefore, the interaction between polyphenols and other digestive enzymes is usually neglected. For better understanding the role of other enzymes on  $\alpha$ -amylase inhibition during *in vitro* digestion, the  $IC_{50}$  values were calculated for whole

pancreatin and purified  $\alpha$ -amylase. As shown in Table 3.1 and Figure S3.1, higher  $IC_{50}$  values were calculated for pancreatin for both TEs. This was likely because the other enzymes from pancreatin could also interact with polyphenols, thus affecting the polyphenol-amylase interaction (McDougall, Kulkarni, & Stewart, 2009). The other components to interact with polyphenols is represented by the food matrix components. Previous studies reported polyphenols to have high affinity for proteins and bond to them by hydrophobic interactions, as well as hydrogen bonds (Jakobek, 2015). Similarly to what has been reported in our previous study with berry polyphenols (mostly anthocyanins and procyanidins), we observed here a strong interaction between tea polyphenols and gluten (Kan et al., 2020). However, the amount of polyphenols bound to starch was even higher, confirming that in a relatively rich source of starch like bread, the contribution of starch in binding polyphenols may be substantially higher than gluten. However, when the supernatant of the samples after gastric digestion was tested for  $\alpha$ -amylase inhibition, no such inhibition was found, suggesting that the role of unbound polyphenols on the observed decrease in starch digestibility is negligible.

The second mechanism for the inhibitory effect of polyphenols on starch digestibility may derive from the direct interaction between tea polyphenols and starch. It was reported that polyphenols can interact directly with starch through hydrophobic forces and hydrogen bonding, thus reducing the available surface of the starch granules to react with enzymes (Amoako & Awika, 2016). The authors in particular speculated that the presence of polyphenols would block the access of amylase to the pores and channels that are typical of cereal starches. This may have happened also in our bread system. In this case we would expect that the presence of gluten would reduce the efficacy of inhibition which is what Figure 3.1D&E seem to suggest. However, it has been reported that the polyphenols that are adsorbed onto starch may exert there an inhibitory activity against  $\alpha$ -amylase (Sun, Gidley, & Warren, 2018). It is difficult to determine experimentally but the inhibition of amylase from polyphenols bound to starch can be tested by measuring the inhibition of amylase in the bread matrix. Clearly, the presence of the gluten matrix may reduce the amount of polyphenols able to interact with starch and thus able to inhibit starch digestion whatever the exact mechanism is in place in close proximity of the glucan chains. Moreover, we cannot exclude that the observed inhibition is partly caused by an indirect effect on the extent of gluten digestion, which would make starch granules more accessible to amylase. It is known that polyphenols can reduce the rate and extent of protein digestion (Bandyopadhyay, Ghosh, & Ghosh, 2012; He et al., 2007; Lamothe, Azimy, Bazinet, Couillard, & Britten, 2014; Ren et al., 2018). This

seems to be confirmed by the particle size distribution data of bread during digestion, where bigger particles are detected in bread co-digested with polyphenols, suggesting that the whole bread is digested at a slower rate in these systems (Table 3). It is also interesting to notice that the starch digestibility of gluten free bread (45%) is much lower than wheat bread (87%). Opposite results were reported in other studies in which the presence of gluten slowed down starch digestion (Camelo-Méndez, Agama-Acevedo, Rosell, de J. Perea-Flores, & Bello-Pérez, 2018). The finding of this study could be attributed to the much weaker hydration properties of gluten free bread compared to wheat bread (Table 3), which might hinder *in vitro* starch digestibility (Briffaz, Bohuon, Méot, Dornier, & Mestres, 2014; De La Hera et al., 2013; De La Hera, Rosell, & Gomez, 2014).

Although tea polyphenols can inhibit starch digestibility, to achieve a level of inhibition that is physiologically relevant, we considered how realistically the effective amounts reported in this study may be achieved in real life through tea consumption (Table 3.4). To achieve an inhibitory effect from co-digestion of 100 g of bread and 1 g of TEs, 2 cups of black tea and 2.5 cups of green tea would be needed to be co-digested with 100 g of wheat bread as shown in Table 3.4. Higher amounts of tea polyphenols to be co-digested with bread would be hard to achieve through realistic tea consumption habits.

**Table 3.4** Actual amount of tea cups required to achieve the inhibitory effect of BTE or GTE co-digestion with 100 g of wheat bread

Co-digestion	Required tea extract (g)	Yield of tea extract (%)		Required tea powder (g)		Required tea (cups)	
		Black tea	Green tea	Black tea	Green tea	Black tea	Green tea
1%	1			4	5	2	2.5
2.5%	2.5			10	12.5	5	6.3
5%	5	25	20	20	25	10	12.5
10%	10			40	50	20	25
20%	20			80	100	40	50

One cup of tea contained 2 g of tea powder (this information is provided by the tea manufacturer).

### 3.5. Conclusion

In this study, the effect of tea polyphenols on starch digestion of wheat bread and gluten-free bread was investigated. The inhibition of tea polyphenols on starch digestibility was attributed to the multiple interactions among tea polyphenols,  $\alpha$ -amylase, other digestive

enzymes, starch and gluten. The use of a gluten free bread made up almost exclusively by wheat starch allowed us to prove that the presence of gluten has little influence on inhibitory efficacy of monomeric polyphenols on starch digestibility, but clearly reduced the inhibitory efficacy of polymeric polyphenols on starch digestibility. Future investigation should elucidate the exact mechanism behind the observed decrease of starch digestion in presence of polyphenols. Data showed that the presence of tea polyphenols in the digestive medium is a promising strategy for controlling glycaemic index of starchy food products but this strategy must be adapted to the specific food matrix considered.

#### **Declaration of interests**

There are no conflicts of interest to declare.

#### **Acknowledgement**

The authors would like to thank our technicians Geert Meijer and Erik Meulenbroeks for their assistance for the lab work. The author Lijiao Kan received a PhD scholarship from the China Scholarship Council (No. 201706820018).



## Reference

- Amoako, D. B., & Awika, J. M. (2016). Polymeric tannins significantly alter properties and in vitro digestibility of partially gelatinized intact starch granule. *Food Chemistry*. <https://doi.org/10.1016/j.foodchem.2016.03.096>
- Bandyopadhyay, P., Ghosh, A. K., & Ghosh, C. (2012). Recent developments on polyphenol-protein interactions: Effects on tea and coffee taste, antioxidant properties and the digestive system. *Food and Function*. <https://doi.org/10.1039/c2fo00006g>
- Barros, F., Awika, J. M., & Rooney, L. W. (2012). Interaction of tannins and other sorghum phenolic compounds with starch and effects on in vitro starch digestibility. *Journal of Agricultural and Food Chemistry*. <https://doi.org/10.1021/jf3034539>
- Briffaz, A., Bohuon, P., Méot, J. M., Dornier, M., & Mestres, C. (2014). Modelling of water transport and swelling associated with starch gelatinization during rice cooking. *Journal of Food Engineering*. <https://doi.org/10.1016/j.jfoodeng.2013.06.013>
- Camelo-Méndez, G. A., Agama-Acevedo, E., Rosell, C. M., de J. Perea-Flores, M., & Bello-Pérez, L. A. (2018). Starch and antioxidant compound release during in vitro gastrointestinal digestion of gluten-free pasta. *Food Chemistry*, 263, 201–207. <https://doi.org/10.1016/J.FOODCHEM.2018.04.075>
- De La Hera, E., Gomez, M., & Rosell, C. M. (2013). Particle size distribution of rice flour affecting the starch enzymatic hydrolysis and hydration properties. *Carbohydrate Polymers*. <https://doi.org/10.1016/j.carbpol.2013.06.002>
- De La Hera, E., Rosell, C. M., & Gomez, M. (2014). Effect of water content and flour particle size on gluten-free bread quality and digestibility. *Food Chemistry*. <https://doi.org/10.1016/j.foodchem.2013.11.115>
- Dona, A. C., Pages, G., Gilbert, R. G., & Kuchel, P. W. (2010). Digestion of starch: In vivo and in vitro kinetic models used to characterise oligosaccharide or glucose release. *Carbohydrate Polymers*, 80(3), 599–617. <https://doi.org/10.1016/J.CARBPOL.2010.01.002>
- Fei, Q., Gao, Y., Zhang, X., Sun, Y., Hu, B., Zhou, L., Jabbar, S., & Zeng, X. (2014). Effects of Oolong tea polyphenols, EGCG, and EGCG3"Me on pancreatic  $\alpha$ -amylase activity in vitro. *Journal of Agricultural and Food Chemistry*. <https://doi.org/10.1021/jf5032907>

- Forester, S. C., Gu, Y., & Lambert, J. D. (2012). Inhibition of starch digestion by the green tea polyphenol, (-)-epigallocatechin-3-gallate. *Molecular Nutrition and Food Research*. <https://doi.org/10.1002/mnfr.201200206>
- Goh, R., Gao, J., Ananingsih, V. K., Ranawana, V., Henry, C. J., & Zhou, W. (2015). Green tea catechins reduced the glycaemic potential of bread: An in vitro digestibility study. *Food Chemistry*, 180, 203–210. <https://doi.org/10.1016/J.FOODCHEM.2015.02.054>
- He, Q., Lv, Y., & Yao, K. (2007). Effects of tea polyphenols on the activities of  $\alpha$ -amylase, pepsin, trypsin and lipase. *Food Chemistry*. <https://doi.org/10.1016/j.foodchem.2006.03.020>
- Jakobek, L. (2015). Interactions of polyphenols with carbohydrates, lipids and proteins. *Food Chemistry*. <https://doi.org/10.1016/j.foodchem.2014.12.013>
- Kan, L., Nie, S., Hu, J., Wang, S., Bai, Z., Wang, J., Zhou, Y., Zeng, Q., & Song, K. (2018). Comparative study on the chemical composition, anthocyanins, tocopherols and carotenoids of selected legumes. *Food Chemistry*, 260. <https://doi.org/10.1016/j.foodchem.2018.03.148>
- Kan, Lijiao, Oliviero, T., Verkerk, R., Fogliano, V., & Capuano, E. (2020). Interaction of bread and berry polyphenols affects starch digestibility and polyphenols bio-accessibility. *Journal of Functional Foods*. <https://doi.org/10.1016/j.jff.2020.103924>
- Kyrleou, M., Kallithraka, S., Koundouras, S., Chira, K., Haroutounian, S., Spinthiropoulou, H., & Kotseridis, Y. (2015). Effect of vine training system on the phenolic composition of red grapes (<em>Vitis vinifera</em> L. cv. Xinomavro). *OENO One*, 49(1), 71. <https://doi.org/10.20870/oeno-one.2015.49.2.92>
- Lamothe, S., Azimy, N., Bazinet, L., Couillard, C., & Britten, M. (2014). Interaction of green tea polyphenols with dairy matrices in a simulated gastrointestinal environment. *Food and Function*. <https://doi.org/10.1039/c4fo00203b>
- McDougall, G. J., Kulkarni, N. N., & Stewart, D. (2009). Berry polyphenols inhibit pancreatic lipase activity in vitro. *Food Chemistry*. <https://doi.org/10.1016/j.foodchem.2008.11.093>
- Minekus, M., Alming, M., Alvito, P., Ballance, S., Bohn, T., Bourlieu, C., Carrière, F., Boutrou, R., Corredig, M., Dupont, D., Dufour, C., Egger, L., Golding, M., Karakaya, S., Kirkhus, B., Feunteun, S. L., Lesmes, U., Macierzanka, A., Mackie, A., Marze, S.,

- McClements, D. J., Mènard, O., Recio, I., Santos, C. N., Singh, R. P., Vegaru, G. E., Wickam, S.J., Weitschies, W., & Brodtkorb, A. (2014). A standardised static in vitro digestion method suitable for food-an international consensus. *Food and Function*. <https://doi.org/10.1039/c3fo60702j>
- Moradi-Marjaneh, R., Paseban, M., & Sahebkar, A. (2019). Natural products with SGLT2 inhibitory activity: Possibilities of application for the treatment of diabetes. *Phytotherapy Research*. <https://doi.org/10.1002/ptr.6421>
- Pereira-Caro, G., Moreno-Rojas, J. M., Brindani, N., Del Rio, D., Lean, M. E. J., Hara, Y., & Crozier, A. (2017). Bioavailability of Black Tea Theaflavins: Absorption, Metabolism, and Colonic Catabolism. *Journal of Agricultural and Food Chemistry*. <https://doi.org/10.1021/acs.jafc.7b01707>
- Pyner, A., Nyambe-Silavwe, H., & Williamson, G. (2017). Inhibition of human and rat sucrase and maltase activities to assess antiglycemic potential: Optimization of the assay using acarbose and polyphenols. *Journal of Agricultural and Food Chemistry*, 65(39), 8643–8651. <https://doi.org/10.1021/acs.jafc.7b03678>
- Ren, C., Xiong, W., Peng, D., He, Y., Zhou, P., Li, J., & Li, B. (2018). Effects of thermal sterilization on soy protein isolate/polyphenol complexes: Aspects of structure, in vitro digestibility and antioxidant activity. *Food Research International*. <https://doi.org/10.1016/j.foodres.2018.06.034>
- Striegel, L., Kang, B., Pilkenton, S. J., Rychlik, M., & Apostolidis, E. (2015). Effect of black tea and black tea pomace polyphenols on  $\alpha$ -glucosidase and  $\alpha$ -amylase inhibition , relevant to type 2 diabetes prevention, 2(February), 1–6. <https://doi.org/10.3389/fnut.2015.00003>
- Sun, L., Gidley, M. J., & Warren, F. J. (2018). Tea polyphenols enhance binding of porcine pancreatic  $\alpha$ -amylase with starch granules but reduce catalytic activity. *Food Chemistry*. <https://doi.org/10.1016/j.foodchem.2018.03.017>
- Sun, L., Warren, F. J., Netzel, G., & Gidley, M. J. (2016). 3 or 3'-Galloyl substitution plays an important role in association of catechins and theaflavins with porcine pancreatic  $\alpha$ -amylase: The kinetics of inhibition of  $\alpha$ -amylase by tea polyphenols. *Journal of Functional Foods*. <https://doi.org/10.1016/j.jff.2016.07.012>
- Xing, L., Zhang, H., Qi, R., Tsao, R., & Mine, Y. (2019). Recent Advances in the

Understanding of the Health Benefits and Molecular Mechanisms Associated with Green Tea Polyphenols. *Journal of Agricultural and Food Chemistry*.

<https://doi.org/10.1021/acs.jafc.8b06146>

Yang, X., & Kong, F. (2016). Effects of tea polyphenols and different teas on pancreatic  $\alpha$ -amylase activity in vitro. *LWT - Food Science and Technology*.

<https://doi.org/10.1016/j.lwt.2015.10.035>

Yilmazer-Musa, M., Griffith, A. M., Michels, A. J., Schneider, E., & Frei, B. (2012). Grape seed and tea extracts and catechin 3-gallates are potent inhibitors of  $\alpha$ -amylase and  $\alpha$ -glucosidase activity. In *Journal of Agricultural and Food Chemistry*.

<https://doi.org/10.1021/jf301147n>

Zeller, W. E., Sullivan, M. L., Mueller-Harvey, I., Grabber, J. H., Ramsay, A., Drake, C., & Brown, R. H. (2015). Protein precipitation behavior of condensed tannins from *Lotus pedunculatus* and *Trifolium repens* with different mean degrees of polymerization.

*Journal of Agricultural and Food Chemistry*. <https://doi.org/10.1021/jf504715p>

Zhang, S., Yang, C., Idehen, E., Shi, L., Lv, L., & Sang, S. (2018). Novel Theaflavin-Type Chlorogenic Acid Derivatives Identified in Black Tea. *Journal of Agricultural and Food Chemistry*, 66(13), 3402–3407. <https://doi.org/10.1021/acs.jafc.7b06044>


## Supplementary materials

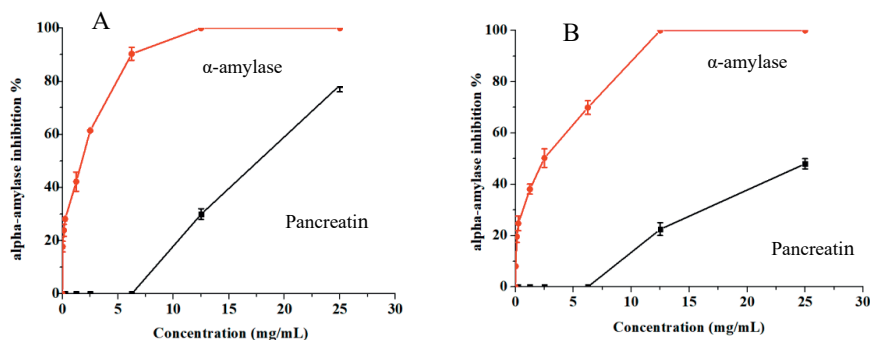


**Figure S3.1.** Inhibition of GTE (A) and BTE (B) on  $\alpha$ -amylase and pancreatin. GTE, green tea extract; BTE, black tea extract.

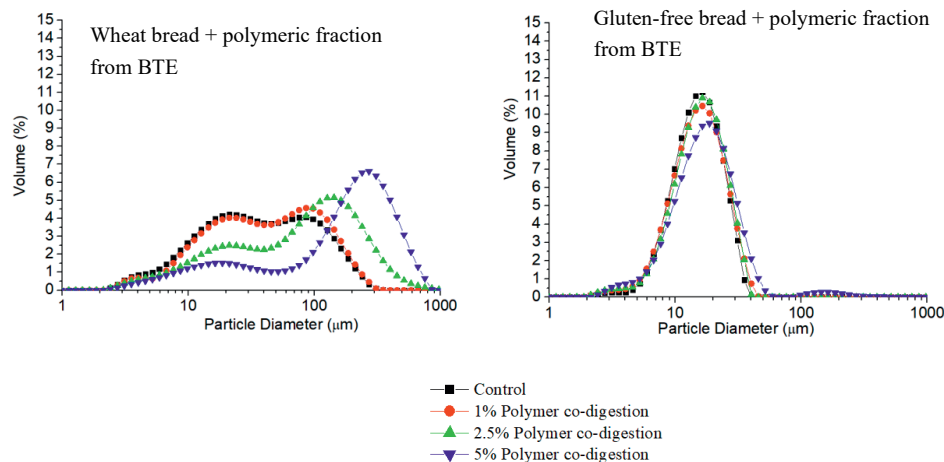


**Figure S3.2.** The breakdown of the bread matrix after co-digestion with different amount of polymeric fractions: size distribution of the intestinal digested bread samples. Note: 5 g of hydrated wheat bread and gluten-free bread was mixed with 0, 50, 125, 250 mg of polymeric fraction from BTE and marked as control, 1, 2.5 and 5%.

The background of the image is composed of several geometric shapes. A large, light gray triangle is in the top-left corner, with its hypotenuse running from the top-left towards the center. A smaller, darker gray triangle is positioned below it, also with its hypotenuse running towards the center. The remaining area on the left is a dark gray triangle. The right half of the image is a solid white background. In the center of this white area is a large, bold, black number '4'.

4

# Chapter 4

Different effects of inclusion and non-inclusion wheat starch-tannic acid complexes on rheological properties and digestibility of wheat starch

This chapter is based on:

Kan, L., Capuano, E., Oliviero, T., & Renzetti, S. Different effects of inclusion and non-inclusion wheat starch-tannic acid complexes on rheological properties and digestibility of wheat starch. Submitted for publication.

**Abstract**

In this study, the interactions of wheat starch (WS) and tannic acid (TA) were investigated for their gelatinization, pasting, structural, and steady and dynamic rheological properties and digestibility of wheat starch. TA was either complexed with starch (WS-TA complexes) or mixed with starch (WS-TA mixtures) right before the characterization of its properties. The increase of melting enthalpy and temperature range ( $T_{\text{peak}} - T_{\text{onset}}$ ) of amylose-lipid complex indicated the formation of inclusion types of complexes. The thermal transition at 130~160 °C indicated the formation of non-inclusion types of complexes. Non-inclusion type of complexes were mostly formed by co-gelatinization WS-TA mixtures, while inclusion complexes were mostly formed by complexation of TA with ungelatinized starch. TA in mixtures resulted in the higher  $G'$  and viscosity and the lower frequency dependency, thus producing a stronger gel. TA in complexes resulted in lower  $G'$  and viscosity and higher frequency dependency at low TA%, thus producing a weak gel, and showed the opposite way at high TA%. The storage moduli  $G'$  increased dependently with effective TA concentration for non-inclusion complexes formation. The formation of cross-linking amylose-TA complexes and inclusion complexes largely slowed down the starch digestibility of gelatinized starch. The insights gained in this study provide opportunities to modulate starch techno-functional properties and digestibility in processing of starchy food.

Key words: wheat starch, tannic acid, inclusion complexes, non-inclusion complexes, rheological properties



## 4.1 Introduction

Starch acts as a thickening, gelling and texturizing ingredient in various formulated food. Industries are enriching starchy food such as bread and pasta with ingredients that contain polyphenols either to develop healthier products or to increase the variety of products (Kan, Oliviero, Verkerk, Fogliano, & Capuano, 2020; Oliviero & Fogliano, 2016). The addition of polyphenols can affect functional properties of starch, such as gelatinization, pasting properties and starch digestibility (Li, Pernell, & Ferruzzi, 2018). Understanding the mechanisms by which polyphenols affect the physicochemical properties of various starch is gaining importance for food applications towards healthy diets (Gao et al., 2021).

The starch-polyphenols interactions has been recently investigated by many researchers by producing starch-polyphenol complexes (Chi et al., 2017; Zheng et al., 2021). One of the important complexes is V-type starch-phenolics complexes that are primarily driven by hydrophobic interactions (Zhu, 2015). In V-type complexes phenolics were hosted in the hydrophobic helical cavity of amylose (Biliaderis & Galloway, 1989). Evidence of V-type complexation have been shown with ferulic acid, gallic acid and green tea polyphenols, caffeic acid (Han, Bao, Wu, & Ouyang, 2020; Liu, Chen, Xu, Liang, & Zheng, 2019; Van Hung, Phat, & Phi, 2013; Zhao, Wang, Zheng, Chen, & Guo, 2019). Limiting factors for the formation of V-complexes are the bulky size, the lack of hydrophobicity of the phenolics, or the size of the cavity in the amylose helix (Zhu, 2015). In such cases some non-inclusion complexes were formed, which were mostly driven by hydrogen bonds (Zhu, 2015). The starch-polyphenols complexes have been extensively characterized by studying gelatinization, retrogradation, pasting and rheological properties and starch digestibility. The effects of starch-polyphenols interactions differed depending on the phenolic and starch types. For instance, complexation with caffeic acid, gallic acid and ferulic acid significantly influenced rheological properties of potato and maize amylopectin, whereas digestibility of both starch was modestly affected by complexing with those three phenolic acids (Li et al., 2018). Complexing with quercetin enhanced crystallinity and compactness and clearly decreased starch digestibility of buckwheat starch (Gao et al., 2021). Although the interaction of a variety of polyphenols and starch has been widely reported, insufficient evidence was provided on the interacting mechanisms, for instance, by forming inclusion and non-inclusion complexes and corresponding forming conditions.

To expand the knowledge of starch-polyphenols interactions, in the present study we investigated the effect of addition of tannic acid (TA), a relatively less studied polyphenol, on

wheat starch (WS) physicochemical properties and digestibility. To better understand the mechanisms of TA interaction with WS under different processing conditions, TA was added to WS in two ways, *i.e.*, by complexing or mixing with WS. WS-TA complexes were prepared by mixing and incubating native starch and tannins solutions and then removing the unbound tannic acid. WS-TA mixtures were prepared by simply mixing native WS and TA just prior to starch characterization. Then the influence of TA on WS physio-chemical changes and the underlying mechanisms were discussed.

## 4.2 Materials and methodology

### 4.2.1 Materials

Wheat starch, tannic acid, pepsin (4268 units/mg), porcine pancreatin (P7545; 4XUSP specifications; amylase activity 40 units/mg), amyloglucosidase (P300 units/mL), bovine serum albumin (BSA), sodium dodecyl sulfate (SDS), 2-Chloro-4-nitrophenyl- $\alpha$ -D-maltotrioxide, triethanolamine (TEA) and ferric chloride were purchased from Sigma–Aldrich (St Louis, MO, USA). All other chemicals were of analytical grade.

### 4.2.2 Preparation of starch-tannins complex

The preparation of starch-tannins complex was performed according to a previous method with some modifications (Li et al., 2018). Wheat starch was mixed with 0%, 5%, 10% and 20% of tannic acid based on dry weight of starch. Then the mixed samples were dispersed in 250 mL of water. The mixture was put in a water bath of 37 °C for 30 min and the suspension was stirred every 5 min. Then it was centrifuged at 3500 g for 10 min. The supernatant was stored for analysis of tannins content, the resulting precipitates were washed with distilled water until no tannins was detected in the supernatant. Then the precipitation was freeze dried to obtain non-gelatinized starch-tannins complexes. According to the initial amount of TA (0%, 5%, 10% and 20%), the wheat starch-tannic acid complexes were marked as C0, C5, C10 and C20, respectively. In addition, starch-tannins mixtures in this study were prepared by simply mixing native starch with tannic acid which dissolved in water just before the starch characterization. According to the initial amount of TA (0%, 5%, 10% and 20%) to be mixed with wheat starch, the wheat starch-tannic acid mixtures were marked as M0, M5, M10 and M20, respectively.

#### 4.2.3 Quantification of bound tannins

The determination of tannins was performed using a BSA precipitation method according to our previous paper (Kan, Capuano, Fogliano, Oliviero, & Verkerk, 2020). This determination has been done only on WS-TA complexes. The bound tannins were calculated by the initial amount of tannins minus the free tannins. The free tannins were defined as the tannic acid which was released in the supernatant upon preparation of starch-tannins complex as described in 2.2.

#### 4.2.4 Determination apparent amylose

Amylose content was estimated by iodine colorimetry according to (H. Li et al., 2019) with slight modifications. This determination has been done only on native wheat starch and wheat starch-tannic acid complexes. A standard curve with amylose content ranging from 0 to 100% was prepared using pure potato amylose (Sigma A0512) and maize amylopectin (Sigma 10120). Native wheat starch, wheat starch-tannic acid complexes, amylose and amylopectin were suspended in 1 M aqueous NaOH (10 mg/mL), followed by heating in a boiling water bath with shaking. After cooling down to room temperature and five-times dilution in water, a 40  $\mu$ L aliquot was added into 1 mL water in a 2 mL Eppendorf tube, followed by adding 200  $\mu$ L iodine solution (0.0025 M I<sub>2</sub>/0.0065 M KI mixture) and 760  $\mu$ L water to make up 2 mL solution. The solution was mixed vigorously and then allowed to develop color for 15 min. The absorbance was read at 600 nm. A standard starch (labelled as 68% amylose content) of K-AMYL Kit (Megazyme, Ireland) tested with the iodometric assay as reference gave  $66.4 \pm 0.6\%$  amylose content at 600 nm. The moisture content of all starches was determined for the calculation of amylose content on a dry weight basis.

#### 4.2.5 Determination of amylose leaching, swelling power and solubility

Amylose leaching, swelling factor and solubility were determined according to a previous method with some modifications (Guo, Zhao, Chen, Chen, & Zheng, 2019). Briefly, 1 g of wheat starch-tannic acid complexes prepared in 2.2 was mixed with 25 mL of water. For the mixture samples, 1 g of wheat starch was mixed with 0, 0.05, 0.1, 0.2 g of tannic acid, and then 25 mL of water was added. Then the starch suspensions were put in a boiled water-bath for 30 min. After cooling down to room temperature, all the samples was centrifuged at 3500 g for 10 min. Leached amylose content in the supernatant was determined by the above-mentioned iodine binding technique. The supernatant and pellet were dried at 105 °C overnight. The dried supernatant and the water in swollen granules were weighed. The

solubility was defined as the ratio of the weight of dried supernatant to the weight of starch samples (g/ 100g). The swelling power was defined as the ratio of the wet weight of the pellet to the dry weight of starch (g/g).

#### 4.2.6 DSC analysis

The melting behaviour of crystalline structures in starch-tannins complex samples and mixture samples was determined by a Q 200 differential scanning calorimeter (TA Instruments, New Castle, DE, USA) (Bin Zhang, Huang, Luo, & Fu, 2012). Regarding the starch-tannins complexes, 7.5 mg of freeze dried starch-tannins complexes were placed in high-volume, high-pressure aluminium pans. Then, 22.5 mL of demineralized water were added and the samples were kept overnight to equilibrate analysis. Regarding the wheat starch-tannic acid mixtures, 7.5 mg of wheat starch was mixed with 22.5 mL of tannic acid solutions. For providing 0%, 5%, 10% and 20% of wheat starch (based on 7.5 mg), the concentrations of tannic acid were 0, 0.017, 0.033, 0.066 mg/mL, respectively. Upon start, the samples were held at 5°C for 5 min, then scanned from 5°C to 160°C at 10°C/min. A 2<sup>nd</sup> scan was performed from 5°C to 160°C. Onset ( $T_{\text{onset}}$ ), peak ( $T_{\text{peak}}$ ) and conclusion ( $T_{\text{conclusion}}$ ) temperatures, as well as the enthalpy were determined. Analysis was done with TA Instruments Universal Analysis 2000 software, version 4.5A, build 4.5.0.5 (TA Instruments, New Castle, DE, USA).

#### 4.2.7 XRD analysis

The X-ray diffraction (XRD) experiments were performed using an X-ray diffractometer (D8 Advance, Bruker Inc., Germany) with the  $2\theta$  (°) range of 5-55° (Zhang, Li, Liu, Xie, & Chen, 2013). Native wheat starch and wheat starch-tannic acid complexes prepared in section 2.2 were directly analysed by XRD. Gelatinization of wheat starch-tannic acid complexes and mixtures were performed according to section 2.5. After cooling down to room temperature, the samples were dried in a freeze dryer (Alpha 2-4 LD plus, Christ). Then the gelatinized wheat-starch-tannic acid complexes and mixtures were analysed by XRD. The relative crystallinity (RC) was quantitatively estimated as a ratio of the crystalline area of the total area (crystalline regions plus amorphous regions) using Difffrac.eva.V5.2 software.

#### 4.2.8 RVA analysis

Pasting behaviour was investigated using a Rapid Visco Analyser Super 4 (Perten, Hägersten, Sweden), according to a previous method with slight modifications (Liu et al.,

2019). Regarding the starch-tannin complexes, inside a suitable canister  $3.00 \pm 0.01$  g of wheat starch-tannic acid complexes (dry basis) is mixed manually with  $22.0 \text{ g} \pm 0.1$  g of distilled water until no lumps were visual anymore. Regarding the wheat starch-tannic acid mixtures, 0.15, 0.3, 0.6 g of tannic acid was added into  $22.0 \text{ g} \pm 0.1$  g of distilled water, then  $3.00 \pm 0.01$  g of wheat starch was added. The experiment was started with an initial stirring speed of 960 rpm at  $50^\circ\text{C}$  for 60 seconds. Then, the stirring speed is decreased to 160 rpm while the temperature is increased to  $95^\circ\text{C}$  within 3 min 42 s. Hold at  $95^\circ\text{C}$  for 2 min 30 s minutes. Then cool to  $50^\circ\text{C}$  within 3 min 48 s and hold at  $50^\circ\text{C}$  for 4 min.

#### 4.2.9 Small amplitude oscillatory rheology of starch-tannic acid gels

Wheat starch suspensions (5%, w/v) were prepared. Briefly, 1.25 g of wheat starch-tannic acid complexes (dry weight basis of starch) was dispersed in 23.75 g of water. Wheat starch-tannic acid mixtures were simply prepared by mixing 1.25 g of wheat starch (dry weight basis) with 62.5, 125 and 250 mg of tannic acid and then 23.75 g of water was added. The starch gelatinization was done using RVA as described in 2.8. The samples were left at room temperature for 1 h to reach  $25^\circ\text{C}$ . Then the rheological properties of the gelatinized samples were evaluated.

Dynamic viscoelastic properties of gels were determined using a rotary rheometer (Discovery, HR-3, TA instrument Inc., USA) equipped with a parallel plate geometry (40 mm) at 1.0 mm gap. Amplitude sweep experiment tests were conducted to record the storage modulus ( $G'$ ) and loss modulus ( $G''$ ) as function of a strain from 0.01 to 1000%. Frequency was set at 1 Hz. Frequency sweeps tests were performed at an angular frequency range of 1-100  $\text{rad/s}^{-1}$  with a strain of 1%, which was within the linear visco-elastic region (as determined by the amplitude sweeps). The frequency sweep data were fitted with a power law model as shown below.

$$G' = k' \times w^{n'} \quad (1)$$

Where  $w$  is the oscillation frequency, and  $k'$  is model constants. The constant  $n'$  is the slope in a log-log plot of  $G'$  versus  $w$ .

The steady shear flow behavior was conducted using the same rheometer set. Viscous flow behavior was obtained at strain-controlled mode with shear rates going from 0.1 to  $100 \text{ s}^{-1}$ .

#### 4.2.10 *In vitro* digestibility

A standard *in vitro* simulated process was used in this study which was modified for the amount of  $\alpha$ -amylase (Minekus et al., 2014). Four different sets of samples were prepared for the *in vitro* digestion experiments: 1) Wheat starch-tannic acid complexes (C0, C5, C10 and C20 prepared in section 2.2) were directly used for *in vitro* digestion. 2) Wheat starch-tannic acid mixtures were prepared by simply mixing 2.5 g of native wheat starch with 0.125, 0.25 and 0.5 g of tannic acid. 3) & 4) Gelatinized wheat starch-tannic acid complexes and mixtures were prepared according to section 2.5. After cooling down to room temperature, they were freeze dried and used for digestion experiments and resistant starch measurement. The resistant starch content was measured by the Resistant Starch Assay Kit (Megazyme).

Briefly, 2.5 g of the samples was mixed with 2.5 g of water for hydration. Then the samples were treated with simulated gastric fluids and pepsin (5.86 mg/mL, the pepsin activity is 4268 U/mg). The pH of the mixture was adjusted to 3 and incubated at 37 °C with agitation for 2 h. Then, simulated intestinal fluids and pancreatin (40 mg/mL, the  $\alpha$ -amylase activity is 40 U/mg) were added to the mixture and the pH was adjusted to 7. The mixture was incubated at 37 °C with agitation for 2 h. During the intestinal phase, 0.1 mL of sample was collected at different time points (0, 10, 20, 40, 60, 80, 100, 120 min). Then 0.4 mL of absolute ethanol was added to stop the reaction and the mixture was centrifuged at 13000 g for 10 min. Finally, 2 mL of amyloglucosidase (27.16 U/mL) was added and incubated at 37°C for an extra hour to complete starch digestion. The bio-accessibility of TA after gastric digestion was measured according to our recently published paper (Kan et al., 2020). A first-order kinetics model was applied to describe the kinetics of glucose release from starch digestion (Dona, Pages, Gilbert, & Kuchel, 2010).

$$C_t - C_0 = C_\infty(1 - e^{-kt}) \quad (1)$$

where  $C_t$ ,  $C_0$  and  $C_\infty$  correspond to the percentage of digested starch at time  $t$ , 0 and infinite time, and  $k$  is the kinetic constant. Parameter estimation was performed using the solver function of excel software by minimizing the residual sum of square values.

#### 4.2.11 $\alpha$ -amylase inhibition by tannic acid in wheat starch-tannins complexes and mixtures

The  $\alpha$ -amylase inhibition assay was conducted according to a previous method with some modifications (Okutan, Kongstad, Jäger, & Staerk, 2014). Briefly, 50 mg of porcine pancreatic  $\alpha$ -amylase (10 units/mg, Sigma St. Louis, MO, USA) was dissolved in 10 mL of

100 mmol phosphate buffer (pH 7.0) containing 2 mg/mL bovine serum albumin and used as an enzyme solution. One hundred  $\mu\text{M}$  2-Chloro-4-nitrophenyl- $\alpha$ -D-maltotrioxide was dissolved in the same buffer (pH 7.0) and used as substrate solution. The  $\alpha$ -amylase inhibition of free and bound tannic acid were tested separately. Free tannic acid referred to the tannins that either potentially released from the wheat starch-tannic acid complexes, or did not interacted with starch in the wheat starch-tannins mixtures. For free tannic acid : 50  $\mu\text{L}$  of enzyme solution and 10  $\mu\text{L}$  of phosphate buffer (control) or different concentrations of tannic acid were mixed in a well of a microplate reader. After incubation for 5 min, substrate solution (50  $\mu\text{L}$ ) was added and incubated for another 5 min at room temperature. The absorbance at 405 nm was measured using a microplate reader. Bound tannic acid referred to the tannins that bound to wheat starch. For the bound tannic acid: 100 mg of wheat starch-tannins complex (sample C20, prepared in section 2.2) was mixed with 1 mL of enzyme solution. The mixture was incubated for 5 min at room temperature. Then the mixture was centrifuged (4500 g, 5 min). Then 60  $\mu\text{L}$  of the supernatant was mixed with 50  $\mu\text{L}$  of substrate. The remaining steps were the same as free tannic acid. The inhibition on  $\alpha$ -amylase was calculated by the following equation:

$$\text{Inhibition (\%)} = (A_{\text{control}} - A_{\text{sample}}) / A_{\text{control}} * 100$$

For free tannic acid:  $A_{\text{control}}$  is the absorbance of mixture of phosphate buffer, enzyme and substrate;  $A_{\text{sample}}$  is the absorbance of mixture of tannic acid, enzyme and substrate;

For bound tannic acid:  $A_{\text{control}}$  is the absorbance of mixture of supernatant from complex control (C0), enzyme and substrate.  $A_{\text{sample}}$  is the absorbance of mixture of supernatant from sample C20, enzyme and substrate.

#### 4.2.12 Statistics.

The results were expressed as mean  $\pm$  standard deviation (SD). One-way analysis of variance (ANOVA) followed by the Duncan's multiple range test was used to compare the means among different groups by the SAS 9.4 (SAS Institute Inc., Cary, NC, USA). Differences were considered significant at  $p < 0.05$ .

### 4.3. Results

#### 4.3.1 Swelling power and amylose leaching

In our study, WS-TA (wheat starch-tannic acid) complexes were prepared by mixing WS with different amount of TA for a certain time and removing free TA. As shown in Table 4.1, 22.6, 40.9 and 68.4 mg/g of complexed TA was detected when wheat starch was complexed with 5, 10 and 20% tannic acid on dry weight of starch, respectively, indicating that an amount of TA variable from 30 to 40% had complexed with WS. The effect of those complexed TA on apparent amylose content, swelling power and solubility was investigated. As shown in Table 4.1, a significant increase of the content of apparent amylose was observed in WS-TA complexes, *e.g.*, from 33.0% (C0) to 46.0% (C20). In line with the increase amount of apparent amylose, the amylose leaching also significantly increased *e.g.*, from 14.3 (C0) to 16.8 g/100g (C5), independently from the amount of bound TA. The swelling power and solubility also significantly increased when complexed with different amount of TA. Mixed TA showed opposite effects on amylose leaching of WS, *i.e.*, mixed TA reduced the amylose leaching of WS and the reduction significantly increased with increasing amount of mixed TA. The solubility and swelling power of M5 and M10 was higher than native starch, but decreased significantly in M20. The swelling power and amylose leaching of complex control (C0) was higher than the native WS (M0). TA in complexes and mixtures also shows clear differences in pasting behaviours as shown in Table S4.1 and Figure S4.1. For instance, TA in mixtures caused a progressive reduction in peak viscosity, whereas TA in complexes caused limited reduction in peak viscosity, independently with the amount of TA.

**Table 4.1.** The amount of tannic acid bound to starch, apparent amylose, amylose leaching, solubility and swelling power of wheat starch by complexation or mixing with tannic acid.

	Bound tannic acid mg/g DW of non-gelatinized complex	Apparent amylose (g/100 g DW of starch)	Amylose leaching (g/100 g DW of starch)	Solubility (g/100 g DW of starch)	Swelling power (g/g DW of starch)
C0	0	33.0 ± 0.8 a	14.3 ± 0.2 d	20.0 ± 0.0 e	13.9 ± 0.1 e
C5	22.6 ± 1.4 a	33.4 ± 0.2 ab	16.8 ± 0.2 e	21.1 ± 0.5 f	15.4 ± 0.2 gh
C10	40.9 ± 0.1 b	36.0 ± 0.1 c	16.8 ± 0.21 e	22.1 ± 1.1 fg	15.2 ± 0.2 fg
C20	68.4 ± 1.6 c	46.0 ± 0.4 d	16.7 ± 0.4 e	23.1 ± 1.6 gh	15.0 ± 0.1 f
NWS	na	33.5 ± 0.9 a	14.5 ± 0.2 d	16.0 ± 0.0 b	11.2 ± 0.2 b
M5	na	na	12.6 ± 0.2 c	16.5 ± 0.0 d	11.8 ± 0.2 c
M10	na	na	11.8 ± 0.1 b	16.2 ± 0.1 c	12.4 ± 0.4 d
M20	na	na	5.4 ± 0.0 a	15.0 ± 0.0 a	9.1 ± 0.1 a

C0, C5, C10 and C20 were starch-tannins complexes with increasing amount of bound TA. M5, M10 and M20 were starch-tannins mixtures in this study, which were prepared by simply mixing native starch with 5%, 10% and 20% of tannic acid (dry weight basis of starch) just prior to amylose leaching, solubility and swelling power analysis. NWS, native wheat starch. na: not applicable; Results are expressed as mean ± standard deviation of triplicates. Different letters in the same column indicate a significant difference between means ( $p < 0.05$ ). WS, wheat starch; TA, tannic acid.



#### 4.3.2 DSC

As shown in Figure 4.1 and Table 4.2, the first endothermic transition appeared at around 60°C and it was known as gelatinization peak of amylopectin. Both complexed and mixed TA facilitated the gelatinization of wheat starch with early gelatinization temperatures, and the temperature range ( $T_{\text{peak}} - T_{\text{onset}}$ ) also increased. Complexed TA caused no change on enthalpy of melting, whereas mixed TA caused a lower enthalpy of melting. The first endothermic peak did not appear in the reheating process (Figure 4.1 B&D), indicating complete gelatinization of starch had occurred. The second endothermic transition that appeared at around 100 °C is known as the amylose-lipid complex transition. Both complexed and mixed TA caused a lower melting temperature and higher temperature range ( $T_{\text{peak}} - T_{\text{onset}}$ ), as well as the higher enthalpy of melting of the amylose-lipid complex. In addition, melting enthalpy and temperature range ( $T_{\text{peak}} - T_{\text{onset}}$ ) of amylose-lipid complex was higher in WS-TA complexes than in WS-TA mixtures. During the cooling stage after the initial heating, all samples displayed one exothermic transition, which were attributed to the formation of starch-lipid complex (Supplementary Table S4.2). The third endothermic transition appeared at 130~150 °C, possibly indicating the formation of amylose-tannins complexes. As shown in Figure 4.1, only a small peak appeared in C10 and C20, but much larger peaks appeared in WS-TA mixtures. The enthalpy of this transition increased with the amount of TA complexed or mixed with starch (Figure 4.1 A&C). This peak was not thermo-reversible since it did not appear in the reheating cycle (Figure 4.1 B&D).

**Table 4.2.** The effect of tannic acid on the gelatinization starch by thermal analysis using differential scanning calorimeter

1 <sup>st</sup> peak	T <sub>onset</sub> (°C)	T <sub>peak</sub> (°C)	T <sub>conclusion</sub> (°C)	Δ T <sub>peak</sub> -T <sub>onset</sub> (°C)	Enthalpy (J/g)
C0	54.6 ± 0.3 d	59.0 ± 0.2 bc	65.7 ± 0.4 bc	4.4 ± 0.1 a	12.0 ± 0.4 b
C5	54.2 ± 0.1 bcd	58.9 ± 0.2 bc	65.4 ± 0.2 ab	4.7 ± 0.1 ab	12.3 ± 0.1 b
C10	54.0 ± 0.2 bc	58.6 ± 0.1 ab	65.2 ± 0.3 ab	4.6 ± 0.1 ab	12.4 ± 0.3 b
C20	53.7 ± 0.1 b	58.4 ± 0.1 a	64.8 ± 0.1 ab	4.7 ± 0.0 ab	12.5 ± 0.3 b
NWS	55.6 ± 0.1 e	60.6 ± 0.1 e	67.2 ± 0.3 d	4.9 ± 0.2 b	12.2 ± 0.4 b
M5	54.5 ± 0.0 cd	60.0 ± 0.0 d	66.6 ± 0.3 cd	5.5 ± 0.0 c	12.0 ± 0.1 b
M10	53.8 ± 0.1 b	59.3 ± 0.1 c	65.7 ± 0.1 bc	5.5 ± 0.2 c	11.6 ± 0.3 ab
M20	52.9 ± 0.1a	58.4 ± 0.1 a	64.6 ± 0.3 a	5.5 ± 0.1 c	11.0 ± 0.1 a
2 <sup>nd</sup> peak	T <sub>onset</sub> (°C)	T <sub>peak</sub> (°C)	T <sub>conclusion</sub> (°C)	Δ T <sub>peak</sub> - T <sub>onset</sub> (°C)	Enthalpy (J/g)
C0	94.3 ± 0.6 d	100.5 ± 0.2 e	105.6 ± 0.3 d	6.2 ± 0.4 ab	0.59±0.04 d
C5	85.8 ± 0.3 bc	95.1 ± 0.2 d	101.4 ± 0.4 c	9.4 ± 0.3 cd	0.71±0.08 c
C10	84.0 ± 0.3 ab	94.0 ± 0.1 c	100.8 ± 0.9 bc	10.0 ± 0.3 d	0.89±0.02 c
C20	82.4 ± 0.4 a	93.1 ± 0.7 bc	99.9 ± 0.5 bc	10.8 ± 0.4 d	1.08±0.10 c
NWS	95.2 ± 0.1 d	100.6 ± 0.1 e	106.2±0.2 d	5.4±0.1 a	0.42 ± 0.03 b
M5	86.0 ± 1.0 c	93.6 ± 0.4 c	99.8±0.7 bc	7.6±0.7 bc	0.61 ± 0.09 a
M10	85.5 ± 0.8 bc	92.3 ± 0.2 ab	99.0±0.6 ab	6.8±1.0 ab	0.64 ± 0.09 a
M20	84.7 ± 0.4 bc	91.7 ± 0.2 a	97.8±0.4 a	7.0±0.1 ab	0.61 ± 0.02 a
3 <sup>rd</sup> peak	T <sub>onset</sub> (°C)	T <sub>peak</sub> (°C)	T <sub>conclusion</sub> (°C)	Δ T <sub>peak</sub> - T <sub>onset</sub> (°C)	Enthalpy (J/g)
C0	nd	nd	nd	nd	nd
C5	nd	nd	nd	nd	nd
C10	145.8 ± 0.0 c	151.3 ± 0.0 c	145.8 ± 0.0 bc	5.5 ± 0.0 a	0.21± 0.02 a
C20	140.5 ± 0.1 b	145.2 ± 0.1 b	140.5 ± 0.1 a	4.7 ± 0.1 a	0.24 ± 0.08 a
NWS	nd	nd	nd	nd	nd
M5	141.1 ± 0.0 b	151.5 ± 0.0 c	155.3 ± 0.0 c	10.4±0.0 c	0.89 ± 0.00 b
M10	138.5 ± 2.6 b	146.6 ± 1.5 b	153.2 ± 1.6 b	8.1±1.1 b	1.04 ± 0.08 b
M20	131.5 ± 1.0 a	142.5 ± 0.6 a	150.2 ± 0.3 a	11.0±0.5 c	1.88 ± 0.34 c

T<sub>onset</sub> temperature, it defines the start of the peak. T<sub>peak</sub> temperature, it defines the temperature that causes the largest heat flow difference. T<sub>conclusion</sub> temperature, it defines the end of the peak. Enthalpy shows the melting enthalpy, indicating the amount of energy required to melt the starch granules. All temperatures are expressed in °C. nd; not detected.

Results are expressed as mean ± standard deviation of triplicate. Different letters in the same column indicate significant difference. pH of C0, C5, C10 and C20 were 7.0, 4.7, 4.6 and 4.2, respectively. pH of NWS, M5 TA, M10 and M20 were 7, 4.6, 3.4 and 3.3, respectively.

C0, C5, C10 and C20 were starch-tannins complexes with increasing amount of bound TA. M5, M10 and M20 were starch-tannins mixtures in this study, which were prepared by simply mixing native starch with 5%, 10% and 20% of tannic acid (dry weight basis of starch), NWS, native wheat starch.

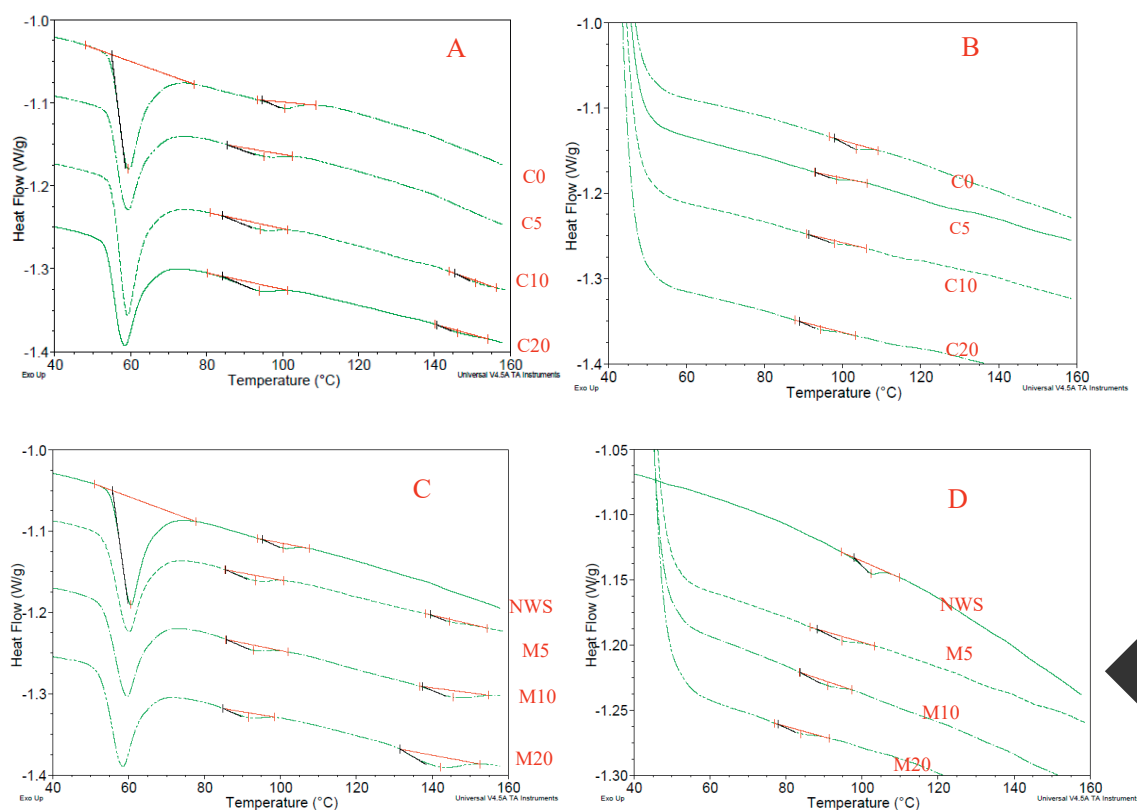


**Figure 4.1:** Thermal behaviour curve of : A) First cycle of wheat starch complexed with 5%, 10% and 20% of tannic acid; B) Second cycle of wheat starch complexed with 5%, 10% and 20% of tannic acid; C) First cycle of wheat starch mixed with 5%, 10% and 20% of tannic acid. D) Second cycle of wheat starch mixed with 5%, 10% and 20% of tannic acid. C0, C5, C10 and C20 were starch-tannins complexes with increasing amount of bound TA. M5, M10 and M20 were starch-tannins mixtures in this study, which were prepared by simply mixing native starch with 5%, 10% and 20% of tannic acid (dry weight basis of starch). NWS, native wheat starch.

## 4.3.3 XRD

The XRD patterns and corresponding crystallinity of native wheat starch, WS-TA complexes, gelatinized WS-TA complexes and gelatinized WS-TA mixtures are shown in Figure 4.2. As shown in Figure 4.2A, native WS presented a typical A-type XRD pattern with strong peaks at  $2\theta = 15^\circ$ ,  $17^\circ$ ,  $18^\circ$  and  $23^\circ$ , and this is generally regarded as the typical A-type starch (Pan et al., 2019). Complexed TA increased the relative crystallinity (RC) of wheat starch, *eg.*, C0 and C1 complex showed a RC value of 33.9% and 36.5%, respectively. The XRD patterns of gelatinized WS-TA complexes and gelatinized WS-TA mixtures were measured and shown in Figure 4.2 C&D. The RC of gelatinized starch was increased dependently with the amount of complexed and mixed TA (Figure 4.2 C&D). The relative increase in RC was much higher for complexes than for mixtures in the gelatinized samples.

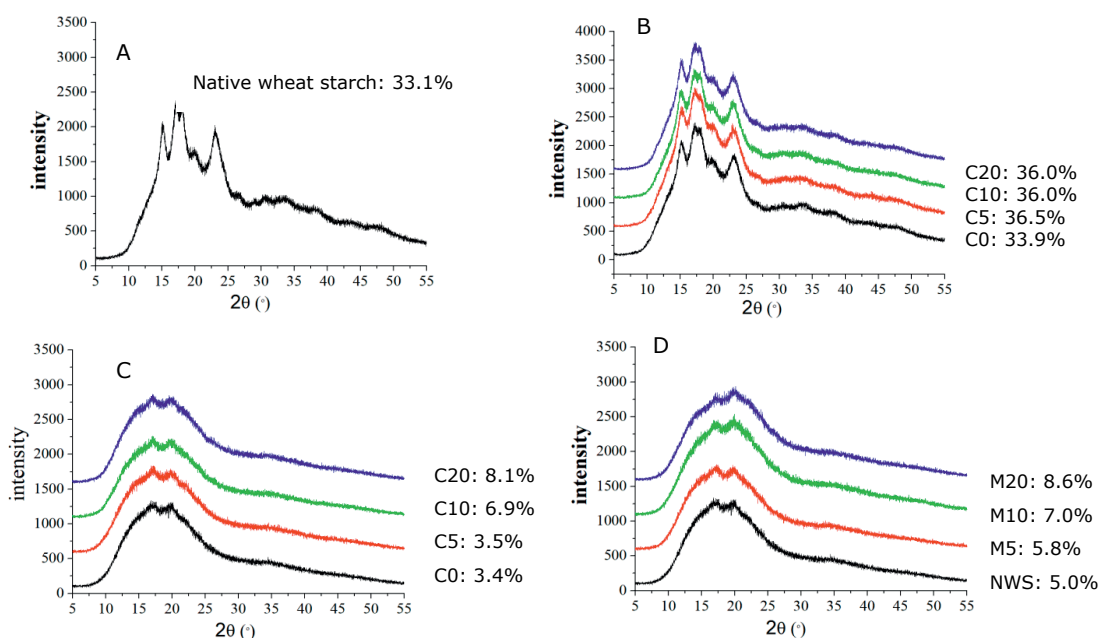


**Figure 4.2.** XRD patterns and relative crystallinity of A) Native wheat starch, B) wheat starch-tannic acid complex, C) gelatinized wheat starch-tannic acid complex, D) gelatinized wheat starch-tannic acid mixtures. Relative crystallinity of each samples was marked on the curve. C0, C5, C10 and C20 were starch-tannins complexes with increasing amount of bound TA. M5, M10 and M20 were starch-tannins mixtures in this study, which were prepared by simply mixing native starch with 5%, 10% and 20% of tannic acid (dry weight basis of starch).

### 4.3.4 Rheological properties

#### 4.3.4.1 Frequency sweep

Frequency dependence of wheat starch gels influenced by complexed and mixed TA is shown in Figure 4.3. Elastic modulus  $G'$  exceeded loss modulus  $G''$  without any crossover point within the frequency range of 0.01–100 rad/s in all the wheat starch gels complexed or mixed with TA except for native wheat starch (NWS) and WS-TA complex with lower amount of TA (C5). A clear crossover point where  $G'$  equals  $G''$  was found in NWS and C5 at around 50 rad/s as marked at Figure 4.3A and 4.3C, respectively, after which  $G''$  started exceed  $G'$ . The power-law model was fitted at frequency range where  $G'$  was higher than  $G''$ . The power-law model's parameters are presented in Table 4.3. Complexed TA and mixed TA showed opposite effects on the power-law model's parameters. Smaller amount of TA in complexes (C5 and C10) significantly lowered the  $k'$  and  $k''$  values and increased the  $n'$  and  $n''$  values. Large amount of TA in complexes (C20) significantly increased the  $k'$  and  $k''$  values and decreased the  $n'$  and  $n''$  values. However, TA in mixtures caused significant increase of  $k'$  and  $k''$  values and significant reduction of  $n'$  and  $n''$  values, though the increase and reduction is not always TA-dose dependent.

**Table 4.3.** The parameters of the power-law model determined by frequency sweep tests and parameters in the LVE region determined by amplitude sweep tests for wheat starch gel in presence of tannic acid

	Frequency sweep tests $G' = k'(\omega)^{n'}$			Amplitude sweep test	
	$k'$	$n'$	$R^2$	$G'_{LVE}$ (Pa)	$\tan(\delta_{LVE})$
C0	16.2 ± 1.2 d	0.11 ± 0.02 bc	0.98 ± 0.01	24.3 ± 0.3 f	0.26 ± 0.00 b
C5	4.2 ± 0.8 a	0.17 ± 0.02 e	0.97 ± 0.02	7.4 ± 0.2 b	0.41 ± 0.01 e
C10	8.2 ± 1.1 b	0.15 ± 0.01 de	0.99 ± 0.00	13.0 ± 0.0 c	0.31 ± 0.00 d
C20	26.8 ± 1.8 e	0.11 ± 0.00 bc	1.00 ± 0.00	41.2 ± 0.2 g	0.17 ± 0.00 a
NWS	4.3 ± 0.4 a	0.13 ± 0.01 cd	0.98 ± 0.01	6.4 ± 0.1 a	0.49 ± 0.02 f
M5	12.5 ± 0.8 c	0.08 ± 0.00 a	0.99 ± 0.00	16.2 ± 0.2 d	0.32 ± 0.01 d
M10	11.5 ± 0.8 c	0.10 ± 0.00 b	0.99 ± 0.01	17.1 ± 0.1 e	0.29 ± 0.01 c
M20	41.8 ± 1.7 f	0.07 ± 0.00 a	0.99 ± 0.00	52.6 ± 0.6 h	0.17 ± 0.00 a

The power-law model was applied to frequency sweep tests were  $G' > G''$ . The parameter  $k'$  is power-law model constants. The parameter  $n'$  is the slope in a log–log plot of  $G'$  and  $G''$  versus oscillation frequency  $\omega$ .  $\tan(\delta_{LVE}) = G''_{LVE} / G'_{LVE}$ ,  $G'_{LVE}$  and  $G''_{LVE}$  - storage modulus and loss modulus; C0, C5, C10 and C20 were starch-tannins complexes with increasing amount of bound TA. M5, M10 and M20 were starch-tannins mixtures in this study, which were prepared by simply mixing native starch with 5%, 10% and 20% of tannic acid (dry weight basis of starch). NWS, native wheat starch. Results are expressed as mean ± standard deviation of triplicate. Different letters in the same column indicate significant difference.

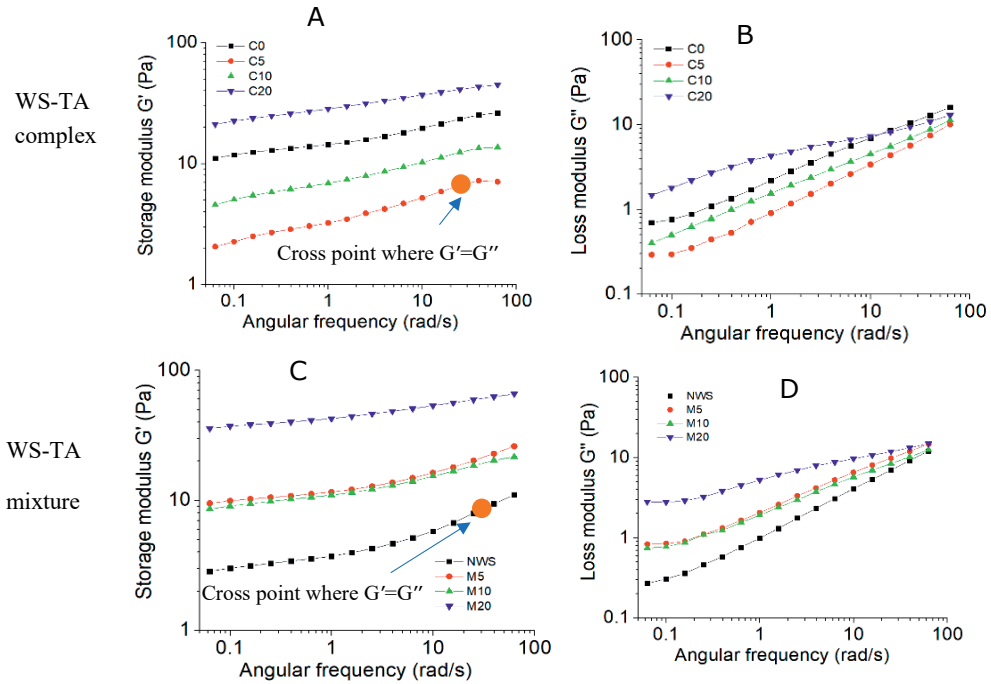


**Figure 4.3.** Frequency dependence of (A) Storage modulus ( $G'$ ) and (B) Loss modulus ( $G''$ ) for the WS-TA complex; Frequency dependence of (C) Storage modulus ( $G'$ ) and (D) Loss modulus ( $G''$ ) for the WS-TA mixtures. WS, wheat starch; TA, tannic acid. C0, C5, C10 and C20 were starch-tannins complexes with increasing amount of bound TA. M5, M10 and M20 were starch-tannins mixtures in this study, which were prepared by simply mixing native starch with 5%, 10% and 20% of tannic acid (dry weight basis of starch).

#### 4.3.4.2 Amplitude sweep

From the results of amplitude experiments (Figure 4.4), two distinct domains including linear viscoelastic (LVE) and non-linear viscoelastic regions were attained. In the LVE region, the  $G'$  and  $G''$  are almost constant and at the non-linear region both start to decrease and at a certain strain both sharply diminishes. A strain hardening behaviour was found indicating by the small peak in  $G'$  and  $G''$  (Figure 4.4). In agreement with the transient network theory, strain hardening evidence a shear-induced increase of the density of elastically active chains through an increase in the proportion of bridging chains (Brassinne, Gohy, & Fustin, 2014). The rheological parameters were shown in Table 4.3. Storage modulus ( $G'_{LVE}$ ) were higher than loss modulus ( $G''_{LVE}$ ) of all samples in the LVE region. Compared to complex control (C0), C5 and C10 decreased  $G'_{LVE}$  and  $G''_{LVE}$ , but C20

enhanced those parameters. Compared to NWS gels,  $G'_{LVE}$  and  $G''_{LVE}$  of WS-TA mixtures were enhanced.

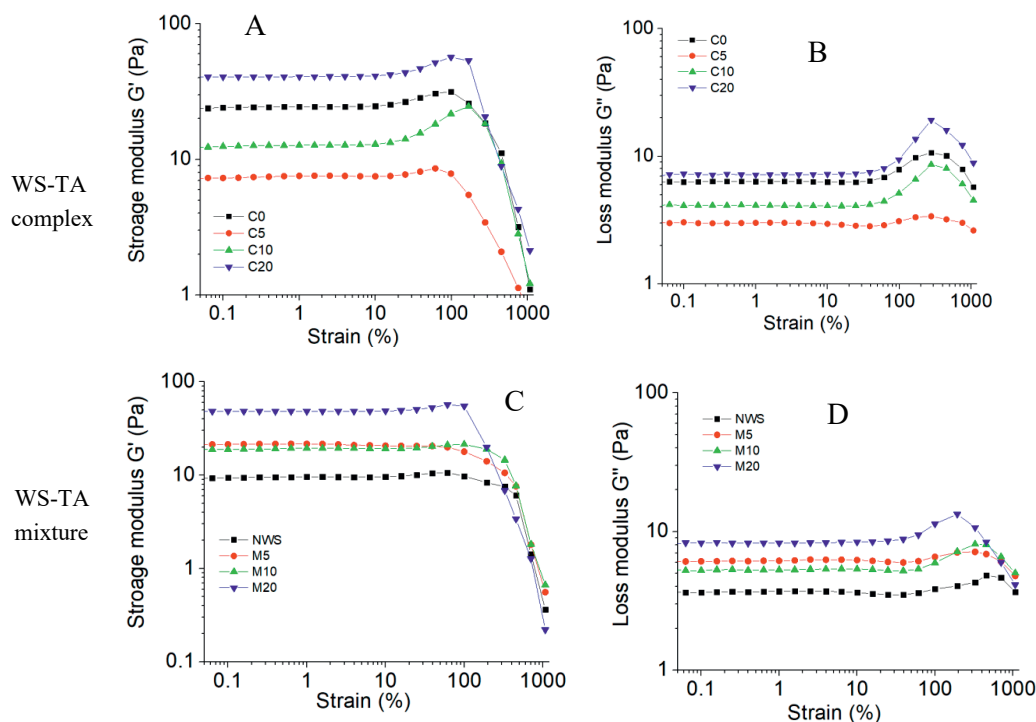


**Figure 4.4.** Amplitude dependence of (A) Storage modulus ( $G'$ ) and (B) Loss modulus ( $G''$ ) for the WS-TA complex; Frequency dependence of (C) Storage modulus ( $G'$ ) and (D) Loss modulus ( $G''$ ) for the WS-TA mixtures. WS, wheat starch; TA, tannic acid. WS-TA0, WS-TA1, WS-TA2 and WS-TA3 were starch-tannins complexes. C0, C5, C10 and C20 were starch-tannins complexes with increasing amount of bound TA. M5, M10 and M20 were starch-tannins mixtures in this study, which were prepared by simply mixing native starch with 5%, 10% and 20% of tannic acid (dry weight basis of starch).

#### 4.3.4.3 Steady flow properties

The flow behaviour of WS-TA complexes and mixtures is shown in Figure S4.2. The viscosity of all starch pastes decreases exponentially with increasing the shear rate. C5 showed lower viscosity than complex control (C0) (Figure S4.2). But C10 and C20 showed higher viscosity than WS-TA0 (Figure S4.2). The starch mixed with TA exhibits higher apparent viscosity than NWS (Figure S4.2) predominantly in the lower shear rate (0.01~1 1/s).

#### 4.3.5 *In vitro* digestibility

The effect of TA in WS-TA complexes and mixtures on starch digestibility was investigated and shown in Figure 4.5. A limited exponential model was fitted to the data and the estimated  $k$  and  $C_{\infty}$  were shown in Table 4.4. Firstly, four WS-TA complexes with different amount of TA was digested. As shown in Figure 4.5A&Table 4.4, complexed TA in C5 showed no inhibition on starch digestibility. Clear inhibition was caused by complexed TA in C10 and C20, *i.e.*, 44.0%, 26.9% and 3.4% of starch was digested in the C0, C10 and C20. Then the four WS-TA complexes were gelatinized and the starch digestibility was measured as well (Figure 4.5C). The starch digestibility of all the gelatinized complexes was decreased compared to the native starch and a clear dose-dependent inhibition by complexed TA was observed. Then starch-tannins mixtures were also prepared by simply mixing native starch with tannic acid just prior to “*in vitro* digestion” and “gelatinization and *in vitro* digestion” as shown in Figure 4.5B&D, respectively. Interestingly, for both non-gelatinized and gelatinized starch, the starch digestibility was significantly inhibited by 5% of mixed TA, and 10% and 20% of mixed almost inhibited all the starch digestibility (Figure 4.5B&D). The inhibition of mixed TA is much stronger than complexed TA in both gelatinized and non-gelatinized samples. Resistant starch (RS) content was measured. Regarding the non-gelatinized WS-TA complex (Table 4.4), more than 70% of RS was detected compared with control (1.73%). Similar results was observed all the gelatinized samples (Table 4.4), *i.e.*, 40%~60% of RS was found in gelatinized WS-TA complex and mixtures, whereas about 6% of RS was found in gelatinized native / control starch.



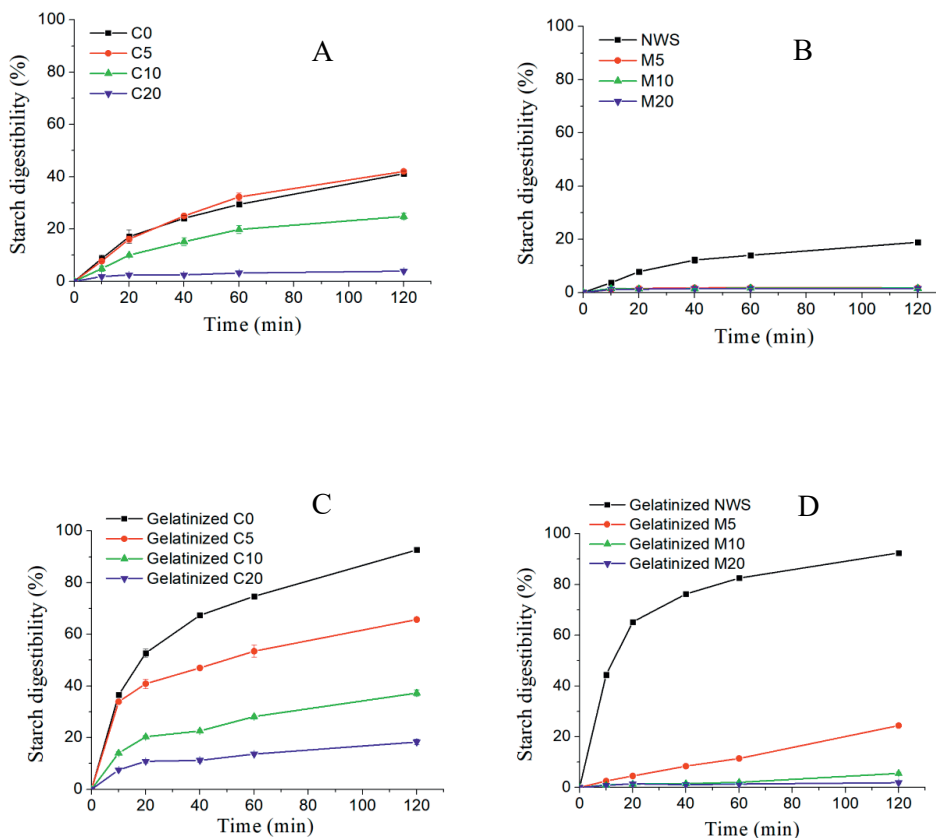


**Figure 4.5:** *In vitro* starch hydrolysis profiles of A) non-gelatinized wheat starch-tannic acid complex; B) non-gelatinized wheat starch-tannic acid mixture;; C) gelatinized wheat starch-tannic acid complex; D) gelatinized wheat starch-tannic acid mixture. C0, C5, C10 and C20 were starch-tannins complexes with increasing amount of bound TA. M5, M10 and M20 were starch-tannins mixtures in this study, which were prepared by simply mixing native starch with 5%, 10% and 20% of tannic acid (dry weight basis of starch).

**Table 4.4:** Estimated kinetic parameters for starch digestion obtained from *in vitro* digestion and resistant starch content and bio-accessibility of TA after gastric phase digestion of A) non-gelatinized starch-tannic acid complex; B) mixture of native starch and tannic acid; C) gelatinized starch-tannic acid complex; D) gelatinized mixture of starch and tannic acid.

Samples A	C0	C5	C10	C20	Samples B	NWS	M5	M10	M20
k (min <sup>-1</sup> )	0.02 ± 0.00	0.02 ± 0.00	0.02 ± 0.00	0.06 ± 0.01	k (min <sup>-1</sup> )	0.02 ± 0.00	NA	NA	NA
C <sub>∞</sub> (%)	44.0 ± 0.0 e	46.2 ± 0.0 d	26.9 ± 1.0 c	3.4 ± 0.1 a	C <sub>∞</sub> (%)	19.9 ± 0.9 b	NA	NA	NA
% * min <sup>-1</sup>	0.9 ± 0.0	0.9 ± 0.1	0.6 ± 0.1	0.2 ± 0.0	% * min <sup>-1</sup>	0.5 ± 0.0	NA	NA	NA
Sum of square	18.4 ± 15.3	2.1 ± 0.7	2.2 ± 1.7	0.8 ± 0.3	Sum of square	2.2 ± 0.5	NA	NA	NA
RS (%)	1.73 ± 0.02 b	73.2 ± 0.5 c	81.6 ± 0.8 d	83.3 ± 0.9 e	RS (%)	0.84 ± 0.00 a	NA	NA	NA
Bio-accessibility	NA	0.35 ± 0.02	0.47 ± 0.01	0.66 ± 0.01	Bio-accessibility	NA	3.27 ± 0.50	7.68 ± 0.74	18.66 ± 0.51
Samples C	Gelatinized C0	Gelatinized C5	Gelatinized C10	Gelatinized C20	Samples D	Gelatinized NWS	Gelatinized M5	Gelatinized M10	Gelatinized M20
k (min <sup>-1</sup> )	0.04 ± 0.00	0.07 ± 0.00	0.04 ± 0.00	0.06 ± 0.00	k (min <sup>-1</sup> )	0.06 ± 0.01	NA	NA	NA
C <sub>∞</sub> (%)	87.0 ± 0.3	58.0 ± 1.1	34.9 ± 0.7	15.1 ± 0.0	C <sub>∞</sub> (%)	87.0 ± 0.3	NA	NA	NA
% * min <sup>-1</sup>	3.8 ± 0.2 c	3.8 ± 0.2 c	1.2 ± 0.0 b	1.0 ± 0.0 a	% * min <sup>-1</sup>	4.9 ± 0.9 d	NA	NA	NA
Sum of square	130.3 ± 6.0	159.1 ± 12.7	50.8 ± 11.2	11.2 ± 0.0	Sum of square	207.9 ± 150.7	NA	NA	NA
RS (%)	6.5 ± 0.05 b	42.1 ± 0.1 c	43.1 ± 0.3 d	46.5 ± 0.2 e	RS (%)	5.9 ± 0.0 a	47.3 ± 0.2 f	49.4 ± 0.3 g	61.9 ± 0.3 h
Bio-accessibility	NA	0.21 ± 0.01	0.19 ± 0.03	0.43 ± 0.03	Bio-accessibility	NA	1.03 ± 0.03	2.59 ± 0.54	5.53 ± 0.55

C0, C5, C10 and C20 were starch-tannins complexes with increasing amount of bound TA. M5, M10 and M20 were starch-tannins mixtures in this study, which were prepared by simply mixing native starch with 5%, 10% and 20% of tannic acid (dry weight basis of starch). NWS, native wheat starch. RS, resistant starch. NA, not applicable. The values were expressed as mean ± standard deviation. The values followed by different letters in the same row of C<sub>∞</sub> and RS values indicate significantly different ( $p < 0.05$ ).

#### 4.4 Discussion.

Starch and phenolic compounds were reported to form either V-types inclusion complexes with amylose single helices facilitated by hydrophobic interactions, or complexes with much weaker binding mostly through hydrogen bonds (Chai, Wang, & Zhang, 2013). Monomeric phenolics and condensed tannins have both been reported to interact with starch to modify physiochemical properties of starch (Amoako & Awika, 2016; Gao et al., 2021). Tannic acid, which belongs to the class of hydrolysable tannins was rarely studied for interaction with starch. Besides, most of the studies focused on V-type inclusion complexes, whereas non-inclusion complexes were not widely reported. Therefore, in our study, TA was used to interact with wheat starch either by binding to wheat starch (preparation of WS-TA complexes) or as solutes in water (WS-TA mixtures), aiming to form different types of interactions.

The differences between WS-TA complexes and mixtures is not only the amount of TA but also the stage at which TA interacts with starch. The concentration of TA in mixtures was much higher than in complexes, since the free TA was removed when preparing WS-TA complexes. Besides, TA in complexes and mixtures interacted with starch at different stages. Under the complex-making conditions (37 °C, 0.5 h), WS was co-incubated with TA

solutions, TA had more time to interact with starch but it only interacted with native starch, preferably the amorphous regions of starch, which are constituted of amylose and non-ordered amylopectin branches. TA in mixtures have possibilities to interact with starch granules during many stages of heating and cooling, for instance, gelatinization and retrogradation (Donald, 2001; Waigh, Gidley, Komanshek, & Donald, 2000) but less time with the native starch. Interestingly, complex control sample (C0), as reference samples in WS-TA complexes, showed different characteristics compared with native wheat starch (Table 4.1-4.4 and Figure 4.1-4.4). This was possibly because that hydrating and swelling occurred under the conditions of WS-TA complexes preparations caused a transition from nematic structure to smectic structure, thus making the complex control different from native wheat starch (Donald, 2001; Renzetti, van den Hoek, & van der Sman, 2021).

TA in complexes and mixtures showed different mechanisms to interact with WS, *i.e.*, V-type inclusion and non-inclusion types of interactions. The presence of V-type inclusion complexes can be evidenced by the significant increase of melting enthalpy and temperature range ( $T_{\text{peak}} - T_{\text{onset}}$ ) of the second endothermic transition *i.e.*, amylose-lipid complex. In agreement with the DSC results, the RC of WS-TA complexes also increased compared to the native starch. The increase in melting enthalpy of amylose-lipid complexes was significantly higher in WS-TA complexes than in the mixtures (Table 4.2), despite the lower amount of TA present in the complexes (Table 4.1). Therefore, V-type inclusion complexes were favoured in WS-TA complexes compared to WS-TA mixtures. However, the exact mechanism for forming inclusion complexes need to be further studied. Some researchers reported that CH- $\pi$  bonds between starch pyranose rings and phenolic aromatic residues may lead to “V-type amylose” formation (Li, Ndiaye, Corbin, Foegeding, & Ferruzzi, 2020). In addition, TA may hamper the interaction between lipids and amylose helix (Chao, Yu, Wang, Copeland, & Wang, 2018), thus causing lower dissociation temperatures of amylose-lipid complex (Table 4.2). The same mechanism may explain the decreased enthalpy of the amylose-lipid related endotherm of WS-TA complexes after re-scan (Table S4.2).

The evidence of non-inclusion WS-TA interaction is the third endothermic transition in DSC results, which is observed at 130~150 °C (Table 4.2 and Figure 4.1). The third endothermic transition was not thermo-reversible since it did not appear in the reheating process (Figure 4.1B&D). Therefore, the WS-TA interactions at the third endothermic transition were possibly non-inclusion complex with much weaker binding most through hydrogen bonds. A positive relation was also found when total enthalpy of 2<sup>nd</sup> and 3<sup>rd</sup> peak

was plotted against the TA concentration (Figure 4.6A). This is because that the enthalpy change of amylose-polyphenols/lipids complexes has been proposed to reflect the amount of complex formed during gelatinization (Chao, Yu, Wang, Copeland, & Wang, 2018). A substantial amount of non-inclusion complexes were formed in WS-TA mixtures. However, for WS-TA complexes, there seemed to be a critical amount of TA needed for formation of non-inclusion complexes. In WS-TA complexes, some amount of TA formed inclusion type of complexes, and the remaining which did not form inclusion complexes was able to form non-inclusion type of complexes. This portion of TA was named as effective TA concentration available for forming non-inclusion complexes. For sample C5, the effective TA concentration for non-inclusion complexes is 0, since all the TA in C5 was used for forming inclusion complexes. Hence, the effective amount of TA for non-inclusion formation in C10 and C20 was estimated by the amount of bound TA in C10 and C20 minus the amount of TA bound to C5 (Table 4.1). As shown in Figure 6B, the melting enthalpy of the 3<sup>rd</sup> peak was positively correlated with the effective amount of TA for non-inclusion formation. The non-inclusion complexes were favoured by gelatinization of a mixture of TA with wheat starch. This could be specifically proved by comparing melting enthalpy of the third peak at the same actual concentration of TA provided by WS-TA complexes (C10) and mixtures (M5) (Figure 4.6B).

Both complexed and mixed TA influenced gelatinization of WS. A reduction in the peak temperature of gelatinization  $T_{peak}$  was observed in both complex and mixture samples (Table 4.2). C0 and NWS had significantly different gelatinization temperatures (Table 2). Therefore,  $T_{peak}/T_{peak0}$ , instead of  $T_{peak}$ , was plotted against the actual amount of TA over WS to show the relation between the amount of TA and gelatinization temperatures (Figure 4.6C). A TA-dose dependent reduction of  $T_{peak}/T_{peak0}$  (Figure 4.6C) was observed. Therefore, TA seemed to act as a plasticizer, facilitating a reduction in  $T_{peak}$ . It was reported that the more effective the solvent is at plasticizing the granule, the less the amount of thermal plasticization necessary to initiate gelatinization (Donald, 2001). Besides, the reduction of  $T_{peak}$  in WS-TA complexes could be also due to the reduction of starch concentration in starch solutions in presence of complexed TA. In addition to the plasticizing effect and the reduction of starch concentration, the acidic pH caused by TA should be considered as well. pH value of the complex and mixture is 4.2~4.7, and 3.4~3.6, respectively. A remarkable pH sensitivity of starch gelatinization was reported and partial hydrolysis of the starch in acidic solutions lowered gelatinization temperature of amylopectin (Builders, Mbah, Adama, & Audu, 2014). The

increase in gelatinization temperature range ( $T_{\text{peak}}-T_{\text{onset}}$ ) in both complexes and mixtures (Table 4.2) implied that the crystallites of starches became heterogeneous due to the addition of TA (Xiao et al., 2011). Green tea polyphenols was also reported to increase the gelatinization temperature range of rice starch (Xiao et al., 2011). Interestingly, no change in gelatinization enthalpy was observed in WS-TA complexes, but a significant decrease was observed in the WS-TA mixtures. This could be attributed to the lower pH and more amount of TA in mixtures than in complexes.

During cooling, a starch gel with three-dimensional network can be formed due to the re-arrangement of starch molecules and studied by means of its dynamic viscoelastic properties (Yousefi & Razavi, 2015). The magnitude of  $G'$  and  $G''$  of all the samples increased with an increase in frequency (Figure 4.3), showing all the tested samples had weak gel behaviour (Pourfarzad, Yousefi, & Ako, 2021). The presence of complexed and mixed TA showed opposite effects on  $G'$  and  $G''$  (Figure 4.3, 4.4 & S4.2). This could be explained by the different amount of inclusion and non-inclusion complexes in WS-TA complexes and mixtures. In the mixtures, a substantial amount of non-inclusion complexes was formed, which are cross-linked amylose-TA complexes. The cross-linked complexes are increasingly formed with increasing TA%, which resulted in the increasing  $G'$  and  $G''$ , as well as the reduction of frequency dependency indicated by the reduction of parameter  $n$  from power-law model (Figure 4.3, Table 4.3). The less frequency dependence evidenced the formation of stronger gel network structures in presence of mixed TA. The cross-linking effect of non-inclusion complexes could be supported by plotting  $G'_{LVE}/G'_{LVE,0}$  against effective TA concentration for non-inclusion complexes (Figure 4.6D).  $G'_{LVE}/G'_{LVE,0}$  increased dependently with the effective TA concentration (Figure 4.6D). The cross-linked complexes formed in WS-TA mixtures could also cause less amylose leaching out or forming insoluble complex of leached amylose, thus influencing the determination of amylose leaching due to its insolubility (Table 4.1). Some other researchers also reported WS and TA could form complexes by three stage, *i.e.*, forming soluble complexes, insoluble complexes or even aggregates with the increasing of TA/WS ratio (Wei, Li, & Li, 2019). Regarding WS-TA complexes, a substantial amount of inclusion complexes were formed and non-inclusion complexes only formed at high TA% (Table 4.2). These inclusion complexes did not form cross-links and also seemed to reduce the amount of amylose which can subtract amylose for re-crystallization, thus reducing  $G'$  and viscosity and increasing frequency dependence when low TA% present in WS-TA complexes (Figure 4.3-4.5 ). When the high TA% was present,

the non-inclusion complexes also formed and hence cross-linked gels, thus increasing  $G'$  and viscosity and decreasing frequency dependence when high TA% present in WS-TA complexes. This could be supported by comparing Figure 4.6D and Figure 4.6E, *i.e.*,  $G'_{LVE}/G'_{LVE0}$  increased dependently with the effective TA concentration for non-inclusion complexes, rather than total TA concentrations added to starch.

Finally, the inhibition of TA on WS digestibility was measured. In our previous study (Kan et al., 2020), we reported that polyphenols inhibit starch digestion by  $\alpha$ -amylase inhibition and starch-polyphenols interactions. In this study, we studied more in detail the effects of inclusion and non-inclusion complexes on starch digestibility. Firstly,  $\alpha$ -amylase inhibition of free and bound TA was measured. Instead of starch, 2-Chloro-4-nitrophenyl- $\alpha$ -D-maltotrioxide was used as substrate to rule out the inhibition resulting from WS-TA interaction. Bound TA showed no inhibition on  $\alpha$ -amylase, whereas free TA was a strong inhibitor ( $IC_{50}=0.16$  mg/mL). Therefore, the inhibitory effects observed on starch digestibility in non-gelatinized WS-TA complexes were predominantly attributed to inclusion complexes, because free TA was removed during sample preparation (Figure 4.5A). The inhibitory effects on starch digestion observed in non-gelatinized WS-TA mixtures was predominantly attributed to  $\alpha$ -amylase inhibition due to the substantial amount of free TA during digestion (Figure 4.5B). Regarding the gelatinized samples, the reduced digestibility ( $C_{\infty}$ ) and the increased RS resulted from the inclusion and non-inclusion complexes formed with amylose. This could be supported by plotting RS values against melting sum enthalpy of peak 2&3 (Figure 4.6F), which represent the sum amount of inclusion and non-inclusion complexes. A clear positive relation was found between RS content and sum enthalpy of peak 2&3 (Figure 4.6F). The presence of non-inclusion complexes could cause cross-linking of amylose-TA, thus reducing starch digestibility. Above a certain level of formation of these non-inclusion complexes, the starch gel is so cross-linked that it is not digested anymore (Figure 4.5D). Therefore, the formation of these cross-links caused by non-inclusion complexes is what largely controls the digestibility of the gelatinized starch in gelatinized WS-TA mixtures. However, inhibition on  $\alpha$ -amylase cannot be completely ruled out in non-gelatinized WS-TA complexes, gelatinized WS-TA complexes/mixtures due to the presence of free TA that is released during digestion of starch (bio-accessibility data in Table 4.4) or free TA that has not bound to starch (in the case of mixtures).

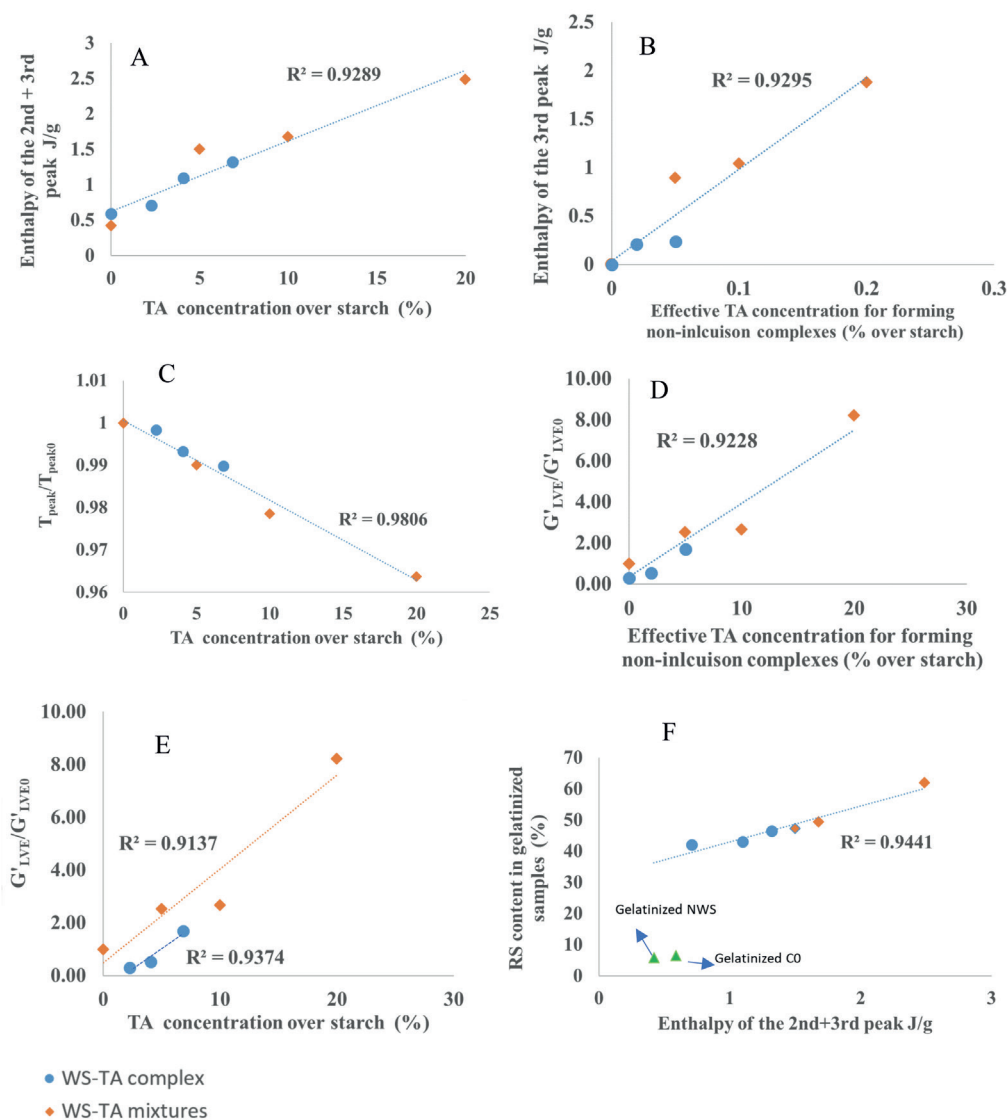


**Figure 4.6:** Plots of (A) enthalpy of the 2<sup>nd</sup> and 3<sup>rd</sup> peak against TA concentration over starch, (B) enthalpy of the 3<sup>rd</sup> peak against effective TA concentration for forming non-inclusion complexes, (C)  $T_{peak}/T_{peak0}$  against TA concentration, (D)  $G'_{LVE}/G'_{LVE,0}$  against effective TA concentration for forming non-inclusion complexes, (E)  $G'_{LVE}/G'_{LVE,0}$  against TA concentration, (F) Resistant starch content against enthalpy of the 2<sup>nd</sup> and 3<sup>rd</sup> peak. The data for plotting was from Table 2, 3 & 4. Regarding WS-TA complexes,  $T_{peak0}$  and  $G'_{LVE,0}$  are the gelatinized temperature and storage moduli of complex control (C0), respectively. Regarding WS-TA mixtures,  $T_{peak0}$  and  $G'_{LVE,0}$  are the gelatinized temperature and storage moduli of native wheat starch (NWS), respectively.

In this study, the effects of tannic acid on the physicochemical properties and *in vitro* digestibility of wheat starch were investigated. Tannic acid was added by complexing and simply mixing with wheat starch. Wheat starch interacted with tannic acid and formed inclusion and non-inclusion complexes. Non-inclusion complexes were better formed during gelatinization from a simple mix with TA than from TA previously associated with ungelatinized starch, while inclusion complexes were better formed from TA previously associated with ungelatinized. Non-inclusion complexes resulted in higher  $G'$  and lower frequency dependency, and while inclusion complexes showed opposite effects on rheology properties of wheat starch. The inclusion and non-inclusion complexes both inhibited the digestibility of the gelatinized starch. This study extends the available knowledge for a better understanding of starch–polyphenol interactions and their effects on physicochemical properties and starch digestibility. Those information can help stimulate further interest in applications of tannic acid in various starchy food.

#### **Declaration of interests**

There are no conflicts of interest to declare.

#### **Acknowledgement**

The author Lijiao Kan received a PhD scholarship from the China Scholarship Council (No. 201706820018).



**References:**

- Amoako, D. B., & Awika, J. M. (2016). Polymeric tannins significantly alter properties and in vitro digestibility of partially gelatinized intact starch granule. *Food Chemistry*, 208, 10-17. <https://doi.org/10.1016/j.foodchem.2016.03.096>.
- Biliaderis, C. G., & Galloway, G. (1989). Crystallization behavior of amylose-V complexes: Structure-property relationships. *Carbohydrate Research*, 189, 31-48. [https://doi.org/10.1016/0008-6215\(89\)84084-4](https://doi.org/10.1016/0008-6215(89)84084-4).
- Brassinne, J., Gohy, J. F., & Fustin, C. A. (2014). Controlling the cross-linking density of supramolecular hydrogels formed by heterotelechelic associating copolymers. *Macromolecules*, 47, 4514-4524. <https://doi.org/10.1021/ma500537t>.
- Builders, P. F., Mbah, C. C., Adama, K. K., & Audu, M. M. (2014). Effect of pH on the physicochemical and binder properties of tigernut starch. *Starch/Staerke*, 66, 281-293. <https://doi.org/10.1002/star.201300014>.
- Chai, Y., Wang, M., & Zhang, G. (2013). Interaction between amylose and tea polyphenols modulates the postprandial glycemic response to high-amylose maize starch. *Journal of Agricultural and Food Chemistry*, 61, 8608-8615. <https://doi.org/10.1021/jf402821r>.
- Chao, C., Yu, J., Wang, S., Copeland, L., & Wang, S. (2018). Mechanisms Underlying the Formation of Complexes between Maize Starch and Lipids. *Journal of Agricultural and Food Chemistry*, 66, 272-278. <https://doi.org/10.1021/acs.jafc.7b05025>.
- Chi, C., Li, X., Zhang, Y., Chen, L., Li, L., & Wang, Z. (2017). Digestibility and supramolecular structural changes of maize starch by non-covalent interactions with gallic acid. *Food and Function*, 8, 720-730. <https://doi.org/10.1039/c6fo01468b>.
- Dona, A. C., Pages, G., Gilbert, R. G., & Kuchel, P. W. (2010). Digestion of starch: In vivo and in vitro kinetic models used to characterise oligosaccharide or glucose release. *Carbohydrate Polymers*, 80, 599-617. <https://doi.org/10.1016/J.CARBPOL.2010.01.002>.
- Donald, A. M. (2001). Plasticization and self assembly in the starch granule. *Cereal Chemistry*, 78, 307-314. <https://doi.org/10.1094/CCHEM.2001.78.3.307>.
- Gao, S., Liu, H., Sun, L., Cao, J., Yang, J., Lu, M., & Wang, M. (2021). Rheological, thermal and in vitro digestibility properties on complex of plasma modified Tartary buckwheat

- starches with quercetin. *Food Hydrocolloids*, 110, 106209.  
<https://doi.org/10.1016/j.foodhyd.2020.106209>.
- Guo, Z., Zhao, B., Chen, J., Chen, L., & Zheng, B. (2019). Insight into the characterization and digestion of lotus seed starch-tea polyphenol complexes prepared under high hydrostatic pressure. *Food Chemistry*, 297, 124992.  
<https://doi.org/10.1016/j.foodchem.2019.124992>.
- Han, M., Bao, W., Wu, Y., & Ouyang, J. (2020). Insights into the effects of caffeic acid and amylose on in vitro digestibility of maize starch-caffeic acid complex. *International Journal of Biological Macromolecules*, 162, 922-930.  
<https://doi.org/10.1016/j.ijbiomac.2020.06.200>.
- Kan, L., Capuano, E., Fogliano, V., Oliviero, T., & Verkerk, R. (2020). Tea polyphenols as a strategy to control starch digestion in bread: the effects of polyphenol type and gluten. *Food & Function*, 11, 5933-5943. <https://doi.org/10.1039/d0fo01145b>.
- Kan, L., Oliviero, T., Verkerk, R., Fogliano, V., & Capuano, E. (2020). Interaction of bread and berry polyphenols affects starch digestibility and polyphenols bio-accessibility. *Journal of Functional Foods*, 68, 103924. <https://doi.org/10.1016/j.jff.2020.103924>.
- Li, H., Dhital, S., Slade, A. J., Yu, W., Gilbert, R. G., & Gidley, M. J. (2019). Altering starch branching enzymes in wheat generates high-amylose starch with novel molecular structure and functional properties, 92, 51-59. *Food Hydrocolloids*.  
<https://doi.org/10.1016/j.foodhyd.2019.01.041>
- Li, M., Ndiaye, C., Corbin, S., Foegeding, E. A., & Ferruzzi, M. G. (2020). Starch-phenolic complexes are built on physical CH- $\pi$  interactions and can persist after hydrothermal treatments altering hydrodynamic radius and digestibility of model starch-based foods. *Food Chemistry*, 308, 125577. <https://doi.org/10.1016/j.foodchem.2019.125577>.
- Li, M., Pernell, C., & Ferruzzi, M. G. (2018). Complexation with phenolic acids affect rheological properties and digestibility of potato starch and maize amylopectin. *Food Hydrocolloids*, 77, 843-852. <https://doi.org/10.1016/j.foodhyd.2017.11.028>.
- Liu, S., Yuan, T. Z., Wang, X., Reimer, M., Isaak, C., & Ai, Y. (2019). Behaviors of starches evaluated at high heating temperatures using a new model of Rapid Visco Analyzer – RVA 4800. *Food Hydrocolloids*, 94, 217-228.  
<https://doi.org/10.1016/j.foodhyd.2019.03.015>.

- Liu, Y., Chen, L., Xu, H., Liang, Y., & Zheng, B. (2019). Understanding the digestibility of rice starch-gallic acid complexes formed by high pressure homogenization. *International Journal of Biological Macromolecules*, 134, 856-863. <https://doi.org/10.1016/j.ijbiomac.2019.05.083>.
- M. Minekus, M. Alminger, P. Alvito, S. Ballance, T. Bohn, C. Bourlieu, F. Carrière, R. Boutrou, M. Corredig, D. Dupont, C. Dufour, L. Egger, M. Golding, S. Karakaya, B. Kirkhus, S. Le Feunteun, U. Lesmes, A. Macierzanka, A. Mackie, S. Marze, D. J. McClements, O. Ménard, I. Recio, C. N. Santos, R. P. Singh, G. E. Vegarud, M. S. J. Wickham, W. Weitschies and A. Brodkorb. (2014). A standardised static *in vitro* digestion method suitable for food – an international consensus. *Food Function*, 5, 1113–1124. <https://doi.org/10.1039/C3FO60702J>.
- Okutan, L., Kongstad, K. T., Jäger, A. K., & Staerk, D. (2014). High-resolution  $\alpha$ -amylase assay combined with high-performance liquid chromatography-solid-phase extraction-nuclear magnetic resonance spectroscopy for expedited identification of  $\alpha$ -amylase inhibitors: Proof of concept and  $\alpha$ -amylase inhibitor in cinnamon. *Journal of Agricultural and Food Chemistry*, 62, 11465-11471. <https://doi.org/10.1021/jf5047283>.
- Oliviero, T., & Fogliano, V. (2016). Food design strategies to increase vegetable intake: The case of vegetable enriched pasta. *Trends in Food Science and Technology*, 51, 58-64. <https://doi.org/10.1016/j.tifs.2016.03.008>.
- Pan, J., Li, M., Zhang, S., Jiang, Y., Lv, Y., Liu, J., Zhu, Y., Zhu, Y., Zhang, H. (2019). Effect of epigallocatechin gallate on the gelatinisation and retrogradation of wheat starch. *Food Chemistry*, 294, 209-215. <https://doi.org/10.1016/j.foodchem.2019.05.048>.
- Pourfarzad, A., Yousefi, A., & Ako, K. (2021). Steady/dynamic rheological characterization and FTIR study on wheat starch-sage seed gum blends. *Food Hydrocolloids*, 111, 106380. <https://doi.org/10.1016/j.foodhyd.2020.106380>.
- Renzetti, S., van den Hoek, I. A. F., & van der Sman, R. G. M. (2021). Mechanisms controlling wheat starch gelatinization and pasting behaviour in presence of sugars and sugar replacers: Role of hydrogen bonding and plasticizer molar volume. *Food Hydrocolloids*, 119, 106880. <https://doi.org/10.1016/j.foodhyd.2021.106880>.
- Van Hung, P., Phat, N. H., & Phi, N. T. L. (2013). Physicochemical properties and antioxidant capacity of debranched starch-ferulic acid complexes. *Starch/Staerke*, 65,

- 382-389. <https://doi.org/10.1002/star.201200168>.
- Waigh, T. A., Gidley, M. J., Komanshek, B. U., & Donald, A. M. (2000). The phase transformations in starch during gelatinisation: A liquid crystalline approach. *Carbohydrate Research*, 328, 165-176. [https://doi.org/10.1016/S0008-6215\(00\)00098-7](https://doi.org/10.1016/S0008-6215(00)00098-7).
- Wei, X., Li, J., & Li, B. (2019). Multiple steps and critical behaviors of the binding of tannic acid to wheat starch: Effect of the concentration of wheat starch and the mass ratio of tannic acid to wheat starch. *Food Hydrocolloids*, 94, 174-182. <https://doi.org/10.1016/j.foodhyd.2019.03.019>
- Xiao, H., Lin, Q., Liu, G. Q., Wu, Y., Tian, W., Wu, W., & Fu, X. (2011). Effect of green tea polyphenols on the gelatinization and retrogradation of rice starches with different amylose contents. *Journal of Medicinal Plants Research*, 5, 4298-4303. <https://doi.org/10.5897/JMPR.9000481>.
- Yousefi, A. R., & Razavi, S. M. A. (2015). Dynamic rheological properties of wheat starch gels as affected by chemical modification and concentration. *Starch/Staerke*, 67, 567-576. <https://doi.org/10.1002/star.201500005>.
- Zhang, Bin, Huang, Q., Luo, F. xing, & Fu, X. (2012). Structural characterizations and digestibility of debranched high-amylose maize starch complexed with lauric acid. *Food Hydrocolloids*, 28, 174-181. <https://doi.org/10.1016/j.foodhyd.2011.12.020>.
- Zhang, Binjia, Li, X., Liu, J., Xie, F., & Chen, L. (2013). Supramolecular structure of A- and B-type granules of wheat starch. *Food Hydrocolloids*, 31, 68-73. <https://doi.org/10.1016/j.foodhyd.2012.10.006>.
- Zhao, B., Wang, B., Zheng, B., Chen, L., & Guo, Z. (2019). Effects and mechanism of high-pressure homogenization on the characterization and digestion behavior of lotus seed starch–green tea polyphenol complexes. *Journal of Functional Foods*, 57, 173-181. <https://doi.org/10.1016/j.jff.2019.04.016>.
- Zheng, Y., Tian, J., Kong, X., Wu, D., Chen, S., Liu, D., & Ye, X. (2021). Proanthocyanidins from Chinese berry leaves modified the physicochemical properties and digestive characteristic of rice starch. *Food Chemistry*, 335, 127666. <https://doi.org/10.1016/j.foodchem.2020.127666>.
- Zhu, F. (2015). Interactions between starch and phenolic compound. *Trends in Food Science*

*& Technology*, 43, 129–143. <https://doi.org/10.1016/J.TIFS.2015.02.003>.

## Supplementary material

Supplementary Materials:

**Table S4.1** Pasting properties of wheat starch-tannic acid complexes and wheat starch mixed with different concentrations of tannic acid

Sample	Peak viscosity	Hold viscosity	Final viscosity	Set Back	Pasting	Peak	Breakdown
C0	4873 ± 24 e	3680 ± 18 f	6516 ± 33 f	2836 ± 14 d	73 ± 0 bc	95 ± 0 a	1193 ± 6a
C5	4615 ± 23 d	2615 ± 13 d	5988 ± 30 e	3373 ± 17 f	73 ± 0 bc	95 ± 0 a	2000 ± 10 f
C10	4780 ± 24 e	2577 ± 13 d	6073 ± 31 e	3496 ± 18 g	72 ± 0 b	95 ± 0 a	2203 ± 11 g
C20	4832 ± 24 e	2558 ± 13 d	5858 ± 30 d	3300 ± 17 e	71 ± 0 ab	95 ± 0 a	2274 ± 11 gh
WS (pH=7)	4694 ± 2 d	3394 ± 33 e	5886 ± 12 d	2492 ± 22 c	69 ± 1 a	95 ± 0 a	1300 ± 32 c
WS (pH=4.6)	4677± 15 d	3364± 23 e	5886 ± 29 d	2489± 27 c	69± 1 a	95 ± 0 a	1290 ± 21 bc
WS (pH=3.3)	4545± 26 d	3321± 19 e	5839 ± 17d	2482± 15 c	70± 0 a	95 ± 0 a	1224± 25 b
M5	4050 ± 71 c	2223 ± 33 c	4656 ± 40 c	2433 ± 7 c	70 ± 1 a	95 ± 0 a	1827 ± 38 e
M10	3873 ± 21 b	2098 ± 9 b	4270 ± 8 b	2172 ± 2 b	71 ± 1ab	95 ± 0 a	1775 ± 12 de
M20	3700 ± 31 a	1981 ± 6 a	3800 ± 24 a	1819 ± 18 a	75 ± 1 c	95 ± 0 a	1719 ± 25 d

The starch concentrations (dry weight basis) of all the samples is 12% (w/w). The amount of complex used was calculated by considering the amount of bound tannins as shown in Table 1. C0, C5, C10 and C20 were starch-tannins complexes with increasing amount of bound TA. M5, M10 and M20 were starch-tannins mixtures in this study, which were prepared by simply mixing native starch with 5%, 10% and 20% of tannic acid (dry weight basis of starch). Different letters in the same column indicate significant difference.

**Table S4.2** The effect of tannic acid on the gelatinization of wheat starch by thermal analysis during cooling and reheating (2<sup>nd</sup> cycle) stage.

2 <sup>nd</sup> peak	Tonset (°C)		Tpeak (°C)		Tconclusion (°C)		Enthalpy (J/g)	
	2nd cycle	cooling	2nd cycle	cooling	2nd cycle	cooling	2nd cycle	cooling
C0	96.61	76.95	102.54	82.61	106.85	85.8	0.6223	0.5776
C5	89.79	72.42	98.83	74.36	104.03	77.62	0.5968	0.2174
C10	90.56	68.6	96.91	74.18	102.27	77.7	0.2536	0.3631
C20	90.42	68.2	95.33	74.12	101.06	77.73	0.1596	0.3265
NWS	97.9	77.21	102.4	82.32	106.25	85.3	0.4272	0.5632
M5	89.32	65.56	95.42	71.34	100.19	75.01	0.266	0.3285
M10	83.78	59.6	90.54	64.68	96.67	67.99	0.3333	0.2359
M20	77.53	54.22	84.46	56.24	90.24	60.04	0.3255	0.1543

C0, C5, C10 and C20 were starch-tannins complexes with increasing amount of bound TA. M5, M10 and M20 were starch-tannins mixtures in this study, which were prepared by simply mixing native starch with 5%, 10% and 20% of tannic acid (dry weight basis of starch).

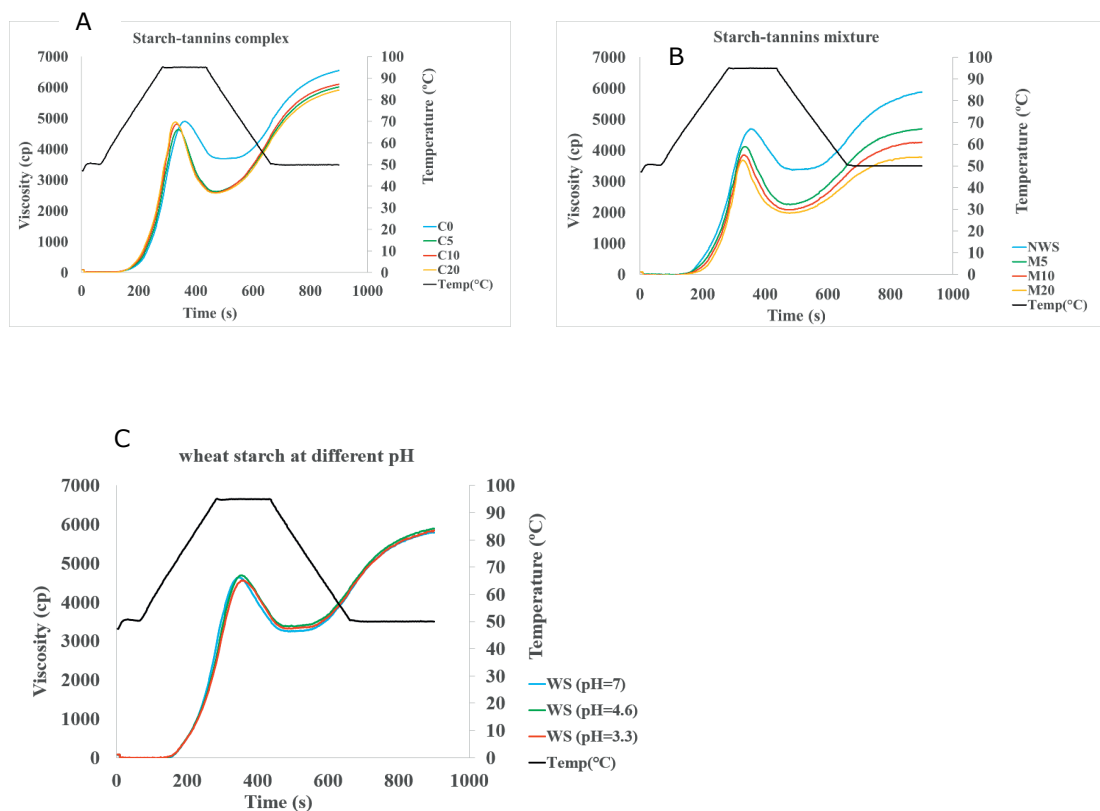



**Figure S4.1:** Pasting properties of wheat starch A) complexed with different concentrations of tannic acid. B) mixed with different concentrations of tannic acid, C) at different pH adjusted by hydrogen chloride. C0, C5, C10 and C20 were starch-tannins complexes with increasing amount of bound TA. M5, M10 and M20 were starch-tannins mixtures in this study, which were prepared by simply mixing native starch with 5%, 10% and 20% of tannic acid (dry weight basis of starch). pH of C0, C5, C10 and C20 were 7.0, 4.7, 4.6 and 4.2, respectively. pH of NWS, M5, M10 and M20 were 7, 4.6, 3.4 and 3.3, respectively.



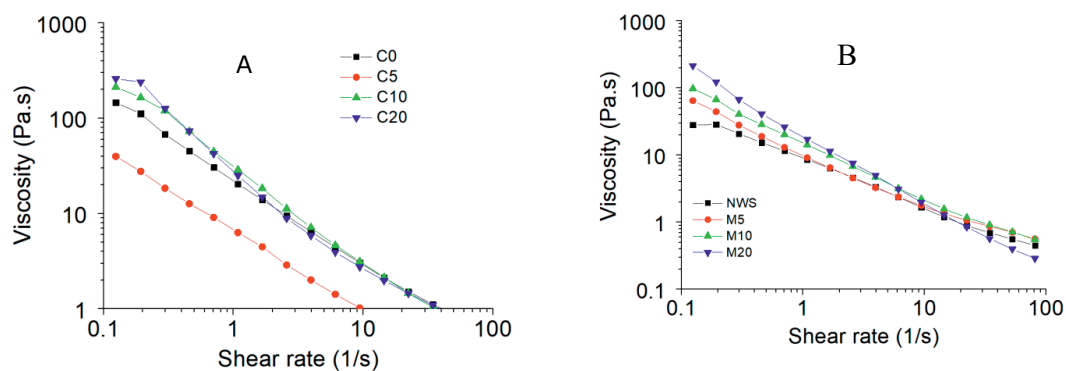


**Figure S4.2.** Shear-dependent flow curves for the A) WS-TA complex, shear rate 0.1~100 1/s; B) WS-TA mixture, shear rate 0.1~100 1/s. C0, C5, C10 and C20 were starch-tannins complexes with increasing amount of bound TA. M5, M10 and M20 were starch-tannins mixtures in this study, which were prepared by simply mixing native starch with 5%, 10% and 20% of tannic acid (dry weight basis of starch).



5

# Chapter 5

Non-inclusion starch-tannins interactions formed in starch differing in crystalline type and different amylose content

This Chapter is based on Kan, Lijiao, Yaw Gyamfi, Capuano, E., Fogliano, V. Oliviero, T., & Renzetti, S. et al. Non-inclusion starch-tannins interactions formed in starch differing in crystalline type and different amylose content (To be submitted for publication)

## Abstract

In this study, potato starch (B-type starch), waxy corn starch (A-type starch) and normal corn starch (A-type starch) were selected to interact with tannic acid by preparing complexes and mixing. Structural changes, thermal properties, pasting properties and starch digestibility were examined. Non-inclusion starch-tannins complexes were found in all three types of starch while inclusion amylose-lipid complex was found only in corn starch. Starch amylose content is one of the major factor influencing the starch-tannins interactions. Non-gelatinized amylopectin had more ability to interact with tannic acid than non-gelatinized amylose, but after gelatinization the TA interaction with amylose became the prevalent one. Physical-chemical properties of potato starch were affected by adding tannic acid most significantly compared to waxy corn starch and normal corn starch. The more open structure of B-type starch (potato) makes it easier to interact with tannic acid than tightly packed A-type starch (corn). Starch-tannins interactions as non-inclusion complexes and starch-lipid interactions as inclusion complexes both contributed to inhibit starch digestibility. These results broaden the application of tannins-modified polyphenols into starch-based food.

Key words: potato starch, corn amylopectin, corn starch, tannic acid, non-inclusion complex

## 5.1 Introduction

Starch is one of the most abundant polysaccharide mainly obtained from cereals and tubers. It has been used since ages in food applications due to its gelling, thickening, bulking and stabilizing abilities (Mahmood et al., 2017). Starch from maize, potato, wheat, tapioca etc. is currently being used by food industries; spanning from the bakery, confectionery, drinks and beverages (Bashir & Aggarwal, 2019). However, starch as ingredient and starch-rich primary products (cereals, legumes, potatoes) have some undesirably nutritional properties such as high glycemic index and functional properties like pH sensitive and heating instability (Liu et al., 2013). Design starch-rich products for modified physical-chemical properties and desired glucose release has become a preferred strategy for diverse food manufacturers. Many ingredients have been used to modify physio-chemical properties of starch, including gum, polysaccharides and salts (Suchen Liu et al., 2020; Ren et al., 2021). Among all the starch modifiers, polyphenols-modified starch have gained in popularity with broader industrial applications with desired functionality and glycemic performance (Pan et al., 2019).

Polyphenol-modified starch holds a great potential for starch-based food design with defined digestibility and altered functionality (Amoako & Awika, 2016). Recent studies reported that polyphenols interact with starch, consequently influencing rheological, structural, pasting, thermal properties and digestibility of starch or starch-based food (Gao et al., 2021). Starch-polyphenols interactions can be non-inclusive and/or inclusive amylose-phenolic complexes and it seems related to types of phenolics, types of starch and preparation methods (Deng, et., 2021). For instance, gallic acid can form inclusion complexes with rich starch and form non-inclusion complexes with maize starch (Chi et al., 2017; Y. Liu, Chen, Xu, Liang, & Zheng, 2019). Sometimes specific method need to be used to prepare inclusion complexes, eg., green tea polyphenols could form V-type inclusion complex with lotus seed starch by high-pressure homogenization and ultrasound-microwave synergistic treatment (Zhao, Sun, et al., 2019; Zhao, Wang, Zheng, Chen, & Guo, 2019). Both inclusion and non-inclusion complexes exhibited lower starch digestibility (Deng, et., 2021). Although digestibility and functionality of starch-phenolic interactions have been characterized within gelatinized starch-based food, molecular mechanisms underlying starch-phenolic complexation have not been fully explored. Insight into the starch structure-functionality relationship for starch-polyphenol interaction especially when it comes into different types of starch is required to master the phenomena and propose this approach in industrial product design.

The present study was designed to advance our understanding of the structure-functionality relationship for starch-phenolic complexes by using different types of starch. Potato starch (B-type starch), waxy corn starch (A-type starch) and normal corn starch (A-type starch) were selected to interact with tannic acid. Tannic acid was added into starch either by preparation of starch-tannins complexes *i.e.*, mixing with native starch followed by incubating and removing of free starch and mixing with native starch just before starch characteristics. Structural changes, thermal properties and pasting properties were examined by X-ray diffraction (XRD), Differential scanning calorimetry (DSC) and Rapid Visco Analysis (RVA), respectively. Finally an *in vitro* digestion was performed to determine the digestibility of starch-polyphenol complexes.

## 5.2 Materials and methodology

### 5.2.1 Materials

Potato starch, waxy corn starch, normal corn starch, potato amylose, tannic acid, pepsin (800–2500 units/mg), pancreatin (P1750; 4X USP specifications), amyloglucosidase (129 U/mg) were purchased from Sigma–Aldrich (St Louis, MO, USA). Absolute ethanol (96%) and other chemicals used were of analytical grade.

### 5.2.2 Preparation of starch-tannins complex

Briefly, 4% (w/v) of starch solution was prepared by adding 5 g of potato starch, corn amylopectin and corn starch into 120 mL of water separately. Then the solution was mixed with 0%, 5%, 10% and 20% of tannic acid based on the weight of starch, *i.e.*, 0, 0.25, 0.5 and 1 g of tannic acid. The samples were mixed thoroughly and incubated in 37°C water-bath for 30 min with continuous stirring at 300 rpm. Then the mixture was cooled to room temperature and then centrifuged at 4700 rpm for 15 min. The supernatants were collected to measure the unbound tannic acid content. The pellets were washed with distilled water several times and centrifuged until no tannic acid were detected in the supernatant. The remaining pellets after washing were freeze-dried and stored at -20 °C for further analysis. The amount of tannins bound to starch were calculated as the results of initial amount of TA added to starch minus amount of TA in washing solutions. In addition, starch-tannic acid mixtures were also prepared by simply mixing native starch and tannic acid just prior to all the analysis in this study. The coding of all the samples were listed below.

Table 5.1 The coding of all the samples used in this study.

Amount of tannic acid based on dry weight of starch	0	5%	10%	20%
Potato starch-tannic acid complexes	P_C0	P_C5	P_C10	P_C20
Potato starch-tannic acid mixtures	NPS	P_M5	P_M10	P_M20
Waxy corn starch (amylopectin)-tannic acid complexes	A_C0	A_C5	A_C10	A_C20
Waxy corn starch (amylopectin)-tannic acid mixtures	NAP	A_M5	A_M10	A_M20
Normal corn starch-tannic acid complexes	C_C0	C_C5	C_C10	C_C20
Normal corn starch-tannic acid mixtures	NCS	C_M5	C_M10	C_M20

### 5.2.3 X-ray diffraction analysis.

The XRD spectra of all the starch-tannins complex prepared in section 2.2 and native starch were measured by using an X-ray diffractometer (Bruker, D8 Advance Diffractometer, Germany). The diffraction angle was scanned from 5 to 55°. All the XRD spectra were processed with Diffraction. EVA 5.2 software.

### 5.2.4 Thermal properties by DSC differential scanning calorimeter

Differential Scanning Calorimetry (DSC) measurements were done using a Q 200 differential scanning calorimeter (TA Instruments, New Castle, DE, USA). Starch-tannin complex prepared in section 2.2 (7.5 mg) were weighed into a high-volume aluminum pan, and 22.5 mL of distilled water was added. In addition, 7.5 mg of native starch was mixed with 22.5 mL of tannic acid solution. The concentration of the tannic acid solution was 0.017, 0.034 and 0.068 mg/mL to match 5%, 10% and 20% of tannic acid, respectively, on starch dry weight. The pan was then hermetically sealed and equilibrated at room temperature overnight to allow adequate starch hydration. Samples were heated from 5 °C to 160 °C at a rate of 5 °C/min and marked as 1<sup>st</sup> cycle. Then the samples were reheated from 40°C to 160 °C and marked as 2<sup>nd</sup> cycle. Data analysis was done with TA Instruments Universal analysis 20000 software, version 4.5 A, USA.

### 5.2.5 Swelling power, solubility and amylose leaching

The swelling power and solubility of the samples were determined using the method by Yadav et al., (2016) with slight modifications. Briefly, 0.5 g of waxy corn starch-tannic acid complex or 0.5 g of normal corn starch-tannic acid complex or 0.25 g of potato starch-tannic

acid complex were suspended in 25 mL of water. In addition, 0.5 g of native waxy corn starch or 0.5 g of native normal corn starch or 0.25 g of potato starch were mixed with 5%, 10% and 20% of TA based on dry weight of starch, and the mixture was suspended in 25 mL of water. All the samples were placed in a water bath (90°C, 30 min). The slurries were mixed thoroughly during the period of heating. Then the samples were cooled down to room temperature followed by centrifuging at 4700 rpm for 15 min. The sediments were weighed. The supernatants were carefully sucked into aluminum pans, weighed and dried in an oven at 105°C for 4 hours. The weight of dried supernatants was weighed.

Thus, the swelling power and solubility of starch were calculated by using the equation:

$$\text{Swelling power (g/g)} = \frac{\text{wet weight of sediments (g)}}{\text{dry weight of the starch (g)}}$$

$$\text{Solubility (g/g)} = \frac{\text{dry weight of supernatants (g)}}{\text{dry weight of the starch (g)}}$$

For amylose leaching determination, 100 µL of the supernatant from solubility determination was diluted for 5 times. Then iodine colorimetry method was used for measuring apparent amylose in supernatant Li et al. (2019). Briefly, 40 µL of diluted samples was mixed with 1 mL of water and 200 µL of iodine solution (2.5 mM I<sub>2</sub>/6.5 mM KI mixture). then 760 µL of water was added to make up 2 mL solution. The solutions were mixed vigorously and allowed to develop color for 15 min. The absorbance was read at 600 nm. Apparent amylose content of native starch and starch-tannins complexes prepared in section 2.2 was also estimated by iodine colorimetry as mentioned above.

#### 5.2.6 RVA analysis

Pasting behaviour of all the samples was investigated using a Rapid Visco Analyser Super 4 (Perten, Hägersten, Sweden), according to a previous method with slight modifications (Siyuan Liu et al., 2019). Briefly, 3.00 ± 0.01 g of waxy corn starch-tannic acid complex or 3.00 ± 0.01 g normal corn starch-tannic acid complex or 1.70 ± 0.01 g of potato starch-tannic acid complex is mixed with 25.00 g ± 0.01 g of distilled water. The amount of starch-tannins complex was dry basis of starch by considering the moisture content and amount of bound tannic acid. In addition, the corresponding amount of native waxy corn starch, normal corn starch and potato starch (dry basis) was mixed with 5%, 10% and 20% of tannic acid, respectively. Then 25.00 g ± 0.01 g of distilled water was added. Then the samples were mixed manually until no lumps were visual anymore. The pasting experiments of corn



amylopectin and corn starch were using RVA standard 1 profile: Initial stirring speed was 960 rpm at 50°C for 60 seconds. Then, the stirring speed is decreased to 160 rpm while the temperature is increased to 95°C within 3 min 42 s. Hold at 95°C for 2 min 30 s minutes. Then cool to 50 °C within 3 min 48 s and hold at 50 °C for 2 min. The pasting experiments of PS using the same method except for the holding time at 95 °C (5 min). The analysis will be done using TCW3 software (Perten, Hägersten, Sweden).

### 5.2.7 *In vitro* digestion of starch and starch-tannin complexes

Preparation of gelatinized starch tannins complexes and mixtures: 1 g of starch-tannins complexes prepared in section 2.2 was mixed with 10 mL of water. In addition, 1 g of native waxy corn starch, normal corn starch and potato starch were mixed with 5%, 10% and 20% of tannic acid based on dry weight of starch, and the mixtures were suspended in 25 mL of water. Then the starch suspensions were put in water-bath (90°C) for 30 min after which they were cooled down to room temperature. Then the cooled starch pastes were directly used for starch digestibility analysis.

Then ungelatinized starch-tannins complexes and gelatinized starch tannins complexes and mixtures were used for *in vitro* digestion experiments. *In vitro* digestion was performed according to a standard digestion method (Minekus et al., 2014) adapted as previously described method (Kan, Capuano, Fogliano, Oliviero, & Verkerk, 2020). During gastric phase digestion, starch-tannins complex or gelatinized pastes were mixed with stimulated gastric fluids, 0.3 M CaCl<sub>2</sub> and pepsin (5.867mg/ml, 4268 U/mg). The sample were incubated at 37°C for 2 h after the pH was adjusted to 3. During intestinal phase, the digested sample from gastric digestion was mixed with stimulated intestinal fluids, bile salts, CaCl<sub>2</sub> and pancreatin (20 mg/mL,  $\alpha$ -amylase activity = 40 U/mL). Then the samples were incubated at 37°C for 2 h after the pH was adjusted to 7. During intestinal digestion, 0.1 mL of samples were collected at time 0, 10, 20, 40, 60 and 120 min, and mixed with 0.4 mL of pure ethanol immediately. Finally, amyloglucosidase was added to complete the starch digestion, followed by the GOPOD kit measurement.

The results obtained were expressed as the percentage of digested starch;

$$\% \text{ Digested starch} = \frac{\text{digested starch}}{\text{initial amount of starch}} \times 100$$

The data were then fitted to the first-order equation as suggested by (Gorri, Garcia-Alonso, & Saura-Calixto, 1997);

$$C_t - C_0 = C_\infty (1 - e^{-kt}) \quad (1)$$

Where,  $C_t$  and  $C_0$  is the percentage of digested starch at time  $t$  and 0 respectively;  $C_\infty$  is the percentage of digested starch at the infinitive time and  $k$  is a pseudo-first-order rate constant. The values of  $k$  and  $C_\infty$  were estimated by minimizing the residual sum of squares values using Solver from Excel.

The inhibition of starch digestion caused by tannic acid addition was calculated as;

$$\text{Inhibition (\%)} = \frac{C_{t \text{ control}} - C_{t \text{ sample}}}{C_{t \text{ control}}} \times 100 \quad (3)$$

Where;  $C_{t \text{ (control)}}$  is the percentage digested starch of the control starch at time  $t$ , and  $C_{t \text{ (sample)}}$  is percentage digested starch-tannin complexes.

### 5.2.8 Statistical analysis

The results of amylose leaching, solubility, swelling power, DSC and *in vitro* digestion were expressed means  $\pm$  standard deviation of triplicates. One-way analysis of variance (ANOVA) was employed followed by Duncan's multiple range test to compare the means among the groups using STATGRAPHICS Centurion XVII (version 17.2.00). All statistical tests were carried out at 95 % confidence level.

## 5.3 Results

### 5.3.1 Apparent amylose, amylose leaching and swelling power

As shown in Table 5.2, the amount of TA bound to starch were in the order: corn amylopectin > potato starch > corn starch. The apparent amylose content of both native corn starch and potato starch is 23.2% and 21.5%, respectively, which is smaller than apparent amylose of corresponding complex control, *i.e.*, 38.5% in AC0 and 33.2% in PC0, respectively. The complexed TA decreased the amount of apparent amylose in normal corn starch, whereas increased apparent amylose in potato starch.

The swelling power, amylose leaching and solubility of starch are also shown in Table 5.2. Among all three types of starch, the highest solubility, amylose leaching and swelling power was found in potato starch. The swelling power of potato starch was reduced significantly by both complexed and mixed TA. However, complexed and mixed TA behaved differently in swelling power of normal corn starch and corn amylopectin. For instance, the swelling power

of amylopectin was slightly increased by complexed TA, whereas significantly reduced by mixed TA. Complexed TA caused no significant differences on swelling power of normal corn starch, whereas mixed TA clearly reduced swelling power of normal corn starch. Regarding all three types of starch, complexed TA caused no significant differences in solubility and amylose leaching, whereas mixed TA caused a significant increase in solubility and amylose leaching.

**Table 5.2.** Amount of bound tannic acid, apparent amylose, swelling power, solubility and amylose leaching of potato starch, corn amylopectin and corn starch complexed and mixed with different amount of tannic acid.

Complexes	Bound TA (mg/g DW)	Apparent amylose g/100g DW	Swelling power (g/g)	Solubility (g/g)	Amylose leaching (g/100g DW)
P-C0	0	33.2 ± 0.5 <sup>b</sup>	99.6 ± 2.2 <sup>f</sup>	0.20 ± 0.009 <sup>c</sup>	18.7 ± 2.0 <sup>c</sup>
P_C50	16.0 ± 0.1 <sup>c</sup>	40.2 ± 0.2 <sup>d</sup>	66.5 ± 1.2 <sup>d</sup>	0.26 ± 0.003 <sup>cd</sup>	20.2 ± 2.0 <sup>c</sup>
P_C10	20.5 ± 0.5 <sup>d</sup>	40.7 ± 1.0 <sup>d</sup>	64.8 ± 2.6 <sup>d</sup>	0.26 ± 0.03 <sup>d</sup>	21.8 ± 3.5 <sup>c</sup>
P_C20	44.2 ± 0.8 <sup>g</sup>	37.4 ± 1.9 <sup>c</sup>	71.4 ± 3.6 <sup>c</sup>	0.27 ± 0.04 <sup>d</sup>	20.2 ± 3.2 <sup>c</sup>
A_C0	0	1.3 ± 0.4 <sup>a</sup>	49.0 ± 1.6 <sup>b</sup>	0.10 ± 0.03 <sup>ab</sup>	5.8 ± 0.5 <sup>a</sup>
A_C5	22.7 ± 0.3 <sup>c</sup>	1.0 ± 0.4 <sup>a</sup>	49.1 ± 1.7 <sup>c</sup>	0.14 ± 0.01 <sup>b</sup>	4.8 ± 0.2 <sup>a</sup>
A_C10	31.0 ± 1.0 <sup>f</sup>	0.3 ± 0.1 <sup>a</sup>	52.7 ± 2.4 <sup>c</sup>	0.12 ± 0.02 <sup>ab</sup>	4.2 ± 0.6 <sup>a</sup>
A_C20	53.1 ± 0.9 <sup>h</sup>	0.1 ± 0.0 <sup>a</sup>	51.8 ± 3.0 <sup>c</sup>	0.14 ± 0.04 <sup>b</sup>	5.3 ± 0.9 <sup>a</sup>
C_C0	0	38.5 ± 2.7 <sup>cd</sup>	12.4 ± 0.3 <sup>a</sup>	0.09 ± 0.003 <sup>a</sup>	16.3 ± 0.4 <sup>b</sup>
C_C5	4.8 ± 0.2 <sup>a</sup>	34.1 ± 1.0 <sup>b</sup>	11.7 ± 0.3 <sup>a</sup>	0.10 ± 0.004 <sup>ab</sup>	15.0 ± 0.2 <sup>b</sup>
C_C10	10.8 ± 0.2 <sup>b</sup>	31.8 ± 1.3 <sup>b</sup>	12.2 ± 0.1 <sup>a</sup>	0.10 ± 0.002 <sup>ab</sup>	15.9 ± 0.4 <sup>b</sup>
C_C20	22.0 ± 1.0 <sup>c</sup>	33.1 ± 2.1 <sup>b</sup>	11.9 ± 0.4 <sup>a</sup>	0.10 ± 0.002 <sup>ab</sup>	15.2 ± 0.2 <sup>b</sup>
Mixtures	Bound TA (mg/g DW)	Apparent amylose g/100g DW	Swelling power (g/g)	Solubility (g/g)	Amylose leaching (g/100g DW)
NPS	na	23.2 ± 1.6 <sup>b</sup>	70.3 ± 1.33 <sup>f</sup>	0.19 ± 0.01 <sup>c</sup> <sup>d</sup>	18.4 ± 0.9 <sup>cf</sup>
P_M50	na	na	41.2 ± 1.9 <sup>c</sup>	0.28 ± 0.01 <sup>cf</sup>	20.5 ± 0.8 <sup>g</sup>
P_M10	na	na	42.9 ± 3.2 <sup>c</sup>	0.33 ± 0.06 <sup>f</sup>	19.5 ± 2.7 <sup>fg</sup>
P_M20	na	na	40.3 ± 1.8 <sup>c</sup>	0.42 ± 0.03 <sup>g</sup>	22.3 ± 0.5 <sup>h</sup>
NAP	na	1.8 ± 0.3 <sup>a</sup>	35.6 ± 0.4 <sup>d</sup>	0.11 ± 0.03 <sup>ab</sup>	4.2 ± 0.3 <sup>a</sup>
A_M5	na	na	33.7 ± 3.0 <sup>d</sup>	0.19 ± 0.06 <sup>cd</sup>	5.9 ± 0.1 <sup>ab</sup>
A_M10	na	na	29.0 ± 1.0 <sup>c</sup>	0.21 ± 0.01 <sup>d</sup>	7.6 ± 0.4 <sup>b</sup>
A_M20	na	na	19.0 ± 3.2 <sup>b</sup>	0.29 ± 0.03 <sup>f</sup>	7.4 ± 1.2 <sup>b</sup>
NCS	na	21.5 ± 0.5 <sup>b</sup>	10.6 ± 0.1 <sup>a</sup>	0.09 ± 0.002 <sup>a</sup>	15.0 ± 0.3 <sup>c</sup>
C_M5	na	na	10.4 ± 0.2 <sup>a</sup>	0.11 ± 0.002 <sup>ab</sup>	15.8 ± 0.6 <sup>cd</sup>
C_M10	na	na	9.8 ± 0.2 <sup>a</sup>	0.14 ± 0.01 <sup>bc</sup>	17.5 ± 0.9 <sup>dc</sup>
C_M20	na	na	8.2 ± 0.1 <sup>a</sup>	0.23 ± 0.01 <sup>dc</sup>	17.2 ± 0.2 <sup>dc</sup>

Results are expressed as mean ± standard deviation of triplicate. Different letters in the same column represent significant difference. The code of the samples are refer to the coding information in Table 5.1.

### 5.3.2 XRD pattern of starch-tannins complexes

The XRD patterns and corresponding crystallinity of native starch and starch-tannins complexes for all three types of starch are shown in Figure 5.1. Native potato starch showed a

typical B-type XRD pattern with the characteristic peak at  $5.5^\circ$  (Figure 5.1A). Native corn amylopectin and normal corn starch showed a typical A-type XRD pattern with the strongest diffraction peak at  $17^\circ$   $2\theta$ , and a few small peaks at around  $2\theta$  with values of around 15, 18 and  $23^\circ$  (Figure 5.1B&C). The relative crystallinity (RC) of starch-tannins complexes were calculated as well. NPS showed the lowest RC value compared to NCS and NAP. The RC value of complex control (P\_C0, C\_C0 and A\_C0) was higher than their corresponding native starch, and this was most significant in potato starch, *i.e.*, 28.6% in NPS and 36.2% in P\_C0. Complexed TA did not change the XRD pattern of three types of starch, but affected their RC, for instance, RC of potato starch was significantly reduced from 36.2 (P\_C0) to 33.9% (P\_C20) by complexed TA. RC of corn amylopectin and normal corn starch increased in presence of lower amount of TA and decreased at higher amount of TA.

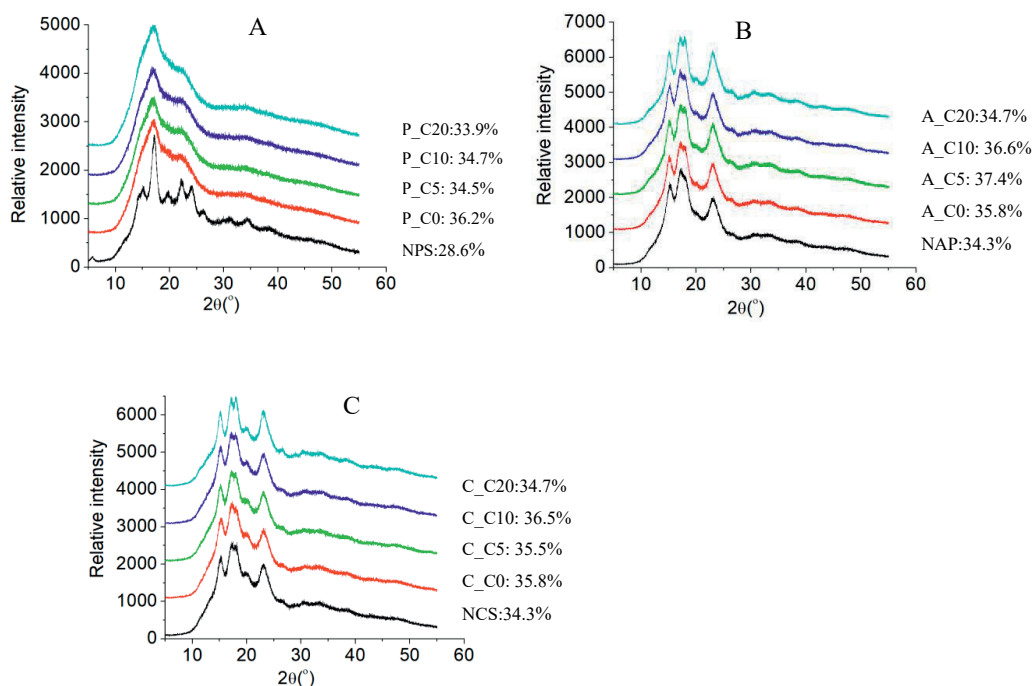


**Figure 5.1.** XRD patterns and relative crystallinity of A) potato starch, B) corn amylopectin, C) corn starch. The code of the samples are refer to the coding information in Table 5.1.

### 5.3.3 DSC of starch-tannins complexes and mixtures

As shown in Table 5.3, the first endothermic transition appeared at around 60-70°C and it corresponds to gelatinization peak of starch. The gelatinization temperature of three native starch were in the order: Native potato starch < native corn amylopectin < native normal corn starch. Both complexed and mixed TA facilitated the gelatinization of all three starch with earlier gelatinization temperatures. Complexed TA caused no change on enthalpy of melting in potato starch and normal corn starch and a small change in corn amylopectin, whereas mixed TA caused a lower enthalpy of melting in three types of starch. The second endothermic transition in corn starch appeared at around 100 °C is known as the amylose-lipid complex transition, which was not detected in potato starch and corn amylopectin. The melting temperature and enthalpy of melting of amylose-lipid in corn starch was reduced by both complexed and mixed TA. An endothermic transition appeared at 130~150 °C in both starch-tannins complexes and mixtures from all three types of starch, possibly indicating the formation of amylose-tannins complexes. The enthalpy of this transition increased with the amount of TA complexed or mixed with starch (Table 5.3). This peak was not thermo-reversible since it did not appear in the reheating cycle (data not shown).

**Table 5.3** The effect of complexed and mixed tannic acid on the gelatinization of potato starch, corn amylopectin and normal corn starch by thermal analysis using differential scanning calorimeter

1 <sup>st</sup> peak	Starch-tannins complexes				
	Tonset (°C)	Tpeak (°C)	Tconclusion (°C)	Tpeak-Tonset (°C)	Enthalpy (J/g)
P_C0	56.4 ± 0.9 <sup>a</sup>	61.8 ± 0.1 <sup>c</sup>	70.4 ± 0.2 <sup>c</sup>	5.4 ± 0.8 <sup>c</sup>	16.7 ± 0.3 <sup>d</sup>
P_C5	56.0 ± 0.1 <sup>a</sup>	61.5 ± 0.1 <sup>b</sup>	70.0 ± 0.2 <sup>bc</sup>	5.5 ± 0.0 <sup>c</sup>	16.8 ± 0.1 <sup>d</sup>
P_C10	55.4 ± 0.2 <sup>a</sup>	61.0 ± 0.0 <sup>a</sup>	69.5 ± 0.1 <sup>ab</sup>	5.6 ± 0.2 <sup>c</sup>	16.9 ± 0.0 <sup>d</sup>
P_C20	55.5 ± 0.2 <sup>a</sup>	61.0 ± 0.1 <sup>a</sup>	69.4 ± 0.1 <sup>a</sup>	5.5 ± 0.1 <sup>c</sup>	16.9 ± 0.8 <sup>d</sup>
A_C0	64.1 ± 0.2 <sup>b</sup>	71.4 ± 0.0 <sup>h</sup>	78.7 ± 0.4 <sup>g</sup>	7.3 ± 0.2 <sup>d</sup>	15.8 ± 0.1 <sup>c</sup>
A_C 5	63.6 ± 0.3 <sup>b</sup>	70.8 ± 0.1 <sup>g</sup>	77.7 ± 0.2 <sup>f</sup>	7.2 ± 0.2 <sup>d</sup>	15.4 ± 0.3 <sup>bc</sup>
A_C 10	63.3 ± 0.2 <sup>b</sup>	70.7 ± 0.2 <sup>g</sup>	77.6 ± 0.3 <sup>f</sup>	7.4 ± 0.0 <sup>d</sup>	15.1 ± 0.6 <sup>bc</sup>
A_C 20	65.2 ± 3.5 <sup>b</sup>	70.6 ± 0.1 <sup>g</sup>	77.8 ± 0.6 <sup>f</sup>	7.4 ± 0.4 <sup>d</sup>	14.6 ± 0.6 <sup>b</sup>
C_C 0	65.3 ± 0.7 <sup>b</sup>	70.2 ± 0.2 <sup>f</sup>	76.4 ± 0.4 <sup>e</sup>	4.9 ± 0.2 <sup>b</sup>	13.2 ± 0.5 <sup>a</sup>
C_C 5	64.6 ± 0.2 <sup>b</sup>	69.2 ± 0.3 <sup>e</sup>	75.9 ± 0.2 <sup>de</sup>	4.6 ± 0.1 <sup>ab</sup>	13.0 ± 0.7 <sup>a</sup>
C_C 10	64.7 ± 0.2 <sup>b</sup>	69.4 ± 0.2 <sup>e</sup>	75.7 ± 0.0 <sup>d</sup>	4.7 ± 0.0 <sup>ab</sup>	13.5 ± 0.4 <sup>a</sup>
C_C 20	63.9 ± 0.2 <sup>b</sup>	69.0 ± 0.1 <sup>d</sup>	76.0 ± 0.6 <sup>de</sup>	5.1 ± 0.1 <sup>b</sup>	13.3 ± 0.3 <sup>a</sup>
1 <sup>st</sup> peak	Starch-tannins mixtures				
	Tonset (°C)	Tpeak (°C)	Tconclusion (°C)	Tpeak-Tonset (°C)	Enthalpy (J/g)
NPS	61.7 ± 0.2 <sup>e</sup>	66.9 ± 0.1 <sup>d</sup>	73.6 ± 0.1 <sup>d</sup>	5.2 ± 0.1 <sup>c</sup>	16.5 ± 0.2 <sup>g</sup>
P_M5	61.1 ± 0.3 <sup>d</sup>	66.2 ± 0.2 <sup>b</sup>	72.8 ± 0.2 <sup>c</sup>	5.1 ± 0.1 <sup>c</sup>	15.26 ± 1.5 <sup>ef</sup>
P_M10	60.3 ± 0.3 <sup>c</sup>	65.5 ± 0.3 <sup>c</sup>	71.9 ± 0.2 <sup>b</sup>	5.2 ± 0.0 <sup>c</sup>	15.9 ± 0.6 <sup>fg</sup>
P_M20	59.0 ± 0.1 <sup>a</sup>	68.5 ± 2.3 <sup>a</sup>	70.8 ± 0.1 <sup>a</sup>	5.6 ± 0.2 <sup>d</sup>	15.7 ± 0.0 <sup>efg</sup>
NAP	64.9 ± 0.1 <sup>i</sup>	71.8 ± 0.1 <sup>j</sup>	78.6 ± 0.2 <sup>j</sup>	6.9 ± 0.0 <sup>e</sup>	15.1 ± 0.1 <sup>ef</sup>
A_M 5	63.7 ± 0.2 <sup>g</sup>	70.6 ± 0.1 <sup>h</sup>	77.4 ± 0.2 <sup>i</sup>	6.9 ± 0.1 <sup>e</sup>	15.0 ± 0.1 <sup>def</sup>
A_M10	62.2 ± 0.2 <sup>f</sup>	69.8 ± 0.2 <sup>g</sup>	76.9 ± 0.2 <sup>h</sup>	7.6 ± 0.0 <sup>f</sup>	14.7 ± 0.2 <sup>de</sup>
A_M 20	59.7 ± 0.1 <sup>b</sup>	67.8 ± 0.1 <sup>e</sup>	75.1 ± 0.3 <sup>f</sup>	8.1 ± 0.0 <sup>g</sup>	14.1 ± 0.4 <sup>cd</sup>
NCS	66.8 ± 0.2 <sup>k</sup>	71.1 ± 0.1 <sup>i</sup>	77.0 ± 0.1 <sup>h</sup>	4.3 ± 0.1 <sup>a</sup>	13.5 ± 0.7 <sup>bc</sup>
C_M 5	65.4 ± 0.2 <sup>j</sup>	70.3 ± 0.1 <sup>h</sup>	76.3 ± 0.1 <sup>g</sup>	4.9 ± 0.1 <sup>b</sup>	12.7 ± 0.2 <sup>ab</sup>
C_M 10	64.5 ± 0.0 <sup>h</sup>	69.9 ± 0.2 <sup>g</sup>	76.0 ± 0.1 <sup>g</sup>	5.4 ± 0.2 <sup>d</sup>	12.1 ± 0.4 <sup>a</sup>
C_M20	63.1 ± 0.0 <sup>g</sup>	68.2 ± 0.1 <sup>f</sup>	74.1 ± 0.1 <sup>e</sup>	5.1 ± 0.1 <sup>c</sup>	12.3 ± 0.2 <sup>a</sup>

Results are expressed as mean ± standard deviation of triplicate. Different letters in the same column represent significant difference. The code of the samples are refer to the coding information in Table 5.1.

Continued Table 5.3

2 <sup>nd</sup> peak	Starch-tannins complexes				
	Tonset (°C)	Tpeak (°C)	Tconclusion (°C)	Tpeak-Tonset (°C)	Enthalpy (J/g)
P_C0	nd	nd	nd	nd	nd
P_C5	nd	nd	nd	nd	nd
P_C10	nd	nd	nd	nd	nd
P_C20	nd	nd	nd	nd	nd
A_C0	nd	nd	nd	nd	nd
A_C 5	nd	nd	nd	nd	nd
A_C 10	nd	nd	nd	nd	nd
A_C 20	nd	nd	nd	nd	nd
C_C 0	93.8 ± 1.0 <sup>b</sup>	100.4 ± 0.7 <sup>b</sup>	104.7 ± 0.4 <sup>a</sup>	6.6 ± 0.3 <sup>c</sup>	0.25 ± 0.1 <sup>a</sup>
C_C 5	92.5 ± 0.7 <sup>a</sup>	98.9 ± 0.4 <sup>a</sup>	105.9 ± 0.8 <sup>a</sup>	6.4 ± 0.3 <sup>c</sup>	0.41 ± 0.0 <sup>b</sup>
C_C 10	92.5 ± 0.9 <sup>a</sup>	98.6 ± 0.6 <sup>a</sup>	103.3 ± 1.9 <sup>a</sup>	6.1 ± 0.3 <sup>b</sup>	0.41 ± 0.1 <sup>b</sup>
C_C 20	92.5 ± 0.4 <sup>a</sup>	98.2 ± 0.6 <sup>a</sup>	104.7 ± 0.4 <sup>a</sup>	5.7 ± 0.2 <sup>a</sup>	0.4 ± 0.1 <sup>b</sup>
2 <sup>nd</sup> peak	Starch-tannins mixtures				
	Tonset (°C)	Tpeak (°C)	Tconclusion (°C)	Tpeak-Tonset (°C)	Enthalpy (J/g)
NPS	nd	nd	nd	nd	nd
P_M5	nd	nd	nd	nd	nd
P_M10	nd	nd	nd	nd	nd
P_M20	nd	nd	nd	nd	nd
NAP	nd	nd	nd	nd	nd
A_M 5	nd	nd	nd	nd	nd
A_M10	nd	nd	nd	nd	nd
A_M 20	nd	nd	nd	nd	nd
NCS	93.7 ± 0.3 <sup>b</sup>	99.7 ± 0.1 <sup>b</sup>	105.3 ± 0.4 <sup>b</sup>	6.0 ± 0.2 <sup>b</sup>	0.23 ± 0.1 <sup>a</sup>
C_M 5	91.3 ± 1.3 <sup>a</sup>	97.3 ± 1.0 <sup>a</sup>	103.7 ± 0.8 <sup>a</sup>	6.0 ± 0.3 <sup>b</sup>	0.24 ± 0.0 <sup>a</sup>
C_M 10	91.1 ± 1.1 <sup>a</sup>	96.5 ± 0.6 <sup>a</sup>	103.2 ± 2.2 <sup>a</sup>	5.4 ± 0.5 <sup>a</sup>	0.35 ± 0.1 <sup>b</sup>
C_M20	90.0 ± 0.8 <sup>a</sup>	96.0 ± 0.8 <sup>a</sup>	102.9 ± 2.5 <sup>a</sup>	6.0 ± 0.0 <sup>b</sup>	0.49 ± 0.1 <sup>d</sup>

Results are expressed as mean ± standard deviation of triplicate. Different letters in the same column represent significant difference. The code of the samples are refer to the coding information in Table 5.1.

Continued Table 5.3

3rd peak	Starch-tannins complexes				
	Tonset (°C)	Tpeak (°C)	Tconclusion (°C)	Tpeak-Tonset (°C)	Enthalpy (J/g)
P_C0	nd	nd	nd	nd	nd
P_C5	126.6 ± 1.0 <sup>e</sup>	133.5 ± 0.5 <sup>a</sup>	134.0 ± 1.0 <sup>a</sup>	6.9 ± 0.5 <sup>d</sup>	0.74 ± 0.02 <sup>e</sup>
P_C10	121.6 ± 0.1 <sup>b</sup>	128.8 ± 0.1 <sup>b</sup>	135.7 ± 0.3 <sup>b</sup>	7.2 ± 0.0 <sup>e</sup>	0.79 ± 0.01 <sup>f</sup>
P_C20	119.4 ± 0.5 <sup>a</sup>	125.7 ± 1.2 <sup>c</sup>	133.0 ± 1.2 <sup>c</sup>	6.3 ± 0.7 <sup>d</sup>	1.04 ± 0.31 <sup>g</sup>
A_C0	nd	nd	nd	nd	nd
A_C 5	138.6 ± 0.7 <sup>f</sup>	146.4 ± 0.0 <sup>c</sup>	152.9 ± 0.8 <sup>c</sup>	7.8 ± 0.7 <sup>e</sup>	0.43 ± 0.15 <sup>d</sup>
A_C 10	137.3 ± 0.2 <sup>c</sup>	145.4 ± 0.9 <sup>c</sup>	150.6 ± 0.8 <sup>d</sup>	8.1 ± 0.7 <sup>e</sup>	0.51 ± 0.09 <sup>d</sup>
A_C 20	134.2 ± 0.0 <sup>d</sup>	144.1 ± 0.7 <sup>d</sup>	149.2 ± 0.8 <sup>d</sup>	7.9 ± 0.7 <sup>e</sup>	0.54 ± 0.06 <sup>d</sup>
C_C 0	nd	nd	nd	nd	nd
C_C 5	149.1 ± 0.0 <sup>i</sup>	153.2 ± 0.0 <sup>g</sup>	155.3 ± 0.0 <sup>f</sup>	4.1 ± 0.0 <sup>a</sup>	0.19 ± 0.00 <sup>a</sup>
C_C 10	147.8 ± 0.1 <sup>b</sup>	152.3 ± 0.2 <sup>fg</sup>	155.0 ± 0.7 <sup>f</sup>	4.5 ± 0.1 <sup>b</sup>	0.23 ± 0.00 <sup>b</sup>
C_C 20	146.6 ± 1.2 <sup>g</sup>	151.8 ± 1.0 <sup>f</sup>	155.9 ± 1.2 <sup>f</sup>	5.2 ± 0.2 <sup>d</sup>	0.32 ± 0.04 <sup>c</sup>
3rd peak	Starch-tannins mixtures				
	Tonset (°C)	Tpeak (°C)	Tconclusion (°C)	Tpeak-Tonset (°C)	Enthalpy (J/g)
NPS	nd	nd	nd	nd	nd
P_M5	131.5 ± 2.4 <sup>c</sup>	138.7 ± 3.4 <sup>c</sup>	145.5 ± 3.3 <sup>bc</sup>	7.2 ± 1.0	1.15 ± 0.31 <sup>cd</sup>
P_M10	127.2 ± 1.6 <sup>b</sup>	135.4 ± 1.2 <sup>b</sup>	138.8 ± 0.2 <sup>b</sup>	8.2 ± 0.4	1.24 ± 0.21 <sup>cd</sup>
P_M20	123.4 ± 0.4 <sup>a</sup>	139.0 ± 4.9 <sup>a</sup>	147.2 ± 4.7 <sup>a</sup>	5.6 ± 4.5	1.34 ± 0.24 <sup>cd</sup>
NAP	nd	nd	Nd	nd	nd
A_M 5	137.3 ± 1.0 <sup>d</sup>	145.5 ± 0.9 <sup>c</sup>	153.0 ± 1.5 <sup>f</sup>	8.2 ± 0.1	0.78 ± 0.19 <sup>a</sup>
A_M10	128.8 ± 0.2 <sup>b</sup>	140.7 ± 0.3 <sup>cd</sup>	149.0 ± 0.3 <sup>de</sup>	11.9 ± 0.1	1.08 ± 0.04 <sup>ab</sup>
A_M 20	123.0 ± 1.3 <sup>a</sup>	134.3 ± 0.1 <sup>ab</sup>	140.6 ± 1.5 <sup>bc</sup>	11.3 ± 1.2	1.24 ± 0.13 <sup>cd</sup>
NCS	nd	nd	nd	nd	nd
C_M 5	139.8 ± 0.4 <sup>c</sup>	145.7 ± 0.3 <sup>c</sup>	152.2 ± 0.5 <sup>ef</sup>	5.9 ± 0.1	1.25 ± 0.11 <sup>cd</sup>
C_M 10	136.6 ± 0.4 <sup>d</sup>	142.6 ± 0.4 <sup>d</sup>	150.6 ± 1.4 <sup>def</sup>	6.0 ± 0.0	1.23 ± 0.01 <sup>cd</sup>
C_M20	130.9 ± 0.4 <sup>c</sup>	136.1 ± 0.9 <sup>b</sup>	147.5 ± 2.5 <sup>cd</sup>	5.2 ± 0.5	1.45 ± 0.05 <sup>d</sup>

Results are expressed as mean ± standard deviation of triplicate. Different letters in the same column represent significant difference. The code of the samples refer to the coding information in Table 5.1.

### 5.3.4 Pasting properties

The effect of TA on pasting properties of starch was investigated and the results are shown in Table 5.4 and Figure 5.2. Potato starch formed pastes at lower temperature than corn starch and corn amylopectin. Pasting properties of complex control (P\_C0, A\_C0 and C\_C0) were statistically different from their corresponding native starch. Compared with waxy corn starch and normal corn starch, potato starch demonstrated more significant alterations in pasting behavior with presence of complexed and mixed TA. Both complexed and mixed TA in potato starch and normal corn starch caused a significant decrease of peak viscosity, set back viscosity



and breakdown viscosity. Complexed TA and mixed TA significantly increased peak temperature of potato starch, whereas had no effect on peak temperature of corn starch. Complexed TA showed little effect on pasting behaviors of corn amylopectin, which can be clearly observed in Figure 5.2C, and while mixed TA caused significant reduction in peak viscosity, set back viscosity as well as pasting temperature.

**Table 5.4 Pasting properties of potato starch, corn amylopectin and corn starch complexed / mixed with different concentrations of tannic acid**

Complexes	Peak viscosity (cp)	Hold viscosity (cp)	Final viscosity (cp)	Set Back (cp)	Pasting temperature (°C)	Peak temperature (°C)	Breakdown (cp)
P_C0	7137 ± 54 <sup>i</sup>	1836 ± 10 <sup>g</sup>	2274 ± 9 <sup>f</sup>	439 ± 1 <sup>d</sup>	66 ± 0 <sup>b</sup>	78 ± 0 <sup>a</sup>	5301 ± 63 <sup>h</sup>
P_C5	5407 ± 61 <sup>h</sup>	1409 ± 10 <sup>e</sup>	1851 ± 1 <sup>e</sup>	442 ± 9 <sup>d</sup>	65 ± 0 <sup>a</sup>	82 ± 0 <sup>c</sup>	3999 ± 52 <sup>g</sup>
P_C10	4528 ± 1.5 <sup>d</sup>	1121 ± 7 <sup>b</sup>	1526 ± 2 <sup>b</sup>	406 ± 4 <sup>c</sup>	66 ± 0 <sup>b</sup>	85 ± 1 <sup>c</sup>	3408 ± 5 <sup>c</sup>
P_C20	3602 ± 90 <sup>a</sup>	811 ± 2 <sup>a</sup>	1135 ± 6 <sup>a</sup>	325 ± 5 <sup>a</sup>	66 ± 0 <sup>b</sup>	83 ± 0 <sup>d</sup>	2791 ± 91 <sup>c</sup>
A_C0	4767 ± 15 <sup>ef</sup>	1504 ± 12 <sup>f</sup>	1836 ± 16 <sup>de</sup>	333 ± 4 <sup>b</sup>	71 ± 0 <sup>c</sup>	80 ± 0 <sup>b</sup>	3264 ± 3 <sup>d</sup>
A_C5	4840 ± 10 <sup>g</sup>	1336 ± 4 <sup>c</sup>	1817 ± 5 <sup>c</sup>	481 ± 1 <sup>f</sup>	71 ± 0 <sup>c</sup>	80 ± 0 <sup>b</sup>	3505 ± 7 <sup>f</sup>
A_C10	4756 ± 14 <sup>c</sup>	1338 ± 2 <sup>c</sup>	1825 ± 6 <sup>cd</sup>	488 ± 4 <sup>f</sup>	71 ± 0 <sup>c</sup>	80 ± 0 <sup>b</sup>	3418 ± 12 <sup>c</sup>
A_C20	4826 ± 13 <sup>fg</sup>	1354 ± 15 <sup>d</sup>	1818 ± 8 <sup>c</sup>	464 ± 8 <sup>c</sup>	71 ± 0 <sup>c</sup>	80 ± 0 <sup>b</sup>	3457 ± 17 <sup>ef</sup>
C_C0	4323 ± 6 <sup>c</sup>	2784 ± 12 <sup>j</sup>	4835 ± 12 <sup>j</sup>	2051 ± 0 <sup>j</sup>	74 ± 0 <sup>c</sup>	95 ± 0 <sup>f</sup>	1540 ± 6 <sup>b</sup>
C_C5	4127 ± 9 <sup>b</sup>	2697 ± 6 <sup>i</sup>	4531 ± 9 <sup>i</sup>	1834 ± 3 <sup>i</sup>	74 ± 0 <sup>c</sup>	95 ± 0 <sup>f</sup>	1430 ± 3 <sup>a</sup>
C_C10	4094 ± 7 <sup>b</sup>	2619 ± 15 <sup>h</sup>	4432 ± 19 <sup>h</sup>	1813 ± 4 <sup>h</sup>	74 ± 0 <sup>c</sup>	95 ± 0 <sup>f</sup>	1475 ± 9 <sup>a</sup>
C_C20	4118 ± 11 <sup>b</sup>	2632 ± 7 <sup>h</sup>	4404 ± 14 <sup>g</sup>	1772 ± 7 <sup>g</sup>	74 ± 0 <sup>c</sup>	95 ± 0 <sup>f</sup>	1486 ± 4 <sup>ab</sup>
Mixtures	Peak viscosity (cp)	Hold viscosity (cp)	Final viscosity (cp)	Set Back (cp)	Pasting temperature (°C)	Peak temperature (°C)	Breakdown (cp)
NPS	4150 ± 24 <sup>i</sup>	1457 ± 0 <sup>g</sup>	1821 ± 10 <sup>h</sup>	364 ± 10 <sup>d</sup>	69 ± 0 <sup>a</sup>	86 ± 1 <sup>c</sup>	2670 ± 24 <sup>g</sup>
P_M5	2870 ± 9 <sup>c</sup>	1271 ± 8 <sup>f</sup>	1681 ± 6 <sup>g</sup>	411 ± 14 <sup>c</sup>	70 ± 0 <sup>a</sup>	95 ± 0 <sup>f</sup>	1600 ± 2 <sup>f</sup>
P_M10	2719 ± 34 <sup>b</sup>	1172 ± 7 <sup>d</sup>	1606 ± 13 <sup>f</sup>	434 ± 6 <sup>c</sup>	70 ± 0 <sup>a</sup>	95 ± 0 <sup>f</sup>	1548 ± 28 <sup>c</sup>
P_M20	2265 ± 25 <sup>a</sup>	1024 ± 7 <sup>b</sup>	1394 ± 4 <sup>d</sup>	371 ± 3 <sup>d</sup>	70 ± 0 <sup>a</sup>	95 ± 0 <sup>f</sup>	1242 ± 19 <sup>d</sup>
NAP	3833 ± 6 <sup>i</sup>	1198 ± 8 <sup>c</sup>	1473 ± 14 <sup>c</sup>	275 ± 21 <sup>c</sup>	73 ± 0 <sup>d</sup>	81 ± 0 <sup>d</sup>	2636 ± 14 <sup>g</sup>
A_M5	3761 ± 1 <sup>h</sup>	1076 ± 9 <sup>c</sup>	1290 ± 6 <sup>c</sup>	215 ± 3 <sup>b</sup>	72 ± 0 <sup>c</sup>	80 ± 0 <sup>c</sup>	2685 ± 8 <sup>g</sup>
A_M10	3781 ± 33 <sup>h</sup>	1018 ± 4 <sup>b</sup>	1217 ± 3 <sup>b</sup>	200 ± 7 <sup>b</sup>	72 ± 0 <sup>c</sup>	80 ± 0 <sup>b</sup>	2764 ± 30 <sup>i</sup>
A_M20	3581 ± 17 <sup>g</sup>	901 ± 13 <sup>a</sup>	1051 ± 15 <sup>a</sup>	150 ± 2 <sup>a</sup>	71 ± 0 <sup>b</sup>	79 ± 0 <sup>a</sup>	2680 ± 4 <sup>g</sup>
NCS	3448 ± 5 <sup>f</sup>	2411 ± 10 <sup>k</sup>	3911 ± 56 <sup>i</sup>	1463 ± 28 <sup>i</sup>	76 ± 0 <sup>g</sup>	95 ± 0 <sup>f</sup>	1065 ± 42 <sup>c</sup>
C_M5	3216 ± 59 <sup>e</sup>	2220 ± 34 <sup>j</sup>	3516 ± 61 <sup>k</sup>	1296 ± 27 <sup>h</sup>	76 ± 1 <sup>fg</sup>	95 ± 0 <sup>f</sup>	997 ± 26 <sup>b</sup>
C_M10	3096 ± 17 <sup>d</sup>	2100 ± 26 <sup>i</sup>	3321 ± 15 <sup>j</sup>	1221 ± 11 <sup>g</sup>	75 ± 0 <sup>ef</sup>	95 ± 0 <sup>f</sup>	996 ± 9 <sup>b</sup>
C_M20	2898 ± 46 <sup>c</sup>	1941 ± 18 <sup>h</sup>	3020 ± 31 <sup>i</sup>	1079 ± 13 <sup>f</sup>	75 ± 0 <sup>c</sup>	95 ± 0 <sup>f</sup>	957 ± 28 <sup>a</sup>

Results are expressed as mean ± standard deviation of triplicate. Different letters in the same column represent significant difference. The code of the samples are refer to the coding information in Table 5.1.

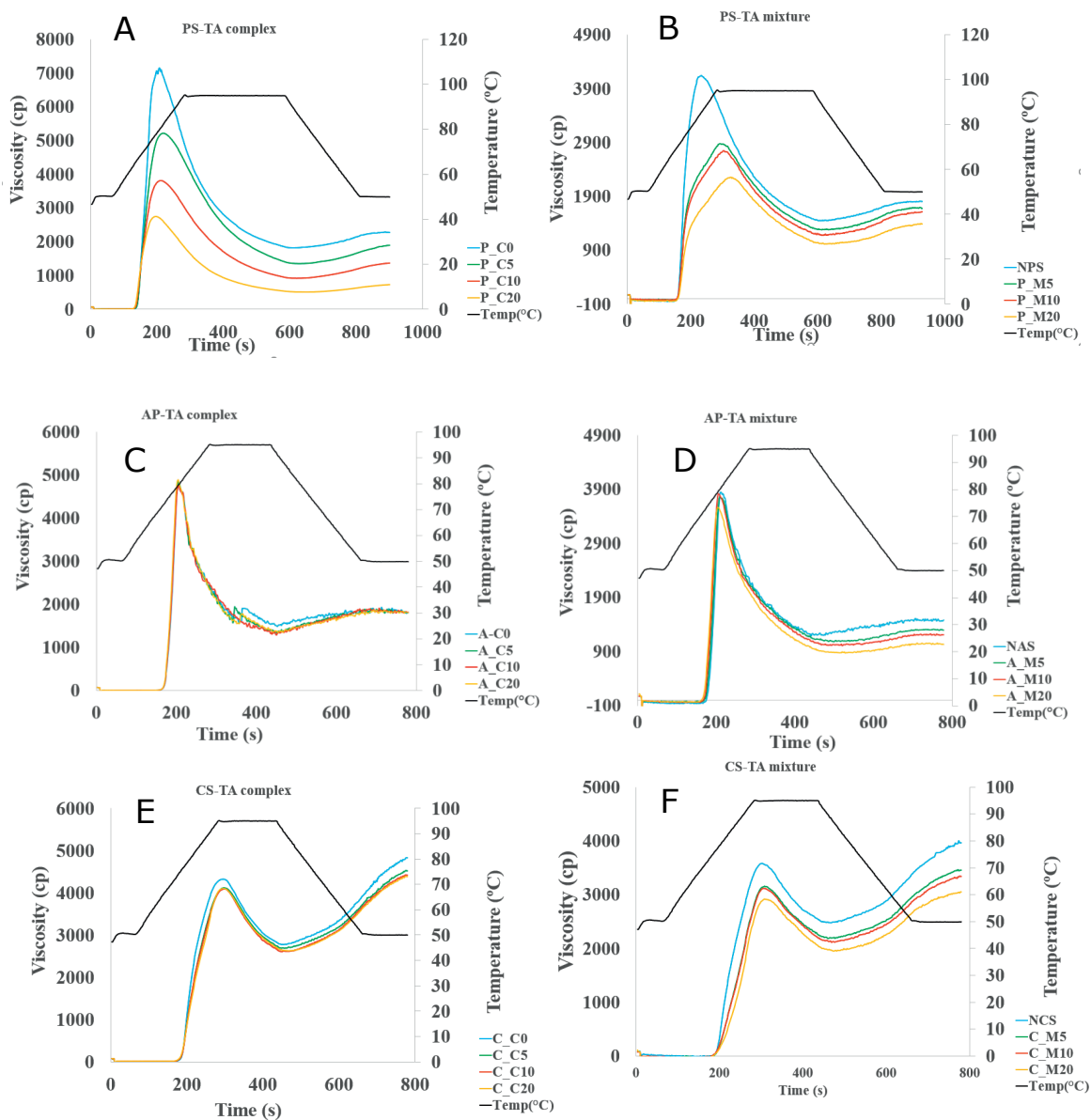


Figure 5.2. Pasting properties of (A) potato starch-tannic acid complex, (B) potato starch-tannic acid mixture, (C) corn amylopectin starch-tannic acid complex, (D) corn amylopectin starch-tannic acid mixture, (E) corn starch-tannic acid complex, (F) corn starch-tannic acid mixture. The code of the samples are refer to the coding information in Table 5.1.

### 5.3.5 *In vitro* digestion

Starch digestibility of gelatinized starch-tannins complexes and mixtures were measured and shown in Figure 5.3. The estimated kinetic parameters and inhibition calculated based on  $C_{\infty}$  values were calculated and shown in Table 5.5. Complexed and mixed TA significantly decreased the amount of starch digestibility ( $C_{\infty}$ ) in all three types of starch. Notably, this inhibitory effect was even more significant for starch-tannins mixtures than starch-tannins complexes, which could be clearly observed in Figure 5.3. When 20% of TA based on starch weight was added to three types of starch, almost no starch digestion occurred.

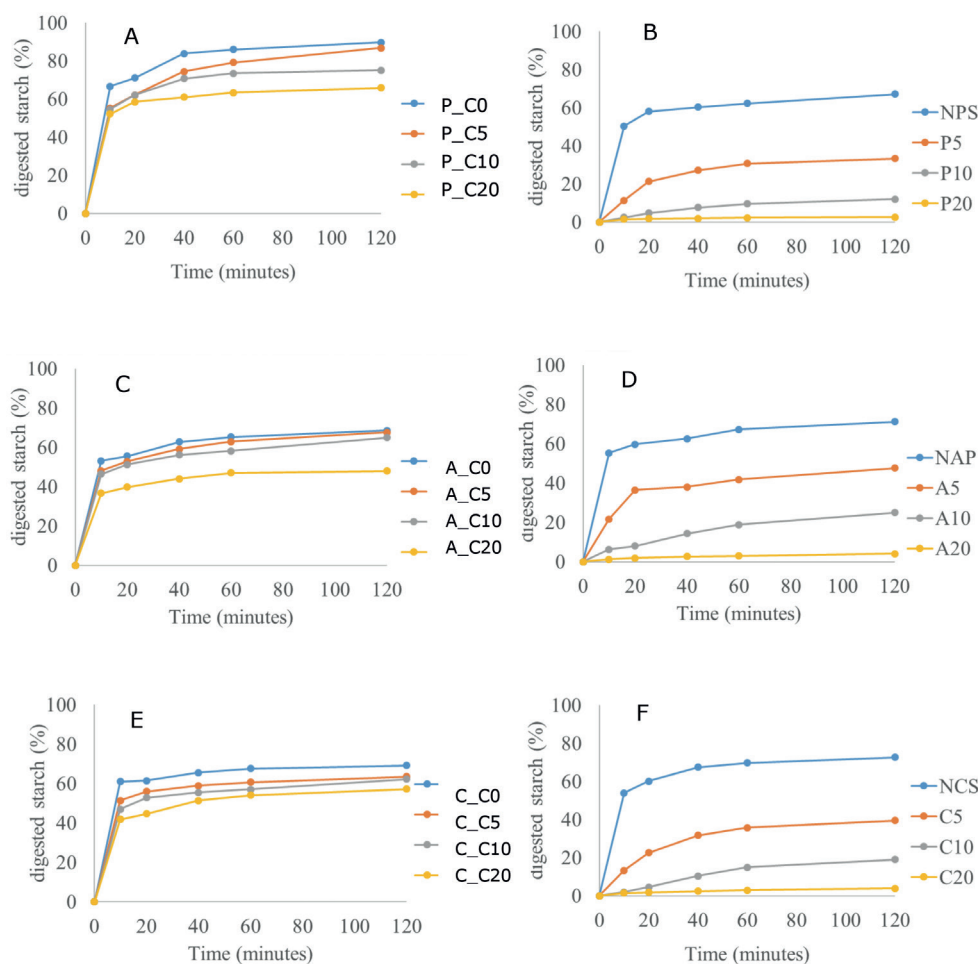


Figure 5.3: *In vitro* starch hydrolysis profiles of A) gelatinized potato starch-tannic acid complex; B) gelatinized potato starch-tannic acid mixture; C) gelatinized corn amylopectin-tannic acid complex; D) gelatinized corn amylopectin-tannic acid mixture; E) gelatinized corn starch-tannic acid complex; F) gelatinized corn starch-tannic acid mixture. The code of the samples are refer to the coding information in Table 5.1.

Table 5.5. Estimated kinetic parameters for *in vitro* starch digestibility of gelatinized potato starch, corn amylopectin and corn starch complexed and mixed with different amounts of tannic acid.

Complexes	C <sub>∞</sub> (%)	Initial rate (%* min <sup>-1</sup> )	k (min <sup>-1</sup> )	Sum of squares	Inhibition %
P_C0	85.7 ± 0.6 <sup>a</sup>	6.6 ± 0.0 <sup>c</sup>	0.13 ± 0.00 <sup>a</sup>	86.6 ± 16.1 <sup>b</sup>	na
P_C5	79.8 ± 0.7 <sup>b</sup>	5.5 ± 0.1 <sup>b</sup>	0.10 ± 0.00 <sup>b</sup>	14.9 ± 16.6 <sup>c</sup>	6.5 ± 0.8 <sup>a</sup>
P_C10	72.5 ± 0.1 <sup>c</sup>	5.4 ± 0.1 <sup>ab</sup>	0.12 ± 0.00 <sup>c</sup>	37.8 ± 0.1 <sup>a</sup>	14.9 ± 90.1 <sup>b</sup>
P_C20	63.0 ± 0.1 <sup>d</sup>	5.2 ± 0.0 <sup>a</sup>	0.17 ± 0.00 <sup>d</sup>	18.3 ± 0.7 <sup>a</sup>	26.1 ± 0.1 <sup>c</sup>
A_C0	64.2 ± 0.2 <sup>a</sup>	5.4 ± 0.1 <sup>c</sup>	0.16 ± 0.01 <sup>c</sup>	60.9 ± 1.3	na
A_C5	63.0 ± 0.6 <sup>b</sup>	4.8 ± 0.0 <sup>b</sup>	0.12 ± 0.00 <sup>a</sup>	67.8 ± 0.4 <sup>c</sup>	2.2 ± 0.9 <sup>a</sup>
A_C10	59.39 ± 0.3 <sup>c</sup>	4.6 ± 0.0 <sup>b</sup>	0.14 ± 0.00 <sup>ab</sup>	65.9 ± 1.9 <sup>c</sup>	7.8 ± 0.5 <sup>b</sup>
A_C20	45.45 ± 0.4 <sup>d</sup>	3.6 ± 0.0 <sup>a</sup>	0.15 ± 0.00 <sup>bc</sup>	23.3 ± 0.7 <sup>a</sup>	29.4 ± 0.6 <sup>c</sup>
C_C0	66.06 ± 0.3 <sup>a</sup>	6.2 ± 0.1 <sup>a</sup>	0.27 ± 0.04 <sup>a</sup>	34.5 ± 6.2 <sup>ab</sup>	na
C_C5	60.47 ± 0.0 <sup>b</sup>	5.2 ± 0.0 <sup>b</sup>	0.18 ± 0.01 <sup>b</sup>	25.0 ± 6.9 <sup>a</sup>	8.8 ± 0.0 <sup>a</sup>
C_C10	57.90 ± 0.2 <sup>c</sup>	4.8 ± 0.0 <sup>c</sup>	0.16 ± 0.00 <sup>b</sup>	41.0 ± 12.4 <sup>ab</sup>	12.7 ± 0.2 <sup>b</sup>
C_C20	53.29 ± 0.3 <sup>d</sup>	4.2 ± 0.8 <sup>d</sup>	0.13 ± 0.01 <sup>b</sup>	55.0 ± 6.1 <sup>b</sup>	19.6 ± 0.4 <sup>c</sup>

Mixtures	C <sub>∞</sub> (%)	Initial rate (%* min <sup>-1</sup> )	k (min <sup>-1</sup> )	Sum of squares	Inhibition %
NPS	63.2 ± 0.5 <sup>a</sup>	5.0 ± 0.1 <sup>c</sup>	0.15 ± 0.00 <sup>a</sup>	38.8 ± 12.4 <sup>a</sup>	na
P_M5	33.1 ± 0.0 <sup>b</sup>	1.2 ± 0.0 <sup>b</sup>	0.05 ± 0.00 <sup>b</sup>	2.4 ± 1.6 <sup>b</sup>	47.3 ± 0.1 <sup>a</sup>
P_M10	13.1 ± 0.1 <sup>c</sup>	0.3 ± 0.0 <sup>ab</sup>	0.02 ± 0.00 <sup>c</sup>	0.5 ± 0.7 <sup>b</sup>	79.2 ± 0.1 <sup>b</sup>
P_M20	2.4 ± 0.2 <sup>d</sup>	0.1 ± 0.0 <sup>a</sup>	0.08 ± 0.01 <sup>d</sup>	0.2 ± 0.0 <sup>b</sup>	96.1 ± 0.3 <sup>c</sup>
NAP	66.1 ± 0.2 <sup>a</sup>	5.5 ± 0.0 <sup>a</sup>	0.17 ± 0.00 <sup>a</sup>	57.3 ± 1.0 <sup>a</sup>	na
A_M5	44.3 ± 0.1 <sup>b</sup>	2.2 ± 0.0 <sup>b</sup>	0.07 ± 0.00 <sup>b</sup>	36.1 ± 1.0 <sup>b</sup>	33.1 ± 0.2 <sup>a</sup>
A_M10	28.7 ± 0.9 <sup>c</sup>	0.6 ± 0.0 <sup>c</sup>	0.02 ± 0.00 <sup>c</sup>	2.9 ± 0.3 <sup>c</sup>	56.7 ± 1.4 <sup>b</sup>
A_M20	4.1 ± 0.1 <sup>d</sup>	0.1 ± 0.0 <sup>d</sup>	0.03 ± 0.00 <sup>d</sup>	0.2 ± 0.0 <sup>d</sup>	93.8 ± 0.1 <sup>c</sup>
NCS	69.5 ± 0.4 <sup>a</sup>	5.4 ± 0.0 <sup>a</sup>	0.14 ± 0.00 <sup>d</sup>	34.7 ± 10.4 <sup>a</sup>	na
C_M5	39.1 ± 0.6 <sup>b</sup>	1.3 ± 0.0 <sup>b</sup>	0.04 ± 0.00 <sup>c</sup>	0.6 ± 0.2 <sup>b</sup>	43.5 ± 0.9 <sup>a</sup>
C_M10	23.9 ± 0.5 <sup>c</sup>	0.2 ± 0.0 <sup>c</sup>	0.01 ± 0.00 <sup>b</sup>	4.7 ± 0.4 <sup>b</sup>	65.5 ± 0.7 <sup>b</sup>
C_M20	3.7 ± 0.1 <sup>d</sup>	0.1 ± 0.0 <sup>c</sup>	0.03 ± 0.00 <sup>a</sup>	0.3 ± 0.0 <sup>b</sup>	94.6 ± 0.1 <sup>c</sup>

Results are expressed as mean ± standard deviation of triplicate. Different letters in the same column represent significant difference. The code of the samples are refer to the coding information in Table 5.1.

## 5.4 Discussion

Influences of polyphenols on physical-chemical properties of starch were widely reported (Amoako & Awika, 2016a; Gao et al., 2021; M. Li, Pernell, & Ferruzzi, 2018), with cereal starches most widely reported for their interaction with phenolics, especially monomeric phenolics such as phenolic acids (Wu, Chen, Li, & Li, 2009). Starch can be classified into A-type, B-type and C-type starch, which represented by cereal starch, tuber starch and legume starch, respectively (Jane, Wong, & McPherson, 1997). In our study, potato starch was selected as example of tuber starch. Waxy corn starch, normal corn starch were chosen as example of

cereal starch. Tannic acid was selected as example of polymeric polyphenols, since it is not commonly used in the interaction experiments.

Taken all the results of this study, starch-tannins interactions are affected by sample preparation method and botanical sources, and the latter includes amylose content, amylopectin architecture and phosphorous content in potato starch.

TA was added to the three selected starches either by preparing complexes or by simply mixing with starch. Complexes had less TA compared to mixtures, since the excess of free TA was removed upon complex preparation. Beside the amount of TA, heat incubation (37°C) during complex preparation might influence the functional properties of the three types of starch and most significantly in potato starch based on XRD patterns, pasting properties, swelling power, etc. This could be confirmed by the big differences between three native starch (NPS, NAP, NCS) and corresponding complex control (P\_C0, A\_C0, C\_C0), which were reflected in the swelling behavior (Table 5.2), gelatinization (Table 5.3), and pasting (Table 5.4) and consistently in the larger decrease of starch digestibility (Table 5.5). Besides, the incubation during complex preparation also caused structural changes in potato starch. This was clearly observed by comparing XRD pattern of potato complex control (P\_C0) and native potato starch (NPS) (Figure 5.1). NPS exhibited the typical B-type X-ray pattern with characteristic peaks at 5.5°, 15.1°, 17.1° 22°, 24 and 26° 2 $\theta$ . NPS also exhibited a peak at 20° 2 $\theta$ , which is known as V-type. V-complex generally reflects V-type crystallinity resulting from amylose-lipid interactions. However, considering trace quantities of bound lipids (~0.08%) in potato starch generally (Varatharajan, Hoover, Liu, & Seetharaman, 2010), the 20° 2 $\theta$  peak probably represents single helices of linear starch chains arranged in a crystalline array, rather than V-type lipid-amylose complexes. In P\_C0 sample, the characteristic peak assigned to “B” type (5.5°) were absent and the peak at 17.1° become broader, indicating the presence of more A-type crystalline unit (Varatharajan et al., 2010). The relative crystallinity also increased from 28.6% to 36.2%. The reduction of the peak intensity at 2 $\theta$  of 5.5° and 22–24°, and a broader peak at 2 $\theta$  of 17° reflected the appearance of A- and B-type polymorphs, *i.e.*, XRD pattern changed from B-type to a mixture of A- and B-type (Yassaroh, Woortman, & Loos, 2019).

The direct evidence of interaction of TA with three types of starch are the thermal transition appearing at around 120 ~160 °C (Table 5.3). These peaks did not appear during cooling and reheating cycle (data not shown). Therefore, these interactions were likely attributed to the non-inclusion complexes with TA, since TA has abundant hydroxyl groups to interact with starch

and it can form non-inclusion complexes by hydrogen bonds (Zhu, 2015). V-type complexes were also found in corn starch (2<sup>nd</sup> peak) and partly attributed to amylose-lipid complexes.

Amylose content influences TA-starch interactions. This was clearly observed when comparing  $\Delta H$  of the 3<sup>rd</sup> peak in waxy starch-TA complexes and normal corn starch-TA complexes. The peak of non-inclusion complexes showed higher melting enthalpy in amylopectin-TA complexes than corn starch-TA complexes (Table 5.3). We found that waxy corn starch bound more TA than normal corn starch (Table 5.1). Considering preparation conditions of complex, TA can only interact with amorphous region of starch, which included linear amylose molecules and probably less ordered amylopectin (Bertoft, 2017). This indicates that branching points of the amylopectin side chains in the amorphous lamellas have more ability to bind TA than amylose. The opposite results were obtained when comparing melting enthalpy of non-inclusion peak (3<sup>rd</sup> peak) in amylopectin-TA and corn starch-TA mixtures (Table 5.3). In complexes, TA interacted with ungelatinized starch, while in mixtures TA co-gelatinized with starch. Therefore, non-gelatinized amylopectin has more ability to interact with TA than non-gelatinized amylose, but gelatinized amylose has more ability to interact with TA than gelatinized amylopectin. This is consistent with a recent report the linear structure of amylose having a more favourable interaction (non-covalent) with condensed tannins than amylopectin due to its less steric hindrance (D. B. Amoako & Awika, 2016a).

Potato starch exhibits distinctive swelling and pasting properties, and those properties were affected by TA presence most significantly compared the other two types of starch. The significant reduction of swelling power and pasting viscosity was observed in potato starch in presence of TA (Table 5.2&5.4). However, TA shows no effect on swelling power and pasting viscosity of corn starch and very small effect on corn amylopectin. The different extent of change which occurs in potato starch is possibly due to its internal long-B amylopectin chains and high level of phosphate esters. To better understand the effects of botanical differences of three types of starch on starch-tannins interactions, the physical and chemical properties of different types of starch used in our starch are shown in Table 5.6.

Table 5.6 Physical and chemical properties of waxy corn starch, normal corn starch and potato starch

Starch		Waxy corn starch	Normal corn starch	Potato starch
Granule diameter ( $\mu\text{m}$ )		16	15	45.8
Crystal type		A	A	B
Chain length distribution DP (mol %)	Average chain length DP	21.1	23.1	31
	DP (6-12)	22.7	21.8	4.6
	DP (13-24)	47.7	38.4	22.1
	DP (25-36)	14	17.1	14.1
	DP (>37)	15.5	22.6	59.2
Apparent amylose %		1.8	21.5	23.2
Relative crystallinity %		34.3	34.3	28.6
Phosphate content %		0	0	0.08

The data of granule diameter and chain length distribution are adapted from (Bertoft, 2017)(Maningat & Seib, 2010)(Martens, Gerrits, Bruininx, & Schols, 2018).

An unique property of potato starch is that it contains the phosphate monoesters. The phosphate monoesters are covalently bound to the amylopectin fraction of the starch and influence pasting properties of potato starch (Craig and others 1989). The highest swelling power of potato starch is attributed to the repulsion created by the negatively charged phosphate monoesters present in adjacent potato starch chains (Singh et al., 2003; Waterschoot, Gomand, & Delcour, 2016; Yadav et al., 2016). Therefore, potato starch granules are also much more susceptible to disintegration (Waterschoot, Gomand, Willebrords, Fierens, & Delcour, 2014), which results in large breakdown viscosity (Table 5.4). As shown in Table 5.2&5.4, physical-chemical properties of potato starch were affected most significantly compared to waxy corn starch, normal corn starch and wheat starch. Therefore, we speculate that the TA presence may interrupt the repulsion of adjacent amylopectin chains, resulting in reducing of swelling power. Besides, polyphenols with hydroxyl groups such as tannins have the potential to induce the formation of cross-links in the structures of starch during gelatinization, which also accounts for the reduction in the swelling of the starches (Amoako & Awika, 2016b; Chen, Chen, Gao, & Zeng, 2020; M. Li, Pernell, & Ferruzzi, 2018).

The other unique properties of potato starch is its internal long-B amylopectin chains (Table 5.6). The different structures of A type (corn starch) and B type-crystalline (potato starch) influenced the interaction of TA with starch. A-type starches have branch points scattered in both amorphous and crystalline regions, and substantial amount of branch-linkages were located within the crystalline region, whereas, the B-type starch have most branch points clustered in the amorphous region, making them more susceptible to the acid hydrolysis or digestive enzymes (Jane et al., 1997). A-type crystalline structure has more short A-chains than B-type structure (Jane et al., 1997). A-type crystalline structure has tightly packed double helices with only 8 water molecules in each monoclinic crystal unit, while the B-type crystalline structure has a more open packing of helices with 36 inter-helical water molecules in each hexagonal crystal unit (Zhang et al., 2014). Therefore, the more open structure of B-type starch makes it easier to interact with TA than tightly packed A-type starch. Overall, the presence of long-B amylopectin chains and high level of phosphate esters make potato starch affected most significantly in functional properties (Table 5.21-5.5) compared to waxy corn starch and normal corn starch.

Finally, starch digestibility of gelatinized starch-tannins complexes and mixtures was measured. As we discussed before, potato starch, corn starch and amylopectin formed non-inclusion complexes with TA in both complexes and mixtures samples. Besides, inclusion complexes formed by amylose-lipid was found in corn starch. To better understand the contribution of non-inclusion starch-tannins complexes and inclusion amylose-lipid complex for the inhibition on starch digestibility, the inhibition % (Table 5.5) was plotted against enthalpy of 2<sup>nd</sup> peak in potato starch and amylopectin and sum enthalpy of 2<sup>nd</sup> and 3<sup>rd</sup> peak in corn starch (Table 5.3). As shown in Figure 5.4, a clear correlation was found between enthalpy and inhibition for all three types of starch. Therefore, non-inclusion complexes from starch-tannins interactions in three selected starches and inclusion complexes from starch-lipid interactions in corn starch contributed predominantly to inhibition of starch digestibility. Besides these effects related to the substrate modification it is worth to remind a direct inhibition on  $\alpha$ -amylase enzyme could also contribute to the inhibition on starch digestibility, since some TA may become free during the *in vitro* digestion (Kan et al., 2020).

Overall, in this study, the effects of botanical source (A or B type) and amylose content of starch on starch-tannins interactions were investigated. These results can help stimulate further interest in applications of starch-tannic acid interactions in various starchy food.



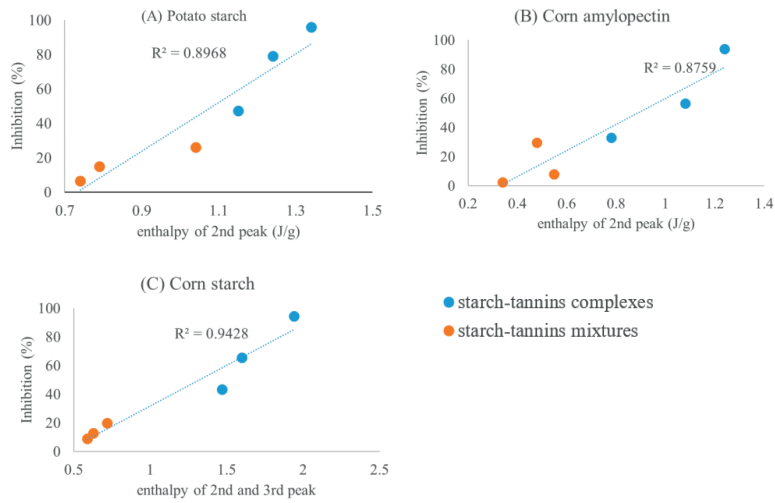


Figure 5.4: Plots of inhibition of starch digestibility against enthalpy of 2<sup>nd</sup> peak in (A) potato starch (B) corn amylopectin (C) plots of inhibition of starch digestibility against enthalpy of 2<sup>nd</sup> and 3<sup>rd</sup> peak in corn starch.

## Reference:


- Amoako, D., & Awika, J. M. (2016). Polyphenol interaction with food carbohydrates and consequences on availability of dietary glucose. *Current Opinion in Food Science*. <https://doi.org/10.1016/j.cofs.2016.01.010>
- Amoako, D. B., & Awika, J. M. (2016a). Polymeric tannins significantly alter properties and in vitro digestibility of partially gelatinized intact starch granule. *Food Chemistry*. <https://doi.org/10.1016/j.foodchem.2016.03.096>
- Amoako, D. B., & Awika, J. M. (2016b). Polymeric tannins significantly alter properties and in vitro digestibility of partially gelatinized intact starch granule. *Food Chemistry*. <https://doi.org/10.1016/j.foodchem.2016.03.096>
- Bashir, K., & Aggarwal, M. (2019). Physicochemical, structural and functional properties of native and irradiated starch: a review. *Journal of Food Science and Technology*. <https://doi.org/10.1007/s13197-018-3530-2>
- Bertoft, E. (2017). Understanding starch structure: Recent progress. *Agronomy*. <https://doi.org/10.3390/agronomy7030056>
- Chao, C., Yu, J., Wang, S., Copeland, L., & Wang, S. (2018). Mechanisms Underlying the Formation of Complexes between Maize Starch and Lipids. *Journal of Agricultural and Food Chemistry*. <https://doi.org/10.1021/acs.jafc.7b05025>
- Chen, N., Chen, L., Gao, H., & Zeng, W. (2020). Mechanism of bridging and interfering effects of tea polyphenols on starch molecules. *Journal of Food Processing and Preservation*, 44(8). <https://doi.org/10.1111/jfpp.14576>
- Chi, C., Li, X., Zhang, Y., Chen, L., Li, L., & Wang, Z. (2017). Digestibility and supramolecular structural changes of maize starch by non-covalent interactions with gallic acid. *Food and Function*. <https://doi.org/10.1039/c6fo01468b>
- Gao, S., Liu, H., Sun, L., Cao, J., Yang, J., Lu, M., & Wang, M. (2021). Rheological, thermal and in vitro digestibility properties on complex of plasma modified Tartary buckwheat starches with quercetin. *Food Hydrocolloids*. <https://doi.org/10.1016/j.foodhyd.2020.106209>
- Gorii, I., Garcia-Alonso, A., & Saura-Calixto, F. (1997). *A STARCH HYDROLYSIS PROCEDURE TO ESTIMATE GLYCEMIC INDEX*. *Nutrition Research* (Vol. 17).

Elsevier Science Inc.

- Jane, J. L., Wong, K. S., & McPherson, A. E. (1997). Branch-structure difference in starches of A and B-type x-ray patterns revealed by their naegeli dextrans. *Carbohydrate Research*. [https://doi.org/10.1016/S0008-6215\(97\)00056-6](https://doi.org/10.1016/S0008-6215(97)00056-6)
- Kan, L., Capuano, E., Fogliano, V., Oliviero, T., & Verkerk, R. (2020). Tea polyphenols as a strategy to control starch digestion in bread: the effects of polyphenol type and gluten. *Food & Function*. <https://doi.org/10.1039/d0fo01145b>
- Li, H., Dhital, S., Slade, A. J., Yu, W., Gilbert, R. G., & Gidley, M. J. (2019). Altering starch branching enzymes in wheat generates high-amylose starch with novel molecular structure and functional properties. *Food Hydrocolloids*. <https://doi.org/10.1016/j.foodhyd.2019.01.041>
- Li, M., Pernell, C., & Ferruzzi, M. G. (2018). Complexation with phenolic acids affect rheological properties and digestibility of potato starch and maize amylopectin. *Food Hydrocolloids*. <https://doi.org/10.1016/j.foodhyd.2017.11.028>
- Liu, Siyuan, Yuan, T. Z., Wang, X., Reimer, M., Isaak, C., & Ai, Y. (2019). Behaviors of starches evaluated at high heating temperatures using a new model of Rapid Visco Analyzer – RVA 4800. *Food Hydrocolloids*. <https://doi.org/10.1016/j.foodhyd.2019.03.015>
- Liu, Suchen, Xie, L., Shen, M., Xiao, Y., Yu, Q., Chen, Y., & Xie, J. (2020). Dual modifications on the gelatinization, textural, and morphology properties of pea starch by sodium carbonate and Mesona chinensis polysaccharide. *Food Hydrocolloids*. <https://doi.org/10.1016/j.foodhyd.2019.105601>
- Liu, X., Wang, Y., Yu, L., Tong, Z., Chen, L., Liu, H., & Li, X. (2013). Thermal degradation and stability of starch under different processing conditions. *Starch/Staerke*. <https://doi.org/10.1002/star.201200198>
- Liu, Y., Chen, L., Xu, H., Liang, Y., & Zheng, B. (2019). Understanding the digestibility of rice starch-gallic acid complexes formed by high pressure homogenization. *International Journal of Biological Macromolecules*. <https://doi.org/10.1016/j.ijbiomac.2019.05.083>
- Luo, D., Li, Y., Xu, B., Ren, G., Li, P., Li, X., ... Liu, J. (2017). Effects of inulin with different degree of polymerization on gelatinization and retrogradation of wheat starch.

- Food Chemistry*. <https://doi.org/10.1016/j.foodchem.2017.02.058>
- Mahmood, K., Kamilah, H., Shang, P. L., Sulaiman, S., Ariffin, F., & Alias, A. K. (2017). A review: Interaction of starch/non-starch hydrocolloid blending and the recent food applications. *Food Bioscience*. <https://doi.org/10.1016/j.fbio.2017.05.006>
- Minekus, M., Alminger, M., Alvito, P., Ballance, S., Bohn, T., Bourlieu, C., ... Brodtkorb, A. (2014). A standardised static *in vitro* digestion method suitable for food – an international consensus. *Food Funct.*, 5(6), 1113–1124. <https://doi.org/10.1039/C3FO60702J>
- Pan, J., Li, M., Zhang, S., Jiang, Y., Lv, Y., Liu, J., ... Zhang, H. (2019). Effect of epigallocatechin gallate on the gelatinisation and retrogradation of wheat starch. *Food Chemistry*. <https://doi.org/10.1016/j.foodchem.2019.05.048>
- Ren, Y., Wu, Z., Shen, M., Rong, L., Liu, W., Xiao, W., & Xie, J. (2021). Improve properties of sweet potato starch film using dual effects: Combination *Mesona chinensis* Benth polysaccharide and sodium carbonate. *LWT*. <https://doi.org/10.1016/j.lwt.2020.110679>
- Singh, N., Singh, J., Kaur, L., Sodhi, N. S., & Gill, B. S. (2003). Morphological, thermal and rheological properties of starches from different botanical sources. *Food Chemistry*. [https://doi.org/10.1016/S0308-8146\(02\)00416-8](https://doi.org/10.1016/S0308-8146(02)00416-8)
- Varatharajan, V., Hoover, R., Liu, Q., & Seetharaman, K. (2010). The impact of heat-moisture treatment on the molecular structure and physicochemical properties of normal and waxy potato starches. *Carbohydrate Polymers*. <https://doi.org/10.1016/j.carbpol.2010.03.002>
- Waterschoot, J., Gomand, S. V., & Delcour, J. A. (2016). Impact of swelling power and granule size on pasting of blends of potato, waxy rice and maize starches. *Food Hydrocolloids*. <https://doi.org/10.1016/j.foodhyd.2015.06.012>
- Waterschoot, J., Gomand, S. V., Willebrords, J. K., Fierens, E., & Delcour, J. A. (2014). Pasting properties of blends of potato, rice and maize starches. *Food Hydrocolloids*. <https://doi.org/10.1016/j.foodhyd.2014.04.033>
- Wu, Y., Chen, Z., Li, X., & Li, M. (2009). Effect of tea polyphenols on the retrogradation of rice starch. *Food Research International*. <https://doi.org/10.1016/j.foodres.2008.11.001>
- Yadav, R. B., Kumar, N., & Yadav, B. S. (2016). Characterization of banana, potato, and rice

- starch blends for their physicochemical and pasting properties. *Cogent Food & Agriculture*, 2(1). <https://doi.org/10.1080/23311932.2015.1127873>
- Yassaroh, Y., Woortman, A. J. J., & Loos, K. (2019). A new way to improve physicochemical properties of potato starch. *Carbohydrate Polymers*.  
<https://doi.org/10.1016/j.carbpol.2018.09.082>
- Zhang, B., Xiong, S., Li, X., Li, L., Xie, F., & Chen, L. (2014). Effect of oxygen glow plasma on supramolecular and molecular structures of starch and related mechanism. *Food Hydrocolloids*. <https://doi.org/10.1016/j.foodhyd.2013.10.034>
- Zhao, B., Sun, S., Lin, H., Chen, L., Qin, S., Wu, W., ... Guo, Z. (2019). Physicochemical properties and digestion of the lotus seed starch-green tea polyphenol complex under ultrasound-microwave synergistic interaction. *Ultrasonics Sonochemistry*.  
<https://doi.org/10.1016/j.ultsonch.2018.11.001>
- Zhao, B., Wang, B., Zheng, B., Chen, L., & Guo, Z. (2019). Effects and mechanism of high-pressure homogenization on the characterization and digestion behavior of lotus seed starch-green tea polyphenol complexes. *Journal of Functional Foods*.  
<https://doi.org/10.1016/j.jff.2019.04.016>
- Zhu, F. (2015). Interactions between starch and phenolic compound. *Trends in Food Science & Technology*, 43(2), 129–143. <https://doi.org/10.1016/J.TIFS.2015.02.003>

The background features a large white triangle pointing towards the top-right corner. The area to the left of this triangle is divided into two sections: a light gray upper section and a dark gray lower section. A small, medium-gray triangle is positioned at the intersection of the white triangle and the dark gray section. A large, black, serif-style number '6' is centered within the white triangular area.

6

# Chapter 6

## Inhibition of $\alpha$ -glucosidases by tea polyphenols in rat intestinal extract and Caco-2 cells grown on Transwell

This chapter has been published as:

Kan, L., Capuano, E., Fogliano, V., Verkerk, R., Mes, J. J., Tomassen, M. M., & Oliviero, T. (2021). Inhibition of  $\alpha$ -glucosidases by tea polyphenols in rat intestinal extract and Caco-2 cells grown on Transwell. *Food Chemistry*, 130047.

### **Abstract**

Inhibition of maltase, sucrase, isomaltase and glucoamylase activity by acarbose, epigallocatechin gallate, epicatechin gallate and four polyphenol-rich tea extract from white, green, oolong, black tea, were investigated by using rat intestinal enzymes and human Caco-2 cells. Regarding rat intestinal enzyme mixture, all four tea extracts were very effective in inhibiting maltase and glucoamylase activity, but only white tea extract inhibited sucrase and isomaltase activity and the inhibition was limited. Mixed-type inhibition on rat maltase activity was observed. Tea extracts in combination with acarbose, produced a synergistic inhibitory effect on rat maltase activity. Caco-2 cells experiments were conducted in Transwells. Green tea extract and epigallocatechin gallate show dose-dependent inhibition on human sucrase activity, but no inhibition on rat sucrase activity. The opposite was observed on maltase activity. The results highlighted the different response in the two model systems studied and show that tea polyphenols are good inhibitors for  $\alpha$ -glucosidase activity.

**Key word:** rat enzyme, Caco-2 cells, tea polyphenols, kinetics, TEER



## 6.1. Introduction

Type-2 diabetes is one of the main diet-related diseases in the world (Mann, 2002). The number of type 2 diabetic patients is estimated to increase to more than 600 million by 2040 (Saeedi et al., 2019). A critical strategy for diabetes prevention is the control of postprandial glucose excursions. The hyperglycaemia can be prevented by some antidiabetic drugs, such as acarbose and voglibose via the inhibition of starch digestive enzyme activities (Lee et al., 2016). Recently, some plant-based polyphenols have been reported as alternatives to modulate starch digestibility, which have similar functions of acarbose (Simsek, Quezada-Calvillo, Ferruzzi, Nichols, & Hamaker, 2015).

Many studies have reported the inhibitory effect of tea polyphenols on various disaccharidases, thereby modulating the blood glucose level (Gao, Xu, Wang, Wang, & Hochstetter, 2013; Lim, Kim, Shin, Hamaker, & Lee, 2019). Although human enzymes are the ideal resources for experiments on enzyme inhibition, many *in vitro* studies used the more readily available rat intestinal enzymes (Simsek et al., 2015). However, rat and human  $\alpha$ -glucosidases are quite different enzymes. Rat  $\alpha$ -glucosidase is composed of two protein complexes, maltase-glucoamylase (MGAM) and sucrase-isomaltase (SI) (Pyner, Nyambe-Silavwe, & Williamson, 2017). Both protein complexes consist of a C-terminal domain (ctMGAM and ctSI) and a N-terminal domain (ntMGAM and ntSI). ctMGAM and ntMGAM are glucoamylase and maltase, respectively. ctSI and ntSI are sucrase and isomaltase, respectively (Pyner et al., 2017). Both MGAM and SI have high  $\alpha$ -1,4 hydrolytic activity on maltose. Each terminal of them have some unique activity, *eg.*, ctMGAM has high hydrolytic activity on larger starch-based oligomers and polymers, ctSI and ntSI have  $\alpha$ -1,2 and  $\alpha$ -1,6 hydrolytic activity, respectively (Lee et al., 2016). Besides rat intestinal  $\alpha$ -glucosidase, human intestinal epithelial cells (Caco-2 cells) can be a more biological alternative to study the modulating effects of dietary compounds towards maltase and sucrase activity (Pyner et al., 2017). Differently from rat and human intestinal enzymes, Caco-2 cells only provide SI, and while MGAM is absent (Hauri, Sterchi, Bienz, Fransen, & Marxer, 1985). Caco-2 cells are human adenocarcinoma cells that spontaneously differentiate into small intestinal enterocytes expressing brush-border enzymes, *i.e.*,  $\alpha$ -glucosidase (Verhoeckx et al., 2015). Enzyme extracts from the Caco-2 cells have been used as sources of sucrase and maltase by some researchers (Pyner et al., 2017). Compared to the use of enzyme extracts from Caco-2, a more physiologically realistic way to simulate disaccharides transport to cells, enzymatic hydrolysis by membrane bound brush-border enzymes and absorption of monosaccharides is to use

Caco-2 cells grown on Transwell inserts, which have been used to study translocation of nutritional compounds from luminal side to the serosal site which would enter the blood (Pico, Corbin, Ferruzzi, & Martinez, 2019). To the best of our knowledge, few researchers have used intact Caco-2 cells grown on Transwell inserts to provide enzymes. Therefore in this study, rat intestinal enzymes and Caco-2 cells grown on Transwell were chosen as the source of  $\alpha$ -glucosidase.

In our previous study, we reported that tea polyphenols can slow down starch digestibility by inhibiting pancreatic  $\alpha$ -amylase (Sigma A4268, 1096 unites/mg) and interacting with starch, thus can potentially modulate the glycaemic index of bread (Kan, Capuano, Fogliano, Oliviero, & Verkerk, 2020). In this study, we further investigated the effect of tea polyphenols on  $\alpha$ -glucosidase activities. Extracts from white, green, oolong and black tea (WTE, GTE, OTE and BTE, respectively) were chosen as source of tea polyphenols. These teas are popular tea among consumers and they have different polyphenols profile because of different processing method. White and green tea are non-fermented tea and white tea is less processed than green tea. Oolong and black tea are half fermented and fully fermented tea, respectively. Two models were used to provide  $\alpha$ -glucosidase, *i.e.*, rat intestinal enzyme and Caco-2 cells in Transwells. Rat intestinal enzyme was used to provide  $\alpha$ -glucosidase, and to study the influence of WTE, GTE, OTE, BTE, EGCG, ECG and polymeric fraction from BTE on  $\alpha$ -glucosidase inhibition. Four substrates has been used to determine individual hydrolytic properties, *i.e.*, maltose, maltodextrin, sucrose and isomaltose. Kinetics of maltase inhibition and synergy of tea polyphenols and acarbose were carried out to further investigate the inhibition mechanisms. Caco-2 cells grown on Transwells were also used to provide  $\alpha$ -glucosidase, and to study the influence of GTE and EGCG on inhibition of compartment Caco-2 derived maltase and sucrase and the effects towards intestinal integrity. The hypothesis of this study is rat and human  $\alpha$ -glucosidase exhibit different sensitivity to tea polyphenol inhibition.

## 6.2. Materials and methods

### 6.2.1. Materials

White tea (LaPlace), green tea (Lipton), and black tea (Pickwick) were purchased from the local supermarket Jumbo in Netherlands. Oolong tea (Pickwick) was provided by Pickwick company in Netherlands. Maltose, sucrose, isomaltose, maltodextrin (dextrose equivalent 4.0-7.0), rat intestinal acetone powders as a source of brush border enzyme, acarbose, EGCG

(epigallocatechin gallate), theaflavin, ECG (Epicatechin gallate), theaflavin-3-gallate, theaflavin-3'-gallate, penicillin-streptomycin solution, phosphate buffered saline (PBS), and fetal bovine serum were purchased from Sigma-Aldrich (Netherlands). Acetonitrile, methanol, ethanol, ethyl acetate, chloroform, BCA kit was purchased from Thermo Fisher Scientific. CaCo-2 cell lines were provided by American Type Culture Collection (ATCC).

#### 6.2.2 Preparation of tea extract and separation of polymeric components

Preparation of tea extracts (TEs), separation of polymeric polyphenols from black tea were done according to our previous method (Kan, Capuano, et al., 2020). Briefly, white tea, green tea, oolong tea and black tea were mixed with absolute methanol (1:10, w/v). Then the mixture was put in an ultrasound equipment (Sonication, China) for 30 min. The extraction was repeated for three times (Sonication, China). After centrifuging (4000 g, 15 min), the supernatants were collected as tea extracts and dried on a freeze dryer (Alpha 2-4 LD plus, Christ). Then the polymeric fraction was separated from BTE. Briefly, BTE solution was prepared by dissolving BTE in 5% of aqueous ethanol. The monomeric and oligomeric fractions were removed by adding ethyl acetate into BTE solution. The remaining aqueous fraction was collected as polymeric fraction, and dried via freeze drying (Alpha 2-4 LD plus, Christ).

Quantification of tea polyphenols was performed according to our previously published paper (Kan, Capuano, et al., 2020). Monomeric polyphenols composition of tea extract was analysed by HPLC-DAD (diode array detector). The tannins content in the tea extract was measured by BSA precipitation method.

#### 6.2.3 Preparation of rat intestinal $\alpha$ -glucosidase

The preparation of intestinal  $\alpha$ -glucosidase was according to a previous report with some modifications (Shin et al., 2019). Rat intestinal enzyme was mixed with 100 mM sodium phosphate buffer (pH 6.8) to give a final concentration of 25 and 50 mg/mL, respectively. The solution was stored at 4 °C for 24 h to extract crude  $\alpha$ -glucosidases. The mixture was centrifuged (13500 g, 25 min) and the supernatant was stored at -20 °C as the enzyme working solutions. The protein concentration of the enzyme working solution was determined with the BCA protein kit.

#### 6.2.4 Hydrolytic properties of rat intestinal $\alpha$ -glucosidases

The glucose produced from hydrolysis of maltose ( $\alpha$ -1,4), sucrose ( $\alpha$ -1,2), isomaltose ( $\alpha$ -1,6) and maltodextrin (dextrose equivalent 4.0-7.0) was determined respectively. Briefly, 150  $\mu$ L of solvent blank (methanol) was mixed with 450  $\mu$ L of maltose (10 mM), sucrose (30 mM), isomaltose (20 mM) or maltodextrin (2 mg/mL). All these substrates were dissolved in 100 mM sodium phosphate buffer (pH 6.8). Then 150  $\mu$ L of enzyme working solution was added (25 mg/mL for maltose and maltodextrin, 50 mg/mL for sucrose and isomaltose) to start the reaction. The  $\alpha$ -glucosidase activity was stopped by adding 750  $\mu$ L of 0.5 M TRIS buffer. Several time points were chosen for the reaction (10, 20, 30, 40, 50, 60 min) and individual tubes were used for each time point. GOPOD kit was used to measure the amount of produced glucose as previously method (Kan, Capuano, et al., 2020). The amount of produced glucose ( $\mu$ mol) from each substrate was plotted against the selected time (10 - 60 min), which showed a linear curve. The slope ( $k$ ) of the linear curve was used for calculation of enzyme activity. One unit of enzyme activity was defined as the amount of glucose ( $\mu$ mol) hydrolysed from the corresponding substrate per minute in the assay.

#### 6.2.5 Rat mucosal enzyme inhibition assay

All the inhibitors were dissolved in methanol and diluted to different concentrations: white, green, oolong, black tea extract and polymeric fraction from BTE were diluted to 0.05~10 mg/mL; EGCG, ECG and theaflavins were diluted to 0.01~1 mg/mL. Briefly, 150  $\mu$ L of solvent blank (methanol) or different concentrations of inhibitors was mixed with 450  $\mu$ L of substrate (maltose (10 mM), sucrose (30 mM), isomaltose (20 mM) or maltodextrin (2 mg/mL)) and 150  $\mu$ L of enzyme working solution. The reaction time was selected according to the result of section 2.4, to have enough glucose released for GOPOD kit measurement, *i.e.*, 30 min for the hydrolysis of maltose and maltodextrin and 60 min for the hydrolysis of sucrose and isomaltose. Finally, TRIS buffer (0.5 M) was added to stop the reaction. The inhibition of the alpha-glucosidase was calculated according to equation below.

$$\text{Inhibition (\%)} = ((C_{\text{control}} - C_{\text{inhibitor}}) / C_{\text{control}}) \times 100$$

Where  $C_{\text{control}}$  was the concentration of glucose produced from individual substrate with solvent blank, and  $C_{\text{inhibitor}}$  was the concentration of glucose produced from individual substrate with inhibitors. Finally, the inhibition of alpha glucosidase was expressed as  $\text{IC}_{50}$  value. The  $\text{IC}_{50}$  value is the concentration of inhibitor required to inhibit 50 % of the enzyme

activity expressed as milligram sample per millilitre solvent. The IC<sub>50</sub> values were calculated using the CompuSyn software.

### 6.2.6 Kinetics analysis of rat maltase inhibition assay

The inhibition type exerted by phenolic-rich samples on maltase was assessed by a kinetic analysis (Yu, Fan, & Duan, 2019). Michaels-Menten plot, Lineweaver-Burk equation combined with Dixon plot and Cornish-Bowden were applied in this study. The formula models for different inhibition types are as follows:

$$\text{Competitive inhibition } \frac{1}{v} = \frac{K_m}{V_{max}} \left(1 + \frac{[i]}{K_i}\right) \frac{1}{[a]} + \frac{1}{V_{max}} \quad (1)$$

$$\text{Non-competitive inhibition } \frac{1}{v} = \frac{K_m}{V_{max}} \left(1 + \frac{[i]}{K_i}\right) \frac{1}{[a]} + \frac{1}{V_{max}} \left(1 + \frac{[i]}{K_i}\right) \quad (2)$$

$$\text{Un-competitive inhibition } \frac{1}{v} = \frac{K_m}{V_{max}} \frac{1}{[a]} + \frac{1}{V_{max}} \left(1 + \frac{[i]}{K_i}\right) \quad (3)$$

$$\text{Mixed inhibition } \frac{1}{v} = \frac{K_m}{V_{max}} \left(1 + \frac{[i]}{K_i}\right) \frac{1}{[a]} + \frac{1}{V_{max}} \left(1 + \frac{[i]}{K_{ia}}\right) \quad (4)$$

Where  $v$  is the reaction rate.  $V_{max}$  and  $K_m$  are maximum reaction rate and Michaelis-Menten constant, respectively.  $K_i$  and  $K_{ia}$  are free enzyme inhibition constant and bound enzyme inhibition constant, respectively.  $[a]$  is the concentration of substrate.  $[i]$  is the concentrations of the inhibitors.

$K_i$  can be calculated by plotting  $1/v$  against  $i$  at several  $a$  values and it equals the absolute value of the intersection abscissa of the plots.  $K_{ia}$  can be achieved by plotting  $a/v$  against  $i$  and it equals the absolute value of the intersection abscissa of the plots.

To calculate the apparent maximum reaction velocity ( $V_{max}^{app}$ ) and the apparent Michaelis constant ( $K_m^{app}$ ), the equation (4) can be written as follows:

$$\frac{1}{v} = \frac{1}{V_{max}^{app}} + \frac{K_m^{app}}{V_{max}^{app}} \frac{1}{[a]} \quad (5)$$

Equation (5) indicates that a plot of  $1/v$  against  $1/[a]$  at a constant value of  $[i]$  is linear.

Therefore the  $V_{max}^{app}$ ,  $K_m^{app}$ , can be calculated as follows:

$$\text{Slope} = \frac{K_m^{app}}{V_{max}^{app}} = \frac{K_m}{V_{max}} \left(1 + \frac{[i]}{K_i}\right) \quad (6)$$

$$\text{Intercept} = \frac{1}{V_{max}^{app}} = \frac{1}{V_{max}} \left(1 + \frac{[i]}{K_{ia}}\right) \quad (7)$$

Where  $V_{max}^{app}$  and  $K_{max}^{app}$  are apparent maximum reaction velocity and apparent Michaelis constant, respectively.

### 6.2.7 Synergetic effect of phenolic inhibitors and acarbose on rat maltase inhibition

The synergetic effect of the polyphenol-acarbose interaction on maltase inhibition was determined by the combination index (CI) using CompuSyn software (Chou, 2006). It is based on the median-effect principle. The combined inhibition assay of tea polyphenols and acarbose was performed at a constant ratio (1mg/mL:1μg/mL). Then a series of concentrations (from 0.25 IC<sub>50</sub> to 4 IC<sub>50</sub>) of tea extracts, tea polyphenols and acarbose were prepared. The combined “Dose-effect” relationships of tea extracts or polyphenols with acarbose for α-glucosidase were constructed, and “Dose” represents the total dose of tea extracts or tea polyphenols and acarbose.

The equation for the median-effect principle is as follows:

$$\log\left(\frac{f_a}{f_u}\right) = m \log D - m \log D_m$$

where D is the dose of the inhibitor,  $f_a$  is the fraction affected by dose D (eg., if the enzyme activity is inhibited by 30%, then  $f_a = 0.3$ ),  $f_u$  is the unaffected fraction ( $f_u = 1 - f_a$ ), m is the coefficient, and  $D_m$  is the median-effect dose (IC<sub>50</sub> in this paper).

The equation for the CI is expressed as follows:

$$CI = \frac{(D)_1}{(D_x)_1} + \frac{(D)_2}{(D_x)_2}$$

where (D)<sub>1</sub> and (D)<sub>2</sub> are the doses of inhibitors that produce a certain level of inhibition in the combination system, and (Dx)<sub>1</sub> and (Dx)<sub>2</sub> are the doses of inhibitors added alone that lead to the same level of inhibition. The type of polyphenol-acarbose interaction was scored as synergistic (CI < 1), additive (CI = 1) or antagonistic (CI > 1).

### 6.2.8 Caco-2 cell culture

Caco-2 cells (American Type Culture Collection) from passage 30 to 40 were cultured and maintained in DMEM containing 10% v/v FBS in 75 cm<sup>2</sup> plastic flasks. Cells were seeded in 12-well polyester insert plates (Corning Inc., Oneonta, USA). The cell density was  $1.25 \times 10^5$  cells per cm<sup>2</sup>. The cells were grown and differentiated for 21 days under a humidified atmosphere of air, 5% CO<sub>2</sub> and at 37 °C. Then highly differentiated monolayers with a TEER > 450 ohm were selected for enzyme studies.

### 6.2.9 Maltase and sucrase inhibition using Caco-2

Fresh medium was placed on apical and basolateral sides of Transwells the day before performing the experiments. Before starting the experiment, TEER voltage was measured to ensure membrane integrity prior to enzyme experiments ( $> 450$  ohm). Then phenol medium was replaced with 1500 mL of phenol-free medium with antibiotics at the basolateral side, and 800  $\mu$ L of prepared inhibitors which dissolved in phenol-free DMEM was added on the apical side. Two wells per plate were employed for the control solution composed of phenol-free DMEM. Another two wells per plate was employed for the blank solution composed of a mixture of maltose (4 mM in phenol-free DMEM) and sucrose (75 mM in phenol-free DMEM). TEER value was measured at 1, 3, 6, 9 and 24 hour. After 24 h, samples were collected from the apical and basolateral side.

Maltose and fructose content of the samples collected from apical and basolateral side were detected by HPLC-ELSD as we previously reported (Kan, Oliviero, Verkerk, Fogliano, & Capuano, 2020). The maltase and sucrase inhibition was calculated by the reduction of the amount of maltose and the production of the fructose, respectively.

$$\text{Maltase inhibition (\%)} = \frac{C_0 - C_a - C_b}{C_0 - C'_a - C'_b} \times 100$$

Where  $C_0$  is the original amount of maltose added in the apical side,  $C_a$  is the amount of maltose detected in the apical side without inhibitors after time 24 hours,  $C_b$  is the amount of maltose detected in the basolateral side without inhibitors after 24 hours,  $C'_a$  is the amount of maltose detected in the apical side with inhibitors after 24 hours,  $C'_b$  is the amount of maltose detected in the basolateral side with inhibitors after 24 hours.

$$\text{Sucrase inhibition (\%)} = \frac{C'_a + C'_b}{C_a + C_b} \times 100$$

Where  $C_a$  is the amount of fructose detected in the apical side without inhibitors after 24 hours,  $C_b$  is the amount of fructose detected in the basolateral side without inhibitors after 24 hours,  $C'_a$  is the amount of fructose detected in the apical side with inhibitors after 24 hours,  $C'_b$  is the amount of fructose detected in the basolateral side with inhibitors after 24 hours.

### 6.2.10 Statistics analysis

The results were expressed as mean  $\pm$  standard deviation (SD). One-way analysis of variance (ANOVA) followed by the Duncan's multiple range test was used to compare the

means among different samples by the SAS 9.4 (SAS Institute Inc., Cary, NC, USA). Differences were considered significant at  $P < 0.05$ .

### 6.3 Results and discussion

#### 6.3.1 Hydrolytic properties of rat intestinal $\alpha$ -glucosidase on different substrates.

Rat intestinal  $\alpha$ -glucosidase shows hydrolytic properties on different  $\alpha$ -glycosidic linkages, e.g.,  $\alpha$ -1,2,  $\alpha$ -1,4 and  $\alpha$ -1,6 linkages (Lim et al., 2019). First, the specific hydrolytic activity of rat  $\alpha$ -glucosidase toward maltose, maltodextrin, sucrose and isomaltose was studied. The rat  $\alpha$ -glucosidase is composed of two enzyme complexes, maltase-glucoamylase (MGAM) and sucrase-isomaltase (SI). All four subunits exhibit maltase activities (*i.e.* against  $\alpha$ -1,4 bonds) (Shin et al., 2019). This is in line with our results as shown in Table 6.1, showing the  $\alpha$ -glucosidase has the highest activities toward maltose (13.77 U/g protein). The glucoamylase subunit shows higher activity toward maltodextrin. The sucrase subunit shows distinctive  $\alpha$ -1,2 glycosidic activity toward sucrose, whereas the isomaltase subunit displays high  $\alpha$ -1,6 hydrolytic activity toward isomaltose. Since different enzymatic subunits may exert hydrolytic activity toward the same substrate (e.g., toward maltose), the hydrolytic activity of individual subunits cannot be determined using the rat  $\alpha$ -glucosidase that has been used in this study. However, this source of  $\alpha$ -glucosidase allows a more realistic assessment of the overall hydrolytic activity. Therefore, the rat intestinal extract is a suitable model to study multiple types of inhibitions on membrane bound disaccharidases. Others also highlighted the advantage of using this model for a more realistic assessment of the hydrolytic activity of disaccharidases (Lim et al., 2019; Shin et al., 2019).

Table 6.1. Specific hydrolytic activities of rat  $\alpha$ -glucosidases on different types of substrates.

$\alpha$ -glucosidase	Substrate	Activity (U/g protein)	Activity (U/g solid)
Maltase	maltose	13.77 $\pm$ 0.06 a	2.41 $\pm$ 0.01 a
Glucoamylase	maltodextrin	7.69 $\pm$ 0.09 b	1.35 $\pm$ 0.01 b
Sucrase	sucrose	1.20 $\pm$ 0.06 d	0.21 $\pm$ 0.01 d
Isomaltase	isomaltose	1.60 $\pm$ 0.06 c	0.28 $\pm$ 0.01 c

The protein content of the rat intestinal extract was 17.5  $\pm$  0.14 g/100g solid.

One unit of enzyme activity was defined as the amount of glucose ( $\mu$ mol) produced from corresponding substrate per minute in the assay.

Results were expressed as means  $\pm$  SD of triplicate analysis. Different letters in the same column indicate a significant difference between means ( $P < 0.05$ ).



### 6.3.2 Inhibition properties of tea extracts on rat $\alpha$ -glucosidase using different substrates

To better understand the hydrolytic inhibition of four TEs on rat  $\alpha$ -glucosidase, the polyphenol composition was investigated and the results are shown in Table 6.2. The total polyphenol content, ECG and EGCG content in TEs was in the order WTE > GTE > OTE > BTE, whereas the tannins content was in the order BTE > OTE > WTE > GTE. This was in line with the previous report, showing that fermented tea (oolong tea and black tea) contains more tannins than non-fermented tea (white and green tea) (Sun, Warren, Netzel, & Gidley, 2016). Then, the individual hydrolytic inhibition of tea polyphenols on individual hydrolytic property toward maltose, maltodextrin, sucrose and isomaltose was studied. As shown in Table 6.3, all four tea extracts are very effective in the inhibition of maltase and glucoamylase, but only WTE was weakly effective on sucrase and isomaltase. This inhibition was very weak as indicated by the high  $IC_{50}$  values, 7.6 and 4.2 mg/mL, respectively. The other three TEs did not show any inhibition on sucrase and isomaltase. WTE was the most efficient inhibitor of  $\alpha$ -glucosidase towards maltose and maltodextrin, resulting in  $IC_{50}$  value of 0.26 and 0.073 mg/mL, respectively. The higher inhibition of WTE is possibly due to its higher amount of total phenolic content (55 g/100g) and more specifically to the higher amount of EGCG (31.2 g/100g) which is the peculiar feature of WTE as shown in Table 6.2. EGCG had strong inhibition properties towards maltase ( $IC_{50}$  = 0.021 mg/mL) and glucoamylase ( $IC_{50}$  = 0.018 mg/mL), weak inhibition towards isomaltase ( $IC_{50}$  = 0.44 mg/mL) and no effect towards sucrase. However the inhibitory activity of EGCG against maltase is 30 times lower than the positive control acarbose ( $IC_{50}$  = 0.0006 mg/mL). Other researchers also reported that EGCG showed strong inhibition on maltase by using *Saccharomyces cerevisiae* with a  $IC_{50}$  value of 0.08 mg/mL (Chem & Ii, 2010). Purified rat  $\alpha$ -glucosidase was also used by some researcher who found that 0.14 mg/mL of EGCG had similar inhibition properties toward dextrin, maltose, sucrose and isomaltulose with inhibition of 64.2, 79.8, 76.1, and 64.7%, respectively (Lim et al., 2019).

In our previous study, we found that the polymeric fraction from BTE showed strong inhibition on starch digestibility by inhibiting  $\alpha$ -amylase and interacting with starch, especially in a model of gluten-free bread (Kan, Capuano, et al., 2020). In this study, we further found that polymeric fraction from BTE, *i.e.* the tannins-rich fraction, showed strong inhibition on maltase (0.31 mg/mL) and glucoamylase (0.06 mg/mL) and weak inhibition on sucrase (2.34 mg/mL) and isomaltase (5.14 mg/mL). The tannins fraction was also reported for its  $\alpha$ -glucosidase inhibitory capacity. For example, tea tannins from *Ampelopsis*

*grossedentata* leaves inhibited maltase from *Saccharomyces cerevisiae* using p-nitrophenyl- $\alpha$ -D-glucopyranoside as substrate with a  $IC_{50}$  value of 1.94  $\mu$ g/mL (Geng et al., 2016). In our study, ECG showed to have a more selective inhibitory activity towards isomaltose ( $IC_{50}$  = 0.32 mg/mL, 0.72 mM) compared to antidiabetic drug acarbose ( $IC_{50}$  = 1.09 mg/mL, 1.69 mM). Lim et al., (2019) also found 0.3 mM of ECG and acarbose showed a similar inhibition of 77.7 and 87.1 % towards isomaltulose as substrate. Therefore, WTE, EGCG and ECG could reduce postprandial glucose uptake in maltodextrin-rich, maltose-rich and isomaltose-rich food, respectively (Ao et al., 2007).

However, the enzyme working solution used in this study is a crude extract from rat intestine without any purification. Consequently, the enzyme working solution contains not only  $\alpha$ -glucosidase but also  $\alpha$ -amylase, protease and other impurities (Shin et al., 2019).  $\alpha$ -amylase can also produce glucose from the substrates used in our study. Therefore, the maltase and glucoamylase activities in Table 6.1 were likely to be overestimated due to the contribution from  $\alpha$ -amylolytic activity of the rat extract. In our previous study, we confirmed the inhibitory effect of tea polyphenols on  $\alpha$ -amylase (Kan, Capuano, et al., 2020). The presence of  $\alpha$ -amylase in rat enzyme preparation can thus interfere with the inhibitory effects of polyphenols on maltase and glucoamylase, since  $\alpha$ -amylase can generate glucose from maltose and maltodextrins. Therefore, the results of inhibitory effect on maltase and glucoamylase in Table 6.3 could be a combined inhibition on  $\alpha$ -glucosidase and  $\alpha$ -amylase. Some researchers have used centrifugal filter unit, with a molecular weight cut-off of 100 kDa to purify the crude  $\alpha$ -glucosidase working solution, resulting in a reduction of  $\alpha$ -amylase activity from 150.7 U to 101.9 U (Shin et al., 2019). In addition, the presence of other impurities, for instance, non-enzyme proteins may reduce the amount of polyphenols that was able to bind and inhibit brush border enzymes, thus reducing their inhibitory effects.

Table 6.2. Polyphenol composition of WTE, GTE, OTE and BTE (g/100g).

Polyphenols	WTE	GTE	OTE	BTE
EGCG	31.2 $\pm$ 0.2 a	27.2 $\pm$ 0.2 a	5.0 $\pm$ 0.0 a	7.3 $\pm$ 0.1 a
ECG	10.0 $\pm$ 0.1 b	6.1 $\pm$ 0.1 b	4.9 $\pm$ 0.1 ab	7.1 $\pm$ 0.1 b
Theaflavin	nd	nd	0.5 $\pm$ 0.0 e	2.3 $\pm$ 0.1 d
Theaflavin 3-gallate	nd	nd	0.4 $\pm$ 0.0 f	1.3 $\pm$ 0.0 f
Theaflavin 3'-gallate	nd	nd	0.8 $\pm$ 0.0 d	1.8 $\pm$ 0.0 e
tannins	2.2 $\pm$ 0.0 c	0.8 $\pm$ 0.0 c	3.3 $\pm$ 0.1 c	5.0 $\pm$ 0.1 c
total	55.0 $\pm$ 0.1	42.9 $\pm$ 0.5	15.0 $\pm$ 0.0	24.7 $\pm$ 0.1

Values are expressed as mean from triplicate analysis  $\pm$  standard deviation. Different letters in the same column (except for the total amount) indicate a significant difference between means ( $P < 0.05$ ).

WTE: white tea extract; GTE, green tea extract; BTE, black tea extract; OTE, oolong tea extract; EGCG, epigallocatechin gallate, nd, not detected.

Table 6.3: IC<sub>50</sub> value (mg/mL) of the  $\alpha$ -glucosidase inhibition using different substrates

Inhibitors	maltose	maltodextrin	sucrose	Isomaltose
WTE	0.26 ± 0.01 f	0.073 ± 0.002 f	7.6 ± 0.1 a	4.2 ± 0.3 b
GTE	0.67 ± 0.01 c	0.10 ± 0.01 e	ND	ND
OTE	1.15 ± 0.01 b	0.57 ± 0.02 b	ND	ND
BTE	1.59 ± 0.08 a	0.47 ± 0.03 c	ND	ND
EGCG	0.021 ± 0.001 / 45.8 $\mu$ M g	0.018 ± 0.001 / 39.2 $\mu$ M h	ND	0.44 ± 0.01 / 121.5 $\mu$ M d
ECG	0.57 ± 0.03 / 1.29 mM d	0.35 ± 0.01 / 0.79 mM d	ND	0.32 ± 0.01 / 0.72 mM e
Theaflavin	ND	ND	ND	ND
Theaflavin 3-gallate	ND	0.48 ± 0.02 c	ND	ND
Theaflavin 3'-gallate	ND	0.99 ± 0.02 a	ND	ND
Polymeric fraction	0.31 ± 0.01 e	0.06 ± 0.01 g	2.34 ± 0.03 b	5.14 ± 0.06 a
Acarbose	0.00061 ± 0.00001 / 0.94 $\mu$ M h	0.00025 ± 0.00001 / 0.39 $\mu$ M i	0.011 ± 0.001 / 15.5 $\mu$ M c	1.09 ± 0.02 / 1687.3 $\mu$ M c

WTE: white tea extract; GTE, green tea extract; BTE, black tea extract; OTE, oolong tea extract; EGCG, epigallocatechin gallate. ND, not detected. IC<sub>50</sub> values of EGCG, ECG and acarbose were expressed as two units, the unit of left value was mg/mL, and the unit of the right value was  $\mu$ M. Values are expressed as mean from triplicate analysis  $\pm$  standard deviation. Different letters in the same column indicate a significant difference between means ( $P < 0.05$ ).

### 6.3.3 Kinetics of $\alpha$ -glucosidase inhibition toward maltose and type of inhibition

As shown before, all four enzymatic subunits of MGAM and SI exhibit maltase activities (*i.e.* against  $\alpha$ -1,4 bonds) and maltose is a common product from starch digestion by pancreatic  $\alpha$ -amylase. To better understand the inhibitory mechanism on maltase, *e.g.*, the type of inhibition, a more detailed kinetic characterisation of the inhibition using maltose as substrate was carried out (Fig. 6.1 and Supplementary material). The exact type of inhibition can be analysed and defined by the combined use of Dixon and Cornish-Bowden plots and Lineweaver-Burk plots as summarized in Table 6.4. Regarding acarbose, the Dixon plots intersect at one point, while the Cornish-Bowden plots run parallel with each other (Fig. 6.1B&C). This demonstrated that acarbose is a competitive inhibitor for  $\alpha$ -glucosidase, which was in line with the previous report (Bischoff, 1995; Calder & Geddes, 1989). This was also confirmed by the values of  $K_m^{app}$  and  $V_{max}^{app}$  calculated from Lineweaver-Burk plots (Table 6.5, Fig. 6.1D). As shown in Table 6.5, the  $K_m^{app}$  increases while  $V_{max}^{app}$  remains the same. Besides, the Lineweaver-Burk plots intersected the y axis. Those are the typical characteristics of competitive inhibition (Sun et al., 2016). Regarding all the TEs and tea polyphenols, both the Dixon and Cornish-Bowden lines intersect at one point (Fig. 1B&C), indicating that they are mixed-type inhibitors. This was further confirmed by the decrease of  $V_{max}^{app}$  (Table 6.5). Based on mixed-type inhibition mechanism, TEs and tea polyphenols can compete with maltose in binding with  $\alpha$ -glucosidase (competitive), as well as can bind with the  $\alpha$ -glucosidase-maltose complex (uncompetitive). Hydrophobic association and hydrogen

bonding have been reported to be the main mechanisms of polyphenols-enzymes interactions (Martinez-Gonzalez et al., 2017).  $K_m^{app}$  of all the TEs and polyphenols increases, indication that the mixed-type inhibition of those inhibitors more closely mimic competitive binding (Table 6.4&6.5). This was in line with that  $K_i$  was smaller than  $K_{ia}$  for all the mixed-type inhibitors (Table 6.5). This suggests that they bind more tightly with free  $\alpha$ -glucosidase than with the  $\alpha$ -glucosidase-maltose complex. Interestingly, the order of  $IC_{50}$  values of four tea extracts correspond to that of the inhibition constants (both  $K_i$  and  $K_{ia}$ ), this was in line with previous report for  $\alpha$ -amylase inhibition (Sun et al., 2016).

As our TEs is a mixture of monomeric and polymeric polyphenols and all the subunits of rat  $\alpha$ -glucosidase shows hydrolytic activity towards maltose, the combination of different mechanisms is expected. Our results are consistent with a previous report where black tea extract was shown to exert a mixed-type inhibition for mammalian  $\alpha$ -glucosidase, using maltose as substrate (Sato, Igarashi, Yamada, Takahashi, & Watanabe, 2015). Some researchers reported different results on inhibition of yeast  $\alpha$ -glucosidase by TEs or tea polyphenols, using 4-Nitrophenyl  $\beta$ -D-glucopyranoside as substrate. For instance, it was reported that gallic acid (GCG) and green tea extract inhibited yeast  $\alpha$ -glucosidase by non-competitively (Wu et al., 2018; X. Yang & Kong, 2016). Non-competitive inhibition is sometimes considered as a special case of mixed-type inhibition, *i.e.*, the competitive constant and un-competitive constant calculated from Dixon and Cornish-Bowden are exactly the same ( $K_i = K_{ia}$ ). Commonly, Lineweaver-Burk plots was used to identify the inhibition type. But the Dixon and Cornish-Bowden can be used to assist in analysing the inhibition to further confirm the inhibition type.

**Table 6.4.** The characteristics of different inhibition types

Inhibition type	Lineweaver-Burk plots ( $1/v$ against $1/s$ )	Dixon plots ( $1/v$ against $i$ )	Cornish-Bowden plots ( $a/v$ against $i$ )
Competitive	1) Intersection; 2) $K_m^{app}$ increased, while $V_{max}^{app}$ remains more or less the same.	Intersection	No intersection (parallel lines);
Uncompetitive	1) No intersection (parallel lines); 2) Both $K_m^{app}$ and $V_{max}^{app}$ decreased.	No intersection (parallel lines);	Intersection
Non-competitive binding	1) Intersection; 2) $V_{max}^{app}$ decreased, $K_m^{app}$ remains the same	Intersection	Intersection
Mixed	1) Intersection; 2) $V_{max}^{app}$ decreased, $K_m^{app}$ increase (more closely to competitive binding), or $K_m^{app}$ decrease (more closely to uncompetitive binding).	Intersection	Intersection

The information of this table was summarized according to previous studies (Peng, Zhang, Liao, & Gong, 2016; Sun, Gidley, & Warren, 2017; Sun et al., 2016).

**Table 6.5.** Michaelis-Menten parameters for  $\alpha$ -glucosidase inhibition by tea polyphenol

Inhibitor	$K_m^{app}$ (mg/mL)					$V_{max}^{app}$ (mM glucose / min)					$K_i$ mg/mL	$K_{ia}$ mg/mL	Inhibition type
	A	B	C	D	E	A	B	C	D	E			
WTE	4.861	5.816	6.098	7.460	8.241	0.062	0.049	0.040	0.029	0.017	0.102 <sup>c</sup>	0.196 <sup>d</sup>	mixed
GTE	4.772	4.639	5.059	5.347	5.933	0.056	0.047	0.040	0.029	0.017	0.735 <sup>c</sup>	1.091 <sup>c</sup>	mixed
BTE	4.201	4.605	4.938	4.901	4.998	0.056	0.051	0.045	0.035	0.022	1.267 <sup>b</sup>	1.509 <sup>b</sup>	mixed
OTE	4.525	5.074	5.558	5.534	5.433	0.059	0.055	0.052	0.044	0.029	1.956 <sup>a</sup>	2.366 <sup>a</sup>	mixed
EGCG	4.872	5.426	5.387	5.800	5.823	0.057	0.046	0.034	0.023	0.014	0.026 <sup>f</sup>	0.035 <sup>c</sup>	mixed
Polymeric fraction	4.333	4.906	6.121	5.631	6.509	0.084	0.072	0.068	0.041	0.030	0.149 <sup>d</sup>	0.198 <sup>d</sup>	mixed
Acarbose *	3.362	5.532	8.773	20.472	65.700	0.076	0.076	0.074	0.086	0.129	0.121 <sup>g</sup>	NA	competitive

\*The units of  $K_m^{app}$ ,  $K_i$  and  $K_{ia}$  for acarbose is  $\mu\text{g/mL}$ . Values are expressed as mean from triplicate analysis. Different letters in the same column indicate a significant difference among means ( $P < 0.05$ ).

The characters (A to E) represent the concentrations of inhibitors, as shown in Fig. 2A (A=0, E=highest concentration, increasing order from A to E). NA, not applicable. WTE, white tea extract; GTE, green tea extract; BTE, black tea extract; OTE, oolong tea extract; EGCG, epigallocatechin gallate.

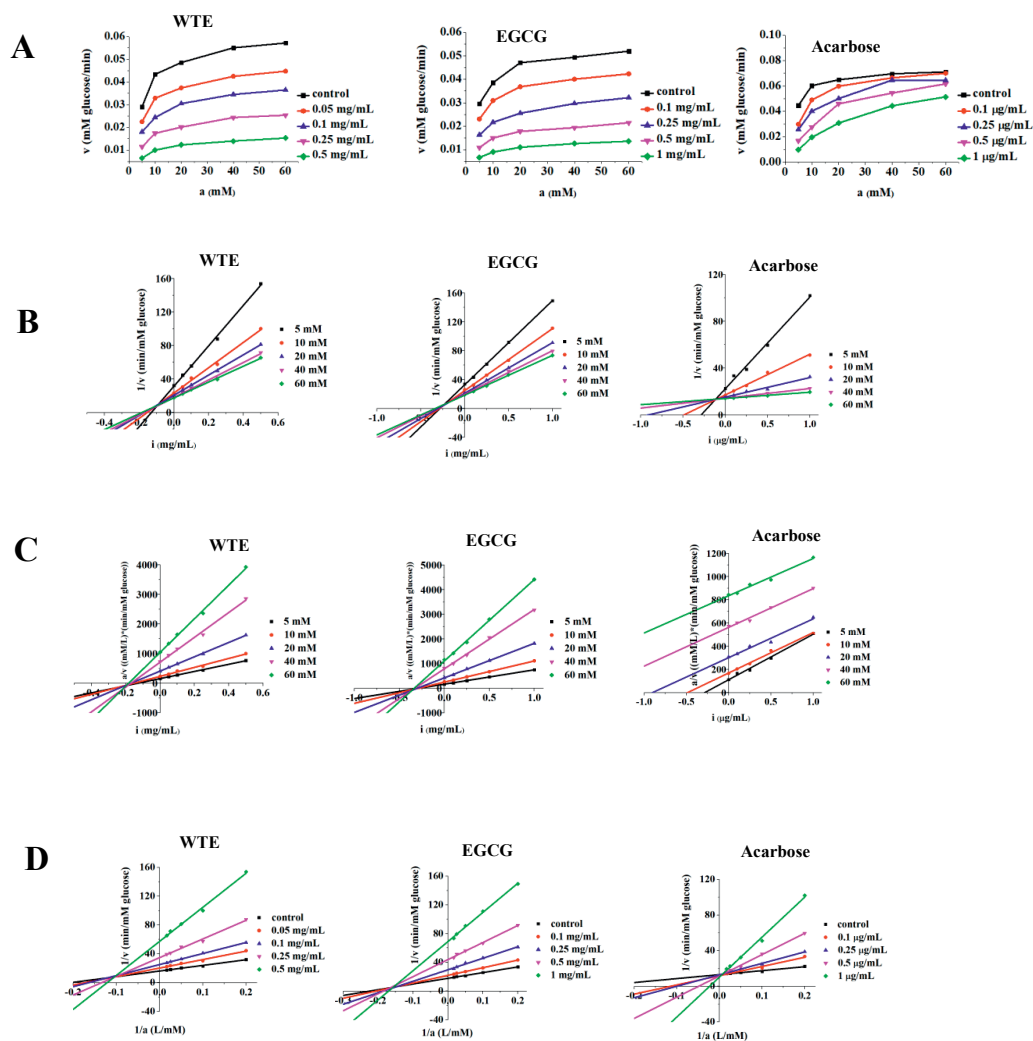


**Figure 6.1.** Kinetics of  $\alpha$ -glucosidase inhibition by tea extracts or tea polyphenols using maltose as substrate. A: Michaelis–Menten plots for  $\alpha$ -glucosidase inhibition by WTE, EGCG, and acarbose. B: Dixon plots for  $\alpha$ -glucosidase inhibition by WTE, EGCG, and acarbose. C: Cornish-Bowden plots for  $\alpha$ -glucosidase inhibition by WTE, EGCG, and acarbose. D: Lineweaver-Burk plots for  $\alpha$ -glucosidase inhibition by WTE, EGCG, and acarbose; WTE: white tea extract; EGCG, epigallocatechin gallate.

#### 6.3.4 Synergy determination for maltase inhibition

To investigate the combined effect of polyphenols and acarbose, we used the method reported by Chou and Talalay to distinguish among synergistic, antagonistic, and additive effects (Chou, 2010). In this method, CI value was calculated by CompuSy to distinguish the three types of effects. As shown in Figure 6.2, except for some lowest concentrations, the combination of all the TEs and EGCG with acarbose showed slight antagonistic inhibition, since the CI values were slightly higher than 1. The combination of polymeric fraction from BTE with acarbose strongly reduced their inhibition, since their CI value was higher than 4. Other researchers also found antagonistic inhibition when combined catechin with acarbose (Zhang et al., 2017). However, some researchers reported different results using baker's yeast  $\alpha$ -glucosidase, *i.e.*, the combination of green tea polyphenols with acarbose had synergistic and antagonistic effects on  $\alpha$ -glucosidase at low and high concentrations, respectively (Gao et al., 2013). The different results could be explained by different enzyme resources, *i.e.*, baker's yeast enzymes and rat enzymes have different amino acid sequences at the catalytic site. There are also some *in vivo* reports about the synergistic effect of tea polyphenols and acarbose. One of the examples is black tea extract, in combination with acarbose, produced a synergistic inhibitory effect on sucrase activity, resulting in decrease of plasma glucose levels of Goto Kakizaki rat *in vivo* (Satoh et al., 2015).

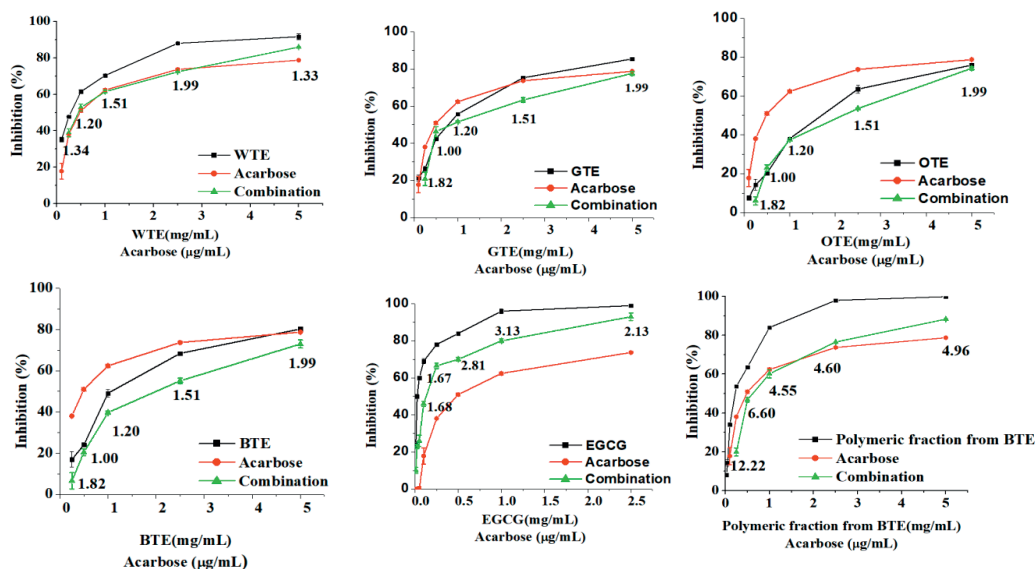


**Figure 6.2.** The inhibitory effect of the combination of acarbose with white tea extract (WTE), green tea extract (GTE), oolong tea extract (OTE), black tea extract (BTE), epigallocatechin gallate (EGCG), and the polymeric fraction from BTE against rat  $\alpha$ -glucosidase, using maltose as substrate. The dose of the combination samples is the total dose of tea extracts or tea compounds and acarbose. The ratio of the tea extracts and acarbose for the combination samples is 1mg/mL:1 $\mu$ g/mL, respectively. The unites of Axis X: acarbose,  $\mu$ g/mL; Tea extracts or EGCG or polymeric fraction from BTE: mg/mL. CI values are indicated as numbers in black along the combination samples and were calculated by CompuSyn software. CI < 1, CI = 1, and CI > 1 indicate synergism, additive effect, and antagonism, respectively. The values shown are the means of duplicate analyses  $\pm$  standard deviation.

### 6.3.5 Inhibitory effect of tea polyphenols on human maltase and sucrase

To investigate the effect of tea polyphenols on human maltase and sucrase and their effect on tight junctions, GTE, EGCG and acarbose were tested on Caco-2 grown on Transwell insert plates. First, the hydrolytic properties of maltase and sucrase was measured based on amount of hydrolysed maltose and produced fructose in both apical and basolateral side, respectively. As shown in [Figure 6.3A](#), within 24h, 3.4 mM of maltose was hydrolysed and no maltose was found in basolateral side. Within 24 h, 16.1 and 4.1 mM of fructose were detected in the apical and the basolateral side, respectively. Fructose could be absorbed by Caco-2 cells, which explains its presence in the basolateral side ([Andrade, Araújo, Correia-Branco, Carletti, & Martel, 2017](#)). TEER values are strong indicators of the integrity of the cell monolayers before their use to study transport of drugs or chemicals ([Srinivasan et al., 2015](#)). As shown in [Figure 6.3A](#), cells exposed to 4 mM of maltose and 75 mM of sucrose



caused a small (around 5%) reduction of TEER in the first 9 hours, but TEER recovered to 100% within 24 h. Therefore, those concentrations of maltose and sucrose were selected for further experiments.

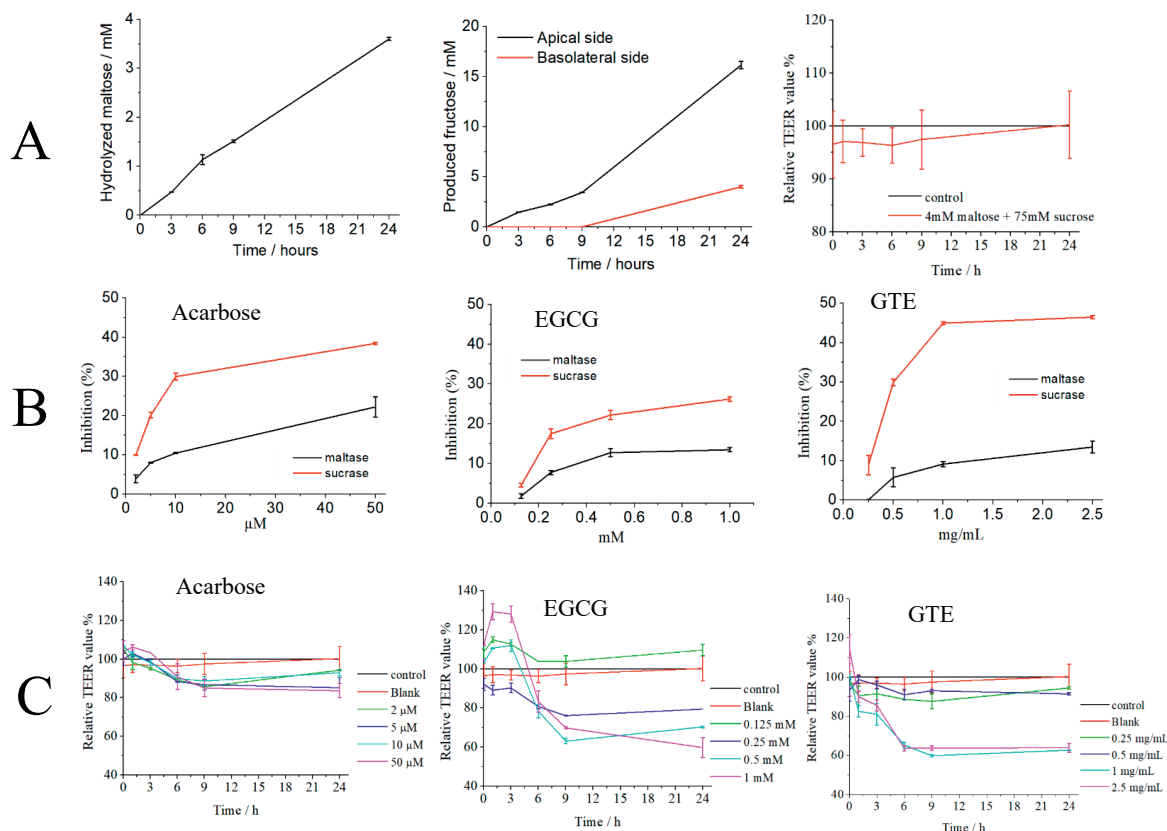


Figure 6.3. A) Amount of hydrolysed maltose and produced fructose in apical and basolateral side without any inhibitors, and TEER value with/without maltose and sucrose. B) Inhibition of acarbose, EGCG and GTE on maltase and sucrase from differentiated Caco-2 cells in apical and basolateral side after 24 h. C) Effect of tested inhibitors on TEER value of Caco-2 cells. All the TEER measurement are at time 0, 0.01, 1, 3, 6, 9, 24 h. TEER at time point 0 represent the TEER value before adding any substrate or inhibitors. TEER value at T=0 is 100% for all the samples. TEER at time point 0.01 represent the immediate TEER value after adding the substrate and inhibitors. Results are expressed as mean  $\pm$  SD (n=3). GTE, green tea extract; EGCG, epigallocatechin gallate.

Then, the inhibitory effect of acarbose, EGCG and GTE was investigated. As shown in Figure 6.3B, GTE, EGCG and acarbose exhibited an inhibitory effect on sucrase and maltase activity expressed by Caco-2 cells grown on Transwells. The inhibitory activity of all the tested compounds was dose-dependent. Interestingly, the inhibition on sucrase was much higher than on maltase, which was the opposite as found for the experiments with rat enzyme (Table 6.3). This is possibly because Caco-2 only provide SI, while MGAM is absent (Hauri, Sterchi, Bienz, Fransen, & Marxer, 1985). Therefore, the use of enzymes produced by Caco-2 can be considered as a better *in vitro* simulation model when evaluating effects for the human intestinal tract, since SI hydrolyses the majority of maltose in human intestine (Pyner et al., 2017). Our data also suggest that the tested inhibitors are more effective on Caco-2 sucrase than rat sucrase. In contrast, the opposite was observed when assessing maltase activity, e.g.: IC<sub>50</sub> of EGCG was 45.8  $\mu$ M for rat maltase (Table 6.3), but 1000  $\mu$ M of EGCG, the highest concentration used in the study, did not reach 50% of inhibition in human enzyme (Figure 6.4B). This is in line with the fact that the homology between human and rat sucrase–isomaltase is only 74%, and so this could possibly explain the difference between human and rat enzyme (Van Beers, Büller, Grand, Einerhand, & Dekker, 1995). Finally the influence of inhibitors on TEER value was measured simultaneously with sugar analysis. As shown in Figure 6.4C, cells exposed to 2–50  $\mu$ M of acarbose maintained a TEER above 80% during the 24 h measurement and the same happens for the low concentrations of GTE (0.25 and 0.5 mg/mL). Acarbose is commonly used for the type-2 diabetes treatment. The dosage of acarbose that people take as medicine is 25–50 mg per time, three times per day, *i.e.*, the concentration of acarbose is 1.11–2.22  $\mu$ M by considering the volume of intestinal fluids as 105 mL (Rosenstock et al., 1998; Schiller et al., 2005). Therefore, our results about the efficacy of the acarbose in Caco-2 cells were as expected, which indicated the Caco-2 grown on Transwells could be a reliable system for investigating human sucrase and maltase inhibition, as well as the effects on tight junction. The higher concentration of GTE (1 and 2.5 mg/mL) caused a dramatic decrease of TEER during the first 6 hours which did not recover after 24 hours. Lower concentration of EGCG (0.125 mM) caused an increase of the TEER value during the 24 hours. This was in line with the previous reports that EGCG has protective effect towards epithelial integrity in Caco-2 cell monolayers (Carrasco-Pozo, Morales, & Gotteland, 2013). But the high concentrations (0.25, 0.5, 1 and 2 mM) of EGCG caused a significant increase of TEER for the 1<sup>st</sup> three hours, then decreased dramatically to 75%, 65% and 60% at 6<sup>th</sup>, 9<sup>th</sup>, and 24<sup>th</sup> hour, respectively. Therefore, the enzyme inhibition of high concentrations of EGCG and GTE could be underestimated due to the reduce of TEER.

This may happen because the inhibitors may migrate to basolateral compartment due to the reduction of tight junction, and less inhibitors are available in apical compartment to inhibit enzyme activity. This could be one of the reasons that the inhibition curves in Figure 6.3B tend to flatten at higher concentrations of inhibitors. The increase of the TEER caused by lower concentration of GTE and EGCG could be used for regulating the intestinal junction and barrier function. Many researchers reported that polyphenols can regulate the intestinal barrier function (Hervert-Hernández & Goñi, 2011; G. Yang, Bibi, Du, Suzuki, & Zhu, 2017). Although tea polyphenols are promising for sucrase and maltase inhibition, an effective concentration of polyphenol through tea consumption should be considered. As reported previously, one cup of tea could provide 5–20 mg of EGCG, so the final concentration in the small intestine may less than 10  $\mu$ M by considering the dilution by gastric and intestinal fluids (Kan, Capuano, et al., 2020; Rosenstock et al., 1998). This amount is much lower than the tested concentration as shown in Figure 6.3. Although an effective concentration of polyphenol to inhibit human maltase and sucrase can be hardly achieved through daily tea drinking, a feasible strategy may be to combine tea polyphenols or acarbose with sugar-rich or starch-rich food to modulate glucose release in the small intestine.

The main conclusion of this study is that maltase and sucrase activities showed different sensitivity to polyphenols by using rat acetone extract and human Caco-2 cells. That can be mainly attributed to the different intrinsic characteristics of the enzymes and the different experimental system. In human and rat, MGAM and SI are both present on the brush border membrane of small intestinal enterocytes (Semenza, Auricchio, & Rubino, 1965). Both MGAM and SI show maltase activity (Pyner et al., 2017). In humans, the amount of MGAM protein is 40–50 times lower than the amount of SI in the human intestine (Semenza et al., 1965). However, MGAM still contributes 30–40% of the total maltase activity due to its higher Ct subunit hydrolytic activity (Quezada-Calvillo et al., 2008). In rat the MGAM has higher maltase activity and produce higher intestinal glucogenesis, while SI has lower maltase activity and sustains slower glucogenesis (Quezada-Calvillo et al., 2007). Human Caco-2 cells is commonly used to provide human disaccharides, but Caco-2 cells only provide SI (Pyner et al., 2017). Therefore, maltase activity in Caco-2 cells is only from SI. Besides, the different experimental conditions used may also explain the different sensitivity observed. Rat enzyme inhibition was performed in test tubes by mixing enzymes, substrates and inhibitors, whereas human enzyme inhibition was measured by intact Caco-2 cells in Transwells. The rat enzymes are a mixture of enzymes free in solutions, whereas Caco-2 enzymes are located in

the membranes of the monolayer of cells. Caco-2 cells have been used by many researchers to provide human  $\alpha$ -glucosidase by using either cell homogenates or membrane-enriched preparations (Pyner et al., 2017). In our study, intact cells grown in Transwells were used without damaging the cell monolayer, which is a physiologically realistic way to simulate enzymatic hydrolysis. Moreover, we used different substrate concentrations to determine the enzyme activity of rat and Caco-2 cell enzymes. This is because different detection and calculation method for maltase and sucrase activity are applied to enzymes from rat acetone extract and Caco-2 cells. Regarding enzymes from rat acetone extract, the calculations of maltase and sucrase activity were based on glucose release from corresponding substrate, which were measured by GOPOD kit. Therefore, 10 mM of maltose and 30 mM of sucrose were selected to make sure enough glucose to be produced to have sufficient color reaction with GOPOD reagent. Regarding experiments in Caco-2 cells, the glucose release cannot be measured because large amounts of glucose are present in DMEM cell culture media. Then, the calculations of maltase and sucrase activity in Caco-2 cells were based on the amount of remaining maltose and produced fructose, which are measured by HPLC-ELSD. Therefore, 4 mM of maltose and 75 mM of sucrose were selected to make sure the remaining amount of maltose and produced fructose are within the detection limit of HPLC-ELSD. Clearly, other polyphenols should be tested to draw firm conclusion on the different sensitivity of rat and human enzymes to polyphenols.

#### **6.4 Conclusion**

This study investigated the inhibitory effects of tea polyphenols on  $\alpha$ -glucosidase activities, using rat intestinal enzymes and Caco-2 cells. Four tea extracts were selected, *i.e.*, white, green, oolong, and black tea extract. All these tea extracts showed a significant enzyme-inhibiting capacity when using dextrin and maltose as substrate. White tea extract is the most effective inhibitor probably because of the high concentration of EGCG. Mixed-type of inhibition was found for the maltase inhibition, and the tea extracts and EGCG showed slightly antagonism effect when combined with acarbose. Therefore, drinking tea at a different time when taking acarbose is recommended. The inhibition of maltase and sucrase from Caco-2 cells is quite different from rat enzyme. Human sucrase activity was more susceptible than the rat enzyme to inhibition by green tea extract and EGCG, while the opposite result was observed when evaluating maltase activity. Tight junction was also influenced when the cells were exposed to tea polyphenols indicated by the reduction of TEER value. In conclusion, tea polyphenols are potential inhibitors for both rat and human  $\alpha$ -

glucosidase with different sensitivity. Rat acetone extract is a convenient tool for measuring enzymatic hydrolysis by using various substrates, *i.e.*, maltose, maltodextrin, isomaltose, and sucrose. Caco-2 cells grown on Transwells can be used to simulate enzymatic hydrolysis in a more physiologically realistic way.

### **Acknowledgement**

The authors would like to thank Luana Kolkman for her assistance for the lab work. The author Lijiao Kan received a PhD scholarship from the China Scholarship Council (No. 201706820018).

**References:**

- Andrade, N., Araújo, J. R., Correia-Branco, A., Carletti, J. V., & Martel, F. (2017). Effect of dietary polyphenols on fructose uptake by human intestinal epithelial (Caco-2) cells. *Journal of Functional Foods*, 36, 429-439. <https://doi.org/10.1016/j.jff.2017.07.032>.
- Ao, Z., Simsek, S., Zhang, G., Venkatachalam, M., Reuhs, B. L., & Hamaker, B. R. (2007). Starch with a slow digestion property produced by altering its chain length, branch density, and crystalline structure. *Journal of Agricultural and Food Chemistry*, 11, 4540–4547. <https://doi.org/10.1021/jf063123x>.
- Bischoff, H. (1995). The mechanism of  $\alpha$ -glucosidase inhibition in the management of diabetes. *Clinical and Investigative Medicine*, 18, 303-311. <https://europepmc.org/article/med/8549017>.
- Calder, P. C., & Geddes, R. (1989). Acarbose is a competitive inhibitor of mammalian lysosomal acid  $\alpha$ -d-glucosidases. *Carbohydrate Research*, 80, 1081-1087. [https://doi.org/10.1016/0008-6215\(89\)85047-5](https://doi.org/10.1016/0008-6215(89)85047-5).
- Carrasco-Pozo, C., Morales, P., & Gotteland, M. (2013). Polyphenols protect the epithelial barrier function of Caco-2 cells exposed to indomethacin through the modulation of occludin and zonula occludens-1 expression. *Journal of Agricultural and Food Chemistry*, 61, 5291-5297. <https://doi.org/10.1021/jf400150p>.
- Chem, F., & Li, T. (2010). Inhibition of three selected beverage extracts on  $\alpha$ -glucosidase and rapid identification of their active compounds using HPLC-DAD-MS/MS and biochemical detection. *Journal of Agricultural and Food Chemistry*, 58, 6608–6613. <https://doi.org/10.1021/jf100853c>.
- Chou, T. C. (2010). Drug combination studies and their synergy quantification using the chou-talalay method. *Cancer Research*, 70, 440-446. <https://doi.org/10.1158/0008-5472.CAN-09-1947>.
- Gao, J., Xu, P., Wang, Y., Wang, Y., & Hochstetter, D. (2013). Combined effects of green tea extracts, green tea polyphenols or epigallocatechin gallate with acarbose on inhibition against  $\alpha$ -amylase and  $\alpha$ -glucosidase *in vitro*. *Molecules*, 18, 11614-11623. <https://doi.org/10.3390/molecules180911614>.
- Geng, S., Chen, Y., Abbasi, A. M., Ma, H., Mo, H., & Liu, B. (2016). Tannin fraction from

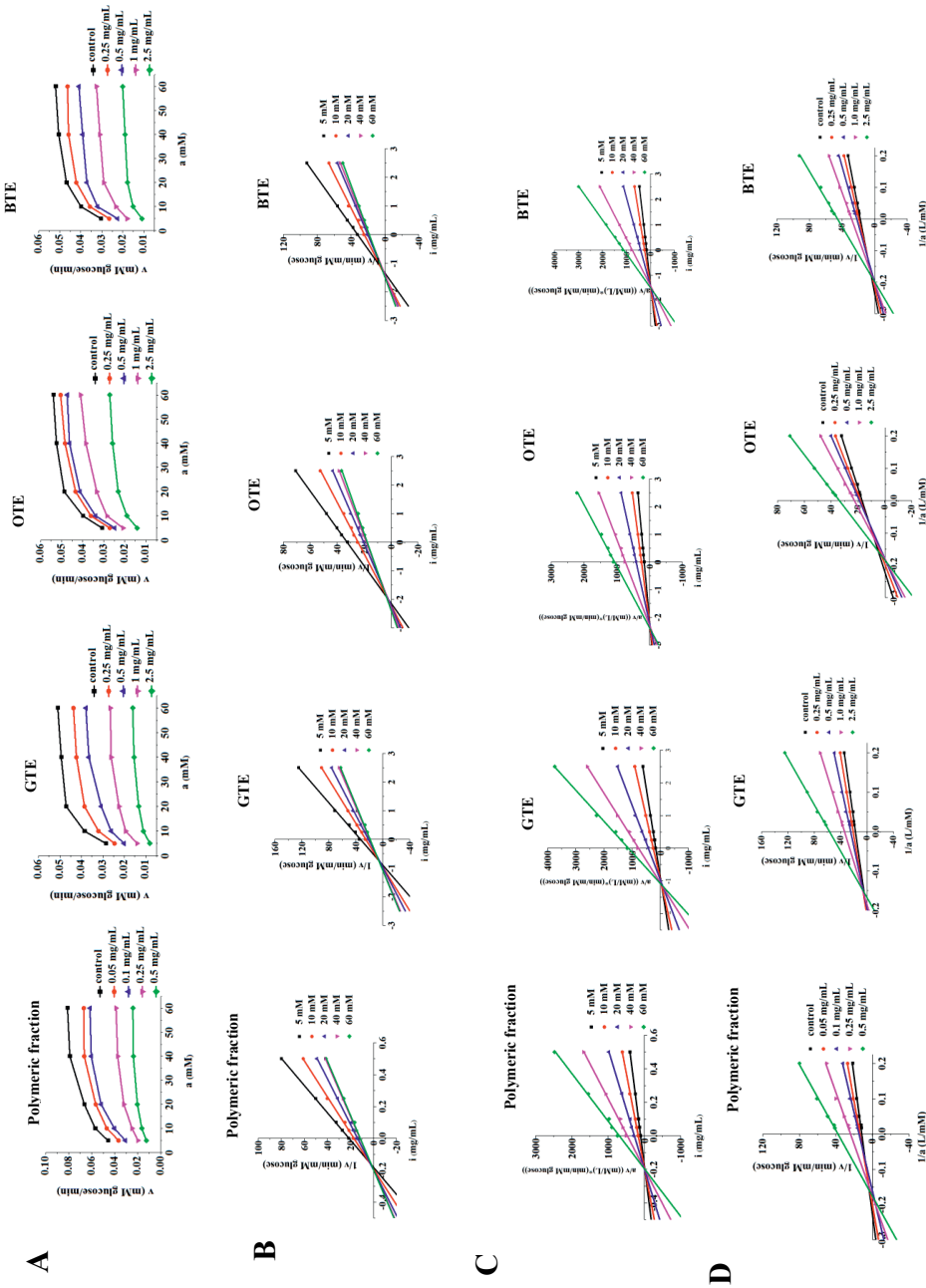
- Ampelopsis grossedentata* leaves tea (Tengcha) as an antioxidant and  $\alpha$ -glucosidase inhibitory nutraceutical. *International Journal of Food Science & Technology*, *51*, 2692–2700. <https://doi.org/10.1111/ijfs.13259>.
- Hauri, H. P., Sterchi, E. E., Bienz, D., Fransen, J. A. M., & Marxer, A. (1985). Expression and intracellular transport of microvillus membrane hydrolases in human intestinal epithelial cells. *Journal of Cell Biology*, *101*, 838-851. <https://doi.org/10.1083/jcb.101.3.838>.
- Hervet-Hernández, D., & Goñi, I. (2011). Dietary polyphenols and human gut microbiota: A review. *Food Reviews International*, *27*, 154-169. <https://doi.org/10.1080/87559129.2010.535233>.
- Kan, L., Capuano, E., Fogliano, V., Oliviero, T., & Verkerk, R. (2020). Tea polyphenols as a strategy to control starch digestion in bread: the effects of polyphenol type and gluten. *Food & Function*, *11*, 5933-5943. <https://doi.org/10.1039/d0fo01145b>.
- Kan, L., Oliviero, T., Verkerk, R., Fogliano, V., & Capuano, E. (2020). Interaction of bread and berry polyphenols affects starch digestibility and polyphenols bio-accessibility. *Journal of Functional Foods*, *68*, 103924. <https://doi.org/10.1016/j.jff.2020.103924>.
- Lee, B. H., Rose, D. R., Lin, A. H. M., Quezada-Calvillo, R., Nichols, B. L., & Hamaker, B. R. (2016). Contribution of the Individual Small Intestinal  $\alpha$ -Glucosidases to Digestion of Unusual  $\alpha$ -Linked Glycemic Disaccharides. *Journal of Agricultural and Food Chemistry*, *64*, 6487-6494. <https://doi.org/10.1021/acs.jafc.6b01816>.
- Lim, J., Kim, D. K., Shin, H., Hamaker, B. R., & Lee, B. H. (2019). Different inhibition properties of catechins on the individual subunits of mucosal  $\alpha$ -glucosidases as measured by partially-purified rat intestinal extract. *Food and Function*, *10*, 4407-4413. <https://doi.org/10.1039/c9fo00990f>.
- Martinez-Gonzalez, A. I., Díaz-Sánchez, Á. G., De La Rosa, L. A., Vargas-Requena, C. L., Bustos-Jaimes, I., & Alvarez-Parrilla, E. (2017). Polyphenolic compounds and digestive enzymes: *In vitro* non-covalent interactions. *Molecules*, *22*, 669. <https://doi.org/10.3390/molecules22040669>.
- Peng, X., Zhang, G., Liao, Y., & Gong, D. (2016). Inhibitory kinetics and mechanism of kaempferol on  $\alpha$ -glucosidase. *Food Chemistry*, *190*, 207-215. <https://doi.org/10.1016/j.foodchem.2015.05.088>.

- Pico, J., Corbin, S., Ferruzzi, M. G., & Martinez, M. M. (2019). Banana flour phenolics inhibit trans-epithelial glucose transport from wheat cakes in a coupled: In vitro digestion/Caco-2 cell intestinal model. *Food and Function*, *10*, 6300-6311. <https://doi.org/10.1039/c9fo01679a>.
- Pyner, A., Nyambe-Silavwe, H., & Williamson, G. (2017). Inhibition of human and rat sucrase and maltase activities to assess antiglycemic potential: Optimization of the assay using acarbose and polyphenols. *Journal of Agricultural and Food Chemistry*, *65*, 8643–8651. <https://doi.org/10.1021/acs.jafc.7b03678>.
- Quezada-Calvillo, R., Robayo-Torres, C. C., Opekun, A. R., Sen, P., Ao, Z., Hamaker, B. R., Quaroni, A., Brayer, G. D., Wattler, S., Nehls, M. C., Sterchi, E. E., Nichols, B. L. (2007). Contribution of mucosal maltase-glucoamylase activities to mouse small intestinal starch  $\alpha$ -glucogenesis. *Journal of Nutrition*, *137*, 1725-1733. <https://doi.org/10.1093/jn/137.7.1725>.
- Quezada-Calvillo, R., Sim, L., Ao, Z., Hamaker, B. R., Quaroni, A., Brayer, G. D., Sterchi, E. E., Robayo-Torres, C. C., Rose, D. R., Nichols, B. L. (2008). Luminal starch substrate “brake” on maltase-glucoamylase activity is located within the glucoamylase subunit. *Journal of Nutrition*, *138*, 685-692. <https://doi.org/10.1093/jn/138.4.685>.
- Rosenstock, J., Brown, A., Fischer, J., Jain, A., Littlejohn, T., Nadeau, D., Nadeau, D., Sussman, A., Taylor, T., Krol, A., & Magner, J. (1998). Efficacy and safety of acarbose in metformin-treated patients with type 2 diabetes. *Diabetes Care*, *21*, 2050-2055. <https://doi.org/10.2337/diacare.21.12.2050>.
- Saeedi, P., Petersohn, I., Salpea, P., Malanda, B., Karuranga, S., Unwin, N., ... Williams, R. (2019). Global and regional diabetes prevalence estimates for 2019 and projections for 2030 and 2045: Results from the International Diabetes Federation Diabetes Atlas, 9th edition. *Diabetes Research and Clinical Practice*. <https://doi.org/10.1016/j.diabres.2019.107843>
- Satoh, T., Igarashi, M., Yamada, S., Takahashi, N., & Watanabe, K. (2015). Inhibitory effect of black tea and its combination with acarbose on small intestinal  $\alpha$ -glucosidase activity. *Journal of Ethnopharmacology*, *161*, 147-155. <https://doi.org/10.1016/j.jep.2014.12.009>.
- Schiller, C., Fröhlich, C. P., Giessmann, T., Siegmund, W., Mönnikes, H., Hosten, N., & Weitschies, W. (2005). Intestinal fluid volumes and transit of dosage forms as assessed




- by magnetic resonance imaging. *Alimentary Pharmacology and Therapeutics*, 22, 971-979. <https://doi.org/10.1111/j.1365-2036.2005.02683.x>.
- Semenza, G., Auricchio, S., & Rubino, A. (1965). Multiplicity of human intestinal disaccharidases I. Chromatographic separation of maltases and of two lactases. *BBA Section Nucleic Acids And Protein Synthesis*, 96, 487-497. [https://doi.org/10.1016/0005-2787\(65\)90565-4](https://doi.org/10.1016/0005-2787(65)90565-4).
- Shin, H., Seo, D. H., Seo, J., Lamothe, L. M., Yoo, S. H., & Lee, B. H. (2019). Optimization of in vitro carbohydrate digestion by mammalian mucosal  $\alpha$ -glucosidases and its applications to hydrolyze the various sources of starches. *Food Hydrocolloids*, 87, 470-476. <https://doi.org/10.1016/j.foodhyd.2018.08.033>.
- Simsek, M., Quezada-Calvillo, R., Ferruzzi, M. G., Nichols, B. L., & Hamaker, B. R. (2015). Dietary phenolic compounds selectively inhibit the individual subunits of maltase-glucoamylase and sucrase-isomaltase with the potential of modulating glucose release. *Journal of Agricultural and Food Chemistry*, 63, 3873-3879. <https://doi.org/10.1021/jf505425d>.
- Srinivasan, B., Kolli, A. R., Esch, M. B., Abaci, H. E., Shuler, M. L., & Hickman, J. J. (2015). TEER measurement techniques for *in vitro* barrier model systems. *Journal of Laboratory Automation*, 20, 107-126. <https://doi.org/10.1177/2211068214561025>.
- Sun, L., Gidley, M. J., & Warren, F. J. (2017). The mechanism of interactions between tea polyphenols and porcine pancreatic  $\alpha$ -amylase: Analysis by inhibition kinetics, fluorescence quenching, differential scanning calorimetry and isothermal titration calorimetry. *Molecular Nutrition and Food Research*, 61, 1-13. <https://doi.org/10.1002/mnfr.201700324>.
- Sun, L., Warren, F. J., Netzel, G., & Gidley, M. J. (2016). 3 or 3'-Galloyl substitution plays an important role in association of catechins and theaflavins with porcine pancreatic  $\alpha$ -amylase: The kinetics of inhibition of  $\alpha$ -amylase by tea polyphenols. *Journal of Functional Foods*, 26, 144-156. <https://doi.org/10.1016/j.jff.2016.07.012>.
- Van Beers, E. H., Büller, H. A., Grand, R. J., Einerhand, A. W. C., & Dekker, J. (1995). Intestinal brush border glycohydrolases: Structure, function, and development. *Critical Reviews in Biochemistry and Molecular Biology*, 30, 197-262. <https://doi.org/10.3109/10409239509085143>.

- Verhoeckx, K., Cotter, P., López-Expósito, I., Kleiveland, C., Lea, T., Mackie, A., Requena, D., Swiatecka, D., & Wichers, H. (2015). The impact of food bioactives on health: In vitro and Ex Vivo models. *Springer Nature*, 338. <https://doi.org/10.1007/978-3-319-16104-4>.
- Wu, X., Ding, H., Hu, X., Pan, J., Liao, Y., Gong, D., & Zhang, G. (2018). Exploring inhibitory mechanism of gallic acid on  $\alpha$ -amylase and  $\alpha$ -glucosidase relevant to postprandial hyperglycemia. *Journal of Functional Foods*, 48, 200-209. <https://doi.org/10.1016/j.jff.2018.07.022>.
- Yang, G., Bibi, S., Du, M., Suzuki, T., & Zhu, M. J. (2017). Regulation of the intestinal tight junction by natural polyphenols: A mechanistic perspective. *Critical Reviews in Food Science and Nutrition*, 57, 3830-3839. <https://doi.org/10.1080/10408398.2016.1152230>.
- Yang, X., & Kong, F. (2016). Evaluation of the *in vitro*  $\alpha$ -glucosidase inhibitory activity of green tea polyphenols and different tea types. *Journal of the Science of Food and Agriculture*, 96, 777-782. <https://doi.org/10.1002/jsfa.7147>.
- Yu, Q., Fan, L., & Duan, Z. (2019). Five individual polyphenols as tyrosinase inhibitors: Inhibitory activity, synergistic effect, action mechanism, and molecular docking. *Food Chemistry*, 297, 124910. <https://doi.org/10.1016/j.foodchem.2019.05.184>
- Zhang, B. W., Li, X., Sun, W. L., Xing, Y., Xiu, Z. L., Zhuang, C. L., & Dong, Y. S. (2017). Dietary Flavonoids and Acarbose Synergistically Inhibit  $\alpha$ -Glucosidase and Lower Postprandial Blood Glucose. *Journal of Agricultural and Food Chemistry*, 65, 8319-8330. <https://doi.org/10.1021/acs.jafc.7b02531>.



**Supplementary Figure 6S1.** The kinetics of  $\alpha$ -glucosidase inhibition by tea extracts or tea polyphenols using maltose as substrate. A: Michaelis–Menten plots for  $\alpha$ -glucosidase inhibition by Polymeric fraction from BTE, GTE, OTE and BTE. B: Dixon plots for glucosidase inhibition by Polymeric fraction from BTE, GTE, OTE and BTE. C: Cornish-Bowden plots for glucosidase inhibition by Polymeric fraction from BTE, GTE, OTE and BTE. D: Lineweaver-Burk plots for  $\alpha$ -glucosidase inhibition by Polymeric fraction from BTE, GTE, OTE and BTE; GTE, green tea extract; OTE, oolong tea extract; BTE, black tea extract.

The background features a diagonal split. The upper-left portion is a light gray, and the lower-right portion is a dark gray. A white diagonal band runs from the top-right to the bottom-left. A large, black, stylized number '7' is positioned in the center of the white band.

7

# Chapter 7

## General Discussion

## 7.1 Introduction

Starchy foods are the main source of carbohydrates with high energy density. The consumption of starchy foods can potentially cause a high glycaemic index, thus causing overweight or type-2 diabetes (Behall, Scholfield, Yuhaniak, & Canary, 1989). Various strategies have been proposed to reduce the glycaemic index of starchy foods. Recently, the inhibitory effects of certain phenolics on starch digestibility are gaining attention to reduce glycaemic index (Carini, Curti, Spotti, & Vittadini, 2012; Wang, Brennan, Serventi, & Brennan, 2021). The overall aim of this thesis is to study the nutritional and physicochemical properties of starch/starchy food as influenced by the addition of phenolics. Phenolics have been widely reported for their inhibitory effects on digestive enzymes (Zhang, Chen, & Wang, 2014). However, food does not just contain starch, but many different compounds. The interaction between phenolics and other compounds, for instance, starch and gluten significantly influence the activity of digestive enzymes.

In Chapter 2&3 I investigated the influence of food matrix on inhibitory efficacy of phenolics on starch digestibility by using bread as a starchy food model. The interactions of tannic acid and wheat starch, potato starch, corn starch, and corn amylopectin were investigated in Chapter 4&5. The inhibitory effects of phenolics on  $\alpha$ -glucosidase were widely studied by using both rat intestinal enzymes and Caco-2 cells as the source of  $\alpha$ -glucosidase (Chapter 6). The present chapter intends to discuss the main findings obtained in this study and to offer a broader perspective about future research in this field. The overall summary of this thesis is shown in Table 7.1.

Table 7.1 Summary of the main results obtained in this thesis.

Aim	Main findings
Study the presence of food matrix affects inhibitory efficacy of phenolics on starch digestibility (Chapter 2&3)	<ul style="list-style-type: none"> <li>• The inhibition of starch digestion obtained by co-digesting berry extracts and bread was much higher than the inhibition obtained by digesting berry-fortified bread. (Chapter 2)</li> <li>• Interactions of phenolics with matrix reduced phenolics bio-accessibility, thus reducing the amount of phenolics available for <math>\alpha</math>-amylase inhibition. (Chapter 2)</li> <li>• Monomeric and polymeric phenolics differently affected starch digestion. (Chapter 3)</li> <li>• Gluten lowered the capacity of tea tannins to inhibit starch digestibility. (Chapter 3)</li> <li>• Gluten had little effect on the inhibition of starch digestion by monomeric phenolics. (Chapter 3)</li> </ul>
Study the effects of tannic acid on rheological properties and starch digestibility of wheat starch (Chapter 4)	<ul style="list-style-type: none"> <li>• Co-gelatinization of starch and TA mostly produced non-inclusion complexes.</li> <li>• Complexation of TA with ungelatinized starch mostly produced inclusion complexes.</li> <li>• Inclusion and non-inclusion complexes had opposite effects on rheological properties.</li> <li>• Inclusion and non-inclusion complexes both inhibited starch digestion.</li> </ul>
Understand how different starch types influence the starch-tannins interactions (Chapter 5)	<ul style="list-style-type: none"> <li>• Non-inclusion starch-tannins complexes were found in potato starch, corn starch and corn amylopectin.</li> <li>• Non-gelatinized amylopectin binds more tannins than non-gelatinized amylose.</li> <li>• Gelatinized amylose binds more tannins than gelatinized amylopectin.</li> <li>• Potato starch (B-type starch) was mostly affected by tannins addition compared to corn starch and corn amylopectin.</li> <li>• Non-inclusion starch-tannins complexes inhibit starch digestibility.</li> </ul>
Study inhibition of $\alpha$ -glucosidases by tea phenolics in rat intestinal extract and <i>in vitro</i> Caco-2 cells-based model system (Chapter 6)	<ul style="list-style-type: none"> <li>• Mixed type inhibition on rat maltase was observed.</li> <li>• Slight antagonistic effect was observed when tea extract combined with acarbose.</li> <li>• Caco-2 cells sucrase was more susceptible than the rat enzyme.</li> <li>• Caco-2 cells maltase was less susceptible than the rat enzyme.</li> </ul>

## 7.2 Interpretation and discussion of the main findings

### 7.2.1 Role of phenolics-food matrix interaction in limiting starch digestion

The small intestine is the main place where starch digestion occurs (Levin, 1994). Digestive enzymes, such as  $\alpha$ -amylase and  $\alpha$ -glucosidase are present in the lumen and brush border of the small intestine, respectively (Levin, 1994). The inhibitory effect of phenolics on digestive enzymes is one of the important mechanisms for slowing down starch digestibility. The first inhibitory effect of phenolics on  $\alpha$ -amylase can be found in the beginning of the intestinal phase. Therefore, bio-accessible phenolics after gastric digestion was considered as the initially efficient phenolics that can inhibit  $\alpha$ -amylase at least in the beginning of the intestinal digestion. The presence of food matrix could interact with phenolics and thus affect the efficient amount of phenolics that can inhibit digestive enzymes. The role of the food matrix can be directly evidenced in Figure 7.1 based on the results of Chapter 2, *i.e.*, stronger inhibition was found in co-digestion of bread and berry extracts comparing to berry-fortified bread. For berry-fortified bread, berry extract is mixed with wheat flour, thus phenolics are embedded within native starch and gluten proteins matrix. Those escaping the food matrix react in part to other digestive enzymes. As a result, a relatively smaller fraction is available to bind to, and inhibit, amylase. In co-digestion experiments, phenolics are not entrapped in the bread matrix, thus, there is less interaction with starch and gluten proteins. As a result, a bigger fraction of phenolics is available to bind to, and inhibit,  $\alpha$ -amylase.

Besides the lower phenolics bio-accessibility caused by the bread matrix, the multiple interactions during bread baking should be considered as well. In phenolics-fortified bread, phenolics can interact with the bread component in each moment of the breadmaking process and influence the formation of the food matrix by affecting starch gelatinization, protein denaturation, and crust formation (Hadiyanto, 2005). In co-digestion experiments, polyphenols are not involved in the baking process and do not influence the formation of the food matrix, and can directly interact with gelatinized starch or gluten. Moreover, degradation of polyphenols upon baking should be considered in the fortified samples. As shown in Table 2.2, almost half of the berry polyphenols were degraded upon baking conditions, but the inhibitory effects on  $\alpha$ -amylase were not affected. This suggests that degraded products from berry polyphenols could also have an inhibitory effect on  $\alpha$ -amylase (Sui, Yap, & Zhou, 2015).



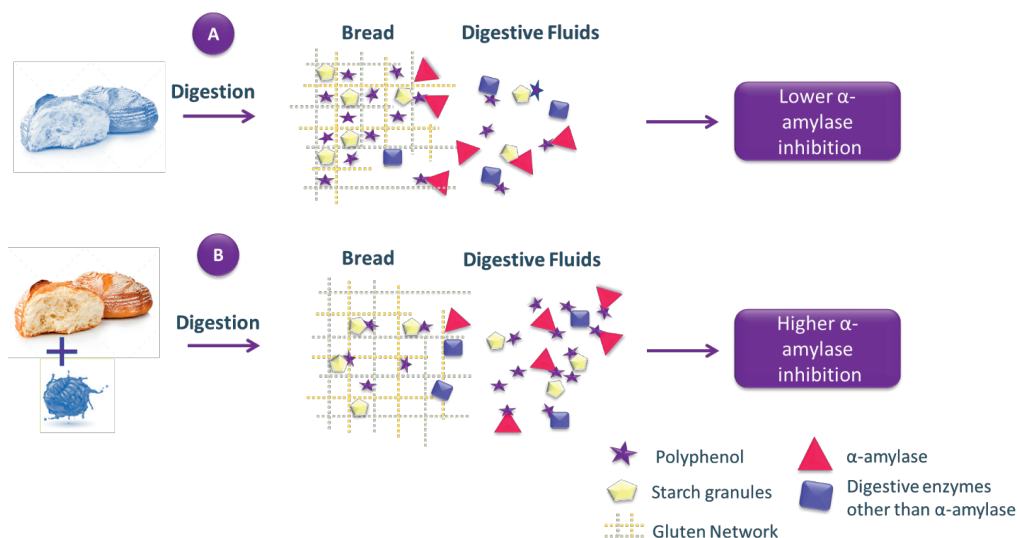


Figure 7.1 Wheat bread fortified (A) or co-digested (B) with berry extracts and influences on  $\alpha$ -amylase inhibition.

### 7.2.2 Role of phenolics types and gluten presence in limiting starch digestibility

The types of phenolics can also influence the inhibition on starch digestibility. This was clearly evidenced by the fact that black tea extract which contains a larger amount of tannins shows stronger inhibition than green tea extract which contains a larger amount of monomeric phenolics (Chapter 3). Besides  $\alpha$ -amylase inhibition, phenolics-starch interaction is also a crucial mechanism for inhibiting starch digestibility. This could be clearly evidenced by the stronger inhibition of raspberry extract than blueberry extract, despite its lower inhibitory effects on  $\alpha$ -amylase (Chapter 2). That means that some types of raspberry polyphenols, most likely the high molecular weight tannins, interacted with starch and then inhibit starch digestion. Whatever are the mechanisms of inhibition on starch digestion, *i.e.*,  $\alpha$ -amylase inhibition and starch-polyphenols interaction, the gluten presence definitely interferes with both mechanisms.

Gluten is the important ingredient in the wheat-flour based matrix. This interaction of polyphenols and gluten not only reduces the polyphenols bio-accessibility, hence reducing

inhibition on  $\alpha$ -amylase but also reduces the amount of polyphenols to interact with starch. By calculating the relative contribution of monomeric and polymeric phenolics in normal wheat bread and gluten-free bread, I confirmed for the first time that the gluten presence lowered the inhibitory efficacy of polymeric phenolics, whereas it has little effect on the inhibitory efficacy of monomeric phenolics (Chapter 3). It has been reported that low and high molecular weight of phenolics show different effects on the functions of gluten. Monomeric phenolics can improve the flexibility of the gluten network, whereas high molecular tannins can increase the density and strength of gluten network, crosslink gluten polymers thus creating a stronger gluten network (Schroeder, 1976). In addition, tannins can also interact with different gluten proteins. Gliadins and glutenins are two components of gluten. Glutenins are alcohol-insoluble and have a more rod-like structure while the gliadins are alcohol-soluble and more spherical (Girard, Bean, Tilley, Adrianos, & Awika, 2018). I did not consider the specific role of gliadins and glutenins regarding their respective effect on phenolics-gluten interaction, but there is an evidence from a previous study that showed that tannins interact with gliadin through hydrogen bonds, while tannins-glutenin interactions were formed by hydrogen bonding and hydrophobic interactions, thus making a more stable complex (Girard et al., 2018). Besides gluten, dietary fibres are also important ingredients in food matrix. Non-covalent polyphenol-dietary fibres interactions affect polyphenol bio-accessibility (Jakobek & Matić, 2019). Therefore, the specific food matrix should be considered when choosing phenolics as a strategy to slow down starch digestibility. Moreover, the presence of enzymes other than  $\alpha$ -amylase lowered the inhibitory efficacy of phenolics on starch digestibility by subtracting polyphenols from binding to  $\alpha$ -amylase. Taken all the results of this thesis, multiple interactions are responsible for the effect on starch digestibility, including phenolics- $\alpha$ -amylase interactions, phenolics- $\alpha$ -glucosidase interactions, phenolics-starch interactions, polyphenol-gluten interactions, etc., as shown in Figure 7.2.

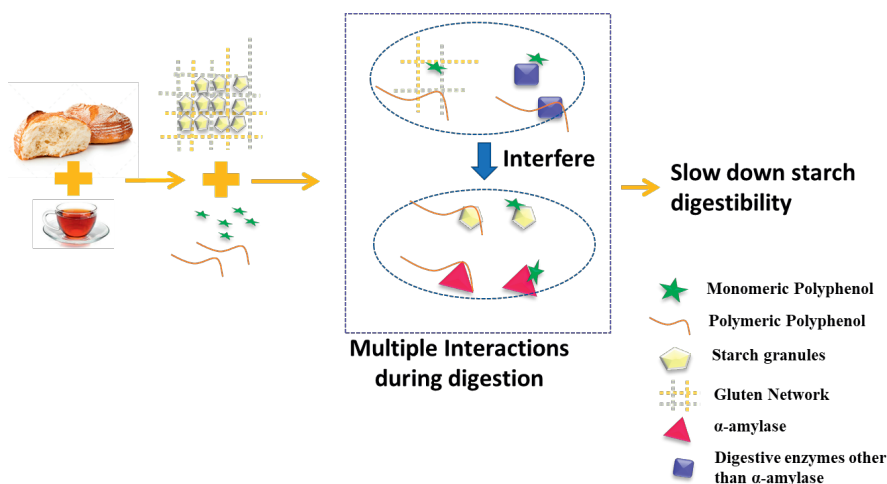


Figure 7.2 Multiple interactions of tea phenolics, digestive enzymes, starch, and gluten during co-digestion of bread and tea extract. Interaction of polyphenols with gluten and digestive enzymes other than  $\alpha$ -amylase lowered the efficiency amount of polyphenols for  $\alpha$ -amylase inhibition and phenolics-starch interaction.

### 7.2.3 Role of starch-phenolics interactions in limiting starch digestibility

Evidence from [Chapter 2&3](#) confirmed the important role of the starch-phenolics interaction for the inhibition of starch digestion. For instance, as results in [Figure 3.1 & 3.2](#), it can be noticed that despite no tea tannins were released during intestinal digestion, but a clear inhibition was obtained achieved by adding tannins. Tannins, as polymeric phenolics, can provide a large amount of hydroxyl groups for hydrogen bonding and more hydrophobic domains than monomeric phenolics ([Amoako & Awika, 2016](#)). Therefore, tannic acid was selected to study the starch-tannins interaction in [Chapter 5&6](#).

Two forms of the starch-tannins complex are reported in my study: V-type inclusion complex ([Chapter 5](#)) and non-V-type complex ([Chapter 5&6](#)). Both types of complexes are resistant to enzymatic digestion. This was clearly confirmed by the positive relation found between the total amount of inclusion and non-inclusion complexes and the amount of resistant starch ([Chapter 5&6](#)). The V-complexes normally involve the inclusion of small guest molecules within the amylose single helix (eg., amylose-lipid) or in the inter-helical space (eg., amylose-phenolics) ([Amoako & Awika, 2019](#); [Cohen, Orlova, Kovalev, Ungar, & Shimoni, 2008](#)). Amylose-lipid complexes are complexes between amylose and lipid that forms amorphous or

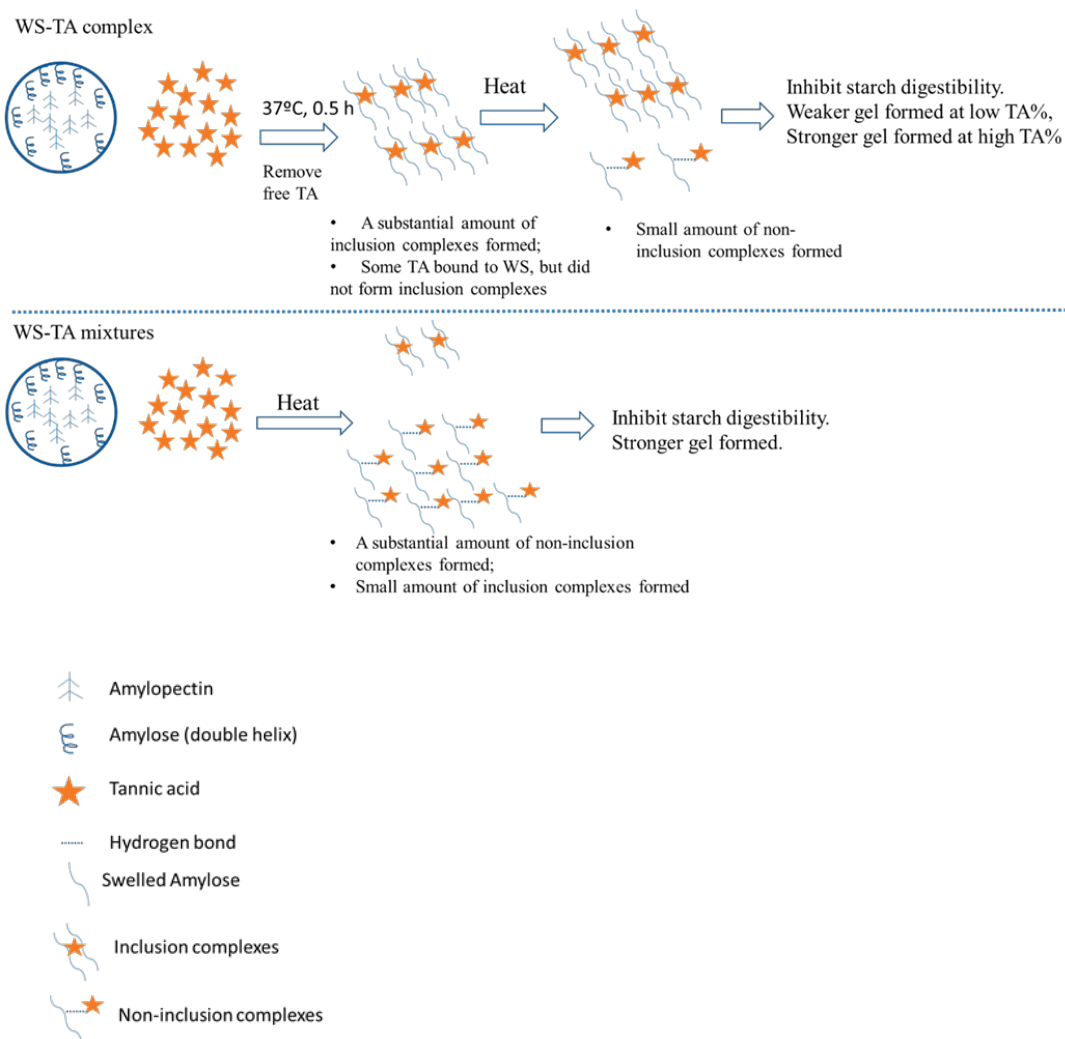


Figure 7.3 Proposed mechanisms of wheat starch-tannic acid interactions and how they consequently influence the rheological properties and starch digestibility. TA tannic acid, WS, wheat starch. TA was either complexed with starch (WS-TA complexes) or mixed with starch (WS-TA mixtures) right before the characterization of its properties. Non-inclusion types of complexes were mostly formed by co-gelatinization WS-TA mixtures, while inclusion complexes were mostly formed by complexation of TA with ungelatinized starch.

highly crystalline structures, and it occur naturally in cereal starch (Morrison, Law, & Snape, 1993). Within the cavity of amylose helices is a hydrophobic environment and small guest molecules, like lipid, are tightly complexed inside the cavity to form inclusion complexes (Putseys, Lamberts, & Delcour, 2010). V-type inclusion starch-phenolics complex usually includes smaller molecules such as phenolic acids instead of bulky molecules such as tannins (Zhu, 2015). However, evidence from Chapter 5 confirmed tannins could interact directly with amylose to form inclusion starch-phenolics complexes. The non-V-type complexes are formed through hydrogen bonds and/or electrostatic and ionic interactions (Zhu, 2015). They are a loose complex compared with V-type inclusion complexes and they usually do not change the crystalline type of the starch (Zhu, 2015). Besides, I reported for the first time that the formation of inclusion and non-inclusion complexes is influenced by whether the tannic acid is complexed with ungelatinized starch in advance or mixed with wheat starch before characterization (Figure 7.3). Considering the different roles of inclusion and non-inclusion complexes in modifying functional properties of wheat starch, starchy food with various functional properties could be produced by the addition of phenolics at different stages. Moreover, different types of starch can affect starch-phenolics interactions. The more open structure and high level of phosphate esters of potato starch make it easier to interact with tannic acid than tightly packed A-type corn starch. These results can help stimulate further interest in applications of starch-tannic acid interactions in various starchy food.

#### 7.2.4 Inhibitory effects of phenolics on brush border enzymes

Starch is firstly hydrolysed into maltose, dextrin, or other oligosaccharides by salivary and pancreatic  $\alpha$ -amylase, and then those products are further hydrolysed into glucose by brush border enzymes, *i.e.*,  $\alpha$ -glucosidase.  $\alpha$ -glucosidase exhibits activities towards various substrates, for instance, maltose, sucrose, isomaltose, dextrin, or even starch. The specific substrate needs to be considered when talking about the inhibitory effects on  $\alpha$ -glucosidase. Tea polyphenols show different inhibitory efficacy towards different substrates, *i.e.*, tea polyphenols were very effective in inhibiting  $\alpha$ -glucosidase activity towards maltose and maltodextrin, but very little inhibition on  $\alpha$ -glucosidase towards sucrose and isomaltose. Tea polyphenols inhibit on rat maltase by a mixed type of inhibition, which means tea phenolics not only compete with maltose in binding  $\alpha$ -glucosidase (competitively), but also bind with  $\alpha$ -glucosidase-maltose complexes (uncompetitively). But tea phenolics bind more tightly to  $\alpha$ -glucosidase than to  $\alpha$ -glucosidase-maltose complexes, indicated by the increase of apparent Michaelis constant ( $K_m^{app}$ ) as shown in Table 6.5. Acarbose is a commercial medicine for

treatment of type 2 diabetes and it is a competitive inhibitor for  $\alpha$ -glucosidase. The combination of polyphenols into acarbose caused a slight antagonistic effect. Consumption of tea phenolics can be used as a prevention strategy for overweight or type-2 diabetes, but drinking tea with acarbose at the same time is not recommended. Human Caco-2 cells were selected to provide  $\alpha$ -glucosidase as well. Interestingly, different sensitivity of rat and Caco-2 cells  $\alpha$ -glucosidase to tea phenolics' inhibition was found. Tea phenolics show higher inhibitory effects on maltase from rat enzyme, but no inhibitory effects on maltase from Caco-2 cells. The opposite results were obtained when comparing the inhibitory effects on sucrase. This could be explained by different intrinsic characteristics of different sources of enzymes and different experimental conditions as shown in Figure 7.4.

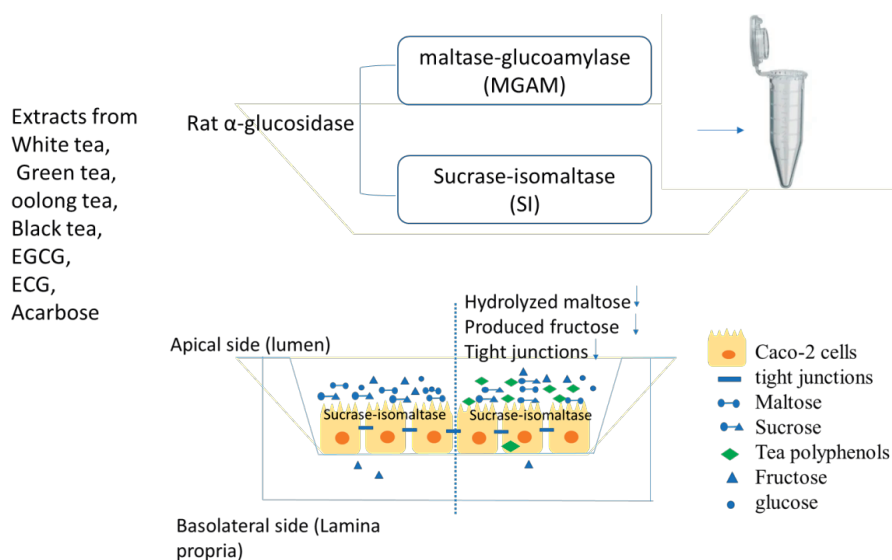


Figure 7.4. The inhibitory activities on maltase, sucrase, isomaltase and glucoamylase of acarbose, epigallocatechin gallate (EGCG), epicatechin gallate (ECG) and four polyphenol-rich tea extract from white, green, oolong, black tea, were investigated by using rat intestinal enzymes and human Caco-2 cells grown on transwell. MGAM, maltase-glucoamylase; SI, sucrase-isomaltase; Nt, N-terminal subunit; Ct, C-terminal subunit.

### 7.3 Methodological considerations

#### 7.3.1 *In vitro* digestion model

*In vitro* digestion model has been used throughout the whole thesis. Compared to *in vivo* models, *i.e.*, animal and humans studies, the *in vitro* models are cheaper and easily performed despite physiological differences to humans. The knowledge obtained based on *in vitro* studies could be used to provide information for *in vivo* studies, thus bridging the gap between the lab and the clinic. *In vitro* approach used in my study consist of a gastric stage and a subsequent small intestinal stage, but the oral stage is skipped. This is because the food samples are prepared as powders or slurry to reduce the experimental time. An oral digestion step is an intrinsic system for the human body to provide mechanical grinding and enzymatic starch hydrolysis with salivary  $\alpha$ -amylase. The contributions of salivary  $\alpha$ -amylase to the final starch hydrolysis are not exactly known yet. One study reported that oral stage can hydrolyse 50% of starch in bread (Hoebler et al., 1998). Meanwhile, a human study reported that the exposure to prolonged exposure to saliva during the chewing of starchy foods did not make contributions to the hydrolysis of starch during the gastrointestinal digestion process (Woolnough, Bird, Monro, & Brennan, 2010). Besides, the concentration of salivary  $\alpha$ -amylase in humans varies with age, psychosocial stress, and other factors. What's more, *in vitro* digestion protocols do not typically include brush border enzymes, though simulating intestinal digestion with brush border enzymes hydrolases can provide physiologically relevant results. During my thesis, I experienced some practical issues to limit the inclusion of those enzymes into an *in vitro* digestion model. For instance, the sources of brush border enzymes with high purity are limited. Instead of being incorporated into *in vitro* digestion model, the brush border enzymes are separately used for evaluating enzyme activities and enzyme inhibitory experiments as shown in Figure 7.4.

#### 7.3.2 Evaluation of inhibitory effects on $\alpha$ -glucosidase

The selection of  $\alpha$ -glucosidase from various sources is one of the most important steps for evaluating the inhibitory effects on  $\alpha$ -glucosidase. Intrinsic differences of  $\alpha$ -glucosidase need to be taken into account when selecting different resources of  $\alpha$ -glucosidase. Rat intestinal extract and Caco-2 cell monolayers were used to provide  $\alpha$ -glucosidase in my study. Rat  $\alpha$ -glucosidase contains two protein complexes, sucrase-isomaltase (SI) and maltase-glucoamylase (MGAM), while Caco-2 cells only express SI. (Hauri, Sterchi, Bienz, Fransen, & Marxer, 1985). ctSI and ntSI are sucrase and isomaltase, respectively (Pyner, Nyambe-

Silavwe, & Williamson, 2017). ctMGAM and ntMGAM are glucoamylase and maltase, respectively. Both MGAM and SI have high  $\alpha$ -1,4 hydrolytic activity on maltose. Besides maltase, all the subunits have their unique activities. For instance, the glucoamylase, sucrase, and isomaltase subunits show higher activity toward maltodextrin, sucrose and isomaltose, respectively. In addition, yeast  $\alpha$ -glucosidase is also used as maltase by many researchers, but they have low homology with mammals  $\alpha$ -glucosidase (Kimura et al., 1992). Some researchers also reported that a chemical substance that inhibits yeast  $\alpha$ -glucosidase activity will not necessarily inhibit mammalian  $\alpha$ -glucosidase (Shai, Magano, Lebelo, & Mogale, 2011). Although human Caco-2 cells were used to provide  $\alpha$ -glucosidase, the enzymes from Caco-2 cells cannot represent the brush border enzymes in humans. That is because Caco-2 cells only provide SI, while the human intestine provides both SI and MGAM. That means maltase in human Caco-2 cells only provided by SI, while maltase in the human intestine is provided by both MGAM and SI. Human and rat intestine both provide MGAM and SI, but the enzyme activities of specific unite are quite different (Hauri et al., 1985; Semenza, Auricchio, & Rubino, 1965). To further study inhibitory mechanisms of tea phenolics on  $\alpha$ -glucosidase, I used several kinetics models, *i.e.*, Lineweaver-Burk plot, Dixon plot, Cornish-Bowden plots to obtain exact inhibitory types, which include the competitive, non-competitive and uncompetitive and mixed type of inhibition. Since all subunits of brush border enzymes exhibit maltase activity, I used maltose as a substrate for the kinetics experiments.

The purification of  $\alpha$ -glucosidase is also an important factor that affect evaluating inhibitory effects on  $\alpha$ -glucosidase. Rat  $\alpha$ -glucosidase used in my study is a crude extract from rat intestine without any further purification and thus includes  $\alpha$ -glucosidase,  $\alpha$ -amylase and other non-enzyme proteins.  $\alpha$ -amylase can also produce glucose from the substrates used in our study. On one hand, it is difficult to discriminate the inhibition from  $\alpha$ -glucosidase and  $\alpha$ -amylase. On the other hand, using a mix of glucosidases would give a more realistic impression of the inhibition as it is *in vivo*, where the individual subunit of glucosidase cannot be discriminated. In addition, the specific experimental condition can also influence determination inhibitory effects on  $\alpha$ -glucosidase. Regarding the experimental conditions, inhibition on rat enzymes is determined in tested tubes, while inhibition on human Caco-2 cell is determined using Transwells. The advantage of using Caco-2 grown on Transwells is to use the enzyme in a more physiologically realistic way. However, the changes of tight junction



indicated by TEER value could possibly influence the inhibitory efficacy due to the transport of polyphenols from the apical side to the basolateral side.

### 7.3.3 The preparation of starch-phenolic complexes

I used two different ways to add tannic acid to starch by making starch-tannins complexes and starch-tannins mixtures as shown in Figure 7.3. The method used in this study is different from the method that has been reported. Various methods have been developed for making starch-phenolic complexes, such as ultrasound-microwave synergistic treatment, alcohol method, and high-temperature water method (Deng et al., 2021). Those methods requires that starch is “de-structured” at high temperature and converted to random coils before the addition of guest compounds. Then the inclusion complexes are favored by the hydrophobic interaction between starch helical interior and guest compounds. No matter which preparation method is chosen, the preparation of starch phenolic complexes will be influenced by temperature, interact time, solvent properties, and pH. Under the preparation conditions in my study, a substantial amount of inclusion and non-inclusion complexes are produced by interacting wheat starch and tannic acid and only non-inclusion complexes are produced by interacting corn starch, corn amylopectin, and potato starch with tannic acid. The amount of inclusion and non-inclusion complexes could be different if the other processing method is applied.

### 7.4 Implications and future perspectives

In this study, I have used different approaches to study the effects of phenolics on starch digestibility and the physicochemical properties of starch. I brought new insights into the most crucial factors that modulate those effects. However, I believe that there is still plenty of space for research to bring more insights into the polyphenol-starch field. In this section, I will discuss implications from this study and some points that are worth exploring in the future.

All the findings in this thesis could make contributions to other fields such as human nutrition. One of the key messages from this thesis is that polyphenols slowdown starch digestibility, and thus possibly produce resistant starch. For nutritional properties, digestibility has been so far only investigated *in vitro*, no study is available *in vivo*. More *in vivo* data are needed for the biological effects of starch-phenolics complexes. For instance, the impact of starch-phenolics complexes on postprandial blood glucose and insulin response in healthy adults can be studied. Researchers can design meal by using the starch-phenolics complexes

which produced in my study. Subjects consumed a standard meal or designed meal containing starch-phenolic complexes with the same amount of starch. Serum glucose, serum insulin, and capillary glucose were measured at different time points within 2 hours after meal consumption.

The knowledge in this study can also provide contributions to the microbiology field. I reported that resistant starch (RS) is possibly formed in presence of tannic acid. V-type resistant starch is formed due to starch-lipid interaction or starch-tannic acid interaction. Starch-lipid V-type complexes have traditionally been classified as RS5. Starch-phenolics interactions may be seen as a new type of RS5, *i.e.* a new type of resistant starch produced by complexation with phenolics (Gutiérrez & Tovar, 2021). RS entirely passes the small intestine and reaches the colon, where it can be fermented by gut microbiota, generating SCFAs (short-chain fatty acids) (Tiwari, Singh, & Jha, 2019). Therefore, the impacts of this specific new kind of RS after digestion on SCFA production and the modulation of gut microbiota during fermentation in the large intestine are worth exploring. A recent publication from this year (Li et al., 2021) reported that the production of SCF and the growth of beneficial bacteria such as *Prevotella* could be enhanced by complexation with apple phenolics compared to pure wheat starch. Based on that, we can widely explore the investigation on the behaviour of starch-phenolics complexes upon fermentation, and how different types of starch and phenolics govern this effect.

This thesis can provide fundamental knowledge for the researchers who work with  $\alpha$ -glucosidase and human nutrition. A comprehensive comparison among rat, human and Caco-2  $\alpha$ -glucosidase has been reported and a comprehensive system has been set up by using various substrates and different experimental conditions. However, the downstream passage through the mucus layer and the unavoidable contact with brush border enzymes before hydrolysis and absorption are never taken into account. Therefore, it would be interesting for further studies on the interaction between phenolics and gastrointestinal mucus and how these interactions influence the way these compounds act regarding the inhibitory effect on carbohydrate digestion. However, the established method for studying polyphenols-mucus interactions is limited. This could be due to several reasons. One of the reasons is that the commercial mucus is mostly from gastric extract, and the intestinal mucus is hardly provided commercially.

### 7.5 Conclusive remarks.

In summary, the research presented in this thesis showed that phenolics can not only modify the nutritional properties of starchy food by modulating starch digestibility, but also modify the physicochemical properties of starch by forming inclusion and non-inclusion complexes. Complex mechanisms were found for the inhibition of phenolics on starch digestibility, *i.e.*, 1) Inhibitory effects of phenolics on  $\alpha$ -amylase were influenced by the presence of food matrix. 2) Interaction of starch and phenolics inhibited starch digestibility by forming inclusion and non-inclusion complexes, but reduced the efficient amount of phenolics to inhibit  $\alpha$ -amylase. Besides the nutritional properties, phenolics also affected the physicochemical properties of starch. 3) Inhibitory effects of phenolics on  $\alpha$ -glucosidase was influenced by intrinsic characteristic of rat and Caco-2 enzymes and experimental conditions. Therefore, this thesis provides strategies for reducing glycaemic index and understand the behaviour of starch when processing starchy food in presence of phenolics.

## References

- Amoako, D. B., & Awika, J. M. (2016). Polymeric tannins significantly alter properties and in vitro digestibility of partially gelatinized intact starch granule. *Food Chemistry*. <https://doi.org/10.1016/j.foodchem.2016.03.096>
- Amoako, D. B., & Awika, J. M. (2019). Resistant starch formation through intrahelical V-complexes between polymeric proanthocyanidins and amylose. *Food Chemistry*. <https://doi.org/10.1016/j.foodchem.2019.01.173>
- Behall, K. M., Scholfield, D. J., Yuhaniak, I., & Canary, J. (1989). Diets containing high amylose vs amylopectin starch: Effects on metabolic variables in human subjects. *American Journal of Clinical Nutrition*. <https://doi.org/10.1093/ajcn/49.2.337>
- Carini, E., Curti, E., Spotti, E., & Vittadini, E. (2012). Effect of Formulation on Physicochemical Properties and Water Status of Nutritionally Enriched Fresh Pasta. *Food and Bioprocess Technology*. <https://doi.org/10.1007/s11947-010-0476-4>
- Cohen, R., Orlova, Y., Kovalev, M., Ungar, Y., & Shimoni, E. (2008). Structural and functional properties of amylose complexes with genistein. *Journal of Agricultural and Food Chemistry*. <https://doi.org/10.1021/jf800255c>
- Deng, N., Deng, Z., Tang, C., Liu, C., Luo, S., Chen, T., & Hu, X. (2021). Formation, structure and properties of the starch-polyphenol inclusion complex: A review. *Trends in Food Science and Technology*. <https://doi.org/10.1016/j.tifs.2021.04.032>
- Girard, A. L., Bean, S. R., Tilley, M., Adrianos, S. L., & Awika, J. M. (2018). Interaction mechanisms of condensed tannins (proanthocyanidins) with wheat gluten proteins. *Food Chemistry*. <https://doi.org/10.1016/j.foodchem.2017.11.054>
- Gutiérrez, T. J., & Tovar, J. (2021). Update of the concept of type 5 resistant starch (RS5): Self-assembled starch V-type complexes. *Trends in Food Science and Technology*. <https://doi.org/10.1016/j.tifs.2021.01.078>
- Hadiyanto, H. (2005). Heat and Mass Transfer during Baking: Product Quality aspects. *Numerical Heat Transfer*.
- Hauri, H. P., Sterchi, E. E., Bienz, D., Fransen, J. A. M., & Marxer, A. (1985). Expression and intracellular transport of microvillus membrane hydrolases in human intestinal epithelial cells. *Journal of Cell Biology*. <https://doi.org/10.1083/jcb.101.3.838>

- Hoebler, C., Karinthi, A., Devaux, M. F., Guillon, F., Gallant, D. J. G., Bouchet, B., Melegari, C., & Barry, J. L. (1998). Physical and chemical transformations of cereal food during oral digestion in human subjects. *British Journal of Nutrition*.  
<https://doi.org/10.1017/s0007114598001494>
- Jakobek, L., & Matić, P. (2019). Non-covalent dietary fiber - Polyphenol interactions and their influence on polyphenol bioaccessibility. *Trends in Food Science and Technology*.  
<https://doi.org/10.1016/j.tifs.2018.11.024>
- Kimura, A., Takata, M., Sakai, O., Matsui, H., Takai, N., Takayanagi, T., Nishimura, I., Uozumi, T., & Uozumi, T. (1992). Complete amino acid sequence of crystalline ( $\alpha$ -glucosidase from *aspergillus niger*. *Bioscience, Biotechnology and Biochemistry*.  
<https://doi.org/10.1271/bbb.56.1368>
- Levin, R. J. (1994). Digestion and absorption of carbohydrates - From molecules and membranes to humans. In *American Journal of Clinical Nutrition*.  
<https://doi.org/10.1093/ajcn/59.3.690S>
- Li, D., Yang, Y., Yang, X., Wang, X., Guo, C., Sun, L., & Guo, Y. (2021). Modulation of gelatinized wheat starch digestion and fermentation profiles by young apple polyphenols in vitro. *Food and Function*. <https://doi.org/10.1039/d0fo02752a>
- Morrison, W. R., Law, R. V., & Snape, C. E. (1993). Evidence for inclusion complexes of lipids with  $\alpha$ -amylose in maize, rice and oat starches. *Journal of Cereal Science*.  
<https://doi.org/10.1006/jcrs.1993.1039>
- Putseys, J. A., Lamberts, L., & Delcour, J. A. (2010). Amylose-inclusion complexes: Formation, identity and physico-chemical properties. *Journal of Cereal Science*.  
<https://doi.org/10.1016/j.jcs.2010.01.011>
- Semenza, G., Auricchio, S., & Rubino, A. (1965). Multiplicity of human intestinal disaccharidases I. Chromatographic separation of maltases and of two lactases. *BBA Section Nucleic Acids And Protein Synthesis*. [https://doi.org/10.1016/0005-2787\(65\)90565-4](https://doi.org/10.1016/0005-2787(65)90565-4)
- Shai, L. J., Magano, S. R., Lebelo, S. L., & Mogale, A. M. (2011). Inhibitory effects of five medicinal plants on rat  $\alpha$ -glucosidase: comparison with their effects on yeast  $\alpha$ -glucosidase. *Journal of Medicinal Plants Research*.

- Sui, X., Yap, P. Y., & Zhou, W. (2015). Anthocyanins During Baking: Their Degradation Kinetics and Impacts on Color and Antioxidant Capacity of Bread. *Food and Bioprocess Technology*. <https://doi.org/10.1007/s11947-014-1464-x>
- Tiwari, U. P., Singh, A. K., & Jha, R. (2019). Fermentation characteristics of resistant starch, arabinoxylan, and  $\beta$ -glucan and their effects on the gut microbial ecology of pigs: A review. *Animal Nutrition*. <https://doi.org/10.1016/j.aninu.2019.04.003>
- Wang, J., Brennan, M. A., Serventi, L., & Brennan, C. S. (2021). Impact of functional vegetable ingredients on the technical and nutritional quality of pasta. *Critical Reviews in Food Science and Nutrition*. <https://doi.org/10.1080/10408398.2021.1895712>
- Woolnough, J. W., Bird, A. R., Monro, J. A., & Brennan, C. S. (2010). The effect of a brief Salivary  $\alpha$ -Amylase exposure during chewing on subsequent in vitro starch digestion curve profiles. *International Journal of Molecular Sciences*. <https://doi.org/10.3390/ijms11082780>
- Zhang, X., Chen, F., & Wang, M. (2014). Antioxidant and antiglycation activity of selected dietary polyphenols in a cookie model. *Journal of Agricultural and Food Chemistry*. <https://doi.org/10.1021/jf4045827>
- Zhu, F. (2015). Interactions between starch and phenolic compound. *Trends in Food Science & Technology*, 43(2), 129–143. <https://doi.org/10.1016/J.TIFS.2015.02.003>

# Summary

## Summary

Polyphenols have been reported to modulate starch digestion, thus influencing the glycaemic index of high energy-density food. Modulation of starch digestion may be achieved through phenolic interactions with either digestive enzymes and/or the starch granules. But the mechanisms can be much more complex when components other than starch are present in the food matrix. Therefore, it is essential to understand the complex mechanisms underpinning the role of polyphenols in limiting starch digestibility from different aspects. In this thesis, I studied the influence of the food matrix on the role of polyphenols in limiting starch digestibility (Chapter 2&3), mechanisms of starch-phenolics interactions (Chapter 4&5) and inhibition on brush border enzymes (Chapter 6).

Chapter 2 and 3 were designed to study the role of food matrix in limiting the inhibitory capacity of polyphenols on starch digestibility. In Chapter 2, co-digestion and fortification were used as strategies to investigate how the food matrix influences the role of berry polyphenols on starch digestibility. Blueberry and raspberry extracts were used as sources of polyphenols and wheat bread was chosen as a starchy food. The inhibition obtained by co-digesting bread with berry extract is higher than the inhibition by digestion berry extract-fortified bread. Starch and gluten, as two main components in the bread matrix, interacted with berry phenolics to a large extent and that was indicated by the lower polyphenols bio-accessibility. On one hand, those interactions with food matrix (starch and gluten) lowered the amount of berry phenolics that can bind and inhibit  $\alpha$ -amylase. On the other hand, starch-phenolics interactions themselves can contribute to slow down starch digestibility. Moreover, polyphenols bio-accessibility is not the only factor for inhibiting starch digestibility, phenolic molecular structures being equally important. That is shown by the fact that raspberry extract which contains larger amount of polymeric tannins showed stronger inhibition on starch digestibility. This study shows co-digestion of phenolics with starchy food is a more efficient strategy to slow down starch digestibility in a bread matrix compared to bread fortification.

In Chapter 3, I further studied how the phenolic types and gluten presence affect the inhibitory capacity of polyphenols on starch digestibility. In this study, green tea and black tea were chosen as the polyphenols sources to study different types of polyphenols. Conventional wheat bread and gluten-free bread were prepared for studying the effects of gluten presence. Gluten is an important matrix components in wheat-based products. I found the presence of gluten lowered the inhibitory capacity of polymeric phenolics, but had little effect on the inhibitory capacity of monomeric phenolics. The results show that the tea polyphenols can be a promising strategy for modulating the glycaemic index of starchy food, but this strategy must be adapted to the selected food matrix.

In previous chapters, I have observed that interaction between starch and polyphenols may contribute to starch digestibility, so I studied further this interaction in Chapters 4&5. In Chapter 4, the interactions of wheat starch (WS) and tannic acid (TA) were investigated for



their gelatinization, pasting, structural, and steady and dynamic rheological properties and digestibility of wheat starch. TA was either complexed with starch (WS-TA complexes) or mixed with starch (WS-TA mixtures) right before the characterization of its properties. A substantial amount of inclusion and non-inclusion complexes were produced and the production of both types of complexes is affected by the way of TA addition. Inclusion complexes were mostly produced by interaction of TA with non-gelatinized starch. Non-inclusion complexes were mostly produced by mixing TA with native starch followed by heating. The two different types of complexes influenced rheological properties of wheat starch differently, i.e., inclusion complexes produced weaker gel and non-inclusion complexes produced stronger gel. Both inclusion and non-inclusion complexes largely inhibited starch digestibility.

In Chapter 5, I studied the starch-phenolics interaction by using three types of starch, i.e., potato starch (B type), corn starch (A-type) and corn amylopectin (A-type). The starch-phenolics interactions influenced by starch types and amylose content were discussed. Similar to the addition method in Chapter 4, tannic acid was added by complexing and simply mixing with starch. The amount of TA in mixture samples is higher than that in complex samples. Besides, heat incubation (37°C) during complex preparation influenced the functional properties of three starches and most significantly in potato starch, for instance, the XRD patterns changed from B-type to A- plus B-type. DSC peak at 120 ~160 °C provided evidence of non-inclusion complexes formed by TA with all three types of starch. Gelatinized and non-gelatinized amylose and amylopectin showed different binding abilities to TA, i.e., non-gelatinized amylopectin has more ability to interact with TA than non-gelatinized amylose, but gelatinized amylose have more ability to interact with TA than gelatinized amylopectin. The more open structure of B-type starch makes it easier to interact with TA than tightly packed A-type starch, since physical-chemical properties of potato starch were more affected compared to corn starch and corn amylopectin. The inhibition of starch digestibility was attributed to non-inclusion complexes from starch-tannins interactions and inclusion complexes from starch-lipid interactions, and the latter was only found in corn starch. These results can help stimulate further interest in applications of starch-tannic acid interactions in various starchy food.

In Chapter 6, I studied the inhibitory effects of tea polyphenols on  $\alpha$ -glucosidase.  $\alpha$ -glucosidase is provided by rat intestinal extract and human Caco-2 cells. Various inhibitors were selected including epigallocatechin gallate, epicatechin gallate and four phenolics-rich tea extract from white, green, oolong, black tea. Four substrates were used to study inhibitory effects of tea polyphenols towards different hydrolytic activities including maltase, sucrase, isomaltase and glucoamylase. Maltase and glucoamylase from rats were largely inhibited by tea polyphenols, but rat isomaltase and sucrase were not. A mixed type of inhibition on rat maltase was found, which is composed of competitive and uncompetitive types of inhibition. Tea extracts in combination with acarbose, produced an antagonistic effect on rat maltase

activity. Tea polyphenols show different sensitivity for rat and Caco-2  $\alpha$ -glucosidase. Epigallocatechin gallate and green tea extract exhibit dose-dependent inhibition on human sucrase, but no inhibition on rat sucrase. The opposite was observed when assessing maltase activity. The results highlighted the intrinsic difference among various enzymes and various testing conditions need to be taken into account when reporting inhibitory effects on  $\alpha$ -glucosidase.

Finally, in Chapter 7, a summary of the main findings, some considerations of methodology and implications was provided. The most important conclusion is that the inhibitory effects of polyphenols on starch digestibility are influenced by multiple interactions among polyphenols, digestive enzymes, starch and other components in the food matrix.

# Acknowledgment

## Acknowledgment

Finally, I made it! It is such a great experience to do a PhD. It is a learning process and no one can finish it alone.

I would like to start acknowledging my perfect supervision team: **Vincenzo, Ruud, Edoardo, and Teresa**. I am so lucky to have all your support which made my PhD journey much easier and enjoyable. You gave me so much freedom to conduct my research project and always guide me to find solutions when I met difficulties. **Vincenzo and Ruud**, you are quite supportive not only for my PhD project but also for motivating me to think about my future. I learned a lot from every conversation that we had. **Edoardo**, it has always been very inspiring working with you. Thanks for always keeping me on track and for your quick feedback on my manuscripts, which is always valuable and helpful. **Teresa**, you are so sweet and supportive. You can always understand my unexpressed feelings and needs and speak for me when needed.

My gratitude also goes to my co-supervisors **Jurriaan, Monic, and Stefano**. **Jurriaan and Monic**, thanks a lot for your help and coach with the Caco-2 assays and valuable feedback on my manuscript. I truly value your commitment and support. **Stefano**, thanks for your valuable suggestions on my project. Your insightful feedback always pushed me to sharpen my thinking.

I would like to thank **Prof. Shaoping Nie**, thanks for all your support during my master study. I gained a lot of skills and competence which quantify me for getting a PhD position at Wageningen University & Research.

Being part of FQD group has been an extraordinary experience for me. It has been a pleasure for me to work in such an international and multidisciplinary group. Thanks to all FQD staff members for the nice moments that we shared. I especially would like to thank our sweet secretaries **Kim, Corine, and Lysanne**. You truly make my life easier and you always try your best to help us with all the administrative processes.

I would like to thank the technicians of FQD, **Charlotte, Frans, Xandra, Geert, Erik, Mike, Jelle, and Nienke**. I am truly grateful to **Geert**. You helped me multiple times to fix and maintain the HPLC, and you can always find a time slot for me no matter how busy you are. Many thanks to **Erik**. Thanks for the support for the lab work and a lot of laughs and jokes, which help me to do lab work in a more relaxed way.

Many thanks to my paranymphs **Yao** and **Diana**. Thanks for being my side during my defense. **Yao**, we had so many nice moments for dinner, lunch breaks, and sports classes, and I am sincerely grateful for your friendship and I wish you a lot of success. **Diana**, it is my great pleasure to be your PhD buddy when you start your PhD journey. I hope you enjoy doing your PhD and I wish you a lot of success.

I would like to thank all my MSc and BSc students who were partially involved in my project. **Yanqiao, Ningxin, Luana, Teun, Kristen, Sam, and Yaw**, thanks for all your efforts and valuable contributions to my project. I wish you a lot of success in your future.

Moreover, I would like to thank all my colleagues from FQD. I would like to specially thank **Ana** for your help on my project. **Sara**, we had so many nice memories for dinners, BBQs and PhD trip and a lot of laughs. You are almost there as well and I wish you a lot of success. **Pieter**, you helped Zhijun and me a lot for our living in the Netherlands and we really appreciated it. I was especially touched by the birthday flowers and greetings, and every year you remembered it. I wish you and Teresa all the best.

**Bingbing and Ling**, I really appreciated your friendship. We had so many nice memories of traveling. You are so brave, brilliant, kind, and helpful. I am pretty sure that you will achieve all your wishes and dreams in your life.

My Chinese colleagues Geelu, Hao, Jing, Li, Chunyue, Hongwei, Yuzheng, Ningjing, Zhan, Yajing, Jianing, Zongyao, Yaowei, Tianxiang, Jiaying, Qing Han, Tiantong, Yi, Huifang, Feilong, Keqing, Qing Ren, Xiangnan, Kangni, Zhe, Yifan, Laiyu and Peiheng, thanks for sharing the fantastic journey with me. It's nice to meet you all in the Netherlands.

**Orange and Groot**, my dear cats, thanks for bringing so much happiness to us.

**Zhijun**, we have been together for 10 years. You are always there for me no matter what. Thanks for your love, encouragement and patience.

My dear **father, mother, and sister**, thanks a lot for your support and understanding. I would not make such a great achievement without your support.

Lijiao Kan

2021-08-04

Wageningen

---

## About the author

#### About the author



Lijiao Kan was born on the 19<sup>th</sup> of April 1991 in Hebei, China. She finished her bachelor and master studies in Food science and technology at Nanchang University (China). After obtaining her MSc degree in 2017, she started a PhD project in Food quality and design group of Wageningen University & Research. Her project aims at

possible mechanisms to explain inhibitory effects of polyphenols on carbohydrate digestion. The results of her research are presented in this thesis.

Lijiao Kan: [klijiao@gmail.com](mailto:klijiao@gmail.com); [ncuskkkanlijiao@163.com](mailto:ncuskkkanlijiao@163.com).



## List of publications

**Kan, Lijiao**, Oliviero, T., Verkerk, R., Fogliano, V., & Capuano, E. (2020). Interaction of bread and berry polyphenols affects starch digestibility and polyphenols bio-accessibility. *Journal of Functional Foods*, 68, 103924. <https://doi.org/10.1016/j.jff.2020.10392>.

**Kan, Lijiao**, Capuano, E., Fogliano, V., Oliviero, T., & Verkerk, R. (2020). Tea polyphenols as a strategy to control starch digestion in bread: the effects of polyphenol type and gluten, *Food & Function*, 11, 5933-5943. <https://doi.org/10.1039/d0fo01145>.

**Kan, Lijiao**, Capuano, E., Fogliano, V., Verkerk, R., Mes, J. J., Tomassen, M. M. M., & Oliviero, T. (2021). Inhibition of  $\alpha$ -glucosidases by tea polyphenols in rat intestinal extract and Caco-2 cells grown on Transwell. *Food Chemistry*, 361, 130047. <https://doi.org/10.1016/j.foodchem.2021.130047>.

**Kan, Lijiao**, Capuano, E., Oliviero, T., & Renzetti, S. Different effects of inclusion and non-inclusion wheat starch-tannic acid complexes on rheological properties and digestibility of wheat starch. (Submitted to journal for publication).

**Kan, Lijiao**, Gyamfi, Y., Capuano, E., Oliviero, T., & Renzetti, S. Non-inclusion starch-tannins interactions formed in starch differing in crystalline type and different amylose content (In preparation).

## **Overview of completed training activities**

### **Discipline specific activities**

#### ***Courses***

Reaction kinetics in food science, VLAG, Wageningen, The Netherlands, 2018

Chemometrics, VLAG, Wageningen, The Netherlands, 2018

Advanced food analysis, VLAG, Wageningen, The Netherlands, 2019

Sumer school, Mediterranean Diet Seminar - II EDITION, Biomedia Srl, Ascea, Italy, 2019

The VLAG Online Lecture Series, VLAG, Wageningen, The Netherlands, 2020

Rheology: The do's and don'ts & Symposium: Rheology, VLAG, Wageningen, The Netherlands, 2020

Energy metabolism & body composition, VLAG, Wageningen, The Netherlands, 2021

#### ***Conferences***

2nd International Conference on Food Bioactives & Health\*, Lisbon, Portugal, 2018

33rd EFFoST International Conference \*, Rotterdam, The Netherlands, 2019

F&V Processing 2020 - Third Symposium on Fruit and Vegetable Processing, online, 2020.

Conference 'Science and Technology for Meat Analogues, online, 2021

#### **General courses**

VLAG PhD week, VLAG, Baarlo, The Netherlands, 2018

Introduction to R, VLAG, Wageningen, The Netherlands, 2018

Applied statistics, VLAG, Wageningen, The Netherlands, 2018

Scientific writing, Wageningen into language, Wageningen, The Netherlands, 2018

The essentials of scientific writing and presenting, Wageningen into language, The Netherlands, 2018

Data management, Wageningen Library, Wageningen, The Netherlands, 2018

Scientific Artwork - Vector graphics and images, Wageningen Library, The Netherlands, 2018

Adobe InDesign Essential Training, Wageningen Library, The Netherlands, 2018

Infographics and Iconography, Wageningen Library Wageningen, The Netherlands, 2018

**Other activities**

Preparation of research proposal, FQD group, Wageningen, The Netherlands, 2017-2018

PhD study tour to Australia, FQD group, Wageningen, The Netherlands, 2018 Wageningen, The Netherlands, 2018

Group meetings on project progress and Colloquia, FQD group, Wageningen, The Netherlands, 2018

VLAG: Graduate School for Nutrition, Food Technology, Agrobiotechnology and Health Sciences;

FQD: Food Quality and Design group.

The research described in this thesis was financially supported by the Chinese Scholarship Council.

Financial support from Wageningen University for printing this thesis is gratefully acknowledged.

Cover design by Fenna Schaap / ProefschriftMaken and Lijiao Kan

Printed by ProefschriftMaken